Quark Numbers and Percolation in QCD

Milad Ghanbarpour

Dezember 2024

Dissertation zur Erlangung
des akademischen Grades
Dr. rer. nat.
am Fachbereich 07 der

JUSTUS-LIEBIG-
UNIVERSITÄT
GIESSEN

Dissertation zur Erlangung des akademischen Grades, Dr. rer. nat., am Fachbereich 07 der Justus-Liebig-Universität Gießen.

Titel:	Quark Numbers and Percolation in QCD
Verfasser:	Milad Ghanbarpour
1. Gutachter:	Prof. Dr. Lorenz von Smekal *(Justus-Liebig-Universität Gießen, Deutschland)*
2. Gutachter:	Prof. Dr. Urs Wenger *(Universität Bern, Schweiz)*
eingereicht am	18.12.2024
Fassung vom	02.07.2025
Disputation:	02.07.2025

Anmerkung:
Die hier präsentierten Forschungsarbeiten sind zu Teilen vor der Fertigstellung dieser Dissertation veröffentlicht worden. Hierbei sind die in der Veröffentlichung enthaltenden Arbeiten in Zusammenarbeit mit Dritten entstanden. Eine genaue Trennung und Zuordnung der wissenschaftlichen Beiträge erfolgt an den entsprechenden Stellen dieser Dissertation. Die dazugehörige Veröffentlichung ist unter *M. Ghanbarpour und L. von Smekal, Phys. Rev. D 106, 054513* zu finden.

Kurzzusammenfassung

Die vorliegende Dissertation beschäftigt sich mit der gittereichtheoretischen Formulierung der Quantenchromodynamik. Die Forschungsarbeit gliedert sich in zwei Hauptresultate. Das erste Resultat ist die explizite Konstruktion eines thermodynamischen Ensembles, für welches die Baryonenzahl in einem räumlichen Untervolumen V auf nicht ganzzahlige Werte fixiert wird. Betrachten wir uns nämlich das gesamte periodische Raumvolumen, so können aufgrund der Eichinvarianz und dem daraus resultierenden Gaußschen Gesetz nur Zustände beobachten werden, deren Gesamtquarkteilchenzahl, welche Quarks positiv und Antiquarks negativ zählt, ein Vielfaches von Drei ist, d.h. es werden nur Zustände mit ganzzahligen Baryonenzahlen beobachtet. Dies liegt daran, dass jedes weitere Quark oder Antiquark ein farbelektrischen Fluss erzeugt, der nicht eichinvariant mit den schon vorhandenen Ladungen terminieren kann. Diese Beschränkung gilt jedoch nicht für ein Untervolumen V. Das Untervolumen V kann insgesamt eine nicht ganzzahlige Baryonenzahl haben, sodass der elektrische Fluss durch die Volumenoberfläche nicht verschwindet und mit passenden Ladungen außerhalb von V eichinvariant terminiert. Die Konstruktion des Ensembles bedarf jedoch der Modifikation der Wechselwirkung an der Volumenoberfläche, da die Wechselwirkung ansonsten ignorant gegenüber der arbiträren Wahl des Volumens V wäre. Wir benutzen zwei unterschiedliche Ansätze für die Konstruktion des Ensembles: eine quantenmechanische Formulierung der Gitter-QCD und eine duale Formulierung des Pfadintegrals. Das zweite Hauptresultat dieser Dissertation beschäftigt sich mit der Untersuchung, inwiefern das Phänomen der Perkolation als Mechanismus für Confinement herangezogen werden kann. Wir basieren unsere Untersuchungen auf einer Idee von Satz, welche vorschlägt, dass der Übergang von einer Confinened-Phase zu einer Deconfined-Phase sich in QCD als Perkolationsübergang beschreiben lassen könnte. Hierbei motiviert Satz seine Idee mit der von Spinsystemen bekannten Kertész-Linie. In dieser Vorstellung stimmt der Perkolationsübergang mit dem Übergang der spontanen Z_3-Symmetrieberechung in der reinen Eichtheorie überein und bleibt bei leichten Quarkmassen bestehen. Dies würde eine eindeutige Unterscheidung der Confined-Phase und Deconfined-Phase ermöglichen. Wir schlagen in dieser Arbeit vor, dass die Definition von Perkolation auf Basis von zentrumselektrischen Flüssen den gewünschten Mechanismus liefert. Hierzu definieren wir die Wahrscheinlichkeit, dass perkolierende Strukturen auftreten, leiten das dazugehörige Pfadintegral her und zeigen, dass der Mechanismus den Confinement-Übergang bei unendlichen Quarkmassen erklären kann. Die hier präsentierten theoretischen Resultat werden anschließend in einem einfachen Flux-Tube-Modell, welches die grundlegenden zentrumselektrischen Flussstrukturen mit QCD gemeinsam hat, numerisch demonstriert.

Abstract

In this thesis, we are concerned with Lattice QCD and present two results. First, we construct an ensemble where the baryon number is fixed to fractional values in a spatial subvolume V. Due to gauge invariance and the implied Gauss law, the baryon number cannot be fixed to a fractional value on the whole periodic volume because any state with a net-quark number which is not a multiple of three has additional quarks or antiquarks whose color-electric fluxes cannot terminate in a gauge-invariant manner. For a subvolume V, this restriction does not apply. The fluxes can terminate at corresponding charges outside of V. However, the interaction has to be modified at the surface of V to make the system aware of the arbitrarily chosen subvolume. This is done with two independent approaches: a quantum-mechanical description of Lattice QCD and a dual formulation of the path integral. Second, we investigate the phenomenon of percolation as a mechanism for confinement. To this end, we base our considerations on a suggestion by Satz to describe the transition between confinement and deconfinement by a percolation transition. Similar to the Kertész line of spin systems, the percolation transition then coincides with the notion of confinement based on the spontaneous breaking of the Z_3 symmetry at infinite quark masses but persists at light masses. This allows for an unambiguous distinction between a confined and deconfined phase at all parameters of the theory. We propose the correct mechanism to be given by the percolation of center-electric fluxes, define the spanning probability, derive the path integral and show that the confinement transition at infinite quark masses can be seen as a consequence of our notion of percolation. As a proof of concept, we demonstrate both main results numerically in a simple flux-tube model which shares the necessary center-electric flux structures with QCD.

Danksagung

Ich möchte an dieser Stelle die Gelegenheit nutzen, meinen Dank auszusprechen.

- An erster Stelle möchte ich mich bei Herrn Prof. Dr. Lorenz von Smekal für die Möglichkeit bedanken, dass ich dieses spannende und herausfordernde Forschungsthema bearbeiten durfte. Hierbei ist insbesondere die jahrelange und hervorragende Betreuung und die enorm lehrreiche Zusammenarbeit hervorzuheben.
- Ein weiterer Dank geht an Herrn Prof. Dr. Urs Wenger von der Universität Bern, der sich bereit erklärt hat, die vorliegende Dissertation zu begutachten.
- Ferner bedanke ich mich bei Herrn Prof. Dr. Christian S. Fischer, der über die letzten Jahre mit seinen Ratschlägen, insbesondere im Rahmen der abgehaltenen PhD-Committees, dazu beigetragen hat, dass die Promotion einen positiven und produktiven Verlauf genommen hat.
- Die hier präsentierten Forschungsarbeiten wurden im Rahmen eines Kooperationsabkommens mit dem GSI Helmholtzzentrum für Schwerionenforschung finanziell gefördert. Hierbei bin ich auch dankbar für die Graduate School, HGS-HIRe, welche mir die Teilnahmen an Konferenzen und Fortbildungen ermöglicht hat.
- Ich bedanke mich bei Julian Bernhardt, Joshua Hoffer und Alexander Sekels für die zahlreichen grammatikalischen, stilistischen und inhaltlichen Hinweise.
- Ein großer Dank geht an alle Kolleginnen, Kollegen und Freunde mit denen ich die Zeit am Institut für theoretische Physik verbringen durfte.
- Ein besonders wichtiger Dank geht an meine Familie und meine Freunde, die mich stets unterstützt haben.

Contents

1 Introduction **1**

2 Quantum Field Theory **5**
2.1 The general framework 5
2.2 Canonical quantization 10
2.3 Quantum Chromodynamics 11
2.4 Lattice QCD 15

3 Transfer-matrix formulation **25**
3.1 Quantum-mechanical description 26
3.2 Symmetric transfer operator 39
3.3 Asymmetric transfer operator 54

4 Quark numbers in QCD **63**
4.1 't Hooft's center-electric flux ensembles 65
4.2 Fixed quark number ensembles 78

5 Percolation in QCD **99**
5.1 The phenomena of percolation 100
5.2 Percolation in QCD 103
5.3 Percolation of flux-tube configurations 106

6 Flux-tube model **119**
6.1 Flux-tube model for heavy quarks and strong couplings 120
6.2 Quark numbers in the flux-tube model 127
6.3 Percolation in the flux-tube model 138

7 Conclusion **149**

A Supplementary considerations for Chapter 5 **151**
A.1 Reflection invariance of center-electric fluxes 151
A.2 Infinite-coupling limit for Wilson fermions 154

B Supplementary considerations for Chapter 6 **158**
B.1 Power expansion of $Q(L)$ 158
B.2 Equivalence between Equation (6.2) and the Z_3-Potts model . . 159
B.3 Transfer-matrix formulation for one-dimensional chains 160
B.4 High-temperature expansion of ΔF 162

B.5 Low-temperature expansion of ΔF 168
B.6 Worm algorithm 182
B.7 Fully-dynamic connectivity problem 196

Bibliography **203**

Chapter 1

Introduction

The emergence of hadronic matter through the strong interaction of quarks and gluons is described by the theoretical framework of Quantum Chromodynamics (QCD). In general, Quantum Field Theory, as which QCD is also formulated, describes the embedding of relativistic physics into quantum mechanics leading to the description of most fundamental forces on microscopic scales. In the 1960s, quarks were introduced by Gell-Mann and Zweig as a mean of understanding the hadron spectrum via $\mathrm{SU}(3)$ symmetries [1, 2]. However, only after deep-inelastic scattering experiments at SLAC demonstrating an approximate Bjorken scaling and Feynman's parton model, the certainty arose that hadrons are made of point-like constituents identified as quarks [3–5]. Being driven by further experimental results and theoretical works, Fritzsch and Gell-Mann introduced the concept of color as an additional $\mathrm{SU}(3)$ symmetry into their quark model, and finally Fritzsch, Gell-Mann and Leutwyler extended the quark model to QCD as a non-Abelian gauge theory paving the way to our current understanding of the strong force [6–9]. At the same time, Gross, Politzer and Wilczek showed that non-Abelian gauge theories, such as QCD, are asymptotically free in the sense that the running coupling $\alpha_\mathrm{s}(\mu) \to 0$ of the interaction vanishes for large energy scales $\mu \to \infty$ [10, 11]. This justifies the consideration of quarks and antiquarks as approximately non-interacting at large energies as it is done in the parton model.

Albeit, quarks, antiquarks and gluons being the elementary particles of the strong force, they have never been observed as asymptotically free states in any experiment [12]. They appear to only occur as part of colorless states which are singlet states of the $\mathrm{SU}(3)$-color symmetry. Color confinement is however only one aspect of confinement in QCD. At small baryon-chemical potentials, QCD seems to undergo a phase transition from a confined phase at low temperatures, where the degrees of freedom are hadrons, to a deconfined phase at large temperatures, where a quark-gluon plasma (QGP) forms in which the degrees of freedom are given by quarks and gluons [13]. Experimental findings indicate that the QGP is a strongly-coupled liquid which behaves almost like a perfect fluid [13, 14]. In the infinite temperature limit, when α_s tends to zero, the system approaches the ideal-gas limit of non-interacting particles [13–15]. It is believed that the early universe was in a state of a QGP before cooling down and hadronizing to the confined phase. However, the distinction between the

confined and deconfined phase is not sharp. The thermodynamic quantities are non-singular and the transition is a crossover transition at around $T_c \approx 150 - 160\,\mathrm{MeV}$ [16–21]. This leaves us with the task of understanding the confinement and deconfinement transition and the mechanism of how the system evolves from hadronic degrees of freedom only to a thermodynamical description based on quarks and gluons. How does the system transform from hadrons to a nearly perfect liquid?

Because the analytic behavior of the thermodynamic quantities does not allow for an unambiguous notion of confinement or deconfinement, the phenomenon of confinement is often studied in pure gauge theories where dynamical fermions are absent [22]. A purely gluonic theory possesses a global symmetry with respect to the center Z_3 of the gauge group $SU(3)$. This symmetry breaks spontaneously at a critical temperature T_c marking a confined ($T < T_c$) and deconfined ($T > T_c$) phase. The confined phase is characterized by a linear rising potential between a static quark-antiquark pair, a narrowing of the color-electric fluxes into tubes and an infinite amount of energy required to insert a single static color charge into the system. The theory is confining in the sense that open color charges are suppressed and an infinite energy is required to separate them arbitrary far away from each other. In the deconfined phase, when the symmetry is spontaneously broken, the potential ultimately flattens at large distances such that color charges can be separated with a finite amount of energy. The system is understood to be deconfined because it allows the insertion of open color charges with a finite amount of energy. However, once dynamical quarks are introduced, the symmetry is explicitly broken. Quarks and antiquarks screen color charges yielding a flattening of the potential at all temperatures. The observables which measure the spontaneous symmetry breaking lose their diagnostic value of identifying the confined and deconfined phase, i.e. the notion of confinement based on the Z_3-symmetry is restricted to the heavy quark regime.

Furthermore, a natural extension of the investigation of QCD matter is to consider non-vanishing baryon-chemical potentials $\mu_B > 0$ and therefore exploring the phase diagram on the (μ_B, T)-plane. Experiments at LHC and RHIC make observations of QCD at large temperatures and small baryonic densities. However, future heavy-ion experiments at, for example, FAIR, NICA, and J-PARC aim to explore QCD at high baryon densities [13, 14, 23]. There are many conjectures and estimates for the QCD phase diagram ([24]), and current and future experiments will hopefully shed some light into wide regions of the phase diagram. QCD with zero quark masses exhibits a spontaneously broken chiral symmetry which refers to the axial $SU_A(N_f)$ symmetry of the massless Lagrangian [14, 24, 25]. The order parameter for this phase transition is the chiral condensate. However, QCD is not described by a Lagrangian with massless quarks. The chiral symmetry gets explicitly broken and the transition becomes a crossover at vanishing chemical potentials. It is however conjectured that QCD exhibits a first-order transition line in the (μ_B, T)-plane which ends in a second-order critical endpoint [24]. Unfortunately, regions of large μ_B are not directly accessible to Lattice QCD because of the sign problem [23]. Some notable efforts in the investigation of the crossover region up to

$\mu_B = 400\,\mathrm{MeV}$ have been made in [26, 27], nevertheless.

We are concerned with the phenomena of confinement in this thesis. The presented research results address both aspects of confinement: color confinement and the transition of QCD matter from hadronic degrees of freedom to a QGP. There are two main results in this thesis, and we work in the framework of Lattice QCD with Wilson fermions exclusively.

First, for color confinement, we have seen that QCD only allows colorless states. This property is also given on the lattice, where the total net-quark number can only be a multiple of three. However, this restriction does not apply to a spatial subvolume V where a hadronic structure partly lies in the volume V and its complement $\overline{V}$. We demonstrate the construction of an ensemble which fixes the net-baryon number to fractional values in V. The construction requires the modification of the interaction at the surface of V because the dynamics are otherwise not aware of the arbitrarily chosen volume, and quarks and antiquarks can in principle be created, destroyed or moved between V and $\overline{V}$. The construction is presented in Chapter 4.

Second, we propose a confinement-deconfinement mechanism based on percolation. This goes back to a suggestion made by Satz [28]. He put forward the idea to understand the transition from a confined to a deconfined phase as a percolation transition. Percolation is a geometric phase transition in which the non-percolating phase is described by finite clusters and the percolating phase is given by the formation of an infinitely large cluster. Importantly, percolation does not rely on a singular behavior of the free-energy density. Similar to the Kertész line of spin systems, Satz suggested that confinement in QCD could be described by a percolation transition which coincides with the notion of confinement based on the spontaneous breaking of the Z_3 symmetry at infinite quark masses but persists at light masses. This allows for an unambiguous distinction between a confined and deconfined phase at all parameters of the theory. In Chapter 5, we propose the correct mechanism to be given by the percolation of center-electric fluxes, define the spanning probability, derive the path integral and show that the confinement transition at infinite quark masses can be seen as a consequence of our notion of percolation. Essentially, the notion is based on decomposing the Hilbert space of the theory into flux-tube configurations where the quarks are sources of center charge and the gauge fields are sources of center-electric fluxes. Gauge invariance then implies a local Z_3-Gauss law which the flux-tube configurations must fulfill. The percolation of flux-tube configuration gives an intuitive understanding for confinement which goes back to early ideas by Patel [29]. In the confined phase, only local and finite structures of non-trivial center charges and fluxes exist. Once the percolation transition is reached, an infinite network of non-trivial center-fluxes forms which is identified with the deconfined phase.

We use the transfer-matrix formulation of Lattice QCD which is a quantum-mechanical formulation of QCD on the spatial lattice to formulate the construction of the fixed net-quark number ensembles and the notion of percolation. The transfer-matrix formulation is presented in Chapter 3.

In Chapter 6, we use a simple flux-tube model, sharing the center-electric flux structures with QCD, to demonstrate the presented concepts.

Chapter 1. Introduction

Before diving into the transfer-matrix formulation, we give a brief introduction to Quantum Field Theory and Lattice QCD in the next chapter.

Chapter 2

Quantum Field Theory

The current foundation of all theories describing the realm of microscopic physics and its interactions is the framework of Quantum Field Theory (QFT) – a framework which combines the principles of relativistic physics and quantum physics. It is the framework which gives rise to the notion of particles in flat spacetime and the richness of all the interactions observed between them. In this thesis, the sole focus is Quantum Chromodynamics (QCD) describing the strong interaction which is responsible for all the hadronic structure: protons, neutrons, pions, etc. The first part of this chapter summarizes briefly the general framework of QFT with its most important concepts. This summary is based on [25, 30–33] and the notations used therein. In the last section of this chapter, we will introduce Lattice QCD as the main framework used in this thesis.

2.1 The general framework

The bases for all theoretical descriptions of microscopic physics, especially particle physics, are the principles of quantum mechanics. A system is characterized by a normalized vector $|\psi\rangle \in \mathcal{H}$ of a separable Hilbert space $\mathcal{H}$. The measurement of a quantity is then described by a self-adjoint operator $\hat{A}$ whose spectrum σ of eigenvalues represent all possible outcomes $E \subseteq \sigma$ of the experiment. The theory does not predict which outcome E will be observed. It merely assigns a probability measure $\mu(E)$ to the possible outcomes and predicts that this measure characterizes the results of repeated measurements. For the experimentalist, there seems to be no reason why a certain outcome has occurred. The measurement procedure appears to be a purely random process. Once the measurement is done and a certain outcome E has been reported, the wave-function of the system has collapsed into a new normalized vector $|\psi_E\rangle \propto \hat{P}_E |\psi\rangle$, where $\hat{P}_E$ is the projection operator onto the subspace $\mathcal{H}_E$ spanned by the eigenvectors with eigenvalues $\lambda \in E$. The probability to observe the outcome E is $\mu(E) = \langle\psi| \hat{P}_E |\psi\rangle$. Hence, only the absolute squares $|\langle\phi|\psi\rangle|^2$ of scalar products between vectors $|\psi\rangle, |\phi\rangle \in \mathcal{H}$ are physically significant. As a consequence, all vectors $e^{i\alpha}|\psi\rangle$, $\alpha \in \mathbb{R}$ which differ only by a complex phase from the vector $|\psi\rangle$ describe the same physical state of the

system. A system is, therefore, not characterized by a single normalized vector $|\psi\rangle \in \mathcal{H}$ but by a ray $\Psi = \{e^{i\alpha} |\psi\rangle \mid \alpha \in \mathbb{R}\}$ of normalized vectors. At first glance, this property does not seem to be of great importance because, for example, it plays no significant role in ordinary non-relativistic quantum mechanics. We can compute and discuss all sorts of phenomena without ever considering the global phase of a vector: the hydrogen atom, the harmonic oscillator, a potential well, molecule structures, etc. Nevertheless, as it is described below, the ignorance of the formulation towards a global phase factor plays a crucial role in the existence of particles with half-integer spin.

Poincaré group

In flat spacetime, an observer in an inertial frame describes an event, like the position of a particle, by a vector $x = (x^0, x^1, x^2, x^3) \in \mathbb{R}^4$. The zeroth component is identified as the time $x^0 = t$ and the other coordinates describe the position in space. The same event will be described by different coordinates in general if we transform to the reference frame of another observer. The transformation between two inertial systems $\mathcal{O}_1$ and $\mathcal{O}_2$ is affine and has the general form

$$x'^\mu = \Lambda^\mu{}_\nu x^\nu + a^\mu \,,$$

where x^μ are the coordinates in $\mathcal{O}_1$ and x'^μ are the coordinates in $\mathcal{O}_2$. The matrix Λ is a Lorentz transformation and $a \in \mathbb{R}^4$ is a spacetime shift. The set of all Lorentz transformations L forms a group and is defined by all (4×4)-matrices Λ which fulfill the equation $\Lambda g \Lambda^T = g$, where

$$g_{\mu\nu} = \begin{pmatrix} 1 & 0 & 0 & 0 \\ 0 & -1 & 0 & 0 \\ 0 & 0 & -1 & 0 \\ 0 & 0 & 0 & -1 \end{pmatrix}$$

is the Minkowski metric. This property ensures lightlike distances between events $(x-y)^\mu (x-y)_\mu = 0$ in an inertial system to stay lightlike in all inertial frames; the four-momentum p of a particle, which lies on the light cone ($p^\mu p_\mu = 0$) for one observer, lies on the light cone for all observers. The speed of light is constant in all inertial frames. The Lorentz group together with all spacetime shifts a forms the Poincaré group $P = L \times \mathbb{R}^4$ with the multiplication rule

$$(\Lambda_2, a_2) \cdot (\Lambda_1, a_1) = (\Lambda_2 \Lambda_1, \Lambda_2 a_1 + a_2)$$

representing successive transformations of a vector x^μ with (Λ_1, a_1) and then (Λ_2, a_2). For a Lorentz transformation $\Lambda \in L$, we have the general property $\det \Lambda = \pm 1$ and if two Lorentz transformations Λ_1 and Λ_2 fulfill $\operatorname{sign} (\Lambda_1)^0{}_0 = \operatorname{sign} (\Lambda_2)^0{}_0$, their product $\Lambda_1 \Lambda_2$ has the same sign for its component $(\Lambda_1 \Lambda_2)^0{}_0$. Consequently, the Lorentz group decomposes into four connected subgroups depending on the signs of the determinant $\det \Lambda$ and the matrix element $\Lambda^0{}_0$. The four components are related to each other via the parity transformation $\Lambda_P \in L$, the time-reversal $\Lambda_T \in L$ and the combination $\Lambda_P \Lambda_T$. By considering the identity component $L_1 \subseteq L$, the other components can be represented by

an element of L_1 and a suitable transformation with either Λ_P, Λ_T or $\Lambda_P\Lambda_T$. Parity and time-reversal are transformations which are typically implemented separately in a quantum theory. For the construction of a relativistic theory in general, we only need L_1. The corresponding subgroup of the Poincaré group is denoted $P_1 = L_1 \times \mathbb{R}^4 \subseteq P$. The identity component L_1 is typically referred to as the proper ($\det \Lambda = 1$) orthochronous ($\text{sign } \Lambda^0{}_0 = 1$) Lorentz group.

Projective representations

Special relativity gives us the concept of observers in inertial frames and the transformation between them. However, these transformations only describe mappings on $\mathbb{R}^4$. We do not have any concept of coordinates in our general formulation of a quantum theory. The connection is made in the following way. An observer $\mathcal{O}_1$ describes the quantum system with a certain vector $|\psi_1\rangle \in \mathcal{H}$. Another observer $\mathcal{O}_2$ related with the Poincaré transformation (Λ, a) describes the same system with another vector $|\psi_2\rangle \in \mathcal{H}$ via a transformation $D(\Lambda, a)$:

$$|\psi_2\rangle = D(\Lambda, a)\,|\psi_1\rangle\ .$$

What is the structure of $D(\Lambda, a)$? Certainly, all observers should perceive the same probabilities when a measurement is done on the system. Hence, the transformation must preserve the values $|\langle\phi, \psi\rangle|^2 = |\langle D(\Lambda, a)\phi, D(\Lambda, a)\psi\rangle|^2$. And, because the absolute value is blind towards global phase factors of a state, it is enough to define a transformation $T(\Lambda, a)$ between the rays Ψ_1 and Ψ_2: $\Psi_2 = T(\Lambda, a)\Psi_1$. When the frame of reference is changed, we only state which new ray is to be used. We define a symmetry to be a ray transformation T which is bijective with T and T^{-1} keeping $|\langle\phi, \psi\rangle|^2$ invariant. These are the properties which we intuitively expect from a symmetry transformation. Now, Poincaré transformations are implemented by assigning to each $(\Lambda, a) \in P_1$ a symmetry $T(\Lambda, a)$ with the additional property that $T(\Lambda, a)$ should constitute a representation of P_1:

$$T((\Lambda_1, a_1) \cdot (\Lambda_2, a_2)) = T(\Lambda_1, a_1)T(\Lambda_2, a_2)\,.$$

This property just states that, on the Hilbert space, the combined transformation should be the same as the successive transformations. Nevertheless, for all practical uses, we like to work with a linear transformation D applied to vectors on the Hilbert space. A theorem by Wigner [34] states that for any symmetry transformation T there exists either a unitary or antiunitary transformation D such that for all $|\psi_1\rangle \in \Psi_1$ we have $D\,|\psi_1\rangle \in \Psi_2$ with $\Psi_2 = T\Psi_1$. The map D is unique up to a phase factor. Now, we can assign the map $D(\Lambda, a)$ to each Poincaré transformation $T(\Lambda, a)$. We assume $D(\Lambda, a)$ to be unitary. Because T constitutes a representation, this property is inherited by $D(\Lambda, a)$ in form of a projective representation:

$$D(\Lambda_1, a_1)D(\Lambda_2, a_2) = \mathrm{e}^{\mathrm{i}\omega} D((\Lambda_1, a_1)(\Lambda_2, a_2))\,,$$

where $\omega \in \mathbb{R}$ is a function of (Λ_1, a_1) and (Λ_2, a_2). The phase factor is just a result of $T(\Lambda, a)$ being a transformation between rays only. Because

$D(\Lambda, a)$ is only unique up to a phase factor, one might try to transform out the factor ω by choosing $e^{i\alpha(\Lambda,a)}$ for each $D(\Lambda, a)$ suitably and setting $D(\Lambda, a) \to e^{i\alpha(\Lambda,a)} D(\Lambda, a)$. In this way, $D(\Lambda, a)$ would be an ordinary representation. However, this is not possible for the Lorentz group L_1 in general. But it is still possible to define an ordinary representation with the help of the covering group of L_1. The covering group (see for example [35, Definition 5.12]) of L_1 is the group $\mathrm{SL}(2, \mathbb{C})$ of all complex (2×2)-matrices with determinant one. The covering map is a surjective Lie group homomorphism $\Lambda : \mathrm{SL}(2, \mathbb{C}) \to L_1$ with $\Lambda(A) = \Lambda(-A)\,, A \in \mathrm{SL}(2, \mathbb{C})$. By replacing L_1 in the Poincaré group with $\mathrm{SL}(2, \mathbb{C})$, we get the inhomogeneous $\mathrm{SL}(2, \mathbb{C})$ [32]. This group has the multiplication law

$$(A_2, a_2) \cdot (A_1, a_1) = (A_2 A_1, \Lambda(A_2) a_1 + a_2)\,.$$

Now, the projective representation of P_1 can be replaced with an ordinary representation $D(A, a)$ of the inhomogeneous $\mathrm{SL}(2, \mathbb{C})$ such that

$$D(A, a) = e^{i\alpha(A,a)} D(\Lambda(A), a),\ \alpha(A, a) \in \mathbb{R}\,.$$

In conclusion, Poincaré transformations are implemented by ordinary representations of the inhomogeneous $\mathrm{SL}(2, \mathbb{C})$. Of course, the specific representation $D(A, a)$ depends on the theory in question and is part of the theory's formulation.

Schrödinger equation

Now, spacetime shifts $D(\mathbb{1}, a)$ form an Abelian subgroup and are generated by the four-momentum operators $\hat{P}^\mu$:

$$D(\mathbb{1}, a) = \exp\left(i\hat{P}^\mu a_\mu\right).$$

The Hamilton operator of the theory is $\hat{H} = \hat{P}^0$. Analogously we define the three-momentum operator as $\vec{P} = (\hat{P}^1, \hat{P}^2, \hat{P}^3)$. The Schrödinger equation is now just a simple consequence of shifts in time. Consider the observers $\mathcal{O}_1$ and $\mathcal{O}_2$ related by the spacetime shift $a = (-t, 0, 0, 0)$: $x'^0 = x^0 - t$. The observer $\mathcal{O}_2$ lies either in the future ($t > 0$) or past ($t < 0$) of $\mathcal{O}_1$. Hence, if $\mathcal{O}_1$ perceives the system to be in the state $|\psi_0\rangle$, then $\mathcal{O}_2$ will perceive the same system in the state

$$|\psi(t)\rangle = e^{-i\hat{H}t} |\psi_0\rangle\ .$$

Taking the derivative with respect to time t, we arrive at the Schrödinger equation:

$$i\partial_t |\psi(t)\rangle = \hat{H} |\psi(t)\rangle\ .$$

One-particle states

Once the Poincaré symmetry is implemented, we are able to define the concept of a particle. A stable one-particle system (e.g. proton, electron, photon, hydrogen atom, etc.) of the theory is an irreducible representation $\mathcal{H}' \subseteq \mathcal{H}$ of $D(A, a)$. If the physical system is described by $|\psi\rangle \in \mathcal{H}'$ for one observer, all

observers will describe the same system with a state of $\mathcal{H}'$ because irreducible representations are invariant under all transformations $D(A,a)$. Nonetheless, irreducibility also means that there are no other non-trivial subspaces of $\mathcal{H}'$ which are invariant under $D(A,a)$. As a consequence, we understand a particle to be an invariant subspace which cannot be chosen smaller without breaking invariance. This definition of a particle has two important consequences: mass and spin/helicity. Both classify the irreducible representation $\mathcal{H}'$. Consider some eigenvector $|\psi_p\rangle$ of the four-momentum operators: $\hat{P}^\mu |\psi_p\rangle = p^\mu |\psi_p\rangle$. We have

$$D(\mathbb{1},a)\,|\psi_p\rangle = \mathrm{e}^{\mathrm{i}p^\mu a_\mu}\,|\psi_p\rangle$$

under spacetime shifts. For a pure Lorentz transformation $(A,0)$, we have

$$\begin{aligned}\hat{P}^\mu D(A,0)\,|\psi_p\rangle &= -\mathrm{i}g^{\mu\nu}\frac{\partial}{\partial a^\nu}_{|a=0} D(\mathbb{1},a)D(A,0)\,|\psi_p\rangle \\ &= D(A,0)\bigg(-\mathrm{i}g^{\mu\nu}\frac{\partial}{\partial a^\nu}_{|a=0}\bigg)D(\mathbb{1},\Lambda^{-1}(A)a)\,|\psi_p\rangle \\ &= (\Lambda^\mu{}_\nu(A)p^\nu)D(A,0)\,|\psi_p\rangle\ .\end{aligned}$$

The transformed state $D(A,0)\,|\psi_p\rangle$ is again an eigenvector of the momentum operators $\hat{P}^\mu$ but with the transformed four-momentum $\Lambda(A)p$. Hence, $\mathcal{H}'$ is only spanned by eigenspaces with four-momenta which can pairwise be mapped onto each other with a Lorentz transformation Λ. Otherwise, we would have subspaces spanned by eigenspaces with four-momenta which cannot be mapped onto each other by Poincaré transformations. Both subspaces would be invariant and, therefore, $\mathcal{H}'$ would not be irreducible.

There are six possible kinds of four-momentum shells, where every momentum can be reached from any other four-momentum by some suitable Lorentz transformation. They are classified by the Lorentz invariants $p^\mu p_\mu$ and sign p^0. If $p^\mu p_\mu = m^2 > 0$, we describe a massive particle with mass m. Here, we either have the possibility of positive energies $p^0 > 0$ or negative energies $p^0 < 0$. Massless particles are described by $p^\mu p_\mu = 0$. We again have the possibilities of positive or negative energies. We can also have $p^\mu = 0$ which describes the vacuum of the theory. Finally, the case $p^\mu p_\mu < 0$ gives particles, so-called tachyons, traveling faster than light. In all our current theories, only three of these possibilities are realized: massive and massless particles with positive energies and the vacuum $|\psi_0\rangle$ with $p^\mu = 0$.

The momentum shell does not describe the irreducible representation fully because eigenvectors $|\psi_{p,r}\rangle$ of the four-momentum operators can have additional degeneracies $r \in \{1,\dots,n\}$. These degeneracies are the origin of spin for massive particles or helicity for massless particles. Spin and helicity describe how the degeneracies transform under Poincaré transformations. For example, the degeneracy of massive particles is transformed with a representation of rotations in three dimensions. The irreducible representations of $\mathrm{SO}(3)$ only allow for integer-spin representations. However, because we consider representations of the covering group $\mathrm{SL}(2,\mathbb{C})$, rotations are actually described by the covering group $\mathrm{SU}(2)$ of $\mathrm{SO}(3)$ which also includes half-integer spins. This shows that the measurement outcomes being ignorant towards a global phase factor allows for massive particles with half-integer spin.

2.2 Canonical quantization

After setting the framework, we need to state how the theory is actually formulated, i.e. we need to define the representation $D(A, a)$. The general approach is the canonical quantization of a Lagrangian. Assume a set of quantum fields $\hat{\Psi}_1(x), \ldots, \hat{\Psi}_n(x)$ which we take to be operator-valued functions at spacetime points $x \in \mathbb{R}^4$. The Lagrangian density $\mathcal{L}(\hat{\Psi}_i, \partial_\mu \hat{\Psi}_i)$ is a function of the fields and their derivatives. The density is used to infer the structure of the theory. The action S is defined by

$$S = \int \mathrm{d}^4 x \, \mathcal{L}(\hat{\Psi}_i(x), \partial_\mu \hat{\Psi}_i(x)) \,.$$

For each field, we define a conjugate field

$$\hat{\Pi}_i(x) = \frac{\partial \mathcal{L}}{\partial(\partial_0 \hat{\Psi}_i(x))} \,.$$

The equations of motion, which the operators shall obey, are the Euler-Lagrange equations

$$\partial_\mu \frac{\partial \mathcal{L}}{\partial(\partial_\mu \hat{\Psi}_i(x))} - \frac{\partial \mathcal{L}}{\partial \hat{\Psi}_i(x)} = 0 \,.$$

The solutions of the Euler-Lagrange equations are exactly those for which the action S is stationary: $\delta S = 0$. The Legendre transformation then gives the Hamiltonian $\hat{H}$ of the theory

$$\hat{H} = \sum_i \int \mathrm{d}^3 \vec{x} \, \hat{\Pi}_i(t, \vec{x}) \partial_0 \hat{\Psi}_i(t, \vec{x}) - \int \mathrm{d}^3 \vec{x} \, \mathcal{L}(\hat{\Psi}_i(t, \vec{x}), \partial_\mu \hat{\Psi}_i(t, \vec{x})) \,.$$

However, this is not enough to properly quantize a theory. The Hamiltonian $\hat{H}$ has to consistently be guaranteed to be time-independent and the fields should actually transform according to $\hat{H}$:

$$\hat{\Pi}_i(t, \vec{x}) = \mathrm{e}^{\mathrm{i}\hat{H}t} \hat{\Pi}_i(0, \vec{x}) \mathrm{e}^{-\mathrm{i}\hat{H}t} \qquad \text{and} \qquad \hat{\Psi}_i(t, \vec{x}) = \mathrm{e}^{\mathrm{i}\hat{H}t} \hat{\Psi}_i(0, \vec{x}) \mathrm{e}^{-\mathrm{i}\hat{H}t} \,.$$

Additionally, there are various constraints

$$f_k(\hat{\Psi}_i, \hat{\Pi}_i) = 0$$

put upon the system. Constraints, which typically occur, are vanishing conjugate fields $\hat{\Pi}_i = 0$ and the corresponding constraints due to the Euler-Lagrange equations of those fields. This is just because the Lagrangian density might not depend on the time derivatives $\partial_0 \hat{\Psi}_i$. Furthermore, as it is the case for QCD, gauge-fixing conditions are applied. We assume that all equations by which the system is governed allow to rewrite the Hamiltonian $\hat{H}$ and the constraints $f_k(\hat{\Psi}_i, \hat{\Pi}_i)$ in terms of $\hat{\Psi}_i$, $\hat{\Pi}_i$ and their spatial derivatives.

Canonical variables $\hat{Q}_k(x)$ and $\hat{P}_k(x)$ are introduced to fully quantize the theory. The variables are canonical in the sense that they are taken to fulfill the equal-time (anti-)commutation relations:

$$\begin{aligned} [\hat{Q}_k(t, \vec{x}), \hat{P}_l(t, \vec{y})]_\pm &= \mathrm{i}\delta_{k,l} \delta(\vec{x} - \vec{y}) \,, \\ [\hat{Q}_k(t, \vec{x}), \hat{Q}_l(t, \vec{y})]_\pm &= [\hat{P}_k(t, \vec{x}), \hat{P}_l(t, \vec{y})]_\pm = 0 \,. \end{aligned}$$

Whether the commutator $(-)$ or anticommutator $(+)$ is used, depends on whether bosonic or fermionic fields/particles are considered. The original fields $\hat{\Psi}_i(\hat{Q}_k, \hat{P}_k)$ and their conjugates $\hat{\Pi}_i(\hat{Q}_k, \hat{P}_k)$ are now functions of the canonical variables such that all constraints are fulfilled, i.e. the canonical variables are independent variables on which we are free to impose the (anti-)commutation relations without creating inconsistency with the constraints of the theory. Once the fields $\hat{Q}_k$ and their conjugates $\hat{P}_k$ are identified, the Hamiltonian $\hat{H}$ is expressed in terms of the canonical variables and the equations of motion are (by construction) equivalent to

$$\mathrm{i}[\hat{H}, \hat{Q}_k] = \partial_0 \hat{Q}_k \qquad \text{and} \qquad \mathrm{i}[\hat{H}, \hat{P}_k] = \partial_0 \hat{P}_k \,.$$

In gauge theories, like QCD, the Lagrangian possesses a local gauge symmetry which creates additional complications when quantizing the theory. This is because the local nature of the gauge symmetry does not allow anymore for unique solutions of the equations of motion derived from the Lagrangian. Therefore, we cannot find canonical variables which fulfill the Heisenberg equations of motion because these equations actually are uniquely solvable. This problem is circumvented in gauge theories by introducing additional constrains. Gauge-fixing conditions $g(\hat{A}^\mu_a) = 0$ are imposed on the gauge fields $\hat{A}^\mu_a$ which can always be fulfilled by a suitable gauge transformation of the fields, i.e. we restrict the Lagrange formulation to a subset of gauge fields and only then consider the canonical formalism.

Once the system is quantized, Lorentz invariance can be used to establish the other generators of $D(A, a)$.

2.3 Quantum Chromodynamics

The Lagrangian density of Quantum Chromodynamics (QCD) is defined by

$$\mathcal{L} = \sum_{f=1}^{N_f} \hat{\bar{\Psi}}_f (\mathrm{i}\not{D} - m_f) \hat{\Psi}_f - \frac{1}{4} \sum_{a=1}^{8} F_{a,\mu\nu} F_a^{\mu\nu} \,.$$

for N_f flavors of quarks. Let us give a detailed explanation of the different parts. Without loss of generality, we restrict the considerations to the case $N_f = 1$ and write

$$\mathcal{L} = \hat{\bar{\Psi}} (\mathrm{i}\not{D} - m) \hat{\Psi} - \frac{1}{4} \sum_{a=1}^{8} F_{a,\mu\nu} F_a^{\mu\nu} \,.$$

The quarks and antiquarks of the theory are described by the Dirac spinor fields $\hat{\Psi}^\alpha_a$ with the Dirac indices $\alpha = 0, 1, 2, 3$ and the color indices $a = 1, 2, 3$. Therefore, the operator $(\not{D} - m)$ is thought of being embedded in the Dirac and color space and we just suppress the corresponding indices in $\mathcal{L}$. The operator $\not{D}$ is defined as

$$\not{D} = \gamma^\mu \partial_\mu - \mathrm{i} g_0 \gamma^\mu \sum_{a=1}^{8} T_a \hat{A}_{a,\mu}(x)$$

with the gamma matrices γ^μ fulfilling the Clifford algebra $[\gamma^\mu, \gamma^\nu]_+ = 2g^{\mu\nu}$ and the generators T_a of the su(3)-Lie algebra in the fundamental representation which fulfill the commutator relations

$$[T_a, T_b] = \mathrm{i}\sum_c f_{abc} T_c$$

with the structure constants f_{abc}. We have the definition $\hat{\overline{\Psi}} = \hat{\Psi}^\dagger \gamma^0$ and we have one massless vector field $\hat{A}_a^\mu(x)$ for each generator T_a of the algebra. These are the eight massless gluons of the theory. The tensor $F_{a,\mu\nu}$ is given by

$$F_{a,\mu\nu} = \partial_\mu \hat{A}_{a,\nu} - \partial_\nu \hat{A}_{a,\mu} + g_0 \sum_{b,c} f_{abc} \hat{A}_{b,\mu} \hat{A}_{c,\nu} \,.$$

The Lagrangian density is invariant under the gauge transformations

$$\begin{aligned} \hat{\Psi}(x) &\longrightarrow \Omega(x)\hat{\Psi}(x) \\ \sum_a T_a \hat{A}_a^\mu(x) &\longrightarrow \Omega(x)\left(\sum_a T_a \hat{A}_a^\mu(x)\right)\Omega^\dagger(x) - \frac{\mathrm{i}}{g_0}(\partial_\mu \Omega(x))\Omega^\dagger(x) \end{aligned}$$

of SU(3) with

$$\Omega(x) = \exp\left(\mathrm{i}\sum_a \omega_a(x) T^a\right).$$

This is a local symmetry transformation because we have the function $\omega_a(x)$ which gives us a different transformation for each spacetime point x in general. Furthermore, the transformation is non-Abelian because the symmetry group SU(3) is not Abelian.

Path integral formulation

An equivalent way of formulating the field theory is by writing amplitudes as integrals over the classical Grassmann $\overline{\psi}_a^\alpha(x)$, $\psi_a^\alpha(x)$ and c-fields $A_a^\mu(x)$. These kinds of integrals are referred to as path integrals. For QCD, the path integral representation of the vacuum expectation value relative to the theory's vacuum $|0\rangle$ has the general form

$$\begin{aligned} &\langle 0|\, T\{\ldots \hat{\Psi}_a^\alpha(x_i) \ldots \hat{A}_b^\mu(x_j) \ldots\} \,|0\rangle \\ &\qquad = \frac{\int \mathcal{D}\overline{\psi}\mathcal{D}\psi\mathcal{D}A\mathcal{D}[\ldots]\, \mathrm{e}^{\mathrm{i}S + \mathrm{i}S'} \ldots \psi_a^\alpha(x_i) \ldots A_a^\mu(x_j) \ldots}{\int \mathcal{D}\overline{\psi}\mathcal{D}\psi\mathcal{D}A\mathcal{D}[\ldots]\, \mathrm{e}^{\mathrm{i}S + \mathrm{i}S'}} \quad , \end{aligned} \tag{2.1}$$

where T is the time-ordering operator putting the operators in decreasing time order from left to right. The exponential is the sum of the QCD action $S(\overline{\psi}, \psi, A)$ and additional terms summarized in S'. These terms include auxiliary fields, denoted ghost fields, which are a consequence of gauge fixing. This is because the path integral can formally be derived starting with the canonically quantized theory which has a gauge-fixed Hamiltonian $\hat{H}$. The operator $\hat{H}$ then gives rise to the action S but also due to its gauge-fixed form it introduces the ghost fields in S'. The ghost fields are not physical and do

not correspond to any additional particles in the theory. They are only a consequence of writing the gauge-fixing conditions as an exponential of a function. Gauge fixing can directly be imposed on the level of the path integral by the method of Faddeev and Popov [36]. Because we consider lattice-field theories, the occurrence of ghost fields will not be important and consequently we skip a detailed description of them.

Renormalization

In general, Quantum Field Theories, suffer from UV-divergences, i.e. the Feynman amplitudes of the theory are divergent. This divergences occur because we consider arbitrarily large energies and momenta at which presumably the theory is not defined. If a field theory is renormalizable, the UV-divergences can be removed systematically such that finite and physical results are retained. This is done in two steps. First, the theory is regularized which means that some cutoff Λ is introduced rendering all computations finite. For example, in perturbation theory, we could choose dimensional regularization where all integrals over momenta in $d = 4$ dimensions are replaced with integrals of dimension $d = 4 - \varepsilon$ with $\varepsilon > 0$. Then, all results are finite as long as $\varepsilon > 0$. In the next section, when we discuss Lattice QCD, we regularize the theory by introducing a finite lattice spacing a defining the smallest distance between spacetime points. This gives effectively a momentum cutoff $\Lambda = a^{-1}$ inversely related to the lattice spacing a.

However, to obtain physical results, the cutoff must ultimately be removed ($\Lambda \to \infty$, $\varepsilon \to 0$ or $a \to 0$) which reintroduces the divergences. Hence, the second step is to renormalize amplitudes before removing the cutoff and consequently to define a specific limit for $\Lambda \to \infty$, $\varepsilon \to 0$ or $a \to 0$ such that the renormalized quantities remain finite and yield physical results. To this end, the bare parameters $g_0(\Lambda)$ and $m(\Lambda)$ are taken to be functions of the cutoff Λ (now representing a general cutoff) and the fields are scaled accordingly:

$$\hat{\Psi}^{\alpha}_{\mathrm{R},a}(x) = \frac{1}{\sqrt{Z_2(\Lambda)}}\hat{\Psi}^{\alpha}_{a}(x) \qquad \text{and} \qquad \hat{A}^{\mu}_{\mathrm{R},a}(x) = \frac{1}{\sqrt{Z_3(\Lambda)}}\hat{A}^{\mu}_{a}(x)$$

which defines the renormalized Feynman amplitudes

$$\langle 0|\, T\{\ldots \hat{\Psi}^{\alpha}_{\mathrm{R},a}(x_i)\ldots \hat{A}^{\mu}_{\mathrm{R},b}(x_j)\ldots\}\,|0\rangle\ .$$

The rescaled fields are the renormalized fields whereas the original fields of the Lagrangian are the bare fields. The factors $Z_i(\Lambda)$ are referred to as field-strength renormalizations. They also depend on the cutoff Λ and diverge $Z_i(\Lambda) \to \infty$ in general when $\Lambda \to \infty$. However, they diverge in the way necessary to render the renormalized amplitudes finite in the limit $\Lambda \to \infty$. Importantly, this shows that the UV-divergences are compensated by simply dividing the amplitudes with an infinite constant. The physics of the theory is then encoded in the functional dependence of the renormalized amplitudes, e.g. the positions of poles in momentum space give the masses of the one-particle states of the theory.

The cutoff dependences $g_0(\Lambda)$, $m(\Lambda)$ and $Z_i(\Lambda)$ are set by a specific renormalization scheme. In general, once the theory is regularized, a set of renormalization conditions is imposed which fixes $g_0(\Lambda)$, $m(\Lambda)$ and $Z_i(\Lambda)$. These conditions define what we expect from a physical theory. In setting the conditions, an arbitrary scale μ is chosen at which the renormalized parameters $g_\mathrm{R}(\mu)$ and $m_\mathrm{R}(\mu)$ are defined and set as part of the conditions. Then, the field-strength renormalizations $Z_i(\Lambda, \mu)$ also become μ-dependent. However, the physics of the theory cannot depend on the arbitrary choice of μ. Therefore, the renormalized parameters are proportional to the bare parameters which are independent of μ:

$$g_0(\Lambda) = c_g(\mu, \Lambda) g_\mathrm{R}(\mu) \qquad \text{and} \qquad m(\Lambda) = c_m(\mu, \Lambda) m_\mathrm{R}(\mu)$$

This implies the differential equations

$$\mu \frac{\mathrm{d}}{\mathrm{d}\mu} g_\mathrm{R} = \left(- \frac{\mu}{c_g} \frac{\mathrm{d}c_g}{\mathrm{d}\mu} \right) g_\mathrm{R} \qquad \text{and} \qquad \mu \frac{\mathrm{d}}{\mathrm{d}\mu} m_\mathrm{R} = \left(- \frac{\mu}{c_m} \frac{\mathrm{d}c_m}{\mathrm{d}\mu} \right) m_\mathrm{R} \,.$$

As a consequence, the integration constants Λ_QCD and M of both equations set the theory in a specific renormalization scheme. After setting up the differential equations at some finite Λ, we can infer the differential equation for $\Lambda \to \infty$.

For QCD, the first equation can be written as

$$\mu \frac{\mathrm{d}}{\mathrm{d}\mu} g_\mathrm{R} = \beta(g_\mathrm{R})$$

with the β-function $\beta(g_\mathrm{R})$ which depends on the chosen renormalization scheme. The β-function of QCD is negative such that $g_\mathrm{R}(\mu) \to 0$ for $\mu \to \infty$, i.e. QCD is an asymptotically free theory [10, 11].

Thermal field theory

The path integral can also be used to derive the thermodynamic description of QCD by computing the grand-canonical partition function

$$Z = \mathrm{tr}\left(\mathrm{e}^{-\beta \hat{H} + \beta \mu \hat{N}} \right) \tag{2.2}$$

with the inverse temperature $\beta = 1/T$, the net-quark number operator $\hat{N}$ and the chemical potential μ. The net-quark number operator counts quarks positively whereas antiquarks are counted negatively. Note that the field theory is defined on the whole space and not on a finite volume. Therefore, the partition function Z, as it stands, is only of formal nature because it is actually infinite and not well-defined. The proper way to define thermodynamic observables is to first define some finite volume V on which we consider the thermodynamic description and then to compute densities of observables, like the energy density, before we take the thermodynamic limit $V \to \infty$. Ignoring that Equation (2.2) is ill-defined, we compute the path integral representation of Z [37, 38]:

$$Z = \int \mathcal{D}\overline{\psi} \mathcal{D}\psi \mathcal{D}A \mathcal{D}[...] \, \exp\left(- \int_0^\beta \mathrm{d}\tau \int \mathrm{d}^3x \, (\mathcal{L}_\mathrm{E} - \mu \overline{\psi} \gamma_4 \psi + \mathcal{L}'_\mathrm{E}) \right),$$

where again the gauge-fixing terms are summarized in the Lagrangian density $\mathcal{L}'_{\mathrm{E}}$. There are, however, striking differences compared to the path integral of Equation (2.1) because we consider the Boltzmann factor $\mathrm{e}^{-\beta\hat{H}}$ instead of the time-evolution operator $\mathrm{e}^{-\mathrm{i}t\hat{H}}$. First, the Lagrangian density $\mathcal{L}$ is replaced with the Euclidean Lagrangian density

$$\mathcal{L}_{\mathrm{E}} = \overline{\psi}(\not{D} + m)\psi + \frac{1}{4}\sum_{a=1}^{8} F_{a,\mu\nu}F_a^{\mu\nu}\,,$$

where all gamma matrices γ^μ are now replaced with Euclidean gamma matrices fulfilling $[\gamma_\mu, \gamma_\nu]_+ = 2\delta_{\mu\nu}$, the Minkowski metric $g^{\mu\nu}$ is replaced with the Euclidean metric $\delta_{\mu\nu}$ and the signs in front of the couplings are flipped. Second, the direction of time is replaced with the Euclidean direction of time and, consequently, we also change the counting of spacetime indices to $\mu = 1, 2, 3, 4$, where $\mu = 4$ is the direction of Euclidean time. In deriving the path integral, the inverse temperature β leads to a compactification of the time direction, i.e. the direction of time is now integrated from 0 to β and bosonic (fermionic) fields are taken to be (anti-)periodic:

$$A_a^\mu(0,\vec{x}) = A_a^\mu(\beta,\vec{x})\,, \quad \overline{\psi}_a^\alpha(0,\vec{x}) = -\overline{\psi}_a^\alpha(\beta,\vec{x}) \quad \text{and} \quad \psi_a^\alpha(0,\vec{x}) = -\psi_a^\alpha(\beta,\vec{x})\,.$$

Finally, the net-quark number operator yields an additional term $\mu\overline{\psi}\gamma_4\psi$.

2.4 Lattice QCD

We have seen that QFTs suffer from UV-divergences and must be regularized and renormalized appropriately. One particular renormalization scheme, which we consider in this thesis exclusively, is given by lattice-gauge theories. A small-distance cutoff for the spacetime is introduced, i.e. the smallest distance of spacetime points is set to be given by the spacing a. Formally, we define the theory on a four-dimensional hyper-cubical periodic lattice of extent N_μ in the μ-th direction. Each site $x = (x_1, x_2, x_3, x_4) = (\vec{x}, x_4)$ of the lattice is given by coordinates $x_\mu \in \{0, \ldots, N_\mu - 1\}$. On a periodic lattice, two sites x and y are called neighboring (in the μ-th direction) if and only if it exists exactly one direction μ with

$$|x_\mu - y_\mu| = 1 \qquad \text{or} \qquad |x_\mu - y_\mu| = N_\mu - 1$$

and $y_\nu = x_\nu$ in all other directions $\nu \neq \mu$. For neighboring sites x and y, we define the directed link $\langle x, y\rangle$ which starts at x and ends at y. We put the lattice on a four-dimensional torus by associating the distance a_μ between sites which are neighboring in the μ-th direction. Here, we consider the special case of the spatial directions to have the same lattice spacing $a = a_1 = a_2 = a_3$ and extent $N = N_1 = N_2 = N_3$ whereas the lattice spacing a_4 and extent N_4 in the Euclidean direction of time might be different.

Now, the regularization is done by discretizing the Euclidean action

$$S_{\mathrm{E}} = -\int_0^\beta \mathrm{d}\tau \int \mathrm{d}^3x \left(\mathcal{L}_{\mathrm{E}} - \mu\overline{\psi}\gamma_4\psi\right)$$

on the finite torus. There is some arbitrariness to the discretization and some subtleties which must be considered. Let us first state the discretized path integral formulation in its full form before we explain its different parts. Here, we choose to discretize the gauge action by the Wilson plaquette action ([39–41])

$$S_{\mathrm{G}}(U) = \frac{a}{a_4}\frac{2}{g_0^2}\sum_{x,k}\mathrm{ReTr}\, U_{\partial p_{x,k4}} + \frac{a_4}{a}\frac{2}{g_0^2}\sum_{x,k<m}\mathrm{ReTr}\, U_{\partial p_{x,km}} \tag{2.3}$$

and the fermionic action with the Hasenfratz-Karsch action of Wilson fermions ([41–43])

$$\begin{aligned} S_{\mathrm{F}}(U,\overline{\psi},\psi) = {} & s(a_4,a)\sum_x\left[\overline{\psi}_x\Lambda^+_{x,4}\psi_{x+\hat{4}} + \overline{\psi}_{x+\hat{4}}\Lambda^-_{x,4}\psi_x\right] \\ & + \frac{a_4}{a}s(a_4,a)\sum_{x,k}\left[\overline{\psi}_x\Lambda^+_{x,k}\psi_{x+\hat{k}} + \overline{\psi}_{x+\hat{k}}\Lambda^-_{x,k}\psi_x\right] - \sum_x\overline{\psi}_x\psi_x \end{aligned} \tag{2.4}$$

with

$$\begin{aligned} \Lambda^+_{x,\mu} &= ((1-\delta_{\mu,4}) + \mathrm{e}^{+a_4\mu}\delta_{\mu,4})(1-\gamma_\mu)U_{\langle x,x+\hat{\mu}\rangle}\,, \\ \Lambda^-_{x,\mu} &= ((1-\delta_{\mu,4}) + \mathrm{e}^{-a_4\mu}\delta_{\mu,4})(1+\gamma_\mu)U^\dagger_{\langle x,x+\hat{\mu}\rangle}\,, \end{aligned}$$

and

$$s(a_4,a) = \frac{1}{2a_4(m+3a^{-1})+2}\,.$$

The partition function now reads

$$Z = \int \mathcal{D}U\mathcal{D}\overline{\psi}\mathcal{D}\psi\,\mathrm{e}^{S_{\mathrm{G}}(U)+S_{\mathrm{F}}(U,\overline{\psi},\psi)}\,,$$

and expectation values of observables are given by

$$\langle\mathcal{O}(U,\overline{\psi},\psi)\rangle = \frac{1}{Z}\int \mathcal{D}U\mathcal{D}\overline{\psi}\mathcal{D}\psi\,\mathcal{O}(U,\overline{\psi},\psi)\mathrm{e}^{S_{\mathrm{G}}(U)+S_{\mathrm{F}}(U,\overline{\psi},\psi)}\,.$$

The inverse temperature β, which enters over the integral bounds of the Euclidean time direction in the continuum, now enters via the lattice extent in direction of Euclidean time: $\beta = N_4 a_4$.

First, we consider the discretization of the fields. The fermion fields are simply defined on the lattice sites x, i.e. we associate Grassmann generators $\overline{\psi}_x^{a,\alpha}$ and $\psi_x^{a,\alpha}$ with each value of the color index a, Dirac index α and site x. Then, the integral measure over the fermionic fields is given by successively conducting Berezin integrals in the order

$$\mathcal{D}\overline{\psi}\mathcal{D}\psi = \prod_x\prod_{a,\alpha}\mathrm{d}\overline{\psi}_x^{a,\alpha}\mathrm{d}\psi_x^{a,\alpha}\,.$$

The gauge fields are defined by associating elements $U_{\langle x,y\rangle} \in \mathrm{SU}(3)$ of the gauge group SU(3) with links $\langle x,y\rangle$ of the lattice such that $U_{\langle x,y\rangle} = U^\dagger_{\langle y,x\rangle}$ by definition. Hence, associating an element $U_{\langle x,x+\hat{\mu}\rangle}$ with every positively orientated link $\langle x,x+\hat{\mu}\rangle$ defines a gauge configuration $U = \{\ldots, U_{\langle x,x+\hat{\mu}\rangle},\ldots\}$.

The integration over all gauge configurations U is defined by integrating every link variable $U_{\langle x,x+\hat{\mu}\rangle}$ separately:

$$\mathcal{D}U = \prod_{\langle x,x+\hat{\mu}\rangle} \mathrm{d}U_{\langle x,x+\hat{\mu}\rangle}\,,$$

where $\mathrm{d}U_{\langle x,x+\hat{\mu}\rangle}$ is the left-invariant Haar measure of $\mathrm{SU}(3)$ normalized to one:

$$\int \mathrm{d}U_{\langle x,x+\hat{\mu}\rangle} = 1\,.$$

Furthermore, we use a vector and matrix notation in the discretized action such that all color and Dirac indices are suppressed. The action also implicitly contains the antiperiodicity of the fermionic fields in direction of Euclidean time by defining

$$\overline{\psi}_{(\vec{x},N_4)} = -\overline{\psi}_{(\vec{x},0)} \qquad \text{and} \qquad \psi_{(\vec{x},N_4)} = -\psi_{(\vec{x},0)}\,.$$

On the lattice, we define plaquettes $p_{x,\mu\nu}$ which are orientated minimal rectangles starting at x, following along the direction μ and then ν such that $\partial p_{x,\mu\nu}$ is the orientated boundary of the rectangle. For each plaquette $p_{x,\mu\nu}$, we associate the value

$$U_{\partial p_{x,\mu\nu}} = U_{\langle x,x+\hat{\mu}\rangle} U_{\langle x+\hat{\mu},x+\hat{\mu}+\hat{\nu}\rangle} U_{\langle x+\hat{\mu}+\hat{\nu},x+\hat{\nu}\rangle} U_{\langle x+\hat{\nu},x\rangle}$$

which is just the product of gauge variables along the plaquette's boundary.

There are many ways to discretize the action and not all choices are physically sensible. For example, discretizing the fermionic action yields additional poles in the fermion propagator which manifest as additional fermionic particles entering the theory and interacting via the gauge fields [38, 44]. These particles are lattice artifacts influencing computations done within the theory. This problem is referred to as the fermion doubling problem. Wilson's formulation of fermions avoids this problem by making the additional fermionic degrees of freedom infinitely heavy for vanishing lattice spacings $a_4, a \to 0$ [45]. The influence of the additional particles vanishes in the continuum limit. Another well-established approach are staggered fermions ([46]) which we are not using in this thesis. Removing fermion doublers from the theory, however, breaks chiral symmetry on the lattice and actually the removal of fermion doublers and chiral symmetry on the lattice are shown to be incompatible by the famous Nielsen-Ninomiya theorem [47]. Furthermore, the naive discretization of the term $\mu\overline{\psi}\gamma_4\psi$ as $\mu\overline{\psi}_x\gamma_4\psi_x$ creates additional divergences when taking the continuum limit $a_4, a \to 0$ [42]. The chemical potential is properly formulated on the lattice via the Hasenfratz-Karsch action (2.4) which, as we are going to see in the next chapter, is a natural consequence of considering the lattice action as the path-integral formulation of a quantum-mechanical system defined on the spatial lattice.

The actions S_G and S_F are invariant under gauge transformations

$$\begin{aligned}
\overline{\psi}_x &\longrightarrow \overline{\psi}_x \Omega_x\,,\\
\psi_x &\longrightarrow \Omega_x^\dagger \psi_x\,,\\
U_{\langle x,y\rangle} &\longrightarrow \Omega_x^\dagger U_{\langle x,y\rangle} \Omega_y\,,
\end{aligned}$$

where a gauge transformation Ω is the association of a group element $\Omega_x \in \mathrm{SU}(3)$ for every site x of the lattice. This invariance allows to choose a certain gauge without influencing any expectation values as long as the observables in question are also gauge-invariant. We are particularly interested in the maximal-temporal gauge, where all timelike links are set to one except between the zeroth and first layer of Euclidean time. The explicit construction of the maximal-temporal gauge is given as follows. Consider the expectation value of a gauge-invariant observable $\mathcal{O}(U, \overline{\psi}, \psi)$. Then, gauge invariance implies

$$\langle \mathcal{O} \rangle = \frac{1}{Z} \int \mathcal{D}U \mathcal{D}\overline{\psi} \mathcal{D}\psi \, \mathcal{O}(U', \overline{\psi}', \psi') \mathrm{e}^{S_\mathrm{G}(U') + S_\mathrm{F}(U', \overline{\psi}', \psi')} \,,$$

where the fields $U' = \Omega^\dagger(U) U \Omega(U)$, $\overline{\psi}' = \overline{\psi}\Omega(U)$ and $\psi' = \Omega^\dagger(U)\psi$ are gauge-transformed fields and the gauge transformation $\Omega(U)$ depends on the gauge configuration U. Consider now the gauge transformation

$$\Omega_{(\vec{x},\tau+1)} = U^\dagger_{\langle(\vec{x},\tau),(\vec{x},\tau+1)\rangle} \Omega_{(\vec{x},\tau)}$$

for all $\tau \in \{1, \ldots, N_4 - 1\}$, $\Omega_{(\vec{x},1)} = \mathbb{1}$ and $\Omega_{(\vec{x},N_4)} = \Omega_{(\vec{x},0)}$ due to periodic boundary conditions. The recursion relation implies

$$\Omega_{(\vec{x},0)} = U^\dagger_{\langle(\vec{x},N_4-1),(\vec{x},0)\rangle} U^\dagger_{\langle(\vec{x},N_4-2),(\vec{x},N_4-1)\rangle} \cdots U^\dagger_{\langle(\vec{x},1),(\vec{x},2)\rangle} \,.$$

A timelike gauge link is now transformed as

$$U_{\langle(\vec{x},\tau),(\vec{x},\tau+1)\rangle} \longrightarrow \Omega^\dagger_{(\vec{x},\tau)} U_{\langle(\vec{x},\tau),(\vec{x},\tau+1)\rangle} \Omega_{(\vec{x},\tau+1)} \,.$$

The definition of Ω_x gives

$$\begin{aligned} \Omega^\dagger_{(\vec{x},\tau)} U_{\langle(\vec{x},\tau),(\vec{x},\tau+1)\rangle} \Omega_{(\vec{x},\tau+1)} &= \Omega^\dagger_{(\vec{x},\tau)} U_{\langle(\vec{x},\tau),(\vec{x},\tau+1)\rangle} U^\dagger_{\langle(\vec{x},\tau),(\vec{x},\tau+1)\rangle} \Omega_{(\vec{x},\tau)} \\ &= \mathbb{1} \end{aligned}$$

for $\tau \in \{1, \ldots, N_4 - 1\}$. However, we have

$$\begin{aligned} \Omega^\dagger_{(\vec{x},0)} U_{\langle(\vec{x},0),(\vec{x},1)\rangle} \Omega_{(\vec{x},1)} &= \Omega^\dagger_{(\vec{x},0)} U_{\langle(\vec{x},0),(\vec{x},1)\rangle} \\ &= U_{\langle(\vec{x},1),(\vec{x},2)\rangle} \ldots U_{\langle(\vec{x},N_4-1),(\vec{x},0)\rangle} U_{\langle(\vec{x},0),(\vec{x},1)\rangle} \end{aligned}$$

if $\tau = 0$. With this transformation, all timelike links except the ones between the time layers $\tau = 0$ and $\tau = 1$ are set to unity. The initial gauge transformation still leaves us with transformed fermionic and spatial gauge variables:

$$\begin{aligned} \overline{\psi}_x &\longrightarrow \overline{\psi}_x \Omega_x(U) \,, \\ \psi_x &\longrightarrow \Omega^\dagger_x(U) \psi_x \,, \\ U_{\langle x, x+\hat{k}\rangle} &\longrightarrow \Omega^\dagger_x(U) U_{\langle x, x+\hat{k}\rangle} \Omega_{x+\hat{k}}(U) \,. \end{aligned}$$

We first conduct the Berezin integrals and transform the fields according to

$$\overline{\psi}_x \longrightarrow \overline{\psi}_x \Omega^\dagger_x(U) \qquad \text{and} \qquad \psi_x \longrightarrow \Omega_x(U) \psi_x \,.$$

This removes the gauge transformations from the fermionic fields. Next, we integrate over the spatial gauge variables $U_{\langle x,x+\hat{k}\rangle}$. The gauge transformations $\Omega_x(U)$ only depend on timelike gauge variables and consequently we can use

$$\int \mathrm{d}U_{\langle x,x+\hat{k}\rangle}\, f(\Omega_x^\dagger(U) U_{\langle x,x+\hat{k}\rangle} \Omega_{x+\hat{k}}(U)) = \int \mathrm{d}U_{\langle x,x+\hat{k}\rangle}\, f(U_{\langle x,x+\hat{k}\rangle})$$

which is a consequence of ([48])

$$\int \mathrm{d}U\, f(U) = \int \mathrm{d}U\, f(GU) \qquad \text{and} \qquad \int \mathrm{d}U\, f(U) = \int \mathrm{d}U\, f(U^{-1})$$

with $G \in \mathrm{SU}(3)$. Finally, we have to conduct the integration over the timlike variables. In this case, we first integrate over $U_{\langle(\vec{x},0),(\vec{x},1)\rangle}$ and use the fact that the Haar measure is left-invariant. Then, actually, all timelike integrations except for $U_{\langle(\vec{x},0),(\vec{x},1)\rangle}$ drop out. We end with the lattice formulation gauge-fixed in maximal-temporal gauge.

Continuum limit

To get physical results, we have to state a proper renormalization scheme in which the cutoffs a_4 and a are taken to zero. We consider the isotropic case $a_4 = a$ and postpone the consideration of anisotropic lattices to the next chapter, where it becomes relevant. In the case $a_4 = a$, the action reduces to

$$S_{\mathrm{G}}(U) = \frac{2}{g_0^2} \sum_{x,\mu<\nu} \mathrm{ReTr}\, U_{\partial p_{x,\mu\nu}}$$

and

$$S_{\mathrm{F}}(U,\overline{\psi},\psi) = \kappa \sum_{x,\mu} \left[\overline{\psi}_x \Lambda^+_{x,\mu} \psi_{x+\hat{\mu}} + \overline{\psi}_{x+\hat{\mu}} \Lambda^-_{x,\mu} \psi_x\right] - \sum_x \overline{\psi}_x \psi_x\,,$$

where

$$\kappa = \frac{1}{2ma+8}$$

is the hopping parameter.

In this form, it is evident that the cutoff a does not enter explicitly into the lattice formulation and expectation values $\langle \mathcal{O}(U,\overline{\psi},\psi)\rangle$ are formulated in units of the lattice spacing a and are dimensionless. The theory is renormalized by considering the bare parameters $g_0(a)$ and $\kappa(a)$ to depend on the lattice cutoff a such that the continuum limit of a renormalized quantity $\mathcal{O}_{\mathrm{R}}(U,\overline{\psi},\psi)$ is given by

$$\mathcal{O}_{\mathrm{phys}}(T,L) = \lim_{\substack{a\to 0\\ N,N_4\to\infty}} \langle \mathcal{O}_{\mathrm{R}}(U,\overline{\psi},\psi)\rangle\,,$$

where the limit is taken such that the physical extent $L = Na$, the temperature $T = 1/(N_4 a)$ and $\mu/T = N_4(a\mu)$ are kept fixed [38]. This then defines QCD on a finite volume $V = L^3$ for which we can consider the thermodynamic limit $V \to \infty$. In general, the UV-divergences and therefore the renormalization scheme do not depend on the temperature T [37]. The renormalization conditions are set in the vacuum of QCD, i.e. we consider the zero-temperature limit in the infinite-volume limit.

We consider (renormalized) observables

$$H(r, a, g_0(a), \kappa(a))$$

which are defined at some scale r [49]. Then, the continuum limit of this observable is given by

$$\lim_{\substack{a\to 0 \\ N,N_4\to\infty}} H(r, a, g_0(a), \kappa(a)) = H_{\text{phys}}(r, L, T)\,.$$

The renormalization is taken at sufficiently large L and small temperatures T such that we approximate the vacuum of the theory. Near the continuum limit, all observables lose their a-dependence, and therefore

$$H(r, a, g_0(a), \kappa(a)) \approx H_{\text{phys}}(r) + \mathcal{O}(a)\,.$$

A typical renormalization scheme to fix $g_0(a)$ and $\kappa(a)$ is to consider a line of constant physics, where the renormalization conditions are given by fixing multiple observables $H(r, a, g_0(a), \kappa(a))$ at any cutoff a to their continuum values

$$H(r, a, g_0(a), \kappa(a)) = H_{\text{phys}}(r)$$

at the scale r [49, 50]. One might also consider the long-range behavior $r \to \infty$. Inverting the renormalization conditions then gives the dependence $g_0(a)$ and $\kappa(a)$ [49, 51]. Consider the case where we use $(ma)(a)$ instead of $\kappa(a)$. Then, we have the renormalization-group equations

$$a\frac{\partial H}{\partial a} + a\frac{\mathrm{d}g_0}{\mathrm{d}a}\frac{\partial H}{\partial g_0} + a\frac{\mathrm{d}(ma)}{\mathrm{d}a}\frac{\partial H}{\partial (ma)} = a\frac{\mathrm{d}H}{\mathrm{d}a} = 0\,.$$

Similar to continuum physics, we now have the lattice β-function $\beta_{\text{lat}}(g_0)$ with

$$a\frac{\mathrm{d}g_0}{\mathrm{d}a} = \beta_{\text{lat}}(g_0)\,.$$

At small couplings, the first two non-vanishing orders of the weak-coupling expansion of $\beta_{\text{lat}}(g_0)$ are identical to the expansion coefficients of $\beta(g_0)$ from the continuum [49, 50]. Furthermore, these two coefficients are independent of the renormalization scheme. Renormalizing the theory at $g_0 \approx 0$ becomes universal such that continuum physics does not depend on the choice of the renormalization scheme. We refer the reader to [49] for a more detailed consideration on this topic. For the bare quark mass, the continuum limit is reached at $(ma)(a) \to 0$ if $a \to 0$ because the bare quark mass $m(g_0)$ vanishes towards $g_0 \to 0$ [15, 50]. This implies $\kappa(a) \to 1/8$ if $a \to 0$. That κ becomes smaller than $1/6$ becomes important in the next chapter when we consider the transfer-matrix formulation.

An example of how renormalization is done in practice can be found in [52–54]. They consider $(2+1)$-flavor QCD with the light quark mass m_{ud} and the strange quark mass m_{s}. The renormalization conditions are given by setting the dimensionless ratios $m_{\text{K}}/f_{\text{K}}$, m_{K}/m_π between the kaon mass m_{K}, the kaon decay constant f_{K} and the pion mass m_π to their experimental values in the

zero-temperature limit. This then defines the dependence of $(m_{\mathrm{ud}}a)(g_0)$ and $(m_{\mathrm{s}}a)(g_0)$. Setting the scale with the physical value of an observable, which is the third renormalization condition, then defines $a(g_0)$. Near the continuum, inverting $a(g_0)$ gives the full renormalization scheme for $g_0(a)$, $(m_{\mathrm{ud}}a)(a)$ and $(m_{\mathrm{s}}a)(a)$.

Spontaneous symmetry breaking

Spontaneous symmetry breaking describes the phenomenon in which a system prefers maintaining certain states against the symmetries of the underlying dynamics. This phenomenon is an effect of the infinite-volume and most famously known from spin systems. We base the following line of argument partly on [22, 38].

Let us formalize the concept of spontaneous symmetry breaking by the example of the two-dimensional Ising model. The action is just given by the nearest-neighbor interactions between spins $\sigma_i \in \{-1, 1\}$ placed at sites i of the lattice: $S(\{\sigma_i\}) = J\sum_{\langle i,j\rangle} \sigma_i\sigma_j$, $J > 0$. Here, the action is invariant under a collective change of the sign $\{\sigma_i\} \to \{-\sigma_i\}$ for a spin configuration $\{\sigma_i\}$. This is an invariance under $\mathbb{Z}_2$-transformations. The magnetization is defined as

$$m(\{\sigma_i\}) = \frac{1}{N_{\mathrm{s}}}\sum_i \sigma_i\,.$$

Contrary to the action, the magnetization is not invariant under symmetry transformations: $m(\{-\sigma_i\}) = -m(\{\sigma_i\})$. Because m is not invariant but the action is invariant under a symmetry transformation, the expectation value $\langle m\rangle = 0$ vanishes for all parameters and finite volumes N_{s}. The probability to observe m or $-m$ is identical due to the symmetry. Spontaneous symmetry breaking is the phenomena that an observable which vanishes due to its missing invariance towards the symmetry can gain a non-vanishing expectation value in the infinite volume limit. The infinite volume limit is capable of maintaining a symmetry-broken state, i.e. the probability distribution of the observable m becomes skewed towards preferred values in the infinite volume limit despite the fact that the dynamics do not possess such a preference. To be more precise, we first introduce an explicit symmetry breaking parameter h, which for the Ising model is just an external field. The invariance of the action under $\mathbb{Z}_2$ is assumed to vanish if $h > 0$, and, for $h = 0$, the original action is restored. Then, we explicitly break the symmetry with $h > 0$, take the infinite volume limit and, afterwards, restore the symmetry of the action by taking the limit $h \to 0$:

$$\langle m\rangle_\infty = \lim_{h\to 0}\lim_{N_{\mathrm{s}}\to\infty}\langle m\rangle_h\,.$$

Spontaneous symmetry breaking is given if $\langle m\rangle_\infty \neq 0$ at a certain parameter of the theory. In the case of the two-dimensional Ising model, there is a well-known second-order phase transition at the inverse temperature $\beta_{\mathrm{c}} = 1/T_{\mathrm{c}} = \sinh^{-1}(1)/(2J)$ [55]. For temperatures $T > T_{\mathrm{c}}$ above the critical point, the magnetization $\langle m\rangle_\infty = 0$ vanishes. This is the non-broken, symmetric phase. For temperatures $T < T_{\mathrm{c}}$ below the critical point, we have $\langle m\rangle_\infty > 0$ which marks the broken phase.

Naturally, we can ask ourselves to which extent it is possible to adapt this concept to QCD? We have seen that the action of the theory is invariant under local gauge transformations $\Omega(x)$. Hence, we might think of spontaneous symmetry breaking in terms of the local gauge transformations. However, Elitzur's theorem states that local symmetries cannot break spontaneously [22, 56]. Any observable $\mathcal{O}$ which is not gauge-invariant has to vanish $\langle\mathcal{O}\rangle = 0$ for all parameters, and this especially persists if we introduce a symmetry breaking parameter first and take the limit as in the case of the Ising model: $\langle\mathcal{O}\rangle_\infty = 0$. The only possibility of having a non-vanishing expectation value is to consider gauge-invariant observables. Elitzur's theorem prevents spontaneous symmetry breaking for local gauge symmetries, but symmetry breaking is still possible for a global symmetry and gauge-invariant observables which are not invariant under the global symmetry.

In the absence of fermions, the action of the theory reduces to the Wilson plaquette part

$$S_\mathrm{G}(U) = \frac{2}{g_0^2}\sum_{x,\mu<\nu}\mathrm{ReTr}\,U_{\partial p_{x,\mu\nu}}\,.$$

This action is not only gauge-invariant but it possesses a global symmetry under transformations with the center $\mathrm{Z}_3 = \{\mathbb{1}, \mathrm{e}^{\frac{2\pi}{3}\mathrm{i}}\mathbb{1}, \mathrm{e}^{\frac{4\pi}{3}\mathrm{i}}\mathbb{1}\}$ of $\mathrm{SU}(3)$ [22, 38, 57–60]. The transformation is defined as follows. Consider an element $z \in \mathrm{Z}_3$. We choose a time layer τ and multiply all timelike links between the τ-th and $(\tau+1)$-th layer of time with the center element z:

$$U_{\langle(\vec{x},\tau),(\vec{x},\tau+1)\rangle} \longrightarrow z\cdot U_{\langle(\vec{x},\tau),(\vec{x},\tau+1)\rangle}\,.$$

Because the Haar measure is invariant under left multiplications with elements of the group, the partition function does not change under this transformation. Importantly, the action $S_\mathrm{G}(U)$ also stays invariant. Every link which is multiplied with z effects the plaquette variables of timelike plaquettes between both layers of time. However, all these effects cancel each other. To see this, consider a timelike plaquette $p_{x,k4}$ with $k \in \{1,2,3\}$ and $x = (\vec{x},\tau)$. The plaquette variable is

$$U_{\partial p_{x,k4}} = U_{\langle x,x+\hat{k}\rangle}U_{\langle x+\hat{k},x+\hat{k}+\hat{4}\rangle}U_{\langle x+\hat{k}+\hat{4},x+\hat{4}\rangle}U_{\langle x+\hat{4},x\rangle}\,.$$

which contains two timelike links. One link points in positive time direction and one link points in negative time direction. Therefore, the positively (negatively) orientated link is multiplied with z ($z^\dagger$) under a center transformation with $z \in \mathrm{Z}_3$:

$$U_{\partial p_{x,k4}} \longrightarrow \ldots\cdot\, zU_{\langle x+\hat{k},x+\hat{k}+\hat{4}\rangle}\,\cdot\ldots\cdot\, z^\dagger U_{\langle x+\hat{4},x\rangle}\,.$$

Because all center elements commute with all elements of $\mathrm{SU}(3)$, we can permute z and $z^\dagger$ to the front of the expression such that $zz^\dagger = \mathbb{1}$, and the plaquette variable $U_{\partial p_{x,k4}}$ remains unchanged under the center transformation. Hence, the action $S_\mathrm{G}(U)$ is indeed invariant under center transformations. Note, however, that the inclusion of fermions breaks the center symmetry explicitly because of the occurrence of gauge variables in the bilinear forms of the fermion action.

For the phenomena of spontaneous symmetry breaking, we still need an observable which is not invariant under the center symmetry. As we have seen, the observable has additionally to be gauge-invariant due to Elitzur's theorem. An observable which has all these properties is the Polyakov loop

$$L_{\vec{x}} = \mathrm{tr}\left(\prod_{\tau=0}^{N_4-1} U_{\langle(\vec{x},\tau),(\vec{x},\tau+1)\rangle}\right),$$

where the product is ordered from left to right for increasing times τ [22, 38, 58, 59]. The product of gauge variables describes a straight path winding around the positive Euclidean time direction. Therefore, the Polyakov loop is characterized by the spatial site $\vec{x}$. The Polyakov loop $L_{\vec{x}}$ transforms as

$$L_{\vec{x}} \longrightarrow zL_{\vec{x}}$$

under a center transformation because exactly one timelike link of the loop is multiplied with the center element z. As for the magnetization $\langle m\rangle$ of the Ising model, the expectation value of the Polyakov loop vanishes due to the center symmetry:

$$\langle L_{\vec{x}}\rangle = \frac{1}{Z}\int \mathcal{D}U\,(zL_{\vec{x}})\mathrm{e}^{S_\mathrm{G}(U)} = z\langle L_{\vec{x}}\rangle$$

which implies $\langle L_{\vec{x}}\rangle = 0$. Introducing a symmetry breaking part into the action allows to investigate the phenomena of spontaneous symmetry breaking for pure SU(3)-gauge theories. Such a symmetry breaking term could just be the fermionic part of the action at finite quark masses. The symmetry is then restored by taking the infinite mass limit.

The above argument defines spontaneous symmetry breaking for global Z_3-transformations on the lattice. Nevertheless, we are interested in possible phase transitions in the continuum limit $a \to 0^+$. Using the Polyakov loop as an order parameter of phase transitions comes with a major obstacle in the continuum limit. The expectation value $\langle L_{\vec{x}}\rangle$ of the Polyakov loop vanishes in continuum limit due to an UV-divergent free energy $F = -T\ln\langle L_{\vec{x}}\rangle \approx \mathcal{O}(a^{-1})$ for $a \to 0$ [61]. Therefore, for the Polyakov loop to retain any meaning in the continuum limit, it has to be renormalized properly [62–68].

Confinement and deconfinement in the absence of fermions

Spontaneous symmetry breaking has been studied intensively for pure SU(N)-gauge theories. First analyses of a phase transition for pure gauge theories were made in [57, 58, 60, 69, 70] . It was conjectured early on that the critical behavior of the symmetry breaking transition of a $(d+1)$-dimensional pure SU(N)-gauge theory is identical to the corresponding d-dimensional $\mathbb{Z}_N$-spin theory [58]. Therefore, the argument implies a first-order transition for SU(3) because the corresponding spin system is a three states Potts model in three dimensions which is known to possess a first-order transition [71]. Indeed pure SU(3) gauge theory exhibits a first-order transition as it has been demonstrated in [62, 65, 68, 72–74] and references therein.

The global center symmetry is explicitly broken once dynamical fermions are included into the theory. At sufficiently low quark masses, the corresponding non-analytic behavior vanishes, and the expectation value $\langle L_{\vec{x}} \rangle$ of the Polyakov loop $L_{\vec{x}}$ becomes a smooth function of temperature [16, 18, 21, 53, 67, 75, 76].

The spontaneous symmetry breaking of pure gauge theory is interpreted as a confinement-deconfinement transition. Below the critical temperature $T < T_c$, the system is in the confined and symmetric phase. Above $T > T_c$, the system goes into a deconfined and symmetry-broken phase. This terminology of confinement and deconfinement stems from interpreting the expectation value of the Polyakov loop $\langle L_{\vec{x}} \rangle$ as the insertion of an infinitely heavy charge at the spatial site $\vec{x}$ [22, 38, 57, 69, 77]. A very intriguing interpretation is given by [77]. They consider the transfer-matrix formulation of Lattice QCD in which the path integral of Lattice QCD is a consequence of a quantum-mechanical system defined on the spatial lattice. A detailed description of the transfer-matrix formalism is given in Chapter 3.

Intuitively, the confined phase of a non-Abelian gauge theory is understood to be driven by squeezing color-electric fields into narrow, cylindrical flux tubes between a static quark and antiquark [22]. Therefore, the energy $E = \sigma d$ of the field increases linearly and proportional to the string tension σ with increasing distance d between the charges. This is the physical intuition for the linear behavior of the quark-antiquark potential in the confined phase. The squeezing of chromo-electric fields into tubes has been confirmed in various lattice studies. Here, we refer to [78–81] and the references therein.

The interpretation of the confinement-deconfinement transition explicitly relies on the behavior of static charges and the existence of a spontaneous $\mathbb{Z}_3$-symmetry breaking. Consequently, this notion of confinement and deconfinement breaks down once dynamical fermions are included. The expectation value $\langle L_{\vec{x}} \rangle$ of the Polyakov loop smoothens out and the static quark-antiquark potential flattens out at all temperatures due to string breaking. The charges get screened by dynamical fermions. One of the main goals of this thesis is to suggest an observable which coincides with the symmetry breaking transition but does not rely on it and extends to all quark masses, see Section 5.3. Such an observable would allow the unambiguous definition of confinement and deconfinement at all parameters of the theory.

Chapter 3

Transfer-matrix formulation

In this chapter, we discuss the transfer-matrix formulation for Lattice QCD with one flavor of Wilson fermions. The formulation describes the path integral of Lattice QCD (2.4) as the consequence of some quantum-mechanical system defined on the three-dimensional spatial lattice. This quantum-mechanical view allows to define important key concepts used in the later chapters. Primarily, we can define a notion of creation and annihilation operators of quarks and antiquarks at spatial sites and the concept of center-electric fluxes and charges together with a local $\mathbb{Z}_3$-Gauss law. Both concepts are essential when we construct the ensembles of fixed quark numbers in a subvolume and investigate the concept of percolation of fluxes in QCD. The construction itself is based on [41, 77, 82–86]. The dynamics of the quantum-mechanical system are driven by a Hamiltonian $\hat{H}$. The path integral of Lattice QCD is derived by discretizing the Boltzmann factor $\mathrm{e}^{-\beta\hat{H}}$ in Euclidean time and replacing it with $(\hat{T}_{a_4})^{N_4}$, where N_4 is the number of time layers, $a_4 = \beta/N_4$ is the spacing in Euclidean time, β is the inverse temperature, and $\hat{T}_{a_4}$ is the transfer operator. We discuss two different choices for $\hat{T}_{a_4}$. The first choice is the one made by Lüscher [83] which is a strictly positive operator $\hat{T}_{a_4}$. Nevertheless, as we are going to see in the subsequent chapters, this choice is inconvenient for our considerations. Hence, we construct a very specific transfer operator which serves our purposes. The price that we pay for our choice of $\hat{T}_{a_4}$ is the loss of hermiticity at $a_4 > 0$. However, the operator still yields a Hamiltonian $\hat{H}$ in the Euclidean time continuum and gives the path integral of Lattice QCD for $a_4 > 0$. For reasons which become clear later on, the operator of Lüscher is named the symmetric transfer operator, and our operator is named the asymmetric transfer operator. Such a quantum-mechanical approach of Lattice QCD via some Hamiltonian $\hat{H}$ was first described by [46] and is typically also referred to as the Hamiltonian approach. A mathematically rigorous description of the Hamiltonian approach based on operator algebras has been formulated by [87–89]. Hence, the transfer-matrix approach describes the transition between the path integral formulation and the Hamiltonian approach via the Euclidean time continuum [77].

The structure of the chapter is as follows. In Section 3.1, we describe the fundamental concepts of the quantum-mechanical view. We define the Hilbert

space, the physical Hilbert space and spatial gauge transformations. We also state the partition function which implies the path integral of Lattice QCD upon discretization of Euclidean time and explain the crucial role of gauge invariance in deriving the path integral. Additionally, we also demonstrate how gauge invariance yields a local Gauss law. This is then taken as the basis for formulating the local, Abelian $\mathbb{Z}_3$-Gauss law and the concept of center charges and center-electric fluxes. We base the treatise of Gauss's law, the $\mathbb{Z}_3$-law, center charges and center-electric fluxes on [77, 87–89].

In Section 3.2, Lüscher's transfer operator is presented. We introduce all necessary notations, define the transfer operator, demonstrate the derivation of the path integral of Lattice QCD and establish the Hamiltonian $\hat{H}$ in the Euclidean time continuum. The main purpose of Section 3.2 is, however, to set the mathematical stage for the transfer-matrix formulation and to summarize the key steps of deriving the path integral.

The final section, Section 3.3, presents the asymmetric transfer operator. The necessity of the choice is discussed and it is shown that the asymmetric operator also gives the path integral of Lattice QCD. Furthermore, we derive the Hamiltonian $\hat{H}$ in the Euclidean time continuum and show its physical equivalence to the Hamiltonian derived in the symmetric case.

The construction of the asymmetric transfer operator has been published in [90]. The author of this thesis is responsible for the formulation and contribution of the asymmetric transfer operator. Note that the idea of an asymmetric operator is inspired by [91]. They consider the transfer-matrix formulation of a $(1+1)$-dimensional $\mathrm{SU}(N)$-gauge theory with scalar fields. Here and in [90], however, the asymmetric transfer operator is constructed for full Lattice QCD with Wilson fermions in $(3+1)$-dimensions. We will consequently use the notations of [90] in parts.

3.1 Quantum-mechanical description

The idea of the transfer-matrix formulation is to associate an Hilbert space $\mathcal{H}$ with a spatial, periodic, cubic lattice of extent $N > 0$ in all directions. Sites are classified by their coordinates $i \in \{0, \ldots, N-1\}^3$. There are $N_\mathrm{s} = N^3$ sites in total. The physical subspace $\mathcal{H}_\mathrm{phys}$ is given by all gauge-invariant states which are defined further below. The grand-canonical partition function of such a system is then written as

$$Z = \mathrm{tr}\left(\mathrm{e}^{\beta\mu\hat{N}}\mathrm{e}^{-\beta\hat{H}}\hat{P}_0\right), \tag{3.1}$$

where β is the inverse temperature, μ is the chemical potential, $\hat{N}$ is the net-quark number operator, $\hat{H}$ is the Hamiltonian, and $\hat{P}_0$ is the projection operator onto $\mathcal{H}_\mathrm{phys}$ [41, 84–86]. The Hamiltonian $\hat{H}$ and the net-quark number operator $\hat{N}$ are assumed to be gauge-invariant:

$$[\hat{H}, \hat{P}_0] = [\hat{N}, \hat{P}_0] = 0\,.$$

This quantum-mechanical description of QCD on the lattice is referred to as the Hamilton approach of Lattice QCD [46, 77, 87–89, 92]. The quantum-

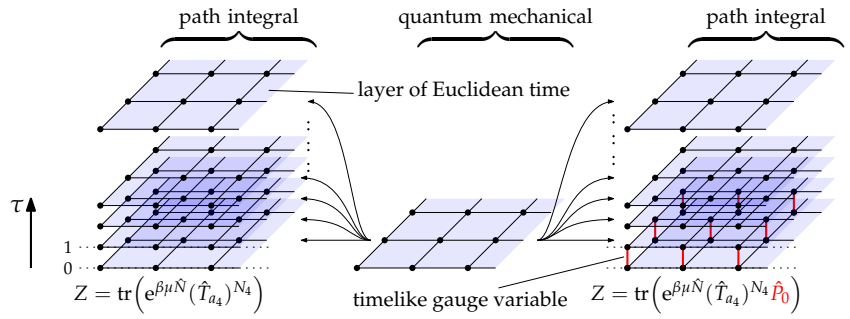

Figure 3.1: Illustration of deriving the path integral with (right) and without (left) gauge invariance. The drawing in the middle represents the spatial lattice with which the Hilbert space $\mathcal{H}$ is associated. The discretization in Euclidean time τ introduces the N_4 layers of time in the resulting path integral. Left, the trace is taken over the full space $\mathcal{H}$; all timelike gauge variables are one and therefore not drawn. Right, the ensemble over the physical Hilbert space $\mathcal{H}_{\mathrm{phys}}$ is shown. The resulting path integral includes the non-trivial timelike gauge variables (red links) between the zeroth and first layer of time.

mechanical system is constructed in such a way that we can derive the Euclidean path integral of Lattice QCD by deriving the path integral of the ensemble (3.1) with some suitable gauge-invariant transfer operator $\hat{T}_{a_4}$ [41, 49, 77, 92, 93]. In doing so, the transfer operator $\hat{T}_{a_4}$ represents the discretization

$$\lim_{N_4\to\infty}\left(\hat{T}_{a_4=\beta/N_4}\right)^{N_4} = e^{-\beta\hat{H}}$$

in direction of Euclidean time, i.e. the evaluation of

$$Z = \mathrm{tr}\left(e^{\beta\mu\hat{N}}(\hat{T}_{a_4=\beta/N_4})^{N_4}\hat{P}_0\right) \tag{3.2}$$

gives the path integral with N_4 layers of time.

Gauge invariance of $\hat{H}$, $\hat{N}$ and $\hat{T}_{a_4}$ is an important assumption because the projection operator $\hat{P}_0$ in Equation (3.1) reduces the full trace to a trace over $\mathcal{H}_{\mathrm{phys}}$, and, then, the thermodynamic ensemble is actually a system of physical states only. The main effect of the projection operator $\hat{P}_0$ is, however, to introduce the timelike gauge variables into the path integral [41, 77, 85, 86]. To be more precise, it introduces the timelike gauge variables between two subsequent layers of time only, see Figure 3.1. All other timelike variables are just one. This is the path integral of Lattice QCD with the temporal direction gauge-fixed maximally to unity, see Section 2.4. Ignoring $\hat{P}_0$ would give a path integral, where all timelike links are one, and the path integral of Lattice QCD cannot be gauge-fixed to such configurations because, then, the expectation value $\langle L_{\vec{x}}\rangle$ of the Polyakov loop $L_{\vec{x}}$ at a site i would be one for all parameters, which is certainly not true.

Continuum limit

The quantum-mechanical formulation and the path integral are related by the continuum limit in direction of Euclidean time. Consider an observable $\hat{O}$ in the

quantum-mechanical system and its corresponding path integral formulation $\mathcal{O}(U,\overline{\psi},\psi)$ on the lattice such that both are related by the temporal continuum $a_4 \to 0$ on the spatial lattice with finite spacing $a > 0$:

$$\langle \hat{O} \rangle = \lim_{\substack{a_4 \to 0 \\ N_4 \to \infty}} \langle \mathcal{O}(U,\overline{\psi},\psi) \rangle \,,$$

where $T = 1/(N_4 a_4)$ stays constant and the expectation values are taken in the respective formulations. In general, for $a_4 > 0$, both observables will not yield the same result due to the discretization introduced in deriving the path integral: $\langle \hat{O} \rangle \neq \langle \mathcal{O}(U,\overline{\psi},\psi) \rangle$. Furthermore, the relation between the quantum-mechanical formulation and the path integral is based on introducing the lattice spacings a and a_4 in the gauge and fermion action in the way necessary that the naive continuum limits give the classical Euclidean action of QCD. Recall that then the action $S = S_\mathrm{G} + S_\mathrm{F}$ of Lattice QCD depending on the lattice spacing reads

$$\begin{aligned} S_\mathrm{G} &= \frac{a}{a_4}\frac{2}{g_0^2}\sum_{x,k} \mathrm{ReTr}\, U_{\partial p_{x,k4}} + \frac{a_4}{a}\frac{2}{g_0^2}\sum_{x,k<m} \mathrm{ReTr}\, U_{\partial p_{x,km}} \,, \\ S_\mathrm{F} &= s(a_4,a)\sum_x \left[\overline{\psi}_x \Lambda^+_{x,4}\psi_{x+\hat{4}} + \overline{\psi}_{x+\hat{4}}\Lambda^-_{x,4}\psi_x\right] \\ &\quad + \frac{a_4}{a}s(a_4,a)\sum_{x,k}\left[\overline{\psi}_x \Lambda^+_{x,k}\psi_{x+\hat{k}} + \overline{\psi}_{x+\hat{k}}\Lambda^-_{x,k}\psi_x\right] - \sum_x \overline{\psi}_x\psi_x \end{aligned} \tag{3.3}$$

with

$$s(a_4,a) = \frac{1}{2a_4(m+3a^{-1})+2} \,,$$

cf. Equation (2.3) and (2.4). However, physical values are not obtained by directly setting a and a_4 in the action but rather the bare parameters $g_0(a)$ and $(ma)(a)$ are adjusted depending on the physical cutoff a for isotropic lattices with $a = a_4$. In this way the theory is renormalized to the correct physical continuum and the renormalized observable $\mathcal{O}_\mathrm{R}$ has the continuum limit

$$\mathcal{O}_\mathrm{phys}(T,L) = \lim_{\substack{a \to 0 \\ N,N_4 \to \infty}} \langle \mathcal{O}_\mathrm{R}(U,\overline{\psi},\psi) \rangle \,,$$

where the limit is taken in the sense of Section 2.4 keeping the physical lattice extent L, the temperature T and $\mu/T = N_4(a\mu)$ fixed. Naturally, we might question to which extent the quantum-mechanical formulation then yields the same physical result $\mathcal{O}_\mathrm{phys}(T,L)$ or whether the quantum-mechanical system can be renormalized at all. This is because, at this point, both formulations are just connected by the naive Euclidean time continuum.

To answer this question, we have to consider Lattice QCD defined on anisotropic lattices with $\xi = a/a_4 > 1$ [40, 43, 49, 94–97]. The lattice spacings a and a_4 are now physical and do not directly occur in the action. We take the continuum limit relative to a fixed $\xi \geq 1$. Because we introduce an anisotropy in the lattice, the asymmetry which it creates between spatial and temporal direction must show up in the action. Rewriting Equation (3.3), we introduce

additional bare parameters such that

$$
\begin{aligned}
S_{\mathrm{G}} &= \xi \frac{2}{g_4^2} \sum_{x,k} \mathrm{ReTr}\, U_{\partial p_{x,\mu 4}} + \frac{1}{\xi} \frac{2}{g_{\mathrm{s}}^2} \sum_{x,k<m} \mathrm{ReTr}\, U_{\partial p_{x,km}}\,, \\
S_{\mathrm{F}} &= s(\gamma_{\mathrm{F}}, ma) \sum_x \left[\overline{\psi}_x \Lambda^+_{x,4} \psi_{x+\hat{4}} + \overline{\psi}_{x+\hat{4}} \Lambda^-_{x,4} \psi_x \right] \\
&\quad + \frac{s(\gamma_{\mathrm{F}}, ma)}{\gamma_{\mathrm{F}}} \sum_{x,k} \left[\overline{\psi}_x \Lambda^+_{x,k} \psi_{x+\hat{k}} + \overline{\psi}_{x+\hat{k}} \Lambda^-_{x,k} \psi_x \right] - \sum_x \overline{\psi}_x \psi_x\,.
\end{aligned}
$$

with

$$
s(\gamma_{\mathrm{F}}, ma) = \frac{1}{2\gamma_{\mathrm{F}}^{-1}(ma+3)+2}\,.
$$

The pure gauge action now includes the anisotropic parameter ξ but the couplings in temporal and spatial directions are chosen differently. Because, we do not consider the naive discretization of the classical action but set up a renormalization scheme for the QFT at physical anisotropy ξ, the choice of the different couplings is a necessity to guarantee the same physical continuum limit [96, 97]. The fermionic action is expressed in the bare parameters ma, which is the quark mass in units of the spatial lattice spacing, and an anisotropy factor γ_{F} which represents the ratio a/a_4 of Equation (3.3). To keep the physics constant, the renormalization scheme gives $\gamma_{\mathrm{F}} \neq \xi$ in general. Based on the chosen renormalization scheme, the bare parameters $g_4(a,\xi)$, $g_{\mathrm{s}}(a,\xi)$, $(ma)(a,\xi)$ and $\gamma_{\mathrm{F}}(a,\xi)$ now depend on the cutoff a and the anisotropy parameter ξ. Expanding the bare parameters relative to $g_0(a)$ of the isotropic case gives ([40, 43, 48, 95–97])

$$
\begin{aligned}
\frac{2}{g_4^2} &= \frac{2}{g_0^2} + c_4(\xi) + \mathcal{O}(g_0^2)\,, \\
\frac{2}{g_{\mathrm{s}}^2} &= \frac{2}{g_0^2} + c_{\mathrm{s}}(\xi) + \mathcal{O}(g_0^2)\,, \\
\gamma_{\mathrm{F}} &= \xi \cdot \left(1 + c_{\mathrm{F}}(\xi) g_0^2 + \mathcal{O}(g_0^4)\right).
\end{aligned}
$$

We are free to choose ξ and obtain the same physical continuum limit:

$$
\mathcal{O}_{\mathrm{phys}}(T,L) = \lim_{\substack{a\to 0 \\ N,N_4\to\infty}} \langle \mathcal{O}_{\mathrm{R}}(U,\overline{\psi},\psi)\rangle_\xi\,.
$$

The Euclidean time continuum is restored in the limit $\xi \to \infty$. Consider the expectation value $\langle \mathcal{O}_{\mathrm{R}}(U,\overline{\psi},\psi)\rangle_\xi$ at fixed physical spacing a and assume $\mathcal{O}_{\mathrm{R}}(U,\overline{\psi},\psi)$ to be a gauge-invariant observable. We gauge-fix the ensemble to maximal temporal gauge such that all timelike links are one, except for the links between the zeroth and first layer of time. Furthermore, we shift all factors $\mathrm{e}^{a_4\mu}$ and $\mathrm{e}^{-a_4\mu}$ into the timelike links between the zeroth and first layer of time such that the corresponding links are multiplied with $\mathrm{e}^{\mu/T}$ or $\mathrm{e}^{-\mu/T}$. Then the expectation value

$$
\langle \mathcal{O}_{\mathrm{R}}(U,\overline{\psi},\psi)\rangle_\xi \longrightarrow \lim_{\substack{\xi\to\infty \\ N_4\to\infty}} \langle \mathcal{O}_{\mathrm{R}}(U,\overline{\psi},\psi)\rangle_\xi
$$

is also pushed towards the Euclidean time continuum $N_4 \to \infty$ for $\xi \to \infty$ if a and T are kept fixed. If we introduce the quark mass $m = (ma)/a$ and $\gamma_\mathrm{F} = a/\tau$ at fixed spatial cutoff a, we see from the g_0-expansion that $\tau \to 0$ as $\xi \to \infty$. Therefore, the limit $\xi \to \infty$ at fixed a and temperature T creates a transition to the quantum-mechanical description as long as $\mathcal{O}_\mathrm{R}(U, \overline{\psi}, \psi)$ has a corresponding gauge-invariant quantum-mechanical operator $\hat{O}_\mathrm{R}$ connected by the naive Euclidean time continuum $a_4 \to 0$. Note that this prescription also defines the renormalization $g_4(a)$, $g_\mathrm{s}(a)$ and $m(a)$ in the quantum-mechanical system and the Hamiltonian $\hat{H}$ depends also directly on the physical cutoff a in general. To be more precise, we replace ξ as a function of γ_F in the pure gauge part via $\gamma_\mathrm{F}/\xi = \eta(a, \xi)$. This ensures that the action depends on the Euclidean time τ. Then the transfer operator is a function of τ such that

$$\hat{T}_\tau^{N_4} \longrightarrow \left(1 + \tau \hat{H}' + \mathcal{O}(\tau^2)\right)^{N_4}.$$

for large anisotropies $\xi \to \infty$. However, the inverse temperature $\beta = N_4 a_4$ is given by the physical lattice spacing a_4. Hence, we write $\tau = a_4/\eta(a, \xi)$ and get

$$\hat{T}_\tau^{N_4} \longrightarrow \mathrm{e}^{-\beta \hat{H}} \qquad (\xi \to \infty)$$

with

$$\hat{H} = \frac{1}{\lim_{\xi \to \infty} \eta(a, \xi)} \hat{H}'.$$

This, of course, requires the factor $\eta(a, \xi)$ to converge to a strictly positive value in the limit $\xi \to \infty$, even beyond the perturbative result for small g_0. Whether this is the case beyond the perturbative regime, is not further investigated in this thesis and must be kept in mind as a future consideration.

In summary, if we define a quantum-mechanical operator $\hat{O}$ and its path integral formulation $\mathcal{O}(U, \overline{\psi}, \psi)$ by connecting both formulations via the naive limit $a_4 \to 0$, we get two formulations which are physically identical in the continuum limit by keeping in mind that the gauge action requires to choose the couplings g_4 and g_s unequal for the temporal and spatial directions.

Hilbert space

We now formulate the Hilbert space $\mathcal{H}$, the physical Hilbert space $\mathcal{H}_\mathrm{phys}$, spatial gauge transformations and the concept of center charges and center-electric fluxes. The Hilbert space $\mathcal{H}$ is constructed as the tensor product $\mathcal{H} = \mathcal{H}_\mathrm{G} \otimes \mathcal{H}_\mathrm{F}$ between the gauge part $\mathcal{H}_\mathrm{G}$ and the fermionic part $\mathcal{H}_\mathrm{F}$. To define $\mathcal{H}_\mathrm{G}$, we associate gauge variables $U_{\langle i, i+\hat{k}\rangle} \in \mathrm{SU}(3)$ with every link $\langle i, i+\hat{k}\rangle$, $k \in \{1, 2, 3\}$. And, as always, we define $U_{\langle i+\hat{k}, i\rangle} = U^\dagger_{\langle i, i+\hat{k}\rangle}$. A spatial gauge configuration $U = \{U_{\langle i, i+\hat{k}\rangle}\}$ is a set of gauge variables $U_{\langle i, i+\hat{k}\rangle}$ for every link $\langle i, i+\hat{k}\rangle$. The space $\mathcal{H}_\mathrm{G}$ is just the space of all complex-valued, square-integrable functions $f(U)$ with respect to the measure

$$\mathcal{D}U = \prod_{i,k} \mathrm{d}U_{\langle i, i+\hat{k}\rangle},$$

where $\mathrm{d}U_{\langle i,i+\hat{k}\rangle}$ denotes the Haar measure for the link variable $U_{\langle i,i+\hat{k}\rangle}$ [77, 83]. The fermionic Fock space $\mathcal{H}_\mathrm{F}$ is spanned by creation and annihilation operators of quarks and antiquarks associated with the spatial sites i [83]: $(\hat{\xi}^\sigma_\mathrm{q})^\dagger_{i,a}$ and $(\hat{\xi}^\sigma_\mathrm{q})_{i,a}$ for quarks and $(\hat{\xi}^\sigma_\mathrm{\overline{q}})^\dagger_{i,a}$ and $(\hat{\xi}^\sigma_\mathrm{\overline{q}})_{i,a}$ for antiquarks. The indices indicate further quantum numbers of the quarks and antiquarks. The index $\sigma = \uparrow, \downarrow$ is the spin state of the fermion, the index $a \in \{1,2,3\}$ is the color state, and i is the site at which the fermion resides. Therefore, there are six possible kinds of quarks (antiquarks) at a site i. The creation and annihilation operators fulfill the standard anti-commutation relations

$$\begin{aligned}
\left[(\hat{\xi}^\sigma_\mathrm{q})^\dagger_{i,a}, (\hat{\xi}^\gamma_\mathrm{q})_{j,b}\right]_+ &= \left[(\hat{\xi}^\sigma_\mathrm{\overline{q}})^\dagger_{i,a}, (\hat{\xi}^\gamma_\mathrm{\overline{q}})_{j,b}\right]_+ = \delta_{ij}\delta_{\sigma\gamma}\delta_{ab}\,, \\
\left[(\hat{\xi}^\sigma_\mathrm{q})_{i,a}, (\hat{\xi}^\gamma_\mathrm{q})_{j,b}\right]_+ &= \left[(\hat{\xi}^\sigma_\mathrm{\overline{q}})_{i,a}, (\hat{\xi}^\gamma_\mathrm{\overline{q}})_{j,b}\right]_+ = \left[(\hat{\xi}^\sigma_\mathrm{q})_{i,a}, (\hat{\xi}^\gamma_\mathrm{\overline{q}})_{j,b}\right]_+ = 0\,, \\
\left[(\hat{\xi}^\sigma_\mathrm{q})^\dagger_{i,a}, (\hat{\xi}^\gamma_\mathrm{\overline{q}})_{j,b}\right]_+ &= 0
\end{aligned}$$

Now, a general state $|\psi\rangle \in \mathcal{H}$ is given by

$$|\psi\rangle = \sum_n \sum_{\alpha_1,\ldots,\alpha_n} f_{\alpha_1,\ldots,\alpha_n}(U) \otimes \hat{\xi}^\dagger_{\alpha_1} \ldots \hat{\xi}^\dagger_{\alpha_n} |0\rangle\,,$$

where $f_{\alpha_1,\ldots,\alpha_n}(U) \in \mathcal{H}_\mathrm{G}$, $|0\rangle$ is the fermionic vacuum state of $\mathcal{H}_\mathrm{F}$, and α_i summarizes all indices of a creation operator. Furthermore, the net-quark number operator $\hat{N}$ is defined as

$$\hat{N} = \sum_i \sum_{a,\sigma} \left[(\hat{\xi}^\sigma_\mathrm{q})^\dagger_{i,a}(\hat{\xi}^\sigma_\mathrm{q})_{i,a} - (\hat{\xi}^\sigma_\mathrm{\overline{q}})^\dagger_{i,a}(\hat{\xi}^\sigma_\mathrm{\overline{q}})_{i,a}\right]\,.$$

Quarks are counted positively, and antiquarks are counted negatively.

Spatial gauge transformations

A gauge transformation Ω associates an element $\Omega_i \in \mathrm{SU}(3)$ with every site i. The transformation is implemented on $\mathcal{H}$ by the unitary operator $\hat{\varrho}(\Omega)$:

$$(\hat{\varrho}(\Omega) f)(U) = f(\{\ldots, \Omega_i^\dagger U_{\langle i,i+\hat{k}\rangle} \Omega_{i+\hat{k}}, \ldots\})\,, \tag{3.4}$$

$$\hat{\varrho}(\Omega)(\hat{\xi}^\sigma_\mathrm{q})_{i,a}\hat{\varrho}^\dagger(\Omega) = \sum_b (\Omega_i^\dagger)_{ab}(\hat{\xi}^\sigma_\mathrm{q})_{i,b}\,, \tag{3.5}$$

$$\hat{\varrho}(\Omega)(\hat{\xi}^\sigma_\mathrm{\overline{q}})_{i,a}\hat{\varrho}^\dagger(\Omega) = \sum_b (\hat{\xi}^\sigma_\mathrm{\overline{q}})_{i,b}(\Omega_i)_{ba}\,. \tag{3.6}$$

Obviously $\hat{\varrho}(\Omega)$ constitutes a representation of the group $(\mathrm{SU}(3))^{N_\mathrm{s}}$ with $N_\mathrm{s} = N^3$. The subspace of physical states is defined by

$$\mathcal{H}_\mathrm{phys} = \overline{\mathrm{span}\,\{|\psi\rangle \in \mathcal{H} \,|\, \hat{\varrho}(\Omega)\,|\psi\rangle = |\psi\rangle \text{ for all } \Omega\}}\,.$$

Because $\mathcal{H}_\mathrm{phys}$ is a closed subspace, it is a Hilbert space. For $|\psi\rangle \in \mathrm{span}\{\ldots\}$, we have $\hat{\varrho}(\Omega)\,|\psi\rangle = |\psi\rangle$ because $\hat{\varrho}(\Omega)$ is linear. Now, if $|\psi\rangle \in \mathcal{H}_\mathrm{phys}$, then there exists a converging sequence $|\psi_n\rangle \in \mathrm{span}\{\ldots\}$ with $|\psi_n\rangle \to |\psi\rangle$ $(n \to \infty)$. The operator $\hat{\varrho}(\Omega)$ is continuous and, therefore, we have

$$\hat{\varrho}(\Omega)\,|\psi\rangle = \lim_{n\to\infty} \hat{\varrho}(\Omega)\,|\psi_n\rangle = \lim_{n\to\infty} |\psi_n\rangle = |\psi\rangle$$

which implies

$$\mathcal{H}_{\text{phys}} = \{|\psi\rangle \in \mathcal{H} \,|\, \hat{\varrho}(\Omega)\,|\psi\rangle = |\psi\rangle \text{ for all } \Omega\}\ .$$

The physical states indeed form a Hilbert space, and the space only consists of states which are invariant under gauge transformations. The projection operator onto $\mathcal{H}_{\text{phys}}$ is ([41, 77, 86, 98])

$$\hat{P}_0\,|\psi\rangle = \int \mathcal{D}\Omega\,\hat{\varrho}(\Omega)\,|\psi\rangle = \int \left(\prod_i \mathrm{d}\Omega_i\right) \hat{\varrho}(\Omega)\,|\psi\rangle \tag{3.7}$$

because the left invariance of the Haar measure implies

$$\hat{\varrho}(G)\hat{P}_0\,|\psi\rangle = \int \left(\prod_i \mathrm{d}\Omega_i\right) \hat{\varrho}(\{\ldots, G_i\Omega_i, \ldots\})\,|\psi\rangle = \hat{P}_0\,|\psi\rangle\ ,$$

and

$$\hat{P}_0^2\,|\psi\rangle = \int \mathcal{D}\Omega_1 \int \mathcal{D}\Omega_2\,\hat{\varrho}(\Omega_1\Omega_2)\,|\psi\rangle = \underbrace{\int \mathcal{D}\Omega_1}_{=1} \int \mathcal{D}\Omega_2\,\hat{\varrho}(\Omega_2)\,|\psi\rangle = \hat{P}_0\,|\psi\rangle\ ,$$

where G is some gauge transformation. More rigorously, the projection operator $\hat{P}_0$ is a consequence of the Peter-Weyl Theorem [98, Theorem 1.12].

Equations (3.5) and (3.6) imply the gauge invariance of the net-quark number operator $\hat{N}$ because

$$\hat{\varrho}(\Omega)\hat{N}\hat{\varrho}^\dagger(\Omega) = \sum_i \sum_{a,b,c,\sigma} \Big[(\hat{\xi}^\sigma_{\mathrm{q}})^\dagger_{i,b} (\Omega_i)_{ba} (\Omega_i^\dagger)_{ac} (\hat{\xi}^\sigma_{\mathrm{q}})_{i,c} - (\Omega_i^\dagger)_{ab} (\hat{\xi}^\sigma_{\mathrm{q}})^\dagger_{i,b} (\hat{\xi}^\sigma_{\mathrm{q}})_{i,c} (\Omega_i)_{ca} \Big] = \hat{N}\ .$$

What are intuitive examples of gauge-invariant states? A simple example is a meson where a quark and an antiquark are connected in a gauge-invariant manner by a line of gauge variables [46]:

$$|\psi\rangle = \sum_{a,b} (\hat{\xi}^\sigma_{\mathrm{q}})^\dagger_{i,a} \left[U_{\langle i,i_1\rangle} \ldots U_{\langle i_n,j\rangle}\right]_{ab} (\hat{\xi}^\gamma_{\overline{\mathrm{q}}})^\dagger_{j,b}\,|0\rangle \tag{3.8}$$

with $i \neq j$. The quarks and antiquarks are sources of color-charge and, therefore, they transform non-trivially under a local gauge transformation:

$$(\hat{\xi}^\sigma_{\mathrm{q}})^\dagger_i \longrightarrow (\hat{\xi}^\sigma_{\mathrm{q}})^\dagger_i \Omega_i\,, \qquad (\hat{\xi}^\gamma_{\overline{\mathrm{q}}})^\dagger_j \longrightarrow \Omega_j^\dagger (\hat{\xi}^\gamma_{\overline{\mathrm{q}}})^\dagger_j\,.$$

Furthermore, the line of gauge variables carries a color-electric flux between the sites and therefore transforms non-trivially at its endpoints:

$$\left[U_{\langle i,i_1\rangle} \ldots U_{\langle i_n,j\rangle}\right] \longrightarrow \Omega_i^\dagger \left[U_{\langle i,i_1\rangle} \ldots U_{\langle i_n,j\rangle}\right] \Omega_j\,.$$

Hence, we immediately observe the gauge invariance of $|\psi\rangle$ because the SU(3)-matrices compensate each other. In this sense, a color charge at a site equals the color-electric fluxes flowing out of the site.

More generally, the concept of gauge invariance implies a local Gauss law on $\mathcal{H}_{\text{phys}}$ [77, 87–89]. Consider the representations $\hat{\Pi}_i(\omega)$ and $\hat{\Pi}_{\langle i,j\rangle}(\omega)$ defined as

$$\hat{\Pi}_i(\omega)(\hat{\xi}^\sigma_{\text{q}})_{j,a}\hat{\Pi}_i^\dagger(\omega) = \begin{cases} \sum_b(\omega^\dagger)_{ab}(\hat{\xi}^\sigma_{\text{q}})_{i,b}\,, & i=j \\ (\hat{\xi}^\sigma_{\text{q}})_{j,a}\,, & i\neq j \end{cases}$$

$$\hat{\Pi}_i(\omega)(\hat{\xi}^\sigma_{\overline{\text{q}}})_{j,a}\hat{\Pi}_i^\dagger(\omega) = \begin{cases} \sum_b(\hat{\xi}^\sigma_{\overline{\text{q}}})_{i,b}\omega_{ba}\,, & i=j \\ (\hat{\xi}^\sigma_{\overline{\text{q}}})_{j,a}\,, & i\neq j \end{cases}$$

and

$$(\hat{\Pi}_{\langle i,j\rangle}(\omega)f)(U) = \begin{cases} f(\{\ldots,\omega^\dagger U_{\langle i,i+\hat{k}\rangle},\ldots\})\,, & \langle i,j\rangle = \langle i,i+\hat{k}\rangle \\ f(\{\ldots,U_{\langle i,i+\hat{k}\rangle}\omega,\ldots\})\,, & \langle j,i\rangle = \langle i,i+\hat{k}\rangle \end{cases}$$

for $\omega\in\text{SU}(3)$. These representations can be combined to establish the gauge transformation

$$\Omega_j = \begin{cases} \omega, & j=i \\ \mathbb{1}, & j\neq i \end{cases}$$

at the site i such that

$$\hat{\varrho}(\Omega) = \hat{\Pi}_i(\omega)\prod_{j\sim i}\hat{\Pi}_{\langle i,j\rangle}(\omega)\,, \tag{3.9}$$

where the notation $j\sim i$ means that j is a nearest neighbor of i. Each representation $\hat{\Pi}_i(\omega)$ and $\hat{\Pi}_{\langle i,j\rangle}(\omega)$ constitutes a part of the gauge transformation $\hat{\varrho}(\Omega)$. If we write $\omega = \exp\left(\text{i}\sum_k \alpha_k T_k\right)$ with the generators T_k, $k\in\{1,\ldots,8\}$ of SU(3), we can define the color-charge operators $\hat{Q}_i^k$ and the color-electric flux operators $\hat{E}^k_{\langle i,j\rangle}$ as infinitesimal transformations of the representations $\hat{\Pi}_i(\omega)$ and $\hat{\Pi}_{\langle i,j\rangle}(\omega)$:

$$\hat{Q}_i^k = -\text{i}\frac{\text{d}}{\text{d}\alpha}_{|\alpha=0}\hat{\Pi}_i\left(\text{e}^{\text{i}\alpha T_k}\right),$$

$$\hat{E}^k_{\langle i,j\rangle} = -\text{i}\frac{\text{d}}{\text{d}\alpha}_{|\alpha=0}\hat{\Pi}_{\langle i,j\rangle}\left(\text{e}^{\text{i}\alpha T_k}\right).$$

Now, we write

$$-\text{i}\frac{\text{d}}{\text{d}\alpha}_{|\alpha=0}\left[\hat{\Pi}_i\left(\text{e}^{\text{i}\alpha T_k}\right)\prod_{j\sim i}\hat{\Pi}_{\langle i,j\rangle}\left(\text{e}^{\text{i}\alpha T_k}\right)\right]|\psi\rangle = 0$$

for $|\psi\rangle\in\mathcal{H}_{\text{phys}}$ which implies the local Gauss law

$$\hat{Q}_i^k = -\sum_{j\sim i}\hat{E}^k_{\langle i,j\rangle} \tag{3.10}$$

on $\mathcal{H}_{\text{phys}}$.

The operators $\hat{Q}_i^k$ and $\hat{E}^k_{\langle i,j\rangle}$ are not gauge-invariant. This can be seen easily by considering the mesonic state (3.8). We have

$$\hat{Q}_i^k|\psi\rangle = \sum_{a,b,c}(\hat{\xi}^\sigma_{\text{q}})^\dagger_{i,c}(T_k)_{ca}\left[U_{\langle i,i_1\rangle}\ldots U_{\langle i_n,j\rangle}\right]_{ab}(\hat{\xi}^\gamma_{\overline{\text{q}}})^\dagger_{j,b}|0\rangle$$

and, therefore,

$$\hat{\varrho}(\Omega)\hat{Q}_i^k \left|\psi\right\rangle = \sum_{a,b,c} (\hat{\xi}_{\mathrm{q}}^{\sigma})_{i,c}^{\dagger} \left(\Omega_i T_k \Omega_i^{\dagger}\right)_{ca} \left[U_{\langle i,i_1\rangle} \dots U_{\langle i_n,j\rangle}\right]_{ab} (\hat{\xi}_{\overline{\mathrm{q}}}^{\gamma})_{j,b}^{\dagger} \left|0\right\rangle \ .$$

In general, $(\Omega_i T_k \Omega_i^{\dagger})$ is an element of the Lie algebra su(3) with $(\Omega_i T_k \Omega_i^{\dagger}) \neq T^k$. Hence, we get $\hat{Q}_i^k \left|\psi\right\rangle \neq \hat{\varrho}(\Omega)\hat{Q}_i^k \left|\psi\right\rangle$, but gauge invariance would require $\hat{Q}_i^k \left|\psi\right\rangle = \hat{\varrho}(\Omega)\hat{Q}_i^k \left|\psi\right\rangle$. An analogous argument can be made for $\hat{E}^k_{\langle i,j\rangle}$.

Center charge and center-electric flux

Normally, a Gauss law is formulated such that it relates a concept of Abelian charges q_i and Abelian fluxes $e_{\langle i,j\rangle}$ to each other. The charges at a site i should be the consequence of the flux flowing out of the site:

$$q_i = -\sum_{j\sim i} e_{\langle i,j\rangle} \ . \tag{3.11}$$

The Abelian character ensures a global Gauss law in which the total charge Q in a volume V equals the flux $-\phi$ through the surface S of the volume. To see this, we replace every q_i in $Q = \sum_{i\in V} q_i$ with the local Gauss law, note that $e_{\langle i,j\rangle}$ and $e_{\langle j,i\rangle} = -e_{\langle i,j\rangle}$ appear in the sum for every $\langle i,j\rangle$ with endpoints in V and reorder the terms such that flux variables lying within the volume cancel each other. Only the links piercing through S remain which give $\phi = \sum_{l\in S^*} e_l$ with the set S^* of links piercing through the surface S. To be more precise, the physical space $\mathcal{H}_{\mathrm{phys}}$ should decompose into sectors $\mathcal{H}_{\{q,e\}}$ for which all $\left|\psi\right\rangle \in \mathcal{H}_{\{q,e\}}$ have some well-defined Abelian charges $q_i \in \{q,e\}$ and fluxes $e_{\langle i,i+\hat{k}\rangle} \in \{q,e\}$ at every site i and link $\langle i, i+\hat{k}\rangle$, and the local Gauss law (3.11) holds for these variables.

However, we cannot use the operators $\hat{Q}_i^k$ and $\hat{E}^k_{\langle i,j\rangle}$ and Gauss's law (3.10) directly to define the notion of Abelian charges and fluxes ([87–89]) because the operators $\hat{Q}_i^k$ and $\hat{E}^k_{\langle i,j\rangle}$ are not gauge-invariant nor can they be diagonalized simultaneously. For example, one might use the Peter-Weyl Theorem ([98, Theorem 1.12]) and decompose the Hilbert space $\mathcal{H}$ into the direct sum of irreducible unitary representations of $\hat{\Gamma}_i(\omega)$ for some site i. Each representation can be labeled by the eigenvalues of the operators

$$\sum_k (\hat{Q}_i^k)^2 \qquad \text{and} \qquad \sum_{klm} d_{klm}\hat{Q}_i^k\hat{Q}_i^l\hat{Q}_i^m \ ,$$

where the coefficients d_{klm} are chosen suitably [99]. Of course, the eigenvalues are Abelian objects, but they cannot serve as the concept of Abelian charges. Due to the fact that $\hat{Q}_i^k$ is not gauge-invariant, we are unable to restrict the operator to a map from $\mathcal{H}_{\mathrm{phys}}$ to $\mathcal{H}_{\mathrm{phys}}$ only, i.e. we are unable to decompose $\mathcal{H}_{\mathrm{phys}}$ into the direct sum of irreducible unitary representations of $\hat{\Gamma}_i(\omega)$. Even if this was possible, the Gauss law (3.10) is linear with respect to $\hat{Q}_i^k$ and $\hat{E}^k_{\langle i,j\rangle}$, but the two operators are non-linear powers of the charge and field operators, and Equation (3.10) would not hold for the eigenvalues.

An Abelian Gauss law can still be derived if we only consider representations of the center $Z_3 = \{1, e^{\frac{2\pi}{3}i}, e^{\frac{4\pi}{3}i}\} \sim \mathbb{Z}_3$ of SU(3) [77, 87–89]. To this end, we define center-charge operators $\hat{Q}_i^z$ and center-electric flux operators $\hat{E}^z_{\langle i,j\rangle}$ as

$$\hat{Q}_i^z (\hat{\xi}^\sigma_{\mathrm{q}})^\dagger_{i,a} (\hat{Q}_i^z)^\dagger = z \ \cdot (\hat{\xi}^\sigma_{\mathrm{q}})^\dagger_{i,a}\,, \tag{3.12}$$

$$\hat{Q}_i^z (\hat{\xi}^\sigma_{\bar{\mathrm{q}}})^\dagger_{i,a} (\hat{Q}_i^z)^\dagger = z^\dagger \cdot (\hat{\xi}^\sigma_{\bar{\mathrm{q}}})^\dagger_{i,a} \tag{3.13}$$

and ([77])

$$(\hat{E}^z_{\langle i,j\rangle} f)(U) = \begin{cases} f(\{\ldots, z^\dagger U_{\langle i,i+\hat{k}\rangle}, \ldots\}), & \langle i,j\rangle = \langle i, i+\hat{k}\rangle \\ f(\{\ldots, z U_{\langle i,i+\hat{k}\rangle}, \ldots\}), & \langle j,i\rangle = \langle i, i+\hat{k}\rangle \end{cases} \tag{3.14}$$

for all $z \in Z_3$. Obviously $\hat{Q}_i^z$ and $\hat{E}^z_{\langle i,j\rangle}$ form unitary representations of Z_3 because

$$\hat{Q}_i^{z_1 z_2} = \hat{Q}_i^{z_1} \hat{Q}_i^{z_2} \qquad \text{and} \qquad \hat{E}^{z_1 z_2}_{\langle i,j\rangle} = \hat{E}^{z_1}_{\langle i,j\rangle} \hat{E}^{z_2}_{\langle i,j\rangle}\,.$$

These operators are essentially the representations $\hat{\Pi}_i(\omega)$ and $\hat{\Pi}_{\langle i,j\rangle}(\omega)$ but restricted to the center of SU(3):

$$\hat{Q}_i^z = \hat{\Pi}_i(z) \qquad \text{and} \qquad \hat{E}^z_{\langle i,j\rangle} = \hat{\Pi}_{\langle i,j\rangle}(z)\,.$$

Therefore, Equation (3.9) implies

$$\hat{\varrho}(\Omega) = \hat{Q}_i^z \prod_{j\sim i} \hat{E}^z_{\langle i,j\rangle}$$

with

$$\Omega_j = \begin{cases} z, & j = i \\ \mathbb{1}, & j \neq i \end{cases}.$$

Hence, we have the local $\mathbb{Z}_3$-Gauss law

$$\hat{Q}_i^z \prod_{j\sim i} \hat{E}^z_{\langle i,j\rangle} |\psi\rangle = |\psi\rangle \tag{3.15}$$

for $|\psi\rangle \in \mathcal{H}_{\mathrm{phys}}$. This form of the $\mathbb{Z}_3$-Gauss law is the same as in [77] but generalized to the case where quarks and antiquarks are included. The operators $\hat{Q}_i^z$ and $\hat{E}^z_{\langle i,j\rangle}$ are gauge-invariant because the center elements $z \in Z_3$ commute with all elements of SU(3). Gauge invariance implies that we can restrict $\hat{Q}_i^z$ and $\hat{E}^z_{\langle i,j\rangle}$ to $\mathcal{H}_{\mathrm{phys}}$ only, and we can utilize the Peter-Weyl Theorem to decompose the physical-state space into the direct sum of irreducible representations of $\hat{Q}_i^z$ and $\hat{E}^z_{\langle i,j\rangle}$. Hence, we can do the very thing which we found out to be not possible for $\hat{\Pi}_i(\omega)$ and $\hat{\Pi}_{\langle i,j\rangle}(\omega)$.

What are the irreducible representations of $\hat{Q}_i^z$ and $\hat{E}^z_{\langle i,j\rangle}$? Consider some general unitary representations $\hat{\Pi}(z)$ of Z_3 and an irreducible representation $\mathcal{H}' \subseteq \mathcal{H}_{\mathrm{phys}}$ of $\hat{\Pi}(z)$. Because Z_3 is Abelian and on the basis of Schur's Lemma (see for example [35, Theorem 4.29],[98, Proposition 1.5]), the irreducible representation must be one-dimensional with $\hat{\Pi}(z)|\psi\rangle = \lambda_z |\psi\rangle$ and $\lambda_z \in \mathbb{C}\backslash\{0\}$

for all $z \in \mathrm{Z}_3$ and $|\psi\rangle \in \mathcal{H}'$. Therefore, the eigenvalues λ_z constitute an unitary representation of Z_3. All these representations are of the form $\lambda_z = z^e$ with some $e \in \mathbb{Z}_3$. This can be shown easily. Because $\hat{\Gamma}(z)$ is unitary, we have $|\lambda_z| = 1$ which implies $\lambda_z = \mathrm{e}^{\mathrm{i}\phi_z}$ with $\phi_z \in \mathbb{R}$. Furthermore, we write

$$1 = \lambda_{z^3} = \lambda_z^3 = \mathrm{e}^{3\mathrm{i}\phi_z}$$

for all $z \in \mathrm{Z}_3$. This implies $3\phi_z = 2\pi \cdot m_z$ with $m_z \in \mathbb{Z}$ and, equivalently,

$$\phi_z = \frac{2\pi}{3} \cdot m_z \,.$$

Therefore, we conclude $\lambda_z \in \mathrm{Z}_3$. Obviously any element $z \in \mathrm{Z}_3$ can be written as $z = u^e$ with some $e \in \mathbb{Z}_3$ and $u = \exp(\frac{2\pi}{3}\mathrm{i})$. Hence, $\lambda_u = z = u^e$. Now, for any element $w \in \mathrm{Z}_3$, we have $w = u^{k_w}$, $k_w \in \mathbb{Z}_3$ and, consequently,

$$\lambda_w = \lambda_{u^{k_w}} = \lambda_u^{k_w} = (u^e)^{k_w} = (u^{k_w})^e = w^e \,.$$

Every irreducible representation $\mathcal{H}'$ of $\hat{\Gamma}(z)$ is classified by some $e \in \mathbb{Z}_3$. This implies the notion of center charges and center-electric fluxes because the irreducible representations of $\hat{Q}_i^z$ and $\hat{E}_{\langle i,j\rangle}^z$ are classified by values $q_i \in \mathbb{Z}_3$ and $e_{\langle i,j\rangle} \in \mathbb{Z}_3$. For example, if we consider an irreducible representation $\mathcal{H}' \subseteq \mathcal{H}_{\text{phys}}$ of $\hat{Q}_i^z$ with center charge q_i, we have

$$\hat{Q}_i^z \,|\psi\rangle = z^{q_i} \,|\psi\rangle$$

for all $|\psi\rangle \in \mathcal{H}'$ and $z \in \mathrm{Z}_3$. In this sense, we say that the state $|\psi\rangle$ has a well-defined center charge q_i or analogously a well-defined center-electric flux $e_{\langle i,j\rangle}$ for irreducible representations of $\hat{E}_{\langle i,j\rangle}^z$.

Sectors of well-defined center charge q_i and center flux $e_{\langle i,j\rangle}$ are defined as

$$\begin{aligned}
\mathcal{H}_i^q &= \overline{\text{span}\left\{|\psi\rangle \in \mathcal{H}_{\text{phys}} \,|\, \hat{Q}_i^z \,|\psi\rangle = z^q \,|\psi\rangle \text{ for all } z \in \mathrm{Z}_3\right\}}\,, \\
\mathcal{H}_{\langle i,j\rangle}^e &= \overline{\text{span}\left\{|\psi\rangle \in \mathcal{H}_{\text{phys}} \,|\, \hat{E}_{\langle i,j\rangle}^z \,|\psi\rangle = z^e \,|\psi\rangle \text{ for all } z \in \mathrm{Z}_3\right\}}\,.
\end{aligned}$$

Because $\hat{Q}_i^z$ and $\hat{E}_{\langle i,j\rangle}^z$ are continuous, we can apply the same argument as for $\mathcal{H}_{\text{phys}}$ which gives

$$\begin{aligned}
\mathcal{H}_i^q &= \left\{|\psi\rangle \in \mathcal{H}_{\text{phys}} \,|\, \hat{Q}_i^z \,|\psi\rangle = z^q \,|\psi\rangle \text{ for all } z \in \mathrm{Z}_3\right\}\,, \\
\mathcal{H}_{\langle i,j\rangle}^e &= \left\{|\psi\rangle \in \mathcal{H}_{\text{phys}} \,|\, \hat{E}_{\langle i,j\rangle}^z \,|\psi\rangle = z^e \,|\psi\rangle \text{ for all } z \in \mathrm{Z}_3\right\}\,.
\end{aligned}$$

The precise formulation of the Peter-Weyl Theorem describes the decomposition into sectors each of which is the closure of a direct sum of equivalent irreducible unitary representations. Therefore, we can always decompose $\mathcal{H}_{\text{phys}}$ into

$$\mathcal{H}_{\text{phys}} = \bigoplus_{q=0}^{2} \mathcal{H}_i^q \qquad \text{and} \qquad \mathcal{H}_{\text{phys}} = \bigoplus_{e=0}^{2} \mathcal{H}_{\langle i,j\rangle}^e$$

for every site i and link $\langle i,j\rangle$. By virtue of the same theorem, we can project onto a sector $\mathcal{H}_i^q$ or $\mathcal{H}_{\langle i,j\rangle}^e$ by taking the discrete Fourier transform over the center Z_3:

$$\hat{P}_i(q) = \frac{1}{3}\sum_{z\in\mathrm{Z}_3} z^{-q}\hat{Q}_i^z \qquad \text{and} \qquad \hat{P}_{\langle i,j\rangle}(e) = \frac{1}{3}\sum_{z\in\mathrm{Z}_3} z^{-e}\hat{E}_{\langle i,j\rangle}^z \tag{3.16}$$

defined on $\mathcal{H}_{\text{phys}}$. We can also check explicitly that these operators give the desired projection operators. Consider $|\psi\rangle \in \mathcal{H}_{\text{phys}}$. We have

$$\hat{Q}_i^u \hat{P}_i(q)\,|\psi\rangle = \frac{1}{3}\sum_{z\in\mathrm{Z}_3} z^{-q}\hat{Q}_i^{uz}\,|\psi\rangle = \frac{1}{3}\sum_{z\in\mathrm{Z}_3} (u^{-1}z)^{-q}\hat{Q}_i^z\,|\psi\rangle = u^q\hat{P}_i(q)\,|\psi\rangle$$

and

$$\hat{P}_i^2(q) = \frac{1}{9}\sum_{z\in\mathrm{Z}_3}\sum_{w\in\mathrm{Z}_3}(zw)^{-q}\hat{Q}_i^{wz} = \frac{1}{9}\left[\sum_{z\in\mathrm{Z}_3}1\right]\sum_{w\in\mathrm{Z}_3} w^{-q}\hat{Q}_i^w = \hat{P}_i(q)\,.$$

Obviously, the same argument applies to $\hat{P}_{\langle i,j\rangle}(e)$.

For the purpose of the $\mathbb{Z}_3$-Gauss law, we like to decompose the physical-state space into sectors $\mathcal{H}_{\{q,e\}}$, where every $|\psi\rangle \in \mathcal{H}_{\{q,e\}}$ has a well-defined center charge and center-electric flux for all sites and links. This is possible because all operators $\hat{Q}_i^z$ and $\hat{E}_{\langle i,j\rangle}^z$ commute pairwise with each other and can be diagonalized simultaneously. We can define the unitary representation $\hat{\Pi}(\{z\})$ of $(\mathrm{Z}_3)^{4N_\mathrm{s}}$ with $\{z\} = (\ldots, z_i, \ldots, z_{\langle i,i+\hat{k}\rangle}, \ldots)$:

$$\begin{aligned}\hat{\Pi} : (\mathrm{Z}_3)^{4N_\mathrm{s}} &\longrightarrow \mathrm{GL}(\mathcal{H}_{\text{phys}}) \\ (\ldots, z_i, \ldots, z_{\langle i,i+\hat{k}\rangle}, \ldots) &\longmapsto \ldots\cdot\hat{Q}_i^{z_i}\cdot\ldots\cdot\hat{E}_{\langle i,i+\hat{k}\rangle}^{z_{\langle i,i+\hat{k}\rangle}}\cdot\ldots\end{aligned}\,.$$

The group $(\mathrm{Z}_3)^{4N_\mathrm{s}}$ is Abelian, therefore, the irreducible representations $\mathcal{H}' \subseteq \mathcal{H}_{\text{phys}}$ are again one-dimensional, and the eigenvalues $\lambda(\{z\})$ constitute a unitary representation of $(\mathrm{Z}_3)^{4N_\mathrm{s}}$. Now, we notice that

$$\begin{aligned}\hat{Q}_i^{z_i} &= \hat{\Pi}(1,\ldots,1,z_i,1,\ldots,1)\,, \\ \hat{E}_{\langle i,j\rangle}^{z_{\langle i,i+\hat{k}\rangle}} &= \hat{\Pi}(1,\ldots,1,z_{\langle i,i+\hat{k}\rangle},1,\ldots,1)\,.\end{aligned}$$

Consequently, the vector $|\psi\rangle \in \mathcal{H}'$ is also an irreducible representation of all operators $\hat{Q}_i^z$ and $\hat{E}_{\langle i,j\rangle}^z$. We have

$$\begin{aligned}\hat{\Pi}(\{z\})\,|\psi\rangle = \lambda(\{z\})\,|\psi\rangle &= \ldots\cdot\hat{Q}_i^{z_i}\cdot\ldots\cdot\hat{E}_{\langle i,i+\hat{k}\rangle}^{z_{\langle i,i+\hat{k}\rangle}}\cdot\ldots|\psi\rangle \\ &= \ldots z_i^{q_i}\ldots z_{\langle i,i+\hat{k}\rangle}^{e_{\langle i,i+\hat{k}\rangle}}\ldots|\psi\rangle\end{aligned}$$

which implies

$$\lambda(\{z\}) = \ldots z_i^{q_i}\ldots z_{\langle i,i+\hat{k}\rangle}^{e_{\langle i,i+\hat{k}\rangle}}\ldots\,.$$

Therefore, irreducible unitary representations of $\hat{\Pi}(\{z\})$ are classified by a set $\{q,e\}$ of center charges $q_i \in \{q,e\}$ and center-electric fluxes $e_{\langle i,i+\hat{k}\rangle} \in \{q,e\}$.

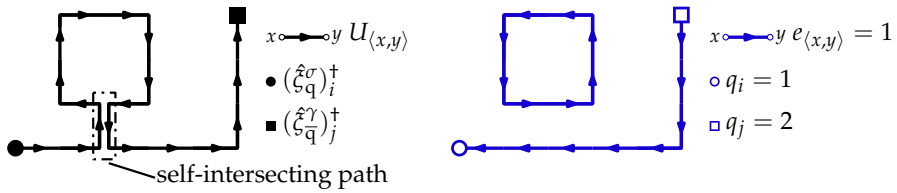

Figure 3.2: Illustration of a mesonic state (3.8). On the left, the creation operators and the path of gauge variables are shown. The product of gauge variables from left to right is taken in direction of the arrows. The path is self-intersecting. The state has well-defined center charge and center-electric fluxes at every site and link. The figure on the right shows the flux-tube configuration $\{q, e\}$ of the state.

This means that the Peter-Weyl Theorem yields the decomposition of $\mathcal{H}_{\mathrm{phys}}$ into sectors $\mathcal{H}_{\{q,e\}}$ of irreducible representations of $\hat{\Pi}(\{z\})$:

$$\mathcal{H}_{\mathrm{phys}} = \bigoplus_{\{q,e\}} \mathcal{H}_{\{q,e\}} \,,$$

where the sum is taken over all possible irreducible unitary representations $\{q, e\}$.

Consider $|\psi\rangle \in \mathcal{H}_{\{q,e\}} \subseteq \mathcal{H}_{\mathrm{phys}}$. Equation (3.15) implies

$$z^{q_i} \prod_{j\sim i} z^{e_{\langle i,j\rangle}} |\psi\rangle = z^{q_i + \sum_{j\sim i} e_{\langle i,j\rangle}} |\psi\rangle = |\psi\rangle \,.$$

This equation can only be fulfilled if $|\psi\rangle = 0$ or

$$q_i + \sum_{j\sim i} e_{\langle i,j\rangle} = 0 \mod 3 \,. \tag{3.17}$$

Hence, either $\mathcal{H}_{\{q,e\}} = \{0\}$ or $\{q, e\}$ must fulfill Equation (3.17). The decomposition of $\mathcal{H}_{\mathrm{phys}}$ can be restricted to the physical configurations $\{q, e\}$ which obey the local $\mathbb{Z}_3$-Gauss law (3.17):

$$\mathcal{H}_{\mathrm{phys}} = \bigoplus_{\{q,e\}_{\mathrm{phys}}} \mathcal{H}_{\{q,e\}} \,. \tag{3.18}$$

The physical configurations $\{q, e\}$ are named flux-tube configurations.

In summary, we have derived a decomposition of the physical-state space $\mathcal{H}_{\mathrm{phys}}$ into sectors $\mathcal{H}_{\{q,e\}}$ of flux-tube configurations $\{q, e\}$ with an Abelian concept of center charges and center-electric fluxes fulfilling a local $\mathbb{Z}_3$-Gauss law. Quarks and antiquarks are sources of center charge and the gauge variables are sources of center-electric flux. The mesonic state (3.8) can be used as an illustrative example. In Figure 3.2, we show an illustration of a mesonic state $|\psi\rangle$ with a self-intersecting path of gauge variables. The quark at the site i gives $\hat{Q}^{z}_{i} |\psi\rangle = z |\psi\rangle$ which corresponds to a center charge $q_i = 1$. The antiquark gives $\hat{Q}^{z}_{j} |\psi\rangle = z^{\dagger} |\psi\rangle$ which corresponds to a center charge $q_j = 2$. Each of the gauge variables $U_{\langle x,y\rangle}$ along the product $U_{\langle i,i_1\rangle} \dots U_{\langle i_n,j\rangle}$ defines

a center-electric flux $e_{\langle x,y\rangle} = 2$ because $\hat{E}^z_{\langle x,y\rangle} |\psi\rangle = z^\dagger |\psi\rangle$. However, the link $\langle x,y\rangle$ at which the path self-intersects yields the occurrence of the gauge variables $U_{\langle x,y\rangle}$ and $U_{\langle y,x\rangle}$ in the product. At this link, the center-electric flux must vanish because the link $U_{\langle x,y\rangle}$ gives the factor $z^\dagger$ and $U_{\langle y,x\rangle}$ gives the factor z upon application of $\hat{E}^z_{\langle x,y\rangle}$. All other sites and links do not occur in $|\psi\rangle$ and, consequently, their center charges and center-electric fluxes are zero. The vector $|\psi\rangle$ has well-defined center values at all sites and links and is part of a sector $\mathcal{H}_{\{q,e\}}$. The second figure of 3.2 shows the non-trivial values of the flux-tube configuration $\{q,e\}$ for $|\psi\rangle$, and the reader might verify easily the validity of the $\mathbb{Z}_3$-Gauss law.

3.2 Symmetric transfer operator

With the quantum-mechanical framework at hand, we can now define the transfer operators. Lüscher's transfer operator ([83]) is presented first. It serves to set up all neccessary notations and definitions and to show the principal procedure of deriving the path integral. Afterwards, we consider the asymmetric transfer operator in the next section. For now, we assume the spatial lattice spacing a and the spacing a_4 in Euclidean time to be one. In general, the transfer operator $\hat{T}$ is written as the integral over some integral kernel $K(U,U')$:

$$\hat{T}(f(U)\otimes|\psi_{\mathrm{F}}\rangle) = \int \mathcal{D}U'\, K(U,U')(f(U')\otimes|\psi_{\mathrm{F}}\rangle)$$

with $f(U)\in\mathcal{H}_{\mathrm{G}}$ and $|\psi_{\mathrm{F}}\rangle\in\mathcal{H}_{\mathrm{F}}$. The integral kernel can be interpreted to act as

$$\begin{aligned} &K(U,U')(f(U')\otimes|\psi_{\mathrm{F}}\rangle) \\ &\quad= \sum_{m,n}\sum_{\substack{\alpha_1,\ldots,\alpha_m\\ \beta_1,\ldots,\beta_n}} \left(K^{\beta_1,\ldots,\beta_n}_{\alpha_1,\ldots,\alpha_m}(U,U')f(U')\right)\otimes\left(\hat{\xi}^\dagger_{\alpha_1}\ldots\hat{\xi}^\dagger_{\alpha_m}\hat{\xi}_{\beta_1}\ldots\hat{\xi}_{\beta_n}|\psi_{\mathrm{F}}\rangle\right). \end{aligned} \tag{3.19}$$

In the derivation of the path integral, the kernel $K(U,U')$ connects a Euclidean time layer $U = U_\tau$ with a subsequent layer $U' = U_{\tau+1}$.

Notations and Definitions

Now, for the construction of the transfer operator, certain preliminary remarks and definitions are in order. We use Euclidean gamma matrices with the convention of [83]:

$$\gamma_k = \begin{pmatrix} 0 & \mathrm{i}\sigma_k \\ -\mathrm{i}\sigma_k & 0 \end{pmatrix} \qquad \text{and} \qquad \gamma_4 = \begin{pmatrix} \mathbb{1}_2 & 0 \\ 0 & -\mathbb{1}_2 \end{pmatrix},$$

where σ_k are the Pauli-spin matrices. Furthermore, we define the matrices $B(U)$ and $c(U)$ as

$$B_{ia\gamma,jb\gamma'} = \frac{1}{2\kappa}\delta_{ij}\delta_{ab}\delta_{\gamma\gamma'} - \frac{1}{2}\delta_{\gamma\gamma'}\sum_k \left[(U_{\langle i,i+\hat{k}\rangle})_{ab}\delta_{i+\hat{k},j} + (U_{\langle j+\hat{k},j\rangle})_{ab}\delta_{j+\hat{k},i}\right] ,$$

$$c_{ia\gamma,jb\gamma'} = \frac{1}{2}\sum_k \left[(U_{\langle i,i+\hat{k}\rangle})_{ab}(\mathrm{i}\sigma_k)_{\gamma\gamma'}\delta_{i+\hat{k},j} - (U_{\langle j+\hat{k},j\rangle})_{ab}(\mathrm{i}\sigma_k)_{\gamma\gamma'}\delta_{j+\hat{k},i}\right]$$

and

$$C(U) = \begin{pmatrix} 0 & c(U) \\ -c(U) & 0 \end{pmatrix} .$$

Note that the matrix $c(U)$ and $B(U)$ are defined as in [83], but $B(U)$ differs by a factor with respect to the matrix stated in [83]. This rescaling is convenient for the construction of the asymmetric transfer operator later on.

The indices i and j denote sites, $a, b \in \{1, 2, 3\}$ are color indices, and $\gamma, \gamma' \in \{\uparrow, \downarrow\}$ are spin indices. The hopping parameter is restricted to $\kappa \in \left(0, \frac{1}{6}\right)$ which guarantees $B(U)$ to be strictly positive for all gauge configurations U [83]. Strict positivity is important because it ensures the existence of $\ln B(U)$ and $B^{\frac{1}{2}}(U)$; both of which are used in the formulation of the transfer operator. To show that $B(U)$ is indeed Hermitian, we write

$$\begin{aligned}
(B^\dagger)_{ia\gamma,jb\gamma'} &= B^*_{jb\gamma',ia\gamma} \\
&= \frac{1}{2\kappa}\delta_{ij}\delta_{ab}\delta_{\gamma\gamma'} - \frac{1}{2}\delta_{\gamma\gamma'}\sum_k \left[\left((U_{\langle j,j+\hat{k}\rangle})_{ba}\right)^* \delta_{j+\hat{k},i} + \left((U_{\langle i+\hat{k},i\rangle})_{ba}\right)^* \delta_{i+\hat{k},j}\right] \\
&= \frac{1}{2\kappa}\delta_{ij}\delta_{ab}\delta_{\gamma\gamma'} - \frac{1}{2}\delta_{\gamma\gamma'}\sum_k \left[(U^\dagger_{\langle j,j+\hat{k}\rangle})_{ab}\delta_{j+\hat{k},i} + (U^\dagger_{\langle i+\hat{k},i\rangle})_{ab}\delta_{i+\hat{k},j}\right] \\
&= B_{ia\gamma,jb\gamma'} ,
\end{aligned}$$

where we used $U_{\langle i,j\rangle} = U^\dagger_{\langle j,i\rangle}$ in the last step. Note that $c(U)$ is also Hermitian via the same line of argument because the Pauli-spin matrices σ_k are Hermitian.

Strict positivity of $B(U)$ is shown with a modification of the proof for the Geršgorin-Circle Theorem [100, 101]. Because $B(U)$ is Hermitian, it can be diagonalized with real eigenvalues. We can think of $B(U)$ as a matrix with site and spin indices whose components $B_{i\gamma,j\gamma'}(U)$ are (3×3)-matrices. Consider an eigenvalue λ and a corresponding eigenvector $u = (\ldots, u_{j\gamma'}, \ldots)$ with $u_{j\gamma'} \in \mathbb{R}^3$. There exists a site i and spin index γ such that $||u_{i\gamma}||_2$ is maximal among all sub-vectors $u_{j\gamma'}$ of u. We define the rescaled vector $v = ||u_{i\gamma}||_2^{-1} u$ such that $||v_{i\gamma}||_2 = 1$, and $||v_{j\gamma'}||_2 \leq 1$. We have

$$(Bv)_{i\gamma} = \frac{1}{2\kappa}v_{i\gamma} - \frac{1}{2}\sum_{j,k}\left[\delta_{i+\hat{k},j}U_{\langle i,i+\hat{k}\rangle}v_{j\gamma} + \delta_{j+\hat{k},i}U_{\langle j+\hat{k},j\rangle}v_{j\gamma}\right] = \lambda v_{i\gamma} .$$

Therefore, we get

$$2\left(\lambda - \frac{1}{2\kappa}\right)v_{i\gamma} = -\sum_{j,k}\left[\delta_{i+\hat{k},j}U_{\langle i,i+\hat{k}\rangle}v_{j\gamma} + \delta_{j+\hat{k},i}U_{\langle j+\hat{k},j\rangle}v_{j\gamma}\right] .$$

Taking the norm on both sides yields

$$\begin{aligned} 2\left|\lambda - \frac{1}{2\kappa}\right| &= \left|\left| \sum_{j,k} \left[\delta_{i+\hat{k},j} U_{\langle i,i+\hat{k}\rangle} v_{j\gamma} + \delta_{j+\hat{k},i} U_{\langle j+\hat{k},j\rangle} v_{j\gamma} \right] \right|\right|_2 \\ &\leq \sum_{j,k} \left[\delta_{i+\hat{k},j} \underbrace{||U_{\langle i,i+\hat{k}\rangle} v_{j\gamma}||_2}_{=||v_{j\gamma}||_2 \leq 1} + \delta_{j+\hat{k},i} ||U_{\langle j+\hat{k},j\rangle} v_{j\gamma}||_2 \right] \\ &\leq \sum_{j,k} \left[\delta_{i+\hat{k},j} + \delta_{j+\hat{k},i} \right] = 6\,. \end{aligned}$$

As a consequence, the eigenvalues must obey $|\lambda - (2\kappa)^{-1}| \leq 3$. The eigenvalues lie in the interval $\lambda \in [(2\kappa)^{-1} - 3, (2\kappa)^{-1} + 3]$. For $\kappa > 0$ and $\kappa < 1/6$, we notice that the interval only contains strictly positive numbers.

To make the coming calculations more comprehensible, we introduce a matrix notation. We suppress the indices of creation and annihilation operators and think of them being ordered in a vector, e.g. we write

$$\hat{\xi}_{\mathrm{q}} = \begin{pmatrix} \vdots \\ (\hat{\xi}^{\sigma}_{\mathrm{q}})_{i,a} \\ \vdots \end{pmatrix}.$$

Matrices M will have indices $M_{ia\gamma,jb\gamma'}$ as it is the case for $B(U)$ and $c(U)$. Hence, we can write matrix-vector products like $M\hat{\xi}_{\mathrm{q}}$. For vector-matrix products as $\hat{\xi}_{\mathrm{q}} M$, we implicitly assume that the vector on the left is written as a row vector $\hat{\xi}_{\mathrm{q}} = (\ldots, (\hat{\xi}^{\sigma}_{\mathrm{q}})_{i,a}, \ldots)$. Gauge transformations Ω assign to each site i an element $\Omega_i \in \mathrm{SU}(3)$. We can also think of them as matrices

$$\Omega_{ia\gamma,jb\gamma'} = \delta_{ij}\delta_{\gamma\gamma'}(\Omega_i)_{ab}\,.$$

Furthermore, we use the short-hand notation $\Omega^\dagger U \Omega$ to denote the gauge transformation of a gauge configuration:

$$\Omega^\dagger U \Omega = \{\ldots, \Omega_i^\dagger U_{\langle i,i+\hat{k}\rangle} \Omega_{i+\hat{k}}, \ldots\}\,.$$

The matrices B and c have the following obvious transformation properties:

$$c(\Omega^\dagger U \Omega) = \Omega^\dagger c(U) \Omega\,, \tag{3.20}$$

$$B(\Omega^\dagger U \Omega) = \Omega^\dagger B(U) \Omega\,. \tag{3.21}$$

Because a gauge transformation Ω is a unitary matrix, we can write

$$\ln\left(\mathrm{e}^{\Omega^\dagger (\ln B(U)) \Omega}\right) = \ln\left(\Omega^\dagger \mathrm{e}^{\ln B(U)} \Omega\right) = \ln\left(\Omega^\dagger B(U) \Omega\right)$$

which implies

$$\ln B(\Omega^\dagger U \Omega) = \Omega^\dagger (\ln B(U)) \Omega\,. \tag{3.22}$$

The same property holds for $B^{\frac{1}{2}}(U)$ because $B^{\frac{1}{2}}(U) = \exp\left(\frac{1}{2}\ln B(U)\right)$.

The derivation of the path integral requires the use of fermionic coherent states. We define the Grassmann generators

$$(\xi_{\mathrm{q}}^{\sigma})_{i,a},\ (\xi_{\overline{\mathrm{q}}}^{\sigma})_{i,a} \qquad \text{and} \qquad (\overline{\xi}_{\mathrm{q}}^{\sigma})_{i,a},\ (\overline{\xi}_{\overline{\mathrm{q}}}^{\sigma})_{i,a}\,.$$

The Grassmann generators are assumed to commute with all creation and annihilation operators. As usual, the fermionic coherent states are defined as

$$|\xi_{\mathrm{q}}, \xi_{\overline{\mathrm{q}}}\rangle = \exp\left(\sum_{i,a,\sigma}\left[(\xi_{\mathrm{q}}^{\sigma})_{i,a}(\hat{\xi}_{\mathrm{q}}^{\sigma})_{i,a}^{\dagger} + (\xi_{\overline{\mathrm{q}}}^{\sigma})_{i,a}(\hat{\xi}_{\overline{\mathrm{q}}}^{\sigma})_{i,a}^{\dagger}\right]\right)|0\rangle\ , \tag{3.23}$$

$$\langle\xi_{\mathrm{q}}, \xi_{\overline{\mathrm{q}}}| = \langle 0|\exp\left(\sum_{i,a,\sigma}\left[(\overline{\xi}_{\mathrm{q}}^{\sigma})_{i,a}(\hat{\xi}_{\mathrm{q}}^{\sigma})_{i,a} + (\overline{\xi}_{\overline{\mathrm{q}}}^{\sigma})_{i,a}(\hat{\xi}_{\overline{\mathrm{q}}}^{\sigma})_{i,a}\right]\right) \tag{3.24}$$

on $\mathcal{H}_{\mathrm{F}}$. This implies

$$(\hat{\xi}_{\mathrm{q}}^{\sigma})_{i,a}\,|\xi_{\mathrm{q}}, \xi_{\overline{\mathrm{q}}}\rangle = (\xi_{\mathrm{q}}^{\sigma})_{i,a}\,|\xi_{\mathrm{q}}, \xi_{\overline{\mathrm{q}}}\rangle\,, \qquad (\hat{\xi}_{\overline{\mathrm{q}}}^{\sigma})_{i,a}\,|\xi_{\mathrm{q}}, \xi_{\overline{\mathrm{q}}}\rangle = (\xi_{\overline{\mathrm{q}}}^{\sigma})_{i,a}\,|\xi_{\mathrm{q}}, \xi_{\overline{\mathrm{q}}}\rangle$$

and

$$\langle\xi_{\mathrm{q}}, \xi_{\overline{\mathrm{q}}}|\,(\hat{\xi}_{\mathrm{q}}^{\sigma})_{i,a}^{\dagger} = \langle\xi_{\mathrm{q}}, \xi_{\overline{\mathrm{q}}}|\,(\overline{\xi}_{\mathrm{q}}^{\sigma})_{i,a}, \qquad \langle\xi_{\mathrm{q}}, \xi_{\overline{\mathrm{q}}}|\,(\hat{\xi}_{\overline{\mathrm{q}}}^{\sigma})_{i,a}^{\dagger} = \langle\xi_{\mathrm{q}}, \xi_{\overline{\mathrm{q}}}|\,(\overline{\xi}_{\overline{\mathrm{q}}}^{\sigma})_{i,a}\,.$$

An important relation, which we are going to use later, is

$$\langle\xi_{\mathrm{q}}, \xi_{\overline{\mathrm{q}}}|\,\mathrm{e}^{\beta\mu\hat{N}} = \langle \mathrm{e}^{\beta\mu}\xi_{\mathrm{q}}, \mathrm{e}^{-\beta\mu}\xi_{\overline{\mathrm{q}}}|\ . \tag{3.25}$$

To prove this identity, the coherent state is expanded:

$$\langle\xi_{\mathrm{q}}, \xi_{\overline{\mathrm{q}}}| = \langle 0|\sum_{k=0}^{\infty}\frac{1}{k!}\sum_{\alpha_1,\ldots,\alpha_k}\hat{\xi}_{\alpha_1}\ldots\hat{\xi}_{\alpha_k}\overline{\xi}_{\alpha_1}\ldots\overline{\xi}_{\alpha_k}\,,$$

where we summarize all indices of the annihilation operators into a common index α_i. Therefore, we have

$$\langle\xi_{\mathrm{q}}, \xi_{\overline{\mathrm{q}}}|\,\mathrm{e}^{\beta\mu\hat{N}} = \langle 0|\sum_{k=0}^{\infty}\frac{1}{k!}\sum_{\alpha_1,\ldots,\alpha_k}\hat{\xi}_{\alpha_1}\ldots\hat{\xi}_{\alpha_k}\overline{\xi}_{\alpha_1}\ldots\overline{\xi}_{\alpha_k}\mathrm{e}^{\beta\mu(n_{\mathrm{q}}-n_{\overline{\mathrm{q}}})}\,.$$

The particle operator $\hat{N}$ just counts the total number of annihilation operators of quarks (n_{q}) and antiquarks ($n_{\overline{\mathrm{q}}}$). Hence, we can factorize $\mathrm{e}^{\beta\mu n_{\mathrm{q}}}$ and $\mathrm{e}^{-\beta\mu n_{\overline{\mathrm{q}}}}$ into factors $\mathrm{e}^{\beta\mu}$ and $\mathrm{e}^{-\beta\mu}$ and reorder them in front of the corresponding Grassmann generators:

$$(\overline{\xi}_{\mathrm{q}}^{\sigma})_{i,a} \longrightarrow \mathrm{e}^{\beta\mu}(\overline{\xi}_{\mathrm{q}}^{\sigma})_{i,a} \qquad \text{and} \qquad (\overline{\xi}_{\overline{\mathrm{q}}}^{\sigma})_{i,a} \longrightarrow \mathrm{e}^{-\beta\mu}(\overline{\xi}_{\overline{\mathrm{q}}}^{\sigma})_{i,a}\,.$$

Undoing the expansion then gives Equation (3.25). Also, we require the transformation law of coherent fermionic states under spatial gauge transformations:

$$\hat{\varrho}(\Omega)\,|\xi_{\mathrm{q}}, \xi_{\overline{\mathrm{q}}}\rangle = |\Omega\xi_{\mathrm{q}}, \xi_{\overline{\mathrm{q}}}\Omega^{\dagger}\rangle\ . \tag{3.26}$$

This identity can be proven by expanding Equation (3.23) and following the proof of Equation (3.25).

The Grassmann generators fulfill the usual identities

$$\mathbb{1} = \int \mathcal{D}\overline{\xi}\mathcal{D}\xi \, \mathrm{e}^{-\overline{\xi}_{\mathrm{q}}\xi_{\mathrm{q}} - \overline{\xi}_{\overline{\mathrm{q}}}\xi_{\overline{\mathrm{q}}}} \left|\xi_{\mathrm{q}}, \xi_{\overline{\mathrm{q}}}\right\rangle \left\langle \xi_{\mathrm{q}}, \xi_{\overline{\mathrm{q}}}\right| , \tag{3.27}$$

$$\mathrm{tr}(\hat{A}) = \int \mathcal{D}\overline{\xi}\mathcal{D}\xi \, \mathrm{e}^{-\overline{\xi}_{\mathrm{q}}\xi_{\mathrm{q}} - \overline{\xi}_{\overline{\mathrm{q}}}\xi_{\overline{\mathrm{q}}}} \left\langle \xi_{\mathrm{q}}, \xi_{\overline{\mathrm{q}}}\right| \hat{A} \left|-\xi_{\mathrm{q}}, -\xi_{\overline{\mathrm{q}}}\right\rangle \tag{3.28}$$

and

$$\left\langle \xi_{\mathrm{q}}, \xi_{\overline{\mathrm{q}}}\right| \mathrm{e}^{\sum_{\alpha\beta} \hat{\xi}^{\dagger}_{\alpha} A_{\alpha\beta} \hat{\xi}_{\beta}} \left|\eta_{\mathrm{q}}, \eta_{\overline{\mathrm{q}}}\right\rangle = \exp\left(\sum_{\alpha\beta} \overline{\xi}_{\alpha} \left(\mathrm{e}^{A}\right)_{\alpha\beta} \eta_{\beta} \right) , \tag{3.29}$$

$$\left\langle \xi_{\mathrm{q}}, \xi_{\overline{\mathrm{q}}}\right| \mathrm{e}^{\sum_{\alpha\beta} \hat{\xi}^{\dagger}_{\alpha} A_{\alpha\beta} \hat{\xi}_{\beta}} \mathrm{e}^{\sum_{\alpha\beta} \hat{\xi}^{\dagger}_{\alpha} B_{\alpha\beta} \hat{\xi}_{\beta}} \left|\eta_{\mathrm{q}}, \eta_{\overline{\mathrm{q}}}\right\rangle = \exp\left(\sum_{\alpha\beta} \overline{\xi}_{\alpha} \left(\mathrm{e}^{A}\mathrm{e}^{B}\right)_{\alpha\beta} \eta_{\beta} \right) . \tag{3.30}$$

on $\mathcal{H}_{\mathrm{F}}$; the indices α and β summarize again all indices of creation and annihilation operators, η_{q} and $\eta_{\overline{\mathrm{q}}}$ are different sets of Grassmann generators, and the matrix A and B are complex-valued.

Transfer operator

The integral kernel of Lüscher's transfer operator is defined as ([83])

$$K(U, U') = T_{\mathrm{F}}^{\dagger}(U) T_{\mathrm{G}}^{\frac{1}{2}}(U) S(U, U') T_{\mathrm{G}}^{\frac{1}{2}}(U') T_{\mathrm{F}}(U')$$

with

$$\begin{aligned} T_{\mathrm{F}}(U) = {} & (2\kappa)^{6N_{\mathrm{s}}} \sqrt{\det B(U)} \\ & \times \exp\left(-\hat{\xi}^{\dagger}_{\mathrm{q}} \left[\frac{1}{2} \ln B(U)\right] \hat{\xi}_{\mathrm{q}} + \hat{\xi}_{\overline{\mathrm{q}}} \left[\frac{1}{2} \ln B(U)\right] \hat{\xi}^{\dagger}_{\overline{\mathrm{q}}} \right) \\ & \times \exp\left(\hat{\xi}_{\overline{\mathrm{q}}} B^{-\frac{1}{2}}(U) c(U) B^{-\frac{1}{2}}(U) \hat{\xi}_{\mathrm{q}} \right) \end{aligned} ,$$

$$T_{\mathrm{G}}(U) = \exp\left(\frac{2}{g_0^2} \sum_{i,k<m} \mathrm{ReTr}\left(U_{\partial p_{i,km}} \right) \right) ,$$

$$S(U, U') = \exp\left(\frac{2}{g_0^2} \sum_{i,k} \mathrm{ReTr}\left(U_{\langle i, i+\hat{k}\rangle} U'_{\langle i+\hat{k}, i\rangle} \right) \right) .$$

The operators $T_{\mathrm{G}}(U)$ and $S(U, U')$ describe the pure gauge part and yield the Wilson plaquette action later on. In particular, $T_{\mathrm{G}}(U)$ describes plaquettes on spatial planes, and $S(U, U')$ describes timelike plaquettes but with the timelike gauge variables set to one. The form of the integral kernel is the apparent reason why the transfer operator of Lüscher is named the symmetric transfer operator. The operators $T_{\mathrm{G}}(U)$ and $T_{\mathrm{F}}(U)$ appear for the gauge configurations U and U'. The factors are symmetrically arranged around the timelike plaquette part $S(U, U')$. This arrangement guarantees $\hat{T}$ to be a Hermitian operator. The transfer operator can be written as

$$\hat{T} = \hat{T}_{\mathrm{F}}^{\dagger} \cdot \hat{T}_{\mathrm{G}}^{\dagger} \cdot \hat{S} \cdot \hat{T}_{\mathrm{G}} \cdot \hat{T}_{\mathrm{F}} ,$$

where $\hat{T}_\mathrm{F}$ and $\hat{T}_\mathrm{G}$ act by simply applying $T_\mathrm{F}(U)$ and $T_\mathrm{G}^{\frac{1}{2}}(U)$, whereas the operator $\hat{S}$ acts as

$$(\hat{S}f)(U) = \int \mathcal{D}U' S(U,U') f(U') \,.$$

The operator $\hat{S}$ is Hermitian because

$$\begin{aligned}\langle \hat{S}g, f\rangle &= \int \mathcal{D}U\mathcal{D}U' \overbrace{S^*(U,U')}^{=S(U',U)} g^*(U') f(U) \\ &= \int \mathcal{D}U'\mathcal{D}U\, g^*(U') S(U',U) f(U) \\ &= \langle g, \hat{S}f\rangle\end{aligned}$$

on $\mathcal{H}_\mathrm{G}$. Therefore, $\hat{T}$ remains invariant under Hermitian conjugation. Boundness and positivity are shown in [83]; there is no need for us to recap the proofs here.

More importantly, $\hat{T}$ is spatially gauge-invariant which, as we remember from above, ensures the thermodynamic ensemble to describe a system of physical states only. The operators $T_\mathrm{G}(U)$ and $T_\mathrm{F}(U)$ transform as

$$\hat{\varrho}(\Omega) T_\mathrm{G}(U) \hat{\varrho}^\dagger(\Omega) = T_\mathrm{G}(\Omega^\dagger U \Omega) = T_\mathrm{G}(U)$$

and

$$\begin{aligned}\hat{\varrho}(\Omega) T_\mathrm{F}(U) \hat{\varrho}^\dagger(\Omega) &= (2\kappa)^{6N_\mathrm{s}} \sqrt{\det B(\Omega^\dagger U \Omega)} \\ &\times \exp\left(- \hat{\xi}^\dagger_\mathrm{q} \Omega \left[\frac{1}{2} \ln B(\Omega^\dagger U \Omega)\right] \Omega^\dagger \hat{\xi}_\mathrm{q} + \hat{\xi}_{\bar{\mathrm{q}}} \Omega \left[\frac{1}{2} \ln B(\Omega^\dagger U \Omega)\right] \Omega^\dagger \hat{\xi}^\dagger_{\bar{\mathrm{q}}} \right) \\ &\times \exp\left(\hat{\xi}_{\bar{\mathrm{q}}} \Omega B^{-\frac{1}{2}}(\Omega^\dagger U \Omega) c(\Omega^\dagger U \Omega) B^{-\frac{1}{2}}(\Omega^\dagger U \Omega) \Omega^\dagger \hat{\xi}_\mathrm{q} \right)\end{aligned} \,. \tag{3.31}$$

Because of Equation (3.20), (3.21) and (3.22), all gauge transformations of U can be extracted from the arguments such that they are then compensated by the gauge transformations of the quarks and antiquarks, and, also,

$$\det B(\Omega^\dagger U \Omega) = \det(\Omega) \det(B(U)) \det(\Omega^\dagger) = \det B(U) \,.$$

Therefore, $T_F(U)$ is gauge-invariant. To see the gauge invariance of $\hat{S}$, we note

$$\begin{aligned}(\hat{\varrho}(\Omega) \hat{S} \hat{\varrho}^\dagger(\Omega) f)(U) &= (\hat{\varrho}(\Omega) \hat{S} f)(\Omega U \Omega^\dagger) \\ &= \int \mathcal{D}U'\, S(\Omega^\dagger U \Omega, U') f(\Omega U' \Omega^\dagger) \\ &= \int \mathcal{D}U'\, \underbrace{S(\Omega^\dagger U \Omega, \Omega^\dagger U' \Omega)}_{=S(U,U')} f(U') \\ &= (\hat{S}f)(U) \,.\end{aligned}$$

Partition function and path integral

The partition function discretized in Euclidean time with all lattice spacings set to one is given by the trace

$$Z = \mathrm{tr}\left(\mathrm{e}^{\beta\mu\hat{N}}\hat{T}^{N_4}\hat{P}_0\right), \tag{3.32}$$

where N_4 is the number of Euclidean time slices. The derivation of the path integral follows the usual line of argument [48, 83–86]. We insert Equation (3.27) between each product of transfer operators $\hat{T}$ and take the trace appropriately. In general, the trace can be computed by considering the trace over $\mathcal{H}_\mathrm{F}$ and $\mathcal{H}_\mathrm{G}$ separately. For an operator

$$\hat{K}(f(U)\otimes|\psi_\mathrm{F}\rangle) = \int \mathcal{D}U'\, K(U,U')(f(U')\otimes|\psi_\mathrm{F}\rangle),$$

we can use Equation (3.19) and write

$$\begin{aligned}\mathrm{tr}\,\hat{K} = \sum_{m,n}\sum_{\substack{\alpha_1,\ldots,\alpha_m\\ \beta_1,\ldots,\beta_n}}\left(\int \mathcal{D}U\, K^{\beta_1,\ldots,\beta_n}_{\alpha_1,\ldots,\alpha_m}(U,U)\right)\\ \times\int \mathcal{D}\overline{\xi}\mathcal{D}\xi\,\mathrm{e}^{-\overline{\xi}_\mathrm{q}\xi_\mathrm{q}-\overline{\xi}_{\overline{\mathrm{q}}}\xi_{\overline{\mathrm{q}}}}\langle\xi_\mathrm{q},\xi_{\overline{\mathrm{q}}}|\,\hat{\xi}^\dagger_{\alpha_1}\ldots\hat{\xi}_{\beta_n}\,|-\xi_\mathrm{q},-\xi_{\overline{\mathrm{q}}}\rangle\end{aligned}.$$

We have used the fact that the trace of an operator

$$(\hat{G}f)(U) = \int \mathcal{D}U'\, G(U,U')f(U')$$

on $\mathcal{H}_\mathrm{G}$ can be written as $\int \mathcal{D}U\, G(U,U)$ under certain prerequisites, see for example [102] and the references therein. The trace over the fermionic part was replaced with Equation (3.28). If we undo the expansion, we get

$$\mathrm{tr}\,\hat{K} = \int \mathcal{D}U\int \mathcal{D}\overline{\xi}\mathcal{D}\xi\,\mathrm{e}^{-\overline{\xi}_\mathrm{q}\xi_\mathrm{q}-\overline{\xi}_{\overline{\mathrm{q}}}\xi_{\overline{\mathrm{q}}}}\langle\xi_\mathrm{q},\xi_{\overline{\mathrm{q}}}|\,K(U,U)\,|-\xi_\mathrm{q},-\xi_{\overline{\mathrm{q}}}\rangle\,. \tag{3.33}$$

As usual, the traces introduce the anti-periodic boundary conditions for the fermionic fields and the periodic boundary conditions for the gauge variables.

Now, we just need to insert Equation (3.27) between the product of transfer operators $\hat{T}$:

$$Z = \mathrm{tr}\left(\mathrm{e}^{\beta\mu\hat{N}}\hat{P}_0\hat{T}\prod_{\tau=1}^{N_4-1}\left[\left(\mathbb{1}_\mathrm{G}\otimes\int\mathcal{D}\overline{\xi}\mathcal{D}\xi\,\mathrm{e}^{-\overline{\xi}\xi}\,|\xi_\mathrm{q},\xi_{\overline{\mathrm{q}}}\rangle\langle\xi_\mathrm{q},\xi_{\overline{\mathrm{q}}}|\right)_\tau\hat{T}\right]\right), \tag{3.34}$$

where the product is written from left to right with increasing τ and the subscript τ defines all Grassmann generators to possess this time index. Before we can continue with the derivation, we need to find an expression for $\hat{P}_0\hat{T}$:

$$\hat{P}_0\hat{T}(f(U)\otimes|\psi_\mathrm{F}\rangle) = \int\mathcal{D}\Omega\int\mathcal{D}U'\,K(U,U',\Omega)(f(U')\otimes\hat{\varrho}(\Omega)\,|\psi_\mathrm{F}\rangle) \tag{3.35}$$

Here, Equation (3.7) is used to replace $\hat{P}_0$, and the integral kernel $K(U, U', \Omega)$ is given by $K(U, U')$ of $\hat{T}$, but the gauge configuration U and all creation and annihilation operators are gauge-transformed:

$$K(U, U', \Omega) = T_{\mathrm{F}}^{\dagger}(U) T_{\mathrm{G}}^{\frac{1}{2}}(U) S(\Omega^{\dagger} U \Omega, U') T_{\mathrm{G}}^{\frac{1}{2}}(U') T_{\mathrm{F}}(U', \Omega)$$

and

$$\begin{aligned} T_{\mathrm{F}}(U', \Omega) = (2\kappa)^{6N_{\mathrm{s}}} \sqrt{\det B(U')} \\ \times \exp\left(-\hat{\xi}_{\mathrm{q}}^{\dagger} \Omega \left[\frac{1}{2} \ln B(U') \right] \Omega^{\dagger} \hat{\xi}_{\mathrm{q}} + \hat{\xi}_{\bar{\mathrm{q}}} \Omega \left[\frac{1}{2} \ln B(U') \right] \Omega^{\dagger} \hat{\xi}_{\bar{\mathrm{q}}}^{\dagger} \right) \\ \times \exp\left(\hat{\xi}_{\bar{\mathrm{q}}} \Omega B^{-\frac{1}{2}}(U') c(U') B^{-\frac{1}{2}}(U') \Omega^{\dagger} \hat{\xi}_{\mathrm{q}} \right) \end{aligned} .$$

Equation (3.25), (3.26), (3.33), (3.34) and (3.35) yield

$$\begin{aligned} Z = \int \mathcal{D}U \mathcal{D}\Omega \mathcal{D}\bar{\xi} \mathcal{D}\xi \, \mathrm{e}^{-\bar{\xi}\xi} \, \langle \mathrm{e}^{\beta\mu} \xi_{\mathrm{q}}^{(0)}, \mathrm{e}^{-\beta\mu} \xi_{\bar{\mathrm{q}}}^{(0)} | \, K(U_0, U_1, \Omega) \, | \Omega \xi_{\mathrm{q}}^{(1)}, \xi_{\bar{\mathrm{q}}}^{(1)} \Omega^{\dagger} \rangle \\ \times \prod_{\tau=1}^{N_4 - 1} \langle \xi_{\mathrm{q}}^{(\tau)}, \xi_{\bar{\mathrm{q}}}^{(\tau)} | \, K(U_\tau, U_{\tau+1}) \, | \xi_{\mathrm{q}}^{(\tau+1)}, \xi_{\bar{\mathrm{q}}}^{(\tau+1)} \rangle \end{aligned} \tag{3.36}$$

with the Euclidean time $\tau \in \{0, \ldots, N_4 - 1\}$, the gauge configuration U_τ of the τ-th layer of time, $U_{N_4} = U_0$ and $\xi^{(N_4)} = -\xi^{(0)}$. Equation (3.36) applies not only to the symmetric transfer operator but to all operators which can be written with a suitable integral kernel. Hence, we are going to use this equation again for the asymmetric transfer operator.

The next step of the derivation is the evaluation of the matrix elements in Equation (3.36). The computation makes use of Equation (3.29) and (3.30). This requires the exponents to be normal-ordered in $T_F(U)$. To this end, we use the anti-commutation relations such that

$$\exp\left(\hat{\xi}_{\bar{\mathrm{q}}} \left[\frac{1}{2} \ln B(U) \right] \hat{\xi}_{\bar{\mathrm{q}}}^{\dagger} \right) = \exp\left(\frac{1}{2} \operatorname{tr} \ln B(U) - \hat{\xi}_{\bar{\mathrm{q}}}^{\dagger} \left[\frac{1}{2} \ln B(U) \right]^{T} \hat{\xi}_{\bar{\mathrm{q}}} \right) \tag{3.37}$$

$$= \sqrt{\det B(U)} \exp\left(-\hat{\xi}_{\bar{\mathrm{q}}}^{\dagger} \left[\frac{1}{2} \ln B(U) \right]^{T} \hat{\xi}_{\bar{\mathrm{q}}} \right) \tag{3.38}$$

and, therefore,

$$\begin{aligned} T_{\mathrm{F}}(U) = (2\kappa)^{6N_{\mathrm{s}}} \det B(U) \\ \times \exp\left(-\hat{\xi}_{\mathrm{q}}^{\dagger} \left[\frac{1}{2} \ln B(U) \right] \hat{\xi}_{\mathrm{q}} - \hat{\xi}_{\bar{\mathrm{q}}}^{\dagger} \left[\frac{1}{2} \ln B(U) \right]^{T} \hat{\xi}_{\bar{\mathrm{q}}} \right) \\ \times \exp\left(\hat{\xi}_{\bar{\mathrm{q}}} B^{-\frac{1}{2}}(U) c(U) B^{-\frac{1}{2}}(U) \hat{\xi}_{\mathrm{q}} \right) \end{aligned} .$$

Now, we can just make use of the properties of coherent states and employ Equation (3.29) and (3.30). The matrix elements, then, read

$$\begin{aligned}
&\langle \xi_{\mathrm{q}}^{(\tau)}, \xi_{\overline{\mathrm{q}}}^{(\tau)} |\, K(U_\tau, U_{\tau+1}) \,| \xi_{\mathrm{q}}^{(\tau+1)}, \xi_{\overline{\mathrm{q}}}^{(\tau+1)} \rangle \\
&\quad = (2\kappa)^{12N_{\mathrm{s}}} \det(B(U_\tau)) \det(B(U_{\tau+1})) T_{\mathrm{G}}^{\frac{1}{2}}(U_\tau) S(U_\tau, U_{\tau+1}) T_{\mathrm{G}}^{\frac{1}{2}}(U_{\tau+1}) \\
&\quad \times \exp\left(\overline{\xi}_{\mathrm{q}}^{(\tau)} B^{-\frac{1}{2}}(U_\tau) c(U_\tau) B^{-\frac{1}{2}}(U_\tau) \overline{\xi}_{\overline{\mathrm{q}}}^{(\tau)} \right) \\
&\quad \times \exp\left(\xi_{\overline{\mathrm{q}}}^{(\tau+1)} B^{-\frac{1}{2}}(U_{\tau+1}) c(U_{\tau+1}) B^{-\frac{1}{2}}(U_{\tau+1}) \xi_{\mathrm{q}}^{(\tau+1)} \right) \\
&\quad \times \exp\left(\overline{\xi}_{\mathrm{q}}^{(\tau)} B^{-\frac{1}{2}}(U_\tau) B^{-\frac{1}{2}}(U_{\tau+1}) \xi_{\mathrm{q}}^{(\tau+1)} - \xi_{\overline{\mathrm{q}}}^{(\tau+1)} B^{-\frac{1}{2}}(U_{\tau+1}) B^{-\frac{1}{2}}(U_\tau) \overline{\xi}_{\overline{\mathrm{q}}}^{(\tau)} \right)
\end{aligned}$$

Analogously, the matrix element between the zeroth and first layer of time is

$$\begin{aligned}
&\langle \mathrm{e}^{\beta\mu} \xi_{\mathrm{q}}^{(0)}, \mathrm{e}^{-\beta\mu} \xi_{\overline{\mathrm{q}}}^{(0)} |\, K(U_0, U_1, \Omega) \,| \Omega \xi_{\mathrm{q}}^{(1)}, \xi_{\overline{\mathrm{q}}}^{(1)} \Omega^\dagger \rangle \\
&\quad = (12\kappa)^{12N_{\mathrm{s}}} \det(B(U_0)) \det(B(U_1)) T_{\mathrm{G}}^{\frac{1}{2}}(U_0) S(\Omega^\dagger U_0 \Omega, U_1) T_{\mathrm{G}}^{\frac{1}{2}}(U_1) \\
&\quad \times \exp\left(\overline{\xi}_{\mathrm{q}}^{(0)} B^{-\frac{1}{2}}(U_0) c(U_0) B^{-\frac{1}{2}}(U_0) \overline{\xi}_{\overline{\mathrm{q}}}^{(0)} \right) \\
&\quad \times \exp\left(\xi_{\overline{\mathrm{q}}}^{(1)} B^{-\frac{1}{2}}(U_1) c(U_1) B^{-\frac{1}{2}}(U_1) \xi_{\mathrm{q}}^{(1)} \right) \\
&\quad \times \exp\Bigg(\overline{\xi}_{\mathrm{q}}^{(0)} B^{-\frac{1}{2}}(U_0) \mathrm{e}^{\beta\mu} \Omega B^{-\frac{1}{2}}(U_1) \xi_{\mathrm{q}}^{(1)} \\
&\qquad\qquad - \xi_{\overline{\mathrm{q}}}^{(1)} B^{-\frac{1}{2}}(U_1) \mathrm{e}^{-\beta\mu} \Omega^\dagger B^{-\frac{1}{2}}(U_0) \overline{\xi}_{\overline{\mathrm{q}}}^{(0)} \Bigg)
\end{aligned}$$

Consequently, Equation (3.36) reduces to

$$\begin{aligned}
Z = (2\kappa)^{12N_{\mathrm{s}}N_4} \int \mathcal{D}U \mathcal{D}\Omega \mathcal{D}\overline{\xi} \mathcal{D}\xi \left[\prod_{\tau=0}^{N_4-1} (\det B(U_\tau))^2 \right] \mathrm{e}^{S_{\mathrm{F}}(U,\Omega,\overline{\xi},\xi)} \\
\times T_{\mathrm{G}}(U_0) S(\Omega^\dagger U_0 \Omega, U_1) \left[\prod_{\tau=1}^{N_4-1} T_{\mathrm{G}}(U_\tau) S(U_\tau, U_{\tau+1}) \right].
\end{aligned}$$

The fermionic action

$$\begin{aligned}
S_{\mathrm{F}}(U,\Omega,\overline{\xi},\xi) = &- \sum_{\tau=0}^{N_4-1} \left(\overline{\xi}_{\mathrm{q}}^{(\tau)} \xi_{\mathrm{q}}^{(\tau)} - \xi_{\overline{\mathrm{q}}}^{(\tau)} \overline{\xi}_{\overline{\mathrm{q}}}^{(\tau)} \right) \\
&+ \sum_{\tau=0}^{N_4-1} \Big(\overline{\xi}_{\mathrm{q}}^{(\tau)} B^{-\frac{1}{2}}(U_\tau) \Big[\delta_{\tau,0} \mathrm{e}^{\beta\mu} \Omega + (1 - \delta_{\tau,0}) \Big] B^{-\frac{1}{2}}(U_{\tau+1}) \xi_{\mathrm{q}}^{(\tau+1)} \\
&\qquad - \xi_{\overline{\mathrm{q}}}^{(\tau+1)} B^{-\frac{1}{2}}(U_{\tau+1}) \Big[\delta_{\tau,0} \mathrm{e}^{-\beta\mu} \Omega^\dagger + (1 - \delta_{\tau,0}) \Big] B^{-\frac{1}{2}}(U_\tau) \overline{\xi}_{\overline{\mathrm{q}}}^{(\tau)} \Big) \\
&+ \sum_{\tau=0}^{N_4-1} \overline{\xi}_{\mathrm{q}}^{(\tau)} B^{-\frac{1}{2}}(U_\tau) c(U_\tau) B^{-\frac{1}{2}}(U_\tau) \overline{\xi}_{\overline{\mathrm{q}}}^{(\tau)} \\
&+ \sum_{\tau=0}^{N_4-1} \xi_{\overline{\mathrm{q}}}^{(\tau+1)} B^{-\frac{1}{2}}(U_{\tau+1}) c(U_{\tau+1}) B^{-\frac{1}{2}}(U_{\tau+1}) \xi_{\mathrm{q}}^{(\tau+1)}
\end{aligned}$$

is just the summary of all bilinear Grassmann forms of the matrix elements. However, this fermionic action is of preliminary nature and we still need to switch to different variables such that we end with the standard Hasenfratz-Karsch action of Equation (2.4). This is done with two subsequent transformations of the variables [83]. The first substitution is given by

$$\begin{aligned} \overline{\xi}_{\mathrm{q}}^{(\tau)} &\to \overline{\xi}_{\mathrm{q}}^{(\tau)} B^{\frac{1}{2}}(U_\tau), & \xi_{\mathrm{q}}^{(\tau)} &\to B^{\frac{1}{2}}(U_\tau)\xi_{\mathrm{q}}^{(\tau)}, \\ \overline{\xi}_{\overline{\mathrm{q}}}^{(\tau)} &\to B^{\frac{1}{2}}(U_\tau)\overline{\xi}_{\overline{\mathrm{q}}}^{(\tau)}, & \xi_{\overline{\mathrm{q}}}^{(\tau)} &\to \xi_{\overline{\mathrm{q}}}^{(\tau)} B^{\frac{1}{2}}(U_\tau). \end{aligned}$$

This transformation removes the matrices $B^{-\frac{1}{2}}(U_\tau)$ from the action and inserts $B(U_\tau)$ into the equal-time part of the action:

$$\begin{aligned} S_{\mathrm{F}}(U,\Omega,\overline{\xi},\xi) = &+ \sum_{\tau=0}^{N_4-1} \Bigg(\overline{\xi}_{\mathrm{q}}^{(\tau)} \Big[\delta_{\tau,0} \mathrm{e}^{\beta\mu} \Omega + (1-\delta_{\tau,0}) \Big] \xi_{\mathrm{q}}^{(\tau+1)} \\ &\quad - \xi_{\overline{\mathrm{q}}}^{(\tau+1)} \Big[\delta_{\tau,0} \mathrm{e}^{-\beta\mu} \Omega^\dagger + (1-\delta_{\tau,0}) \Big] \overline{\xi}_{\overline{\mathrm{q}}}^{(\tau)} \Bigg) \\ &- \sum_{\tau=0}^{N_4-1} \Big(\overline{\xi}_{\mathrm{q}}^{(\tau)} B(U_\tau) \xi_{\mathrm{q}}^{(\tau)} - \xi_{\overline{\mathrm{q}}}^{(\tau)} B(U_\tau) \overline{\xi}_{\overline{\mathrm{q}}}^{(\tau)} \Big) \\ &+ \sum_{\tau=0}^{N_4-1} \overline{\xi}_{\mathrm{q}}^{(\tau)} c(U_\tau) \overline{\xi}_{\overline{\mathrm{q}}}^{(\tau)} + \sum_{\tau=0}^{N_4-1} \xi_{\overline{\mathrm{q}}}^{(\tau)} c(U_\tau) \xi_{\mathrm{q}}^{(\tau)} \end{aligned}.$$

Of course, we have to consider the determinant of the Jacobian matrix. Here, we get the factor $(\det B(U_\tau))^{-2}$ for every layer of Euclidean time; they are fully compensated by the factors $(\det B(U_\tau))^2$ in the partition function Z. To arrive at the desired form of the action, we introduce the Dirac spinors

$$\begin{aligned} (\overline{\xi}_{\mathrm{q}}^{\uparrow})_{i,a}^{(\tau)} &\longrightarrow \overline{\psi}_{(i,\tau)}^{a1}, & (\xi_{\mathrm{q}}^{\uparrow})_{i,a}^{(\tau)} &\longrightarrow \psi_{(i,\tau)}^{a1}, \\ (\overline{\xi}_{\mathrm{q}}^{\downarrow})_{i,a}^{(\tau)} &\longrightarrow \overline{\psi}_{(i,\tau)}^{a2}, & (\xi_{\mathrm{q}}^{\downarrow})_{i,a}^{(\tau)} &\longrightarrow \psi_{(i,\tau)}^{a2}, \\ (\overline{\xi}_{\overline{\mathrm{q}}}^{\uparrow})_{i,a}^{(\tau)} &\longrightarrow \psi_{(i,\tau)}^{a3}, & (\xi_{\overline{\mathrm{q}}}^{\uparrow})_{i,a}^{(\tau)} &\longrightarrow \overline{\psi}_{(i,\tau)}^{a3}, \\ (\overline{\xi}_{\overline{\mathrm{q}}}^{\downarrow})_{i,a}^{(\tau)} &\longrightarrow \psi_{(i,\tau)}^{a4}, & (\xi_{\overline{\mathrm{q}}}^{\downarrow})_{i,a}^{(\tau)} &\longrightarrow \overline{\psi}_{(i,\tau)}^{a4}. \end{aligned}$$

This gives us

$$\begin{aligned} S_{\mathrm{F}}(U,\Omega,\overline{\psi},\psi) = &- \sum_{\tau=0}^{N_4-1} \Bigg(\overline{\psi}^{(\tau)} \frac{1}{2}(1+\gamma_4) \Big[\delta_{\tau,0} \mathrm{e}^{\beta\mu} \Omega + (1-\delta_{\tau,0}) \Big] \psi^{(\tau+1)} \\ &\quad - \overline{\psi}^{(\tau+1)} \frac{1}{2}(1-\gamma_4) \Big[\delta_{\tau,0} \mathrm{e}^{-\beta\mu} \Omega^\dagger + (1-\delta_{\tau,0}) \Big] \psi^{(\tau)} \Bigg) \\ &- \sum_{\tau=0}^{N_4-1} \Big(\overline{\psi}^{(\tau)} \frac{1}{2}(1+\gamma_4) B(U_\tau) \psi^{(\tau)} - \overline{\psi}^{(\tau)} \frac{1}{2}(1-\gamma_4) B(U_\tau) \psi^{(\tau)} \Big) \\ &+ \sum_{\tau=0}^{N_4-1} \overline{\psi}^{(\tau)} \frac{1}{2}(1+\gamma_4) C(U_\tau) \psi^{(\tau)} - \sum_{\tau=0}^{N_4-1} \overline{\psi}^{(\tau)} \frac{1}{2}(1-\gamma_4) C(U_\tau) \psi^{(\tau)} \end{aligned}.$$

We have just renamed the integration variables. Therefore, we have the replacement rule

$$\mathrm{d}(\overline{\xi}^{\sigma}_{\overline{\mathrm{q}}})^{(\tau)}_{i,a}\mathrm{d}(\xi^{\sigma}_{\overline{\mathrm{q}}})^{(\tau)}_{i,a} \longrightarrow \mathrm{d}\psi^{a\alpha}_{(i,\tau)}\mathrm{d}\overline{\psi}^{a\alpha}_{(i,\tau)}$$

for the integration measure of antiquarks. However, we need to permute the variables in order to bring the measure of the path integral into the canonical form $\mathcal{D}\overline{\psi}\mathcal{D}\psi$. Transposing each pair gives a minus sign:

$$\mathrm{d}\psi^{a\alpha}_{(i,\tau)}\mathrm{d}\overline{\psi}^{a\alpha}_{(i,\tau)} = -\mathrm{d}\overline{\psi}^{a\alpha}_{(i,\tau)}\mathrm{d}\psi^{a\alpha}_{(i,\tau)}$$

But there are $6N_{\mathrm{s}}N_4$ pairs which have to be rearranged. Consequently, the global sign is just one. The fermionic action can be condensed further:

$$\begin{aligned} S_{\mathrm{F}}(U,\Omega,\overline{\psi},\psi) = &\sum_{\tau=0}^{N_4-1}\overline{\psi}^{(\tau)}\gamma_4\big[C(U_\tau)-B(U_\tau)\big]\psi^{(\tau)} \\ &-\sum_{\tau=0}^{N_4-1}\Bigg(\overline{\psi}^{(\tau)}\frac{1}{2}(1+\gamma_4)\Big[\delta_{\tau,0}\mathrm{e}^{\beta\mu}\Omega+(1-\delta_{\tau,0})\Big]\psi^{(\tau+1)} \\ &\quad-\overline{\psi}^{(\tau+1)}\frac{1}{2}(1-\gamma_4)\Big[\delta_{\tau,0}\mathrm{e}^{-\beta\mu}\Omega^{\dagger}+(1-\delta_{\tau,0})\Big]\psi^{(\tau)}\Bigg) \quad . \end{aligned} \tag{3.39}$$

The difference between the matrices $C(U_\tau)$ and $B(U_\tau)$ is

$$\begin{aligned} &\big[C(U_\tau)-B(U_\tau)\big]_{ia\alpha,jb\beta} \\ &\quad= -\frac{1}{2\kappa}\delta_{ij}\delta_{ab}\delta_{\alpha\beta}+\frac{1}{2}\sum_k\Big[(U_{\langle i,i+\hat{k}\rangle})_{ab}(1+\gamma_k)_{\alpha\beta}\delta_{i+\hat{k},j} \\ &\qquad\qquad+(U_{\langle j+\hat{k},j\rangle})_{ab}(1-\gamma_k)_{\alpha\beta}\delta_{j+\hat{k},j}\Big]. \end{aligned}$$

Inserting this into the action, applying the second substitution

$$\overline{\psi}^{(\tau)} \longrightarrow \overline{\psi}^{(\tau)}(2\kappa\gamma_4)$$

and reordering the terms appropriately gives

$$\begin{aligned} S_{\mathrm{F}}(U,\Omega,\overline{\psi},\psi) = &-\sum_{\tau=0}^{N_4-1}\overline{\psi}^{(\tau)}\psi^{(\tau)} \\ &+\kappa\sum_{\tau=0}^{N_4-1}\Bigg(\overline{\psi}^{(\tau)}(1+\gamma_4)\Big[\delta_{\tau,0}\mathrm{e}^{\beta\mu}\Omega+(1-\delta_{\tau,0})\Big]\psi^{(\tau+1)} \\ &\qquad+\overline{\psi}^{(\tau+1)}(1-\gamma_4)\Big[\delta_{\tau,0}\mathrm{e}^{-\beta\mu}\Omega^{\dagger}+(1-\delta_{\tau,0})\Big]\psi^{(\tau)}\Bigg) \quad . \\ &+\kappa\sum_{\tau=0}^{N_4-1}\sum_{i,k}\Bigg(\overline{\psi}_{(i,\tau)}\Big(U^{(\tau)}_{\langle i,i+\hat{k}\rangle}\Big)(1+\gamma_k)\psi_{(i+\hat{k},\tau)} \\ &\qquad+\overline{\psi}_{(i+\hat{k},\tau)}\Big(U^{(\tau)}_{\langle i+\hat{k},i\rangle}\Big)(1-\gamma_k)\psi_{(i,\tau)}\Bigg) \end{aligned}$$

This is the Hasenfratz-Karsch action with the temporal direction gauge-fixed maximally to unity if we identify $U_{\langle(i,\tau),(j,\tau)\rangle} = U^{(\tau)}_{\langle i,j\rangle}$ and $U_{\langle(i,0),(i,1)\rangle} = \Omega_i$. The

determinant of this substitution is $(2\kappa)^{-12N_sN_4}$ which is again fully compensated by the prefactor in Z. Certainly, this form of the action still differs from Equation (2.4) because the gamma matrices have a different sign convention. However, the signs in front of the gamma matrices can always be flipped by the unitary transformation

$$-\gamma_\mu = M\gamma_\mu M^\dagger \qquad \text{with} \qquad M = \begin{pmatrix} 0 & \mathbb{1}_2 \\ \mathbb{1}_2 & 0 \end{pmatrix} . \tag{3.40}$$

Finally, we compute the pure gauge part by summarizing the exponents of the transfer operators S and T_F:

$$\mathrm{e}^{S_\mathrm{G}(U,\Omega)} = T_\mathrm{G}(U_0)S(\Omega^\dagger U_0 \Omega, U_1)\left[\prod_{\tau=1}^{N_4-1} T_\mathrm{G}(U_\tau)S(U_\tau, U_{\tau+1})\right]$$

with

$$\begin{aligned} S_\mathrm{G}(U,\Omega) =& \frac{2}{g_0^2}\sum_{\tau=0}^{N_4-1}\sum_{i,k<m}\mathrm{ReTr}\left(U^{(\tau)}_{\partial p_{i,km}}\right) \\ &+\frac{2}{g_0^2}\sum_{\tau=0}^{N_4-1}\sum_{i,k}\mathrm{ReTr}\Big(\Big[\delta_{\tau,0}\Omega_i^\dagger + (1-\delta_{\tau,0})\Big]U^{(\tau)}_{\langle i,i+\hat{k}\rangle} \\ &\qquad\qquad \times\Big[\delta_{\tau,0}\Omega_{i+\hat{k}} + (1-\delta_{\tau,0})\Big]U^{(\tau+1)}_{\langle i+\hat{k},i\rangle}\Big) \end{aligned} . \tag{3.41}$$

Obviously, this is the Wilson plaquette action with all temporal links gauge-fixed maximally to unity if we again identify $U_{\langle(i,0),(i,1)\rangle} = \Omega_i$.

In summary, we have shown that the partition function (3.32) of the transfer operator $\hat{T}$ gives the path integral of Lattice QCD.

Euclidean time continuum

Because we want to think of the path integral as the discretization of some quantum-mechanical system, we have to show that there exists a gauge-invariant Hamiltonian $\hat{H}$ such that

$$\lim_{N_4\to\infty}\left(\hat{T}_{a_4=\beta/N_4}\right)^{N_4} = \mathrm{e}^{-\beta\hat{H}} .$$

To this end, we have to introduce the lattice spacings into the path integral and the transfer operator $\hat{T}_{a_4}$: a_4 is the spacing in the direction of time and a is the spacing in a direction of space. The transfer operator $\hat{T}$ is then just the special case $a_4 = a = 1$.

From the previous chapter, we know that the path integral with asymmetric lattice spacings is given by Equation (2.3) and (2.4). The timelike plaquette part is multiplied with the factor a/a_4, the spatial plaquette part is multiplied with the factor a_4/a, the hopping parameter κ is replaced with $s(a_4, a)$ for timelike hops in S_F, and the hopping parameter κ is replaced with $\frac{a_4}{a}s(a_4, a)$ for spatial hops in S_F. Remember that

$$s(a_4, a) = \frac{1}{2a_4(m + 3a^{-1}) + 2} .$$

The transfer operator $\hat{T}_{a_4}$ is defined by modifying $\hat{T}$ in a suitable way. First, we need to modify the matrix $B(U)$:

$$B_{ia\gamma,jb\gamma'} = \frac{a}{2a_4 s(a_4,a)}\delta_{ij}\delta_{ab}\delta_{\gamma\gamma'} - \frac{1}{2}\delta_{\gamma\gamma'}\sum_k \left[(U_{\langle i,i+\hat{k}\rangle})_{ab}\delta_{i+\hat{k},j} + (U_{\langle j+\hat{k},j\rangle})_{ab}\delta_{j+\hat{k},i}\right] . \quad (3.42)$$

The prefactor of the diagonal part diverges for $a_4 \to 0$:

$$\frac{a}{2a_4 s(a_4,a)} = (m + 3a^{-1}) + \frac{1}{a_4} \longrightarrow \infty .$$

Therefore, if a_4 is sufficiently small, we can guarantee strict positivity of $B(U)$ because strict positivity is guaranteed for sufficiently large $(2\kappa)^{-1}$ in the original form of $B(U)$. Furthermore, we have to modify the different components of the transfer operator. $T_{\mathrm{G}}(U)$ and $S(U,U')$ are modified in the obvious way by inserting the factor a/a_4 into the exponent of $S(U,U')$ and the factor a_4/a into the exponent of $T_{\mathrm{G}}(U)$. In the fermionic operator $T_{\mathrm{F}}(U)$, we replace all matrices $B(U)$ and $c(U)$ with $\frac{a_4}{a}B(U)$ and $\frac{a_4}{a}c(U)$, and we replace the factor $(2\kappa)^{6N_{\mathrm{s}}}$ with $(2s(a_4,a))^{6N_{\mathrm{s}}}$.

The modified transfer operator $\hat{T}_{a_4}$ inserted into Equation (3.32) gives the path integral of Lattice QCD with asymmetric lattice spacings a_4 and a. This can be verified easily by repeating the same derivation as above and using the modified substitutions

$$\overline{\xi}^{(\tau)}_{\mathrm{q}} \to \overline{\xi}^{(\tau)}_{\mathrm{q}}\left[\frac{a_4}{a}B(U_\tau)\right]^{\frac{1}{2}}, \qquad \xi^{(\tau)}_{\mathrm{q}} \to \left[\frac{a_4}{a}B(U_\tau)\right]^{\frac{1}{2}}\xi^{(\tau)}_{\mathrm{q}},$$
$$\overline{\xi}^{(\tau)}_{\overline{\mathrm{q}}} \to \left[\frac{a_4}{a}B(U_\tau)\right]^{\frac{1}{2}}\overline{\xi}^{(\tau)}_{\overline{\mathrm{q}}}, \qquad \xi^{(\tau)}_{\overline{\mathrm{q}}} \to \xi^{(\tau)}_{\overline{\mathrm{q}}}\left[\frac{a_4}{a}B(U_\tau)\right]^{\frac{1}{2}}$$

and

$$\overline{\psi}^{(\tau)} \longrightarrow \overline{\psi}^{(\tau)}(2s(a_4,a)\gamma_4) .$$

To find the Hamiltonian $\hat{H}$, we expand the transfer operator to linear order:

$$\mathcal{N}(a_4)\hat{T}_{a_4} = \mathbb{1} - a_4\hat{H} + \mathcal{O}(a_4^2) ,$$

where $\mathcal{N}(a_4)$ is an additional normalization constant discussed below. We then hope $\hat{H}$ to be Hermitian, gauge-invariant and independent of a_4 such that

$$\lim_{N_4\to\infty}\left(\mathcal{N}(a_4)\hat{T}_{a_4=\beta/N_4}\right)^{N_4} = \lim_{N_4\to\infty}\left(\mathbb{1} - \frac{\beta}{N_4}\hat{H} + \mathcal{O}(a_4^2)\right)^{N_4} = \mathrm{e}^{-\beta\hat{H}} .$$

We decompose the transfer operator $\hat{T}_{a_4}$ into the operators $\hat{T}_{\mathrm{F},a_4}$, $\hat{T}_{\mathrm{G},a_4}$ and $\hat{S}_{a_4}$ and expand each operator separately:

$$\begin{aligned}\mathcal{N}(a_4)\hat{T}_{a_4} &= \hat{T}^{\dagger}_{\mathrm{F},a_4}\cdot\hat{T}^{\dagger}_{\mathrm{G},a_4}\cdot(\mathcal{N}(a_4)\hat{S}_{a_4})\cdot\hat{T}_{\mathrm{G},a_4}\cdot\hat{T}_{\mathrm{F},a_4}\\ &= \ldots\cdot\left(\mathbb{1} - a_4\hat{h}_{\mathrm{S}} + \mathcal{O}(a_4^2)\right)\left(\mathbb{1} - a_4\hat{h}_{\mathrm{G}} + \mathcal{O}(a_4^2)\right)\left(\mathbb{1} - a_4\hat{h}_{\mathrm{F}} + \mathcal{O}(a_4^2)\right)\\ &= \mathbb{1} - a_4\left(\hat{h}_{\mathrm{S}} + \hat{h}_{\mathrm{G}} + \hat{h}^{\dagger}_{\mathrm{G}} + \hat{h}_{\mathrm{F}} + \hat{h}^{\dagger}_{\mathrm{F}}\right) + \mathcal{O}(a_4^2) .\end{aligned}$$

We start the derivation of $\hat{H}$ with the fermionic part $\hat{h}_{\mathrm{F}}$. To this end, we first define the matrix $R(U)$ as the non-diagonal elements of $B(U)$:

$$B(U) = \frac{a}{2a_4 s(a_4, a)} \mathbb{1} + R(U) \,.$$

Furthermore, we have

$$s(a_4, a) = \frac{1}{2} - \frac{m + 3a^{-1}}{2} a_4 + \mathcal{O}(a_4^2) \,.$$

Now, we can compute various expansions which then are just inserted into $\hat{T}_{\mathrm{F},a_4}$:

$$\frac{a_4}{a} B(U) = \frac{1}{2s(a_4, a)} \left(\mathbb{1} + \frac{2a_4}{a} s(a_4, a) R(U) \right) , \tag{3.43}$$

$$\ln\left(\frac{a_4}{a} B(U) \right) = a_4 (m + 3a^{-1}) + \frac{a_4}{a} R(U) + \mathcal{O}(a_4^2) \,, \tag{3.44}$$

$$\begin{aligned} \left(\frac{a_4}{a} B(U) \right)^{\pm \frac{1}{2}} &= \exp\left(\pm \frac{1}{2} \ln\left(\frac{a_4}{a} B(U) \right) \right) \\ &= \mathbb{1} \pm \frac{a_4 (m + 3a^{-1})}{2} \pm \frac{a_4}{2a} R(U) + \mathcal{O}(a_4^2) \end{aligned} \tag{3.45}$$

and, with $\det(1 + \varepsilon M) = 1 + \varepsilon \operatorname{tr} M + \mathcal{O}(\varepsilon^2)$, we get

$$\begin{aligned} \sqrt{\det\left(\frac{a_4}{a} B(U) \right)} &= (2s(a_4, a))^{-3N_{\mathrm{s}}} \det\left(\left[\mathbb{1} + \frac{2a_4}{a} s(a_4, a) R(U) \right]^{\frac{1}{2}} \right) \\ &= (2s(a_4, a))^{-3N_{\mathrm{s}}} \det\left[\exp\left(\frac{1}{2} \ln\left(\mathbb{1} + \frac{2a_4}{a} s(a_4, a) R(U) \right) \right) \right] \\ &= (2s(a_4, a))^{-3N_{\mathrm{s}}} \det\left(\mathbb{1} + \frac{a_4}{2a} R(U) + \mathcal{O}(a_4^2) \right) \\ &= (2s(a_4, a))^{-3N_{\mathrm{s}}} \left(1 + \frac{a_4}{2a} \operatorname{tr} R(U) + \mathcal{O}(a_4^2) \right) \\ &= (2s(a_4, a))^{-3N_{\mathrm{s}}} \left(1 + \mathcal{O}(a_4^2) \right) . \end{aligned}$$

Next, we have

$$\left(\frac{a_4}{a} B(U) \right)^{-\frac{1}{2}} \left(\frac{a_4}{a} c(U) \right) \left(\frac{a_4}{a} B(U) \right)^{-\frac{1}{2}} = \frac{a_4}{a} c(U) + \mathcal{O}(a_4^2) \,.$$

With these expansions, the different parts of the operator $T_{\mathrm{F},a_4}(U)$ are linearized as

$$\begin{aligned} &\exp\left(- \hat{\xi}_{\mathrm{q}}^{\dagger} \left[\frac{1}{2} \ln\left(\frac{a_4}{a} B(U) \right) \right] \hat{\xi}_{\mathrm{q}} + \hat{\xi}_{\overline{\mathrm{q}}} \left[\frac{1}{2} \ln\left(\frac{a_4}{a} B(U) \right) \right] \hat{\xi}_{\overline{\mathrm{q}}}^{\dagger} \right) \\ &\quad = \mathbb{1} - a_4 \Bigg(\hat{\xi}_{\mathrm{q}}^{\dagger} \left[\frac{(m + 3a^{-1})}{2} + \frac{1}{2a} R(U) \right] \hat{\xi}_{\mathrm{q}} \\ &\qquad\qquad - \hat{\xi}_{\overline{\mathrm{q}}} \left[\frac{(m + 3a^{-1})}{2} + \frac{1}{2a} R(U) \right] \hat{\xi}_{\overline{\mathrm{q}}}^{\dagger} \Bigg) + \mathcal{O}(a_4^2) \end{aligned}$$

and

$$\exp\left(\hat{\xi}_{\bar{\mathrm{q}}}\left(\frac{a_4}{a}B(U)\right)^{-\frac{1}{2}}\left(\frac{a_4}{a}c(U)\right)\left(\frac{a_4}{a}B(U)\right)^{-\frac{1}{2}}\hat{\xi}_{\mathrm{q}}\right)$$
$$=\hat{\xi}_{\bar{\mathrm{q}}}\left[\frac{a_4}{a}c(U)\right]\hat{\xi}_{\mathrm{q}}+\mathcal{O}(a_4^2)\,.$$

We also have to consider the prefactor of $T_{\mathrm{F},a_4}(U)$:

$$(2s(a_4,a))^{6N_{\mathrm{s}}}\sqrt{\det\left(\frac{a_4}{a}B(U)\right)}=1-a_4(m+3a^{-1})+\mathcal{O}(a_4^2)\,.$$

If we summarize all linear terms, we get

$$\begin{aligned}\hat{h}_{\mathrm{F}}+\hat{h}_{\mathrm{F}}^{\dagger}=&2(m+3a^{-1})+\hat{\xi}_{\mathrm{q}}^{\dagger}\left[(m+3a^{-1})+\frac{1}{a}R(U)\right]\hat{\xi}_{\mathrm{q}}\\&-\hat{\xi}_{\bar{\mathrm{q}}}\left[(m+3a^{-1})+\frac{1}{a}R(U)\right]\hat{\xi}_{\bar{\mathrm{q}}}^{\dagger}-\hat{\xi}_{\bar{\mathrm{q}}}\left[\frac{1}{a}c(U)\right]\hat{\xi}_{\mathrm{q}}-\hat{\xi}_{\mathrm{q}}^{\dagger}\left[\frac{1}{a}c(U)\right]\hat{\xi}_{\bar{\mathrm{q}}}^{\dagger}\end{aligned}\,.$$

We introduce the creation and annihilation operators

$$\begin{aligned}(\hat{\chi}_i)_{1,a}&=(\hat{\xi}_{\mathrm{q}}^{\uparrow})_{i,a}\,,&(\hat{\chi}_i)_{3,a}&=(\hat{\xi}_{\bar{\mathrm{q}}}^{\uparrow})_{i,a}^{\dagger}\,,\\(\hat{\chi}_i)_{2,a}&=(\hat{\xi}_{\mathrm{q}}^{\downarrow})_{i,a}\,,&(\hat{\chi}_i)_{4,a}&=(\hat{\xi}_{\bar{\mathrm{q}}}^{\downarrow})_{i,a}^{\dagger}\,,\end{aligned}$$

and the fermionic part of the Hamiltonian becomes

$$\begin{aligned}\hat{h}_{\mathrm{F}}+\hat{h}_{\mathrm{F}}^{\dagger}&=\hat{\chi}^{\dagger}\gamma_4\left[(m+3a^{-1})+\frac{1}{a}R(U)\right]\hat{\chi}-\hat{\chi}^{\dagger}\gamma_4\left[\frac{1}{a}C(U)\right]\hat{\chi}+2(m+3a^{-1})\\&=\hat{\chi}^{\dagger}\gamma_4(m+3a^{-1})\hat{\chi}+\frac{1}{a}\hat{\chi}^{\dagger}\gamma_4\left[R(U)-C(U)\right]\hat{\chi}+2(m+3a^{-1})\,,\end{aligned}$$

where the matrix $R(U)$ is embedded diagonally into the Dirac-spinor space. The difference between the matrices is

$$\begin{aligned}&(R(U)-C(U))_{ia\alpha,jb\beta}=\\&\qquad-\frac{1}{2}\sum_k\left[(U_{\langle i,i+\hat{k}\rangle})_{ab}(1+\gamma_k)_{\alpha\beta}\delta_{i+\hat{k},j}+(U_{\langle j+\hat{k},i\rangle})_{ab}(1-\gamma_k)_{\alpha\beta}\delta_{j+\hat{k},i}\right]\end{aligned}$$

Therefore, the fermionic part finally reads

$$\begin{aligned}\hat{h}_{\mathrm{F}}+\hat{h}_{\mathrm{F}}^{\dagger}&=2(m+3a^{-1})+\hat{\chi}^{\dagger}\gamma_4(m+3a^{-1})\hat{\chi}\\&\quad-\frac{1}{2a}\sum_{i,k}\left[\hat{\chi}_i^{\dagger}\gamma_4(1+\gamma_k)U_{\langle i,i+\hat{k}\rangle}\hat{\chi}_{i+\hat{k}}+\hat{\chi}_{i+\hat{k}}^{\dagger}\gamma_4(1-\gamma_k)U_{\langle i+\hat{k},i\rangle}\hat{\chi}_i\right].\end{aligned}\tag{3.46}$$

But this is the Hamiltonian for Wilson fermions on the lattice up to an irrelevant constant shift in energy [48]. The fermionic operator is obviously Hermitian and gauge-invariant.

For the gauge part, we can just use the results of [77]. The operator $\hat{T}_{\mathrm{G},a_4}$ of spatial plaquettes yields

$$\begin{aligned} T^{\frac{1}{2}}_{\mathrm{G},a_4}(U) &= \exp\left(\frac{a_4}{a}\frac{1}{g_0^2}\sum_{i,k<m}\mathrm{ReTr}\left(U_{\partial p_{i,km}}\right)\right) \\ &= 1 - a_4\Big(-\frac{1}{ag_0^2}\sum_{i,k<m}\mathrm{ReTr}\left(U_{\partial p_{i,km}}\right)\Big) + \mathcal{O}(a_4^2)\,. \end{aligned}$$

Consequently, the part of the Hamiltonian which originates form the spatial plaquettes is

$$\hat{h}_{\mathrm{G}} + \hat{h}^{\dagger}_{\mathrm{G}} = -\frac{2}{ag_0^2}\sum_{i,k<m}\mathrm{ReTr}\left(U_{\partial p_{i,km}}\right)\,. \tag{3.47}$$

Obviously, this part is again Hermitian and gauge-invariant. The time continuum of $\hat{S}_{a_4}$ is more involved compared to the other parts because it is a convolution over gauge configurations:

$$\hat{S}_{a_4} f = f(U) * \exp\left(\frac{2a}{a_4 g_0^2}\sum_{i,k}\mathrm{ReTr}\,U_{\langle i,i+\hat{k}\rangle}\right).$$

To take the Euclidean time continuum, we have to multiply $\hat{S}_{a_4}$ with a suitable normalization $\mathcal{N}(a_4)$ such that the transfer operator now reads

$$\mathcal{N}(a_4)\hat{T}_{a_4} = \hat{T}^{\dagger}_{\mathrm{F},a_4}\cdot\hat{T}^{\dagger}_{\mathrm{G},a_4}\cdot(\mathcal{N}(a_4)\hat{S}_{a_4})\cdot\hat{T}_{\mathrm{G},a_4}\cdot\hat{T}_{\mathrm{F},a_4}\,.$$

This normalization factor then appears in the partition function of the path integral when deriving it from Equation (3.2). We have neglected this factor in our derivation of the path integral because it is inconsequential for any expectation value. However, in the limit $a_4 \to 0$, it ensures that the convolution operator is actually one in the zeroth order, compensating an otherwise divergent overall constant [41, 77, 103]:

$$\mathcal{N}(a_4)\hat{S}_{a_4} \longrightarrow \mathbb{1} - a_4\hat{h}_{\mathrm{S}} + \mathcal{O}(a_4^2)\,.$$

The limit is proven in [77] and is given by the Laplace-Beltrami operator:

$$\hat{h}_{\mathrm{S}} = -\frac{g_0^2}{2a}\sum_{\langle i,i+\hat{k}\rangle}\sum_{k}\left(\hat{E}^k_{\langle i,i+\hat{k}\rangle}\right)^2. \tag{3.48}$$

The operators $\hat{E}^k_{\langle i,j\rangle}$ are defined as in Section 3.1.

In summary, we have seen that the symmetric transfer operator can indeed be understood as the discretization of a Hamiltonian $\hat{H}$ in Euclidean time.

3.3 Asymmetric transfer operator

So far, we have used the well-known symmetric transfer operator to set the mathematical stage for describing Lattice QCD as the consequence of a quantum-mechanical system on the spatial lattice. Lüscher's choice of $\hat{T}$ is not

only gauge-invariant, but it also has two additional properties; it is Hermitian and strictly positive [83]. These properties allow to define a Hamiltonian $\hat{H}_{a_4}$ not only in the Euclidean time continuum $a_4 \to 0$ but at all spacings $a_4 > 0$:

$$\hat{T}_{a_4} \propto \mathrm{e}^{-a_4 \hat{H}_{a_4}} .$$

But this property is not a necessity. The only relevant properties are gauge invariance, the existence of $\hat{H}$ in the Euclidean time continuum, and that $\hat{T}_{a_4}$ is a suitable discretization of the Boltzmann factor in the sense that Equation (3.32) gives the path integral of Lattice QCD. These properties suffices to interpret the Lattice QCD partition function as the result of some quantum-mechanical system.

Why are we interested in an alternative formulation of $\hat{T}$? Later on, we would like to consider products of the form $\hat{E}^z_{\langle i,j\rangle}\hat{T}$. Using Equation (3.14) and (3.19), we get

$$\hat{E}^z_{\langle i,j\rangle}\hat{T}(f(U)\otimes|\psi_\mathrm{F}\rangle) = \int \mathcal{D}U'\, K(U^z,U')(f(U')\otimes|\psi_\mathrm{F}\rangle)$$

with

$$U^z = \begin{cases} \{\ldots, z^\dagger U_{\langle i,i+\hat{k}\rangle}, \ldots\}, & \langle i,j\rangle = \langle i, i+\hat{k}\rangle \\ \{\ldots, z U_{\langle i,i+\hat{k}\rangle}, \ldots\}, & \langle j,i\rangle = \langle i, i+\hat{k}\rangle \end{cases} . \tag{3.49}$$

The center-electric flux operator twists the gauge variable $U_{\langle i,j\rangle}$ at the link $\langle i,j\rangle$ with the center value $z^\dagger$. If we choose the symmetric transfer operator, the twist will influence the fermionic part because

$$K(U^z,U') = T_\mathrm{F}(U^z)T_\mathrm{G}^{\frac{1}{2}}(U^z)S(U^z,U')T_\mathrm{G}^{\frac{1}{2}}(U')T_\mathrm{F}(U') . \tag{3.50}$$

The multiplication of gauge variables with center elements results in twists of the plaquettes, i.e. we multiply certain plaquette variables with center values: $U_{\partial p_{i,km}} \to z U_{\partial p_{i,km}}$. The form of the gauge action remains the same, however. This cannot be expected from the fermionic part. Consider the expectation value $\langle \hat{E}^z_{\langle i,j\rangle}\rangle$ as an example:

$$\langle \hat{E}^z_{\langle i,j\rangle}\rangle = \frac{1}{Z}\,\mathrm{tr}\left(\mathrm{e}^{\beta\mu\hat{N}}\hat{E}^z_{\langle i,j\rangle}\hat{T}^{N_4}\hat{P}_0\right).$$

The path integral of the trace can be computed analogously to the path integral of Z. The difference lies in the use of $K(U_0^z, U_1)$ instead of $K(U_0, U_1)$ between the zeroth and first layer of Euclidean time. As described above, the gauge action is simply modified by some suitable twists of plaquettes. The fermionic

action, however, now reads

$$
\begin{aligned}
S_{\mathrm{F}}(U,\Omega,\overline{\xi},\xi) = &- \sum_{\tau=0}^{N_4-1} \left(\overline{\xi}_{\mathrm{q}}^{(\tau)} \xi_{\mathrm{q}}^{(\tau)} - \xi_{\overline{\mathrm{q}}}^{(\tau)} \overline{\xi}_{\overline{\mathrm{q}}}^{(\tau)} \right) \\
&+ \sum_{\tau=0}^{N_4-1} \left(\overline{\xi}_{\mathrm{q}}^{(\tau)} \left[B^{-\frac{1}{2}}(U_0^z)\delta_{\tau,0} \mathrm{e}^{\beta\mu}\Omega + B^{-\frac{1}{2}}(U_\tau)(1-\delta_{\tau,0}) \right] B^{-\frac{1}{2}}(U_{\tau+1}) \xi_{\mathrm{q}}^{(\tau+1)} \right. \\
&\left. - \xi_{\overline{\mathrm{q}}}^{(\tau+1)} B^{-\frac{1}{2}}(U_{\tau+1}) \left[\delta_{\tau,0} \mathrm{e}^{-\beta\mu}\Omega^\dagger B^{-\frac{1}{2}}(U_0^z) + (1-\delta_{\tau,0}) B^{-\frac{1}{2}}(U_\tau) \right] \overline{\xi}_{\overline{\mathrm{q}}}^{(\tau)} \right) \\
&+ \sum_{\tau=0}^{N_4-1} \overline{\xi}_{\mathrm{q}}^{(\tau)} \left[\delta_{\tau,0} B^{-\frac{1}{2}}(U_0^z) c(U_0^z) B^{-\frac{1}{2}}(U_0^z) \right. \\
&\qquad \left. + (1-\delta_{\tau,0}) B^{-\frac{1}{2}}(U_\tau) c(U_\tau) B^{-\frac{1}{2}}(U_\tau) \right] \overline{\xi}_{\overline{\mathrm{q}}}^{(\tau)} \\
&+ \sum_{\tau=0}^{N_4-1} \xi_{\overline{\mathrm{q}}}^{(\tau)} B^{-\frac{1}{2}}(U_\tau) c(U_\tau) B^{-\frac{1}{2}}(U_\tau) \xi_{\mathrm{q}}^{(\tau)}
\end{aligned}
\,.
$$

Normally, the next step is to transform all Grassmann generators such that the matrices $B^{-\frac{1}{2}}(U_\tau)$ are removed from the action, and we only have the matrices $B(U_\tau)$ in the equal-time layers. But we cannot achieve this here because both matrices $B^{-\frac{1}{2}}(U_0^z)$ and $B^{-\frac{1}{2}}(U_0)$ occur in the action. Trying to remove both matrices with suitable substitutions will create products like $B^{\frac{1}{2}}(U_0^z)B^{\frac{1}{2}}(U_0)$. The square roots of both matrices have different arguments and, therefore, cannot be simplified to a matrix equal or similar to $B(U)$, where some suitable gauge configuration U has been chosen. Alternatively, one might try to extract the center value z by means of Equation (3.21). This is not possible because the non-trivial twist of one gauge variable does not represent a full gauge transformation. Therefore, we are essentially stuck with the square root of the matrix B. Of course, one can just accept this result and work with a fermionic action where the matrices $B^{\frac{1}{2}}(U)$ occur. Though, the purpose of this section is to show that there exists a transfer operator $\hat{T}$ where the fermionic action remains unchanged for expectation values like $\langle \hat{E}^z_{\langle i,j \rangle} \rangle$; we only have to twist the timelike plaquettes of the gauge action.

Transfer operator

How do we construct such a transfer operator? A closer inspection of Equation (3.50) reveals that we can reach our goal easily if we define a transfer operator with an asymmetric integral kernel

$$
K(U,U') = S(U,U') T_{\mathrm{G}}(U') T_{\mathrm{F}}(U') \,,
$$

where $S(U,U')$, $T_{\mathrm{G}}(U')$ and $T_{\mathrm{F}}(U')$ are chosen suitably. In this case, the center-electric field operator $\hat{E}^z_{\langle i,j \rangle}$ only influences the timelike plaquettes in $S(U,U')$:

$$
K(U^z,U') = S(U^z,U') T_{\mathrm{G}}(U') T_{\mathrm{F}}(U') \,. \tag{3.51}
$$

We choose $S(U, U')$ and $T_G(U')$ as in the case of Lüscher's transfer operator. The fermionic part is defined by

$$T_F(U') = (2\kappa)^{12N_s} \det(B(U')) \exp\left(\hat{\xi}_q^\dagger c(U') \hat{\xi}_{\bar{q}}^\dagger\right) \times \exp\left(\hat{\xi}_q^\dagger \ln(B(U'))\hat{\xi}_q - \hat{\xi}_{\bar{q}} \ln(B(U'))\hat{\xi}_{\bar{q}}^\dagger\right) \exp\left(\hat{\xi}_{\bar{q}} c(U') \hat{\xi}_q\right).$$

This transfer operator is stated in [90]. Again, the transfer operator decomposes into products of operators

$$\hat{T} = \hat{S} \cdot \hat{T}_G \cdot \hat{T}_F,$$

where $\hat{S}$ acts as in the case of the symmetric transfer operator, $\hat{T}_G$ acts by multiplying a wave function $f(U)$ with $T_G(U)$, and $\hat{T}_F$ acts by multiplying a state $f(U) \otimes |\psi_F\rangle$ with $T_F(U)$.

We already know from the previous section that $\hat{S}$ and $\hat{T}_G$ are gauge-invariant. The fermionic part $\hat{T}_F$ is also gauge-invariant as it can be shown analogously to Equation (3.31). Nonetheless, the asymmetric transfer operator is not Hermitian because $\hat{T}^\dagger = \hat{T}_F^\dagger \cdot \hat{T}_G \cdot \hat{S}$. The operators are not anymore symmetrically arranged around $\hat{S}$ which was crucial in guaranteeing $\hat{T}$ to be Hermitian. Consequently, removing the influence of center-electric flux operators from the fermionic part comes with the price of loosing hermiticity. Non-Hermitian transfer operators have been considered for example in [104]. Additionally, for lattice-gauge theories and in a different context, such an asymmetric choice of a transfer operator is also discussed in [91].

We still need to establish the quantum-mechanical interpretation for the asymmetric transfer operator, i.e. we need to show the equivalence between Equation (3.32) and the path integral of Lattice QCD, and we have to establish the existence of an Hermitian, gauge-invariant Hamiltonian $\hat{H}$ in the Euclidean time continuum.

Partition function and path integral

We derive the path integral along the same line of arguments as in the previous section. First, we bring the exponents of the fermionic part into normal order, cf. Equation (3.38):

$$T_F(U') = (2\kappa)^{12N_s} \exp\left(\hat{\xi}_q^\dagger c(U') \hat{\xi}_{\bar{q}}^\dagger\right) \times \exp\left(\hat{\xi}_q^\dagger \Big[\ln B(U')\Big] \hat{\xi}_q + \hat{\xi}_{\bar{q}}^\dagger \Big[\ln B(U')\Big]^T \hat{\xi}_{\bar{q}}\right) \exp\left(\hat{\xi}_{\bar{q}} c(U') \hat{\xi}_q\right).$$

The next step is to establish

$$K(U, U', \Omega) = S(\Omega^\dagger U \Omega) T_G(U') T_F(U', \Omega)$$

with

$$T_F(U', \Omega) = (2\kappa)^{12N_s} \det(B(U')) \exp\left(\hat{\xi}_q^\dagger \Omega c(U') \Omega^\dagger \hat{\xi}_{\bar{q}}^\dagger\right) \times \exp\left(\hat{\xi}_q^\dagger \Omega \ln(B(U'))\Omega^\dagger \hat{\xi}_q - \hat{\xi}_{\bar{q}} \Omega \ln(B(U'))\Omega^\dagger \hat{\xi}_{\bar{q}}^\dagger\right) \exp\left(\hat{\xi}_{\bar{q}} \Omega c(U') \Omega^\dagger \hat{\xi}_q\right).$$

Remember that $K(U, U', \Omega)$ is the integral kernel where the gauge configuration U and the creation and annihilation operators are gauge-transformed with Ω. We insert $K(U, U')$ and $K(U, U', \Omega)$ into Equation (3.36) and use the normal-ordered form of $T_{\mathrm{F}}(U')$ to get the path integral:

$$Z = (2\kappa)^{12N_{\mathrm{s}}N_4} \int \mathcal{D}U\mathcal{D}\Omega\mathcal{D}\overline{\xi}\mathcal{D}\xi \, \mathrm{e}^{S_{\mathrm{F}}(U,\Omega,\overline{\xi},\xi)} \mathrm{e}^{S_{\mathrm{G}}(U,\Omega)} \,. \tag{3.52}$$

The gauge action $S_{\mathrm{G}}(U, \Omega)$ is the same as in Equation (3.41). The fermionic action is

$$\begin{aligned} S_{\mathrm{F}}(U,\Omega,\overline{\xi},\xi) = &- \sum_{\tau=0}^{N_4-1} \left(\overline{\xi}_{\mathrm{q}}^{(\tau)} \xi_{\mathrm{q}}^{(\tau)} - \xi_{\overline{\mathrm{q}}}^{(\tau)} \overline{\xi}_{\overline{\mathrm{q}}}^{(\tau)} \right) + \sum_{\tau=0}^{N_4-1} \xi_{\overline{\mathrm{q}}}^{(\tau)} c(U_\tau) \xi_{\mathrm{q}}^{(\tau)} \\ &+ \sum_{i=0}^{N_4-1} \overline{\xi}_{\mathrm{q}}^{(\tau)} \Big[\delta_{\tau,0}\Omega + (1-\delta_{\tau,0}) \Big] c(U_{\tau+1}) \Big[\delta_{i,0}\Omega^\dagger + (1-\delta_{\tau,0}) \Big] \overline{\xi}_{\overline{\mathrm{q}}}^{(\tau)} \\ &+ \sum_{\tau=0}^{N_4-1} \Big(\overline{\xi}_{\mathrm{q}}^{(\tau)} \Big[\delta_{\tau,0} \mathrm{e}^{\beta\mu}\Omega + (1-\delta_{\tau,0}) \Big] B(U_{\tau+1}) \xi_{\mathrm{q}}^{(\tau+1)} \\ &\qquad - \xi_{\overline{\mathrm{q}}}^{(\tau+1)} B(U_{\tau+1}) \Big[\delta_{\tau,0} \mathrm{e}^{-\beta\mu}\Omega^\dagger + (1-\delta_{\tau,0}) \Big] \overline{\xi}_{\overline{\mathrm{q}}}^{(\tau)} \Big) \end{aligned} .$$

Now, we apply the transformations

$$\begin{aligned} \overline{\xi}_{\mathrm{q}}^{(\tau)} &\longrightarrow \overline{\xi}_{\mathrm{q}}^{(\tau)} \Big[\delta_{\tau,0} \mathrm{e}^{-\beta\mu}\Omega^\dagger + (1-\delta_{\tau,0}) \Big] , \\ \overline{\xi}_{\overline{\mathrm{q}}}^{(\tau)} &\longrightarrow \Big[\delta_{\tau,0} \mathrm{e}^{\beta\mu}\Omega + (1-\delta_{\tau,0}) \Big] \overline{\xi}_{\overline{\mathrm{q}}}^{(\tau)} \end{aligned}$$

to the Grassmann generators. This gives

$$\begin{aligned} S_{\mathrm{F}}(U,\Omega,\overline{\xi},\xi) = &+ \sum_{\tau=0}^{N_4-1} \overline{\xi}_{\mathrm{q}}^{(\tau)} c(U_{\tau+1}) \overline{\xi}_{\overline{\mathrm{q}}}^{(\tau)} + \sum_{\tau=0}^{N_4-1} \xi_{\overline{\mathrm{q}}}^{(\tau)} c(U_\tau) \xi_{\mathrm{q}}^{(\tau)} \\ &+ \sum_{\tau=0}^{N_4-1} \left(\overline{\xi}_{\mathrm{q}}^{(\tau)} B(U_{\tau+1}) \xi_{\mathrm{q}}^{(\tau+1)} - \xi_{\overline{\mathrm{q}}}^{(\tau+1)} B(U_{\tau+1}) \overline{\xi}_{\overline{\mathrm{q}}}^{(\tau)} \right) \\ &- \sum_{\tau=0}^{N_4-1} \Big(\overline{\xi}_{\mathrm{q}}^{(\tau)} \Big[\delta_{\tau,0} \mathrm{e}^{-\beta\mu}\Omega^\dagger + (1-\delta_{\tau,0}) \Big] \xi_{\mathrm{q}}^{(\tau)} \\ &\qquad - \xi_{\overline{\mathrm{q}}}^{(\tau)} \Big[\delta_{\tau,0} \mathrm{e}^{\beta\mu}\Omega + (1-\delta_{\tau,0}) \Big] \overline{\xi}_{\overline{\mathrm{q}}}^{(\tau)} \Big) \end{aligned} .$$

In the previous section, we have seen that the the matrices $B(U_\tau)$ and $c(U_\tau)$ are combined to give the spatial hops of the τ-th time layer. However, the fermionic action in its current form does not allow the same derivation because the matrices $B(U_{\tau+1})$ connect variables between the layers τ and $\tau + 1$ and do not lie on one layer of time only. Also, the bilinear forms $\mathrm{e}^{\beta\mu}\Omega$ and $\mathrm{e}^{-\beta\mu}\Omega^\dagger$ lie on the zeroth layer of time, but they should actually form the timelike hops. The equal-time (timelike) hops are what we want to be the (equal-time) timelike hops; the roles are reversed. We can fix this rather easily by just shifting all

Grassmann generators $\overline{\xi}_{\mathrm{q}}^{(\tau)}$ and $\overline{\xi}_{\overline{\mathrm{q}}}^{(\tau)}$ one step into the positive time direction:

$$\begin{aligned} \overline{\xi}_{\mathrm{q}}^{(\tau)} &\longrightarrow \overline{\xi}_{\mathrm{q}}^{(\tau+1)}, & \overline{\xi}_{\mathrm{q}}^{(N_4-1)} &\longrightarrow -\overline{\xi}_{\mathrm{q}}^{(0)}, \\ \overline{\xi}_{\overline{\mathrm{q}}}^{(\tau)} &\longrightarrow \overline{\xi}_{\overline{\mathrm{q}}}^{(\tau+1)}, & \overline{\xi}_{\overline{\mathrm{q}}}^{(N_4-1)} &\longrightarrow -\overline{\xi}_{\overline{\mathrm{q}}}^{(0)} \end{aligned}$$

for $\tau < N_4 - 1$. This gives the action

$$\begin{aligned} S_{\mathrm{F}}(U,\Omega,\overline{\xi},\xi) = &+ \sum_{\tau=0}^{N_4-1} \overline{\xi}_{\mathrm{q}}^{(\tau)} c(U_\tau) \overline{\xi}_{\overline{\mathrm{q}}}^{(\tau)} + \sum_{\tau=0}^{N_4-1} \xi_{\overline{\mathrm{q}}}^{(\tau)} c(U_\tau) \xi_{\mathrm{q}}^{(\tau)} \\ &+ \sum_{\tau=0}^{N_4-1} \left(\overline{\xi}_{\mathrm{q}}^{(\tau)} B(U_\tau) \xi_{\mathrm{q}}^{(\tau)} - \xi_{\overline{\mathrm{q}}}^{(\tau)} B(U_\tau) \overline{\xi}_{\overline{\mathrm{q}}}^{(\tau)} \right) \\ &- \sum_{\tau=0}^{N_4-1} \Bigg(\overline{\xi}_{\mathrm{q}}^{(\tau+1)} \left[\delta_{\tau,0} \mathrm{e}^{-\beta\mu} \Omega^\dagger + (1-\delta_{\tau,0}) \right] \xi_{\mathrm{q}}^{(\tau)} \\ &\qquad - \xi_{\overline{\mathrm{q}}}^{(\tau)} \left[\delta_{\tau,0} \mathrm{e}^{\beta\mu} \Omega + (1-\delta_{\tau,0}) \right] \overline{\xi}_{\overline{\mathrm{q}}}^{(\tau+1)} \Bigg) \end{aligned} .$$

The sign in the transition from $N_4 - 1$ to 0 takes the anti-periodicity of the Grassmann generators into account such that $\overline{\xi}^{(N_4)} = -\overline{\xi}^{(0)}$ and $\xi^{(N_4)} = -\xi^{(0)}$ still hold for the resulting action. The overall determinant of the transformation is just one. To see this, we decompose the substitution into a permutation of time layers and a change of sign for the generators of the zeroth layer. A permutation of the Grassmann numbers can be written as a linear transformation with a permutation matrix P. The determinant of P is either 1 or -1 depending on whether the permutation decomposes into an even or odd number of transpositions. Here, the permutation decomposes into transpositions of time layers, but each time layer involves an even number of generators. Therefore, we have an even number of transpositions overall; the determinant of P is one. The multiplication of the generators with minus one gives a Jacobian whose determinant is one because we again have an even number of generators involved.

By introducing the Dirac spinors as in the case of the symmetric transfer operator, the action becomes

$$\begin{aligned} S_{\mathrm{F}}(U,\Omega,\overline{\psi},\psi) = &+ \sum_{\tau=0}^{N_4-1} \overline{\psi}^{(\tau)} \gamma_4 \left[B(U_\tau) + C(U_\tau) \right] \psi^{(\tau)} \\ &+ \sum_{\tau=0}^{N_4-1} \Bigg(\overline{\psi}^{(\tau)} \frac{1}{2} (1-\gamma_4) \left[\delta_{\tau,0} \mathrm{e}^{\beta\mu} \Omega + (1-\delta_{\tau,0}) \right] \psi^{(\tau+1)} \\ &\qquad - \overline{\psi}^{(\tau+1)} \frac{1}{2} (1+\gamma_4) \left[\delta_{\tau,0} \mathrm{e}^{-\beta\mu} \Omega^\dagger + (1-\delta_{\tau,0}) \right] \psi^{(\tau)} \Bigg) \end{aligned} .$$

Again, the matrices $B(U_\tau)$ and $C(U_\tau)$ are added to form the spatial hops in the resulting action. However, contrary to the symmetric case, we do not take the difference $C(U_\tau) - B(U_\tau)$, but we take the sum $C(U_\tau) + B(U_\tau)$. This results mainly in a different sign for the gamma matrices. Summarizing everything

and conducting the final substitution

$$\overline{\psi}^{(\tau)} \longrightarrow \overline{\psi}^{(\tau)}(-2\kappa\gamma_4)\,,$$

we end with the Hasenfratz-Karsch action (2.4) with all timelike links maximally gauge-fixed to unity if we identify $U_{\langle(i,0),(i,1)\rangle} = \Omega_i$:

$$\begin{aligned}
S_{\mathrm{F}}(U,\Omega,\overline{\psi},\psi) = &-\sum_{\tau=0}^{N_4-1}\overline{\psi}^{(\tau)}\psi^{(\tau)} \\
&+\kappa\sum_{\tau=0}^{N_4-1}\Bigg(\overline{\psi}^{(\tau)}(1-\gamma_4)\left[\delta_{\tau,0}\mathrm{e}^{\beta\mu}\Omega+(1-\delta_{\tau,0})\right]\psi^{(\tau+1)} \\
&\qquad\qquad +\overline{\psi}^{(\tau+1)}(1+\gamma_4)\left[\delta_{\tau,0}\mathrm{e}^{-\beta\mu}\Omega^{\dagger}+(1-\delta_{\tau,0})\right]\psi^{(\tau)}\Bigg)\,. \\
&+\kappa\sum_{\tau=0}^{N_4-1}\sum_{i,k}\Bigg(\overline{\psi}_i^{(\tau)}\left(U^{(\tau)}_{\langle i,i+\hat{k}\rangle}\right)(1-\gamma_k)\psi^{(\tau)}_{i+\hat{k}} \\
&\qquad\qquad +\overline{\psi}^{(\tau)}_{i+\hat{k}}\left(U^{(\tau)}_{\langle i+\hat{k},i\rangle}\right)(1+\gamma_k)\psi_i^{(\tau)}\Bigg)
\end{aligned}$$

Note that the prefactor $(2\kappa)^{12N_{\mathrm{s}}N_4}$ in Equation (3.52) is compensated by the determinant of the substitution.

Euclidean time continuum

Finally, it remains to show the existence of a Hamiltonian $\hat{H}$ in the Euclidean time continuum. Again, we have to introduce the lattice spacings first. For $\mathcal{N}(a_4)S_{a_4}(U,U')$ and $T_{\mathrm{G},a_4}(U')$, this is done completely analogous to the symmetric case. The spacings are introduced to the fermionic part in the following way. The matrix $B(U)$ is taken as in Equation (3.42), and we write

$$\begin{aligned}
T_{\mathrm{F},a_4}(U') = &\,(2s(a_4,a))^{12N_{\mathrm{s}}}\det\left(\frac{a_4}{a}B(U')\right)\exp\left(\hat{\xi}^{\dagger}_{\mathrm{q}}\left[\frac{a_4}{a}c(U')\right]\hat{\xi}^{\dagger}_{\overline{\mathrm{q}}}\right) \\
&\times\exp\left(\hat{\xi}^{\dagger}_{\mathrm{q}}\ln\left(\frac{a_4}{a}B(U')\right)\hat{\xi}_{\mathrm{q}}-\hat{\xi}_{\overline{\mathrm{q}}}\ln\left(\frac{a_4}{a}B(U')\right)\hat{\xi}^{\dagger}_{\overline{\mathrm{q}}}\right)\exp\left(\hat{\xi}_{\overline{\mathrm{q}}}\left[\frac{a_4}{a}c(U')\right]\hat{\xi}_{\mathrm{q}}\right)\,.
\end{aligned}$$

Obviously, the special case $a_4 = a = 1$ gives the asymmetric transfer operator $\hat{T}$ from above, and deriving the path integral with lattice spacings introduced gives the action (2.4) if we use the substitution

$$\overline{\psi}^{(\tau)} \longrightarrow \overline{\psi}^{(\tau)}(-2s(a_4,a)\gamma_4)\,.$$

The Euclidean time continuum is taken again by decomposing the transfer operator $\hat{T}_{a_4}$:

$$\begin{aligned}
\mathcal{N}(a_4)\hat{T}_{a_4} &= (\mathcal{N}(a_4)\hat{S}_{a_4})\cdot\hat{T}_{\mathrm{G},a_4}\cdot\hat{T}_{\mathrm{F},a_4} \\
&= \left(\mathbb{1}-a_4\hat{h}_{\mathrm{S}}+\mathcal{O}(a_4^2)\right)\left(\mathbb{1}-a_4\hat{h}_{\mathrm{G}}+\mathcal{O}(a_4^2)\right)\left(\mathbb{1}-a_4\hat{h}_{\mathrm{F}}+\mathcal{O}(a_4^2)\right) \\
&= \mathbb{1}-a_4\left(\hat{h}_{\mathrm{S}}+\hat{h}_{\mathrm{G}}+\hat{h}_{\mathrm{F}}\right)+\mathcal{O}(a_4^2)\,.
\end{aligned}$$

Because the gauge part is, except for some reordering, the same as in the symmetric case, the operator $\hat{h}_\mathrm{S}$ is equivalent to Equation (3.48) from the previous section, and the operator $\hat{h}_\mathrm{G}$ equals the right-hand side of Equation (3.47). The different parts of $T_{\mathrm{F},a_4}(U)$ are expanded to linear order of a_4 where we use Equation (3.43), (3.44) and $\det(1+\varepsilon M) = 1 + \varepsilon \operatorname{tr} M + \mathcal{O}(\varepsilon^2)$:

$$
\begin{aligned}
(2s(a_4,a))^{12N_\mathrm{s}} \det\left(\frac{a_4}{a}B(U)\right) &= 1 - a_4(m+3a^{-1}) + \mathcal{O}(a_4^2)\,,\\
\exp\left(\hat{\xi}_\mathrm{q}^\dagger\left[\frac{a_4}{a}c(U)\right]\hat{\xi}_{\overline{\mathrm{q}}}^\dagger\right) &= \mathbb{1} + a_4\hat{\xi}_\mathrm{q}^\dagger\left[\frac{1}{a}c(U)\right]\hat{\xi}_{\overline{\mathrm{q}}}^\dagger + \mathcal{O}(a_4^2)\,,\\
\exp\left(\hat{\xi}_{\overline{\mathrm{q}}}\left[\frac{1}{a}c(U)\right]\hat{\xi}_\mathrm{q}\right) &= \mathbb{1} + a_4\hat{\xi}_{\overline{\mathrm{q}}}\left[\frac{1}{a}c(U)\right]\hat{\xi}_\mathrm{q} + \mathcal{O}(a_4^2)\,,
\end{aligned}
$$

and

$$
\begin{aligned}
&\exp\left(\hat{\xi}_\mathrm{q}^\dagger \ln\left(\frac{a_4}{a}B(U)\right)\hat{\xi}_\mathrm{q} - \hat{\xi}_{\overline{\mathrm{q}}}\ln\left(\frac{a_4}{a}B(U)\right)\hat{\xi}_{\overline{\mathrm{q}}}^\dagger\right)\\
&\quad= \mathbb{1} + a_4\hat{\xi}_\mathrm{q}^\dagger\left[(m+3a^{-1}) + \frac{1}{a}R(U)\right]\hat{\xi}_\mathrm{q}\\
&\qquad\quad - a_4\hat{\xi}_{\overline{\mathrm{q}}}\left[(m+3a^{-1}) + \frac{1}{a}R(U)\right]\hat{\xi}_{\overline{\mathrm{q}}}^\dagger + \mathcal{O}(a_4^2)
\end{aligned}
$$

Collecting all terms yields the fermionic part

$$
\begin{aligned}
\hat{h}_\mathrm{F} =&(m+3a^{-1}) - \hat{\xi}_\mathrm{q}^\dagger\left[(m+3a^{-1}) + \frac{1}{a}R(U)\right]\hat{\xi}_\mathrm{q}\\
&+ \hat{\xi}_{\overline{\mathrm{q}}}\left[(m+3a^{-1}) + \frac{1}{a}R(U)\right]\hat{\xi}_{\overline{\mathrm{q}}}^\dagger - \hat{\xi}_{\overline{\mathrm{q}}}\left[\frac{1}{a}c(U)\right]\hat{\xi}_\mathrm{q} - \hat{\xi}_\mathrm{q}^\dagger\left[\frac{1}{a}c(U)\right]\hat{\xi}_{\overline{\mathrm{q}}}^\dagger
\end{aligned}
$$

We again introduce the creation and annihilation operators $\hat{\chi}^\dagger$ and $\hat{\chi}$:

$$
\begin{aligned}
\hat{h}_\mathrm{F} &= (m+3a^{-1}) - \hat{\chi}^\dagger\gamma_4\left[(m+3a^{-1}) + \frac{1}{a}R(U)\right]\hat{\chi} - \hat{\chi}^\dagger\gamma_4\left[\frac{1}{a}C(U)\right]\hat{\chi}\\
&= -\hat{\chi}^\dagger\gamma_4(m+3a^{-1})\hat{\chi} - \frac{1}{a}\hat{\chi}^\dagger\gamma_4\left[R(U)+C(U)\right]\hat{\chi} + (m+3a^{-1})\,,
\end{aligned}
$$

where $R(U)$ is embedded diagonally into the Dirac-spinor space. We have

$$
\begin{aligned}
&(R(U)+C(U))_{ia\alpha,jb\beta} =\\
&\quad -\frac{1}{2}\sum_k\left[(U_{\langle i,i+\hat{k}\rangle})_{ab}(1-\gamma_k)_{\alpha\beta}\delta_{i+\hat{k},j} + (U_{\langle j+\hat{k},j\rangle})_{ab}(1+\gamma_k)_{\alpha\beta}\delta_{j+\hat{k},j}\right].
\end{aligned}
$$

The final form of the fermionic part $\hat{h}_\mathrm{F}$ therefore reads

$$
\begin{aligned}
\hat{h}_\mathrm{F} = &(m+3a^{-1}) - \hat{\chi}^\dagger\gamma_4(m+3a^{-1})\hat{\chi}\\
&+ \frac{1}{2a}\sum_{i,k}\left[\hat{\chi}_i^\dagger\gamma_4(1-\gamma_k)U_{\langle i,i+\hat{k}\rangle}\hat{\chi}_{i+\hat{k}} + \hat{\chi}_{i+\hat{k}}^\dagger\gamma_4(1+\gamma_k)U_{\langle i,i+\hat{k}\rangle}\hat{\chi}_i\right]
\end{aligned}
$$

The Hamiltonian $\hat{h}_\mathrm{F}$ is physically equivalent to the Hamiltonian of the symmetric case stated in Equation (3.46) because they only differ by a constant shift of energy and by a different sign convention of the gamma matrices γ_μ; the signs can always be changed by the unitary transformation in Equation (3.40).

Chapter 4

Quark numbers in QCD

This chapter presents the first of two main results of this thesis: the construction of an ensemble with fixed net-quark number $N_V = e \mod 3$ in a spatial subvolume V of the lattice. What is the importance of such a construction? In QCD and on the spatial torus, we can only have states with a total net-quark number $N = 0 \mod 3$, i.e. we only observe integer baryon numbers: mesons, baryons or more complicated hadronic structures. States with additional quarks or antiquarks yielding fractional baryon numbers are prohibited. This is because the physical states of the system are gauge-invariant by definition which implies a local Gauss law where quarks and antiquarks are sources of color-electric flux. Fractional baryon numbers imply the presence of quarks and antiquarks creating color-electric fluxes relative to a hadronic background of $N = 0 \mod 3$. These fluxes are, however, unable to terminate in a gauge-invariant manner with any parts of the background rendering states with $N \neq 0 \mod 3$ unphysical. More precisely, in the previous chapter, we have seen that gauge invariance implies a local $\mathbb{Z}_3$-law on $\mathcal{H}_{\text{phys}}$ and the decomposition (3.18) of $\mathcal{H}_{\text{phys}}$ into sectors $\mathcal{H}_{\{q,e\}}$ of flux-tube configurations $\{q, e\}$. Due to the local $\mathbb{Z}_3$-law (3.17), each flux-tube configuration has a total center charge

$$q = \sum_i q_i = 0 \mod 3$$

on the torus. Hence, physical states have a vanishing total center charge, and because a (anti-)quark is a source of a (negative) positive center charge ($q_i = -1$) $q_i = 1$, physical states can only have a total net-quark number $N = 0 \mod 3$. This restriction to $N = 0 \mod 3$ is also the reason of the well-known Roberge-Weiss symmetry of QCD [105] which states that the partition function at imaginary chemical potential $\beta\mu = \mathrm{i}\Theta$ has a $2\pi/3$-periodicity:

$$Z(T, V, \Theta) = Z\left(T, V, \Theta + \frac{2\pi}{3}\right) .$$

Despite the above argument excluding states with fractional baryon number as a result of Gauss's law and the periodic boundary conditions, the restriction does not apply to a subvolume V of the spatial lattice. Hadronic structures extending in space can lie partially in the volume V yielding a fractional baryon number for V, i.e. $N_V = e \mod 3$. A simple example is a quark-antiquark pair

with the quark residing in V and the antiquark residing in the complement $\overline{V}$. In the language of center charges and fluxes, the total center charge q_V of the subvolume V can be non-vanishing and creates a corresponding center flux through the volume's surface. The surplus quarks or antiquarks of V create a color-electric flux through the surface of V which terminates in a gauge-invariant manner with charges outside of V. Of course, this is an intuitive result and the relation between the net-quark number in V, the center charge of V and the center flux through its boundary has been pointed out early on by [106], and further refined rigorously by [87–89] which have established the decomposition of $\mathcal{H}_{\text{phys}}$ into sectors of center charge q_V.

However, the construction of an ensemble $Z(N_V = e \mod 3)$ with fixed net-quark number is more subtle than just taking the trace over a sector of fixed center charge $q_V = e \mod 3$. The dynamics of the system are blind towards our arbitrary choice of V. Quarks and antiquarks can move in and out of the volume or be created between V and $\overline{V}$. Therefore, an observer restricting its measurement to the subvolume V is expected to observe all possible values $N_V = e \mod 3$, while the naive trace taken over a sector $q_V = e \mod 3$ merely reflects the probability of observing a state of total center charge e in V.

It is the very point of this chapter to properly construct the ensemble $Z(N_V = e \mod 3)$ by modifying the dynamics at the interface between the volume V and $\overline{V}$. This modification can be interpreted as the insertion of a membrane enclosing the volume V. Once the system is initialized in a state of fixed center charge $q_V = e \mod 3$, the modified dynamics only allow changes of the center flux through the interface by multiples of three preventing the system to leave the sector of fixed center charge. Therefore, taking the trace over such a sector and using the modified dynamics actually describes the ensemble $Z(N_V = e \mod 3)$. Then, an observer, restricting its considerations to the volume V only, will indeed perceive a subsystem with QCD dynamics and fractional baryon number.

The structure of this chapter is as follows. In Section 4.1, we first consider the construction of 't Hooft's center-electric flux ensembles because, as it turns out, the construction of $Z(N_V = e \mod 3)$ is of similar structure as 't Hooft's ensembles and can be seen as a form of generalization to them if dynamical fermions are present. Moreover, the first section also introduces notations and definitions which are used throughout this chapter. Additionally, the section is meant to create a bridge between the previous chapter and the construction of the fixed net-quark number ensembles.

The main result of this chapter is then presented in Section 4.2. The ensemble $Z(N_V = e \mod 3)$ is constructed in the transfer-matrix formulation. We establish the necessary local modifications of the Hamiltonian $\hat{H}$ at the interface between V and $\overline{V}$, construct the modified transfer-matrix operator based on the asymmetric operator of Section 3.3 and derive the path integral by discretizing Euclidean time. At the end of the chapter, we derive the path integral again but use the dualization scheme by [107, 108] which does not rely on the Hamiltonian approach. The different approaches are demonstrated to give the same result.

Both approaches to construct $Z(N_V = e \mod 3)$ have been published in

[90], and, consequently, we will base Section 4.2 on the notations and arguments of [90]. The author of this thesis is responsible for the construction within the transfer-matrix formulation. This includes, identifying the failure of naively constructing the ensemble by a simple trace over the charged sectors, defining and using the asymmetric transfer operator to get equivalent results for both approaches, establishing the proper modified Hamiltonian and transfer operator and deriving the path integral. The initial idea of using the dualization scheme of [107, 108] to construct the ensemble and its derivation within this approach are also due to the author of this thesis. However, for the dualization approach, the second author of [90] is responsible for putting forward the ansatz of a continuity equation (4.29) and the need of independently twisting Dirac sheets in all layers of Euclidean time.

4.1 't Hooft's center-electric flux ensembles

We commence with the well-known construction of 't Hooft's center-electric flux ensembles [109, 110].

We use the transfer-matrix formulation of Chapter 3, and, for now, we consider the full formulation with dynamical fermions. In Chapter 3, we already discussed the expectation value

$$\langle \hat{E}^z_{\langle i,j\rangle} \rangle = \frac{1}{Z} \operatorname{tr}\left(\hat{E}^z_{\langle i,j\rangle} \mathrm{e}^{\beta\mu\hat{N}} \mathrm{e}^{-\beta\hat{H}} \hat{P}_0 \right)$$

of the center-electric flux operator $\hat{E}^z_{\langle i,j\rangle}$ with $z \in \mathrm{Z}_3$. The gauge invariance of $\hat{E}^z_{\langle i,j\rangle}$, manifesting itself in $[\hat{E}^z_{\langle i,j\rangle}, \hat{P}_0] = 0$, is crucial because it gives a physical interpretation of the expectation value: it is the expectation value of an observable over a thermodynamic ensemble of physical states only. The path integral of the expectation value is derived by discretizing the Boltzmann factor $\mathrm{e}^{-\beta\hat{H}}$ in Euclidean time τ with the asymmetric transfer operator $\hat{T}_{a_4}$ from Section 3.3. Recall that we have exploited the arbitrariness in the choice of $\hat{T}_{a_4}$ and constructed the asymmetric transfer operator exactly for the purpose of taking expectation values of center-electric flux operators such that only the plaquette action is modified in the resulting path integral. Consequently, by following the computations of Chapter 3, especially Section 3.3, Equation (3.36) gives the path integral

$$\begin{aligned}
&\langle \hat{E}^z_{\langle i,j\rangle} \rangle = \\
&\quad \frac{1}{Z} \int \mathcal{D}U \mathcal{D}\Omega \mathcal{D}\overline{\xi} \mathcal{D}\xi \, \mathrm{e}^{-\overline{\xi}\xi} \, \langle \mathrm{e}^{\beta\mu} \xi^{(0)}_{\mathrm{q}}, \mathrm{e}^{-\beta\mu} \xi^{(0)}_{\overline{\mathrm{q}}} | \, K(U^z_0, U_1, \Omega) \, | \Omega \xi^{(1)}_{\mathrm{q}}, \xi^{(1)}_{\overline{\mathrm{q}}} \Omega^\dagger \rangle \\
&\qquad\qquad \times \prod_{\tau=1}^{N_4-1} \langle \xi^{(\tau)}_{\mathrm{q}}, \xi^{(\tau)}_{\overline{\mathrm{q}}} | \, K(U_\tau, U_{\tau+1}) \, | \xi^{(\tau+1)}_{\mathrm{q}}, \xi^{(\tau+1)}_{\overline{\mathrm{q}}} \rangle \\
&= \frac{1}{Z} \int \mathcal{D}U \mathcal{D}\overline{\psi} \mathcal{D}\psi \, \mathrm{e}^{S_{\mathrm{G}}(z,U)} \mathrm{e}^{S_{\mathrm{F}}(U,\overline{\psi},\psi)}
\end{aligned}$$

of the expectation value for the lattice spacings set to $a_4 = a = 1$. The integral kernel $K(U^z_0, U_1)$ from Equation (3.51) is used, and U^z is defined as in Equation

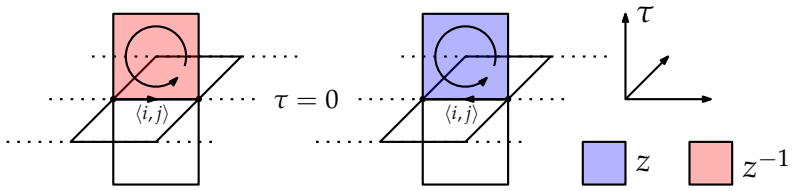

Figure 4.1: Illustration of a single twist which occurs in the action $S_{\mathrm{G}}(z,U)$. The link $\langle i,j \rangle$ is embedded in the zeroth Euclidean time layer. The timelike plaquette between the zeroth and first layer of time which contains the link $\langle i,j \rangle$ or $\langle j,i \rangle$ is twisted with the center element z^{-1} or z.

(3.49). The fermionic action $S_{\mathrm{F}}(U,\overline{\psi},\psi)$ turns out to be the Hasenfratz-Karsch action (2.4), and the gauge action $S_{\mathrm{G}}(z,U)$ is given by

$$S_{\mathrm{G}}(z,U) = \frac{2}{g_0^2} \sum_{x,\mu<\nu} \mathrm{ReTr}\left(z_{\langle i,j \rangle}(p_{x,\mu\nu}) U_{\partial p_{x,\mu\nu}} \right). \tag{4.1}$$

The function $z_{\langle i,j \rangle}(p_{x,\mu\nu})$ is defined as

$$z_{\langle i,j \rangle}(p_{(i,\tau),\mu\nu}) = \begin{cases} z^{-1}, & \tau = 0, \nu = 4, \mu = k, \langle i,j \rangle = \langle i, i+\hat{k} \rangle \\ z, & \tau = 0, \nu = 4, \mu = k, \langle j,i \rangle = \langle i, i+\hat{k} \rangle \\ 1, & \text{else} \end{cases}.$$

What does $z_{\langle i,j \rangle}(p_{(i,\tau),\mu\nu})$ cause? It multiplies exactly one timelike plaquette, which lies between the zeroth and first layer of Euclidean time, with either the center element z or z^{-1} depending on the orientation of $\langle i,j \rangle$. If the link $\langle i,j \rangle$ ($\langle j,i \rangle$) embedded in the zeroth layer of time is part of the boundary $\partial p_{x,\mu\nu}$ of the plaquette $p_{x,\mu\nu}$, then the plaquette variable $U_{\partial p_{x,\nu\mu}}$ is multiplied with z^{-1} (z): $U_{\partial p_{x,\mu\nu}} \to z^{-1} U_{\partial p_{x,\nu\mu}}$ ($U_{\partial p_{x,\mu\nu}} \to z U_{\partial p_{x,\mu\nu}}$). Multiplying plaquettes with center elements in this way is exactly what is meant by twisting a plaquette. The procedure is illustrated in Figure 4.1 for $(2+1)$-dimensions.

Of course, similar to [77], we can also think of more general expectation values

$$\left\langle \prod_{\langle i,j \rangle \in \Gamma} \hat{E}^z_{\langle i,j \rangle} \right\rangle = \frac{1}{Z} \mathrm{tr}\left(\left[\prod_{\langle i,j \rangle \in \Gamma} \hat{E}^z_{\langle i,j \rangle} \right] \mathrm{e}^{\beta\mu\hat{N}} \mathrm{e}^{-\beta\hat{H}} \hat{P}_0 \right), \tag{4.2}$$

where Γ is some set of links on the spatial lattice, and $z \in \mathrm{Z}_3$. The reason to consider these kind of expectation values is that we can define topological objects called vortices (monopoles) in two spatial dimensions and vortex lines ('t Hooft loops) in three spatial dimensions [22, 51, 109, 111–125]. These objects are boundaries $\partial\Gamma^*$ of lines and surfaces Γ^* dual to Γ [51, 111, 112]. The physical significance of vortices is only given in the absence of dynamical fermions because then the expectation value does not depend anymore on the exact choice of Γ, but it only depends on the boundary $\partial\Gamma^*$ [109, 111–113, 116]:

$$\Phi(\partial\Gamma^*, k) = \left\langle \prod_{\langle i,j \rangle \in \Gamma} \hat{E}^{u^k}_{\langle i,j \rangle} \right\rangle$$

with $u = \mathrm{e}^{\frac{2\pi}{3}\mathrm{i}}$ and $k \in \mathbb{Z}_3$. This is similar to Classical Electrodynamics, where the magnetic flux through a surface S does not depend on the shape of S but only on its boundary $\mathcal{C} = \partial S$, i.e. magnetic fluxes of surfaces with the same boundary $\mathcal{C}$ are identical. In this sense, we say that $\Phi(\partial\Gamma^*, k)$ creates the center-magnetic flux k along the loop $\partial\Gamma^*$, and $\Delta F(\partial\Gamma^*, k) = -\beta^{-1} \ln \Phi(\partial\Gamma^*, k)$ is the free energy difference when creating a loop $\partial\Gamma^*$ of center-magnetic flux k [22, 51, 109, 111]. There is however one case which we have skipped in the above argument: $\partial\Gamma^* = 0$. There are two ways in which $\partial\Gamma^* = 0$ can be achieved. The first one is just the case in which Γ^* is a closed surface of a volume. In this case $\Phi(\partial\Gamma^*, k) = 1$ due to Gauss's law. The topology of the torus allows however for a different possibility which does not exist in an infinite volume. The surface Γ^* does not enclose a volume but still has no boundary because it closes by winding around two directions of the torus. The latter case is equivalent to imposing twisted boundary conditions [22, 109–111, 124, 126–132].

Let us give a more detailed account of the above argument. To define the concept of a surface Γ^* and its boundary $\partial\Gamma^*$, we need to state how structures like paths and surfaces are constructed on the spatial lattice. We use the terminology of r-cells which, for our case, are just the elementary objects of the three-dimensional spatial lattice: sites, links, plaquettes and cubes. In doing so, we base the definitions and arguments on [111, 112, 133, 134]. r-cells are abstract objects s_r with the assigned dimension $\dim s_r = r$. They define two important concepts: orientations and boundaries. Sites are 0-cells, links are 1-cells, plaquettes are 2-cells, and cubes are 3-cells. Hence, on the lattice, we have four sets of cells: C_0, C_1, C_2 and C_3. The set C_0 of all 0-cells is given by all sites i of the spatial lattice. The set C_1 of all 1-cells are all links $\langle i, i + \hat{k}\rangle$, $k \in \{1, 2, 3\}$ which point in a positive lattice direction. The set C_2 of 2-cells are all plaquettes $p_{i,km}$ with $k < m$ and $k, m \in \{1, 2, 3\}$. Geometrically, we identify a plaquette with a rectangle which is drawn by starting a line from i, first going one lattice spacing into the direction k, then continuing with one lattice spacing in the direction m and finally closing the path into a rectangle:

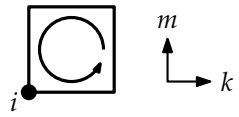

The set C_3 of all 3-cells is the set of all cubes c_i attached to a corner site i and drawn with all faces in positive coordinate directions:

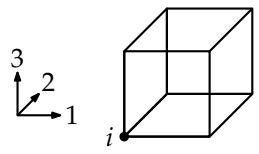

Now, we can introduce a formal linear combination

$$d_r = \sum_{s_r \in C_r} \alpha_{s_r} s_r, \quad \alpha_{s_r} \in \mathbb{Z}$$

of r-cells with integer coefficients which is called a r-chain. To be more precise, we consider the set C_r to form a basis of a left $\mathbb{Z}$-module K_r which is the concept of a vector space defined over the ring $\mathbb{Z}$ instead of the fields $\mathbb{R}$ or $\mathbb{C}$, see for example [135]. For all practical purposes, this means that we have a concept of adding r-chains and r-cells, and we have a scalar multiplication with factors in $\mathbb{Z}$. Because C_r is a basis, the r-cells are linearly independent:

$$\sum_{s_r \in C_r} \alpha_{s_r} s_r = 0$$

if and only if $\alpha_{s_r} = 0$ for all $s_r \in C_r$.

Later on, we will frequently encounter the notation $\pm s_r \in d_r$ which is defined if and only if $\alpha_{s_r} \in \{0, 1, -1\}$ for all r-cells s_r. Then,

$$\pm s_r \in d_r \Longleftrightarrow \alpha_{s_r} = \pm 1\,.$$

For each r-cell $s_r \in C_r$, we can consider also the cell $-s_r$. We define all r-cells to be positively orientated, and, therefore, $-s_r$ is said to be the negatively orientated r-cell of s_r. For links and plaquettes, we have a straightforward geometrical interpretation of the orientation. We identify $\langle i + \hat{k}, i\rangle = -\langle i, i + \hat{k}\rangle$ for all 1-cells $\langle i, i + \hat{k}\rangle \in C_1$. This means that negatively orientated 1-cells $-\langle i, i + \hat{k}\rangle$ are just the links $\langle i, i + \hat{k}\rangle$ pointing in the opposite direction. In the case of plaquettes $p_{i,km} \in C_2$, we define $p_{i,mk} = -p_{i,km}$ which we interpret to be $p_{i,km}$ where the rectangle is drawn in the opposite direction:

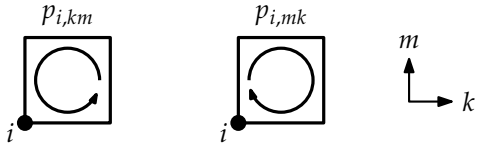

For sites and cubes, we do not have an immediate geometrical interpretation of the orientation. At least, for sites $i \in C_0$, we distinguish i and $-i$ by drawing different dots:

$$i \bullet \qquad \circ\ -i$$

The next step is the concept of a boundary for r-chains. The boundary operator

$$\partial : K_r \to K_{r-1}$$

is a linear operator which is defined for every $r \in \{1, 2, 3\}$, and $\partial = 0$ on K_0. As the name suggests, ∂d_r gives the boundary of a r-chain d_r which is a $(r-1)$-chain. How do we define the boundary of a general r-chain? Because the operator ∂ is considered linear by definition, we just need to define ∂ for every r-cell $s_r \in C_r$ because C_r is a basis of K_r. An important constraint of the definition is the property that the boundary of the boundary vanishes: $\partial^2 = 0$. The boundaries of the r-cells are defined by

$$\begin{aligned}
\partial\langle i, j\rangle &= i - j\,,\\
\partial p_{i,km} &= \langle i, i + \hat{k}\rangle + \langle i + \hat{k}, i + \hat{k} + \hat{m}\rangle + \langle i + \hat{k} + \hat{m}, i + \hat{m}\rangle + \langle i + \hat{m}, i\rangle\,,\\
\partial c_i &= p_{i,13} + p_{i+\hat{2},31} + p_{i,21} + p_{i+\hat{3},12} + p_{i,32} + p_{i+\hat{1},23}\,.
\end{aligned}$$

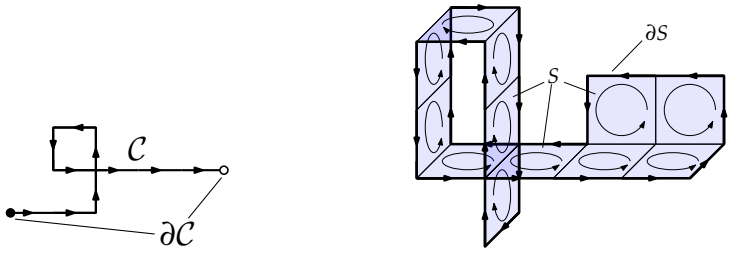

(a) path $\mathcal{C}$ and its boundary $\partial\mathcal{C}$ (b) surface S and its boundary ∂S

Figure 4.2: Illustration of a path $\mathcal{C}$, a surface S and their respective boundaries.

Now, we can define paths and surfaces. A path $\mathcal{C}$ is a 1-chain such that the boundary $\partial\mathcal{C}$ are the endpoints of the path:

$$\mathcal{C} = \langle i, a_1\rangle + \langle a_1, a_2\rangle + \ldots + \langle a_n, j\rangle$$

and

$$\partial\mathcal{C} = i - j\,.$$

A surface S is simply a 2-chain, i.e. a formal sum of plaquettes. In the usual sense, we may consider a surface S to be a 2-chain with an additional constraint. If an edge between sites i and j of the lattice is shared by an even number of plaquettes then the plaquettes are orientated in a way such that $\langle i, j\rangle$ and $\langle j, i\rangle$ do not occur in ∂S. An example of paths, surfaces and their boundaries is shown in Figure 4.2.

We cannot only define a boundary operator ∂, but we can also define a linear operator D which transforms a r-chain d_r into an $(d-r)$-chain $d^*_{d-r} = Dd_r$ on the dual lattice for the dimensions $d = 2$ or $d = 3$. The dual lattice is the spatial lattice shifted half a spacing in all directions. We analogously have r-cells on the dual lattice: sites, links, plaquettes and cubes. We define them as on the spatial lattice but indicate them with an asterisk: i^*, $\langle i, i+\hat{k}\rangle^*$, $p^*_{i,km}$ and c^*_i. Thus, we also have the spaces K^*_r. For $d = 3$, the dual $Dc_i = i^*$ of a cube c_i is the site i^* placed in the middle of the cube c_i, the dual $Dp_{i,km} = \langle i - \hat{n}, i\rangle^*$ of a plaquette $p_{i,km}$ is the link $\langle i - \hat{n}, i\rangle^*$, $n \neq k, m$ which penetrates the plaquette orthogonally in its center, the dual $D\langle i, i+\hat{n}\rangle = p^*_{i-\hat{k}-\hat{m},km}$ of a link $\langle i, i+\hat{n}\rangle$ is the plaquette $p^*_{i-\hat{k}-\hat{m},km}$ which is again penetrated by the link through its center, and finally the dual $Di = c^*_{i-\hat{1}-\hat{2}-\hat{3}}$ of a site i is the cube $c^*_{i-\hat{1}-\hat{2}-\hat{3}}$. For $d = 2$, there are no cubes. The dual $Dp_{i,12} = i^*$ of a plaquette $p_{i,12}$ is the site i^*, the dual

$$D\langle i, i+\hat{k}\rangle = \begin{cases} \langle i - \hat{2}, i\rangle^*, & k = 1 \\ \langle i, i - \hat{1}\rangle^*, & k = 2 \end{cases}$$

of a link $\langle i, i+\hat{k}\rangle$ is again a link, and the dual $Di = p^*_{i-\hat{1}-\hat{2},12}$ of a site i is the plaquette $p^*_{i-\hat{1}-\hat{2},12}$. This self-duality of links can be used for example in showing self-duality for various spin systems in two-dimensions [132, 136, 137].

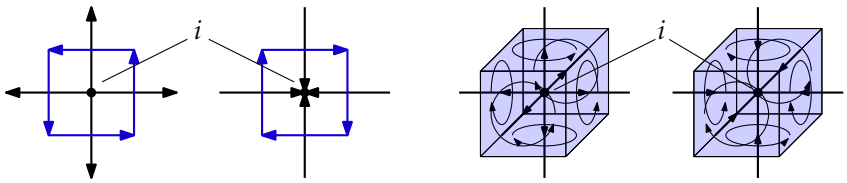

(a) $d = 2$ (b) $d = 3$

Figure 4.3: Illustration of Gauss's law manifesting itself on the lattice (black) and the dual lattice (blue) for two ($d = 2$) and three ($d = 3$) dimensions.

We are ready to redefine Equation (4.2) to the more general case of an arbitrary 1-chain $d_1 = \sum_{s_1 \in C_1} \alpha_{s_1} s_1$ of the spatial lattice:

$$I(d_1, z) = \left\langle \prod_{\langle i, i+\hat{k} \rangle} \left(\hat{E}^z_{\langle i, i+\hat{k} \rangle} \right)^{\alpha_{\langle i, i+\hat{k} \rangle}} \right\rangle \tag{4.3}$$

with $z \in Z_3$. Crucially, we, now, restrict ourselves to the pure gauge case, i.e. we consider the theory without any dynamical fermions. As an immediate consequence, Gauss's law in Equation (3.15) reduces to

$$\prod_{j \sim i} \hat{E}^z_{\langle i,j \rangle} \, |\psi\rangle = |\psi\rangle \tag{4.4}$$

for all $|\psi\rangle \in \mathcal{H}_{\text{phys}}$ and $z \in Z_3$. Hence, this restriction enables us to insert the left-hand side of Equation (4.4) into the expectation value $I(d_1, z)$ as often as we please because it acts as the unit operator. Inserting and rearranging the center-electric flux operators changes the exponents $\alpha_{\langle i, i+\hat{k} \rangle}$ in general. The expectation value $I(d_1, z)$ is, therefore, equivalent to $I(d_1', z)$ with some different 1-chain d_1' after the insertion of the $\mathbb{Z}_3$-law. The chain d_1' is obviously determined by

$$d_1' = d_1 + \sum_{j \sim i} \langle i, j \rangle \quad \left(d_1' = d_1 - \sum_{j \sim i} \langle i, j \rangle \right)$$

if we insert $\prod_{j \sim i} \hat{E}^z_{\langle i,j \rangle}$ $\left(\prod_{j \sim i} \hat{E}^{z^{-1}}_{\langle i,j \rangle} \right)$ at the site i. The $\mathbb{Z}_3$-law manifest itself as the 1-chain $\pm \sum_{j \sim i} \langle i, j \rangle$. On the dual lattice, Gauss's law is a boundless rectangle for $d = 2$ or a boundless cube surface for $d = 3$. This is illustrated in Figure 4.3. Now, consider d_1 and d_1' only differing by Gauss's law $\pm \sum_{j \sim i} \langle i, j \rangle$. Then the boundary of the dual chain

$$\partial D d_1' = \partial D d_1 \pm \partial D \sum_{j \sim i} \langle i, j \rangle = \partial D d_1 \, .$$

is identical for both 1-chains. We can reverse the argument. Assume we define some surface S^* on the dual lattice with $d = 3$. The boundary of the surface is ∂S^* and the dual of the surface is the 1-chain $d_1 = DS^*$ on the spatial lattice. The boundary ∂S^* is the vortex line. This is illustrated in Figure 4.4 for the surface shown in Figure 4.2. Any deformation of the surface S^* by one of the

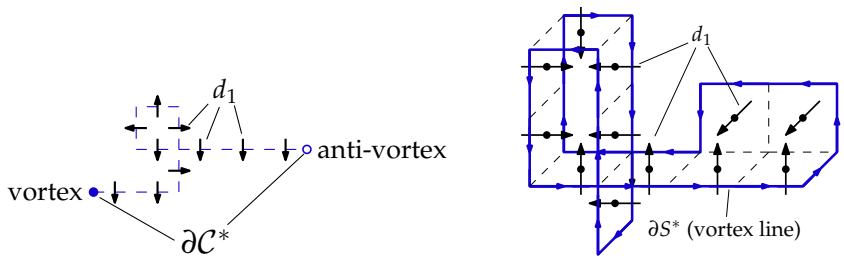

(a) $d = 2$ (b) $d = 3$

Figure 4.4: Illustration of the 1-chain d_1 which is dual to the path $\mathcal{C}^*$ or surface S^* of Figure 4.2. In two-dimensions, $\partial\mathcal{C}^*$ is interpreted as a vortex-antivortex pair. In three dimensions, ∂S^* is interpreted as a vortex line.

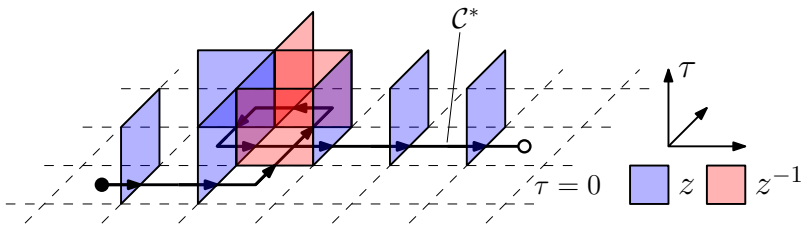

Figure 4.5: Illustration of twists in the path integral of Equation (4.3) of the path $\mathcal{C}^*$ from Figure 4.2. The path $\mathcal{C}^*$ is placed on the dual spatial lattice of the zeroth layer of Euclidean time.

cubes of Figure 4.3 changes the surface S^* and the 1-chain d_1 in general but not the vortex line ∂S^*. Because such changes of the 1-chain d_1 do not change the expectation value $I(d_1, z)$, we conclude that the expectation value $I(d_1, z)$ for a surface S^* is only determined by its boundary ∂S^* in the sense that all deformations due to Gauss's law yield the same expectation value. For two-dimensions, Gauss's law yields deformations of paths $\mathcal{C}^*$ on the dual lattice, and, therefore, the expectation value $I(d_1, z)$ only depends on the boundary $\partial\mathcal{C}^* = i - j$ which is given by its two endpoints i and $-j$. We interpret i as a vortex and $-j$ as an antivortex, see Figure 4.4. A path $\mathcal{C}^*$ is denoted a Dirac string, and a surface S^* is denoted a Dirac sheet.

The path integral of a 1-chain d_1 is computed similar to the case of $\langle \hat{E}^z_{\langle i,j\rangle} \rangle$. The only difference is that we introduce multiple twists depending on the coefficients $\alpha_{\langle i,i+\hat{k}\rangle}$ of d_1. Each operator $\left(\hat{E}^z_{\langle i,i+\hat{k}\rangle}\right)^{\alpha_{\langle i,i+\hat{k}\rangle}}$ twists the timelike plaquette $p_{(i,0),k4}$ with the center element $z^{-\alpha_{\langle i,i+\hat{k}\rangle}}$. The timelike plaquette lies between the zeroth and first layer of Euclidean time. In $(2+1)$-dimensions, we analogously twist the plaquettes for a 1-chain d_1 which is the dual of a path $\mathcal{C}^*$ on the dual lattice. The rules are the same as for three spatial directions. An illustration of the twists imposed by the path $\mathcal{C}^*$ from Figure 4.2 is shown in Figure 4.5.

On the dual lattice of the spatial torus, a surface S^* can be boundless $\partial S^* = 0$ either by being the surface $S^* = \partial V^*$ of a volume V^*, or it can span in two directions of the lattice and close periodically in both directions. In

the former case, the 1-chain d_1 of the surface S^* gives $I(d_1, z) = 1$ because we can deform the surface S^* with Gauss's law till it vanishes, i.e. we can remove all center-electric flux operators from the expectation value. We can therefore write $\Phi(\partial V^*, k) = I(d_1, u^k) = 1$ with $u = \mathrm{e}^{\frac{2\pi}{3}\mathrm{i}}$. Now, consider a surface S^*_{mn} which winds around the directions m and n with $m < n$. The surface is assumed to be a (mn)-plane of the dual lattice with all plaquettes orientated positively. Equivalently, the surface $S^*_{mn} = Dd_1$ is the dual of the 1-chain

$$d_1 = \sum_{a,b=0}^{N-1} \langle a\hat{m} + b\hat{n}, a\hat{m} + b\hat{n} + \hat{r} \rangle \,,$$

where we have attached the surface S^*_{mn} to the origin, and $r \neq m, n$. The path integral of $\Phi(S^*_{mn}, k) = I(d_1, u^k)$, $k \in \mathbb{Z}_3$ is given by twisting with u^{-k} all plaquettes between the zeroth and first layer of time which have a link in d_1 if we think of d_1 to be embedded in the zeroth layer of time. In principle, we are free to impose twists in all three spatial planes S^*_{23}, S^*_{13} and S^*_{12} simultaneously. The corresponding twists are denoted $\vec{k} = (k_1, k_2, k_3) \in \mathbb{Z}_3^3$: k_1 for S^*_{23}, k_2 for S^*_{13} and k_3 for S^*_{12}. The 1-chains of the surfaces are given by $d_1^{(1)}$, $d_1^{(2)}$ and $d_1^{(3)}$. The expectation value generalizes to

$$\Phi(\vec{k}) = \left\langle \prod_{s=1}^{3} \prod_{\langle i,i+\hat{a}\rangle} \left(\hat{E}^{u^{k_s}}_{\langle i,i+\hat{a}\rangle} \right)^{\alpha^{(s)}_{\langle i,i+\hat{a}\rangle}} \right\rangle$$

where $\alpha^{(s)}_{\langle i,i+\hat{a}\rangle} \in \mathbb{Z}$ are the coefficients of $d_1^{(s)}$. We define the ensembles

$$Z(\vec{k}) = Z \cdot \Phi(\vec{k}) = \mathrm{tr}\left(\left[\prod_{s=1}^{3} \prod_{\langle i,i+\hat{a}\rangle} \left(\hat{E}^{u^{k_s}}_{\langle i,i+\hat{a}\rangle} \right)^{\alpha^{(s)}_{\langle i,i+\hat{a}\rangle}} \right] \mathrm{e}^{-\beta \hat{H}} \hat{P}_0 \right).$$

In the terminology of [127–132], the path integral of $Z(\vec{k})$ is an ensemble with temporally twisted boundary conditions.

For every surface S^*_{mn}, the operator

$$\hat{E}^z(S^*_{mn}) = \prod_{\langle i,i+\hat{a}\rangle} \left(\hat{E}^z_{\langle i,i+\hat{a}\rangle} \right)^{\alpha^{(s)}_{\langle i,i+\hat{a}\rangle}}$$

constitutes a representation of Z_3. Furthermore, comparing with Equation (3.16), the operator

$$\hat{P}(S^*_{mn}, e) = \frac{1}{3} \sum_{z \in Z_3} z^{-e} \hat{E}^z(S^*_{mn}),\ e \in \mathbb{Z}_3 \tag{4.5}$$

is a projection operator. Consider $|\psi\rangle \in \mathcal{H}_{\mathrm{phys}}$. We obviously have

$$\hat{E}^z(S^*_{mn}) \hat{P}(S^*_{mn}, e) \,|\psi\rangle = z^e \hat{P}(S^*_{mn}, e) \,|\psi\rangle$$

if we follow the line of argument which comes after Equation (3.16). Therefore, a state $\hat{P}(S^*_{mn}, e) \,|\psi\rangle$ has a well-defined center value $e \in \mathbb{Z}_3$ and constitutes an

irreducible representation of Z_3. We denote e the center-electric flux through the surface S^*_{mn}. This is not merely a definition but motivated by the sectors $\mathcal{H}_{\{q,e\}}$ of flux-tube configurations $\{q,e\}$. The physical Hilbert space $\mathcal{H}_{\text{phys}}$ decomposes into the sectors of flux-tube configurations as we have already seen in Equation (3.18). The projection operator $\hat{P}(S^*_{mn},e)$ acts as

$$\hat{P}(S^*_{mn},e)\,|\psi\rangle = \frac{1}{3}\sum_{z\in Z_3} z^{-e}\hat{E}^z(S^*_{mn})\,|\psi\rangle = \frac{1}{3}\sum_{z\in Z_3} z^{\phi(S^*_{mn})-e}\,|\psi\rangle \tag{4.6}$$

$$= \delta(\phi(S^*_{mn}) = e \mod 3)\,|\psi\rangle \tag{4.7}$$

on a state $|\psi\rangle \in \mathcal{H}_{\{q,e\}}$, where

$$\phi(S^*_{mn}) = \sum_{\langle i,i+\hat{k}\rangle} \alpha^{(s)}_{\langle i,i+\hat{k}\rangle} e_{\langle i,i+\hat{k}\rangle}$$

with $e_{\langle i,i+\hat{k}\rangle} \in \{q,e\}$. The value $\phi(S^*_{mn})$ measures the total center-electric flux through the surface S^*_{mn}. The projection operator $\hat{P}(S^*_{mn},e)\,|\psi\rangle$ either gives $|\psi\rangle$ or zero depending on whether the total center-electric flux $\phi(S^*_{mn})$ through S^*_{mn} equals e up to a multiple of three. Note that $\phi(S^*_{mn})$ measures the total center-electric flux in the sense that it just adds all center-electric flux variables $e_{\langle i,i+\hat{k}\rangle}$ of S^*_{mn}. However, if we want a true total center-electric flux $\phi^{(3)}(S^*_{mn}) \in \mathbb{Z}_3$, we have to take the total sum with the group operation $+_3$ of $\mathbb{Z}_3$. Equations (3.18) and (4.7) give

$$\mathcal{H}(S^*_{mn},e) = \hat{P}(S^*_{mn},e)\mathcal{H}_{\text{phys}} = \bigoplus_{\substack{\{q,e\}_{\text{phys}} \\ \phi(S^*_{mn})=e \bmod 3}} \mathcal{H}_{\{q,e\}}\,.$$

The subspace $\mathcal{H}(S^*_{mn},e)$ is, therefore, the subspace of all states with fixed center-electric flux e through the surface S^*_{mn}. This decomposition is valid with and without fermions included. However, for now, we are concerned with pure gauge theory, where fermions are absent. Therefore, the flux tube configurations are only made of center-electric fluxes $e_{\langle i,i+\hat{k}\rangle} \in \{e\}$.

What is the physical significance of the subspace $\mathcal{H}(S^*_{mn},e)$? The operator $\hat{P}(S^*_{mn},e)$ commutes with the transfer-operator $\hat{T}$ [77]: $[\hat{P}(S^*_{mn},e),\hat{T}] = 0$. To see this, we write

$$\hat{T}\hat{E}^z(S^*_{mn})f(U) = \int \mathcal{D}U'\, S(U,U')T_{\text{G}}(U')f((z(S^*_{mn})U')\,.$$

The factor $z(S^*_{mn})$ multiplies certain gauge variables U' with the center element z. The factor $z(S^*_{mn})$ is due to the application of $\hat{E}^z(S^*_{mn})$ to the state $f(U)$: $\hat{E}^z(S^*_{mn})f(U) = f(z(S^*_{mn})U)$. Each center operator $\hat{E}^z_{\langle i,j\rangle}$ of $\hat{E}^z(S^*_{mn})$ creates a factor z^{-1} for the gauge variable $U_{\langle i,j\rangle}$ as it is stated in Equation (3.14). Because the Haar measure is left-invariant under multiplications of a group element, we can shift the center-dependence into the integral kernel by multiplying all gauge variables affected by $z(S^*_{mn})$ with z:

$$\hat{T}\hat{E}^z(S^*_{mn})f(U) = \int \mathcal{D}U'\, S(U,z^{-1}(S^*_{mn})U')T_{\text{G}}(z^{-1}(S^*_{mn})U')f(U')\,.$$

The function $T_{\mathrm{G}}(U')$ only includes spatial plaquettes. A link $\langle i, i+\hat{r}\rangle$ of the 1-chain $d_1^{(s)}$ of S^*_{mn} is part of two spatial plaquettes attached to the site i. For each of these plaquettes, the border includes a link $\langle j+\hat{r}, j\rangle$ whose inverse $\langle j, j+\hat{r}\rangle$ is also part of $d_1^{(s)}$. Hence, in $T_{\mathrm{G}}(U')$, the plaquette variable includes the factor $U_{\langle i,i+\hat{r}\rangle}$ and $U_{\langle j+\hat{r},j\rangle}$. The operator $z^{-1}(S^*_{mn})$ multiplies $U_{\langle i,i+\hat{r}\rangle}$ with z and $U_{\langle j+\hat{r},j\rangle}$ with z^{-1}. Therefore, the overall twist of the plaquette vanishes, and we have $T_{\mathrm{G}}(z^{-1}(S^*_{mn})U') = T_{\mathrm{G}}(U')$. It is straightforward to see that

$$S(U, z^{-1}(S^*_{mn})U') = S(z(S^*_{mn})U, U')\,,$$

and, therefore,

$$\hat{T}\hat{E}^z(S^*_{mn})f(U) = \int \mathcal{D}U'\, S(z(S^*_{mn})U, U')T_{\mathrm{G}}(U')f(U') = \hat{E}^z(S^*_{mn})\hat{T}f(U)\,.$$

The center operator $\hat{E}^z(S^*_{mn})$ commutes with $\hat{T}$. This means the projection operator $\hat{P}(S^*_{mn}, e)$ also commutes with $\hat{T}$. If we take the continuum limit in Euclidean time, we get

$$[\hat{P}(S^*_{mn}, e), \mathrm{e}^{-\beta\hat{H}}] = \lim_{N_4\to\infty}\left[\hat{P}(S^*_{mn}, e), \left(\mathcal{N}(a_4)\hat{T}_{a_4=\beta/N_4}\right)^{N_4}\right] = 0\,,$$

and, by taking the derivative on the left-hand side at $\beta = 0$, $[\hat{P}(S^*_{mn}, e), \hat{H}] = 0$. The sectors $\mathcal{H}(S^*_{mn}, e)$ are actually invariant under the dynamics: once the center-electric flux e is fixed through the surface S^*_{mn}, it stays fixed for all times. Therefore, we can restrict our quantum theory to a sector $\mathcal{H}(S^*_{mn}, e)$ and define the thermodynamic ensemble $Z_{\mathrm{el.}}(e_s)$ of fixed center-electric flux e_s through the surface S^*_{mn}:

$$Z_{\mathrm{el.}}(e_s) = \mathrm{tr}\left(\hat{P}(S^*_{mn}, e_s)\mathrm{e}^{-\beta\hat{H}}\hat{P}_0\right).$$

This way of constructing ensembles of fixed center-electric flux in the transfer-matrix formulation was formulated first in [77]. We just followed their line of argument.

Evidently, the center-electric flux can be fixed through all surfaces S^*_{23}, S^*_{13} and S^*_{12} separately with the center-electric flux $\vec{e} = (e_1, e_2, e_3) \in \mathbb{Z}_3^3$ and the sector $\mathcal{H}(\vec{e})$ because the corresponding projection operators commute pairwise:

$$Z_{\mathrm{el.}}(\vec{e}) = \mathrm{tr}\left(\hat{P}(S^*_{23}, e_1)\hat{P}(S^*_{13}, e_2)\hat{P}(S^*_{12}, e_3)\mathrm{e}^{-\beta\hat{H}}\hat{P}_0\right).$$

Inserting Equation (4.5) then yields

$$Z_{\mathrm{el.}}(\vec{e}) = \frac{1}{N_{\mathrm{c}}^3}\sum_{\vec{k}\in\mathbb{Z}_3^3}\exp\left(-\frac{2\pi\mathrm{i}}{N}\,\vec{e}\cdot\vec{k}\right)Z(\vec{k}) \tag{4.8}$$

with $N_{\mathrm{c}} = 3$. This is the well-known duality relation between center-electric flux ensembles $Z_{\mathrm{el.}}(\vec{e})$ and temporally twisted ensembles $Z(\vec{k})$ [22, 109, 111, 127, 131, 132].

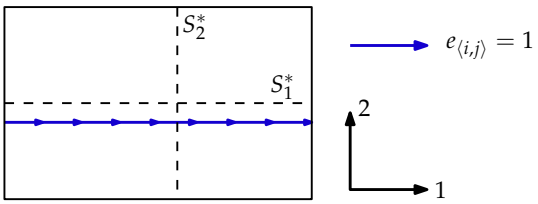

Figure 4.6: Example of a minimally thin string creating the center-electric flux $\vec{e} = (1, 0)$ in two spatial dimensions.

Confinement-deconfinement transition

In Section 2.4, we have discussed the confinement-deconfinement transition of QCD in the absence of fermions. The system possesses a phase transition because of the spontaneous breaking of the global $\mathbb{Z}_3$-symmetry. The order parameter of the transition is the expectation value $\langle L_i \rangle$ of the Polyakov loop L_i. The phase of unbroken symmetry is identified with the confined phase, and the symmetry-broken phase is identified with the deconfined phase.

An alternative observable for this phase transition can be constructed with the center-electric flux ensembles $Z_{\text{el.}}(\vec{e})$. We consider the ratio

$$R(\vec{e}) = \frac{Z_{\text{el.}}(\vec{e})}{Z_{\text{el.}}(0)} \,.$$

The free-energy difference to impose the center-electric flux $\vec{e}$ along the spatial volume is then given by

$$\Delta F = -T \ln R(\vec{e}) \,.$$

What is the physical interpretation of ΔF? The confined phase is characterized by the formation of chromo-electric flux tubes, see Section 2.4. We might suspect that this characteristic manifests itself in the free-energy difference ΔF via an analog mechanism. Due to Gauss's law, the non-trivial flux variables $e_{\langle i,j\rangle} \in \{e\}$ of a flux-tube configuration $\{e\}$ must form closed loops. As a consequence, the only possibility for a configuration $\{e\}$ to create a non-trivial flux through a plane S^*_{mn} is to include a path $\mathcal{C}$ of non-trivial flux variables $e_{\langle i,j\rangle} \neq 0$ which winds around the lattice in the direction orthogonal to S^*_{mn}. Assume $\vec{e} = (1, 0, 0)$. The physical picture of the confined phase is now as follows [109]. In the confined phase, the center-electric fluxes condensate to thin strings, and part of them are forced to wind around the full length N_1 of the first direction because otherwise the center-electric flux $\vec{e} = (1, 0, 0)$ would not be enforced. The thinning happens due to the fact that larger non-trivial flux structures require larger energies in the confined phase. In the zero-temperature limit the thinning of strings becomes maximal in the sense that only the flux-tube configurations with one minimal string of length N_1 winding around the first direction contribute to the partition function $Z_{\text{el.}}(\vec{e})$. An example of such a minimal string is shown in Figure 4.6. The ground state of the system becomes degenerate in the zero-temperature limit. There is one ground state $|\psi_0\rangle \in \mathcal{H}_{\{e\}}$ for every flux-tube configuration $\{e\}$ with a minimally thin string creating the flux $\vec{e} = (1, 0, 0)$. Analog to the chromo-electric fields, the flux-tube configurations with a minimal string are expected

to have an energy proportional to the string tension σ and the length N_1 of the string if N_1, N_2 and N_3 are sufficiently large. The ensemble $Z_{\text{el.}}(0)$ enforces zero center-electric flux through all directions. Here, the energy is minimized by a ground state $|\psi_0\rangle \in \mathcal{H}_{\{e=0\}}$ of the sector with no non-trivial electric flux variables. We conclude

$$R(\vec{e}) \approx \alpha N_2 N_3 \exp\left(-\frac{\sigma a}{T} N_1\right)$$

near the zero-temperature limit [109]. The factor $N_2 N_3$ is the number of configurations with a minimal string winding around the first direction, i.e. $N_2 N_3$ is the number of positions through which the string can penetrate the surface S^*_{23}. The factor α is just an overall proportionality factor. The free-energy difference ΔF is

$$\frac{\Delta F}{T} = \frac{\sigma a}{T} N_1 - \ln(\alpha N_2 N_3)\,,$$

and therefore ([77])

$$\frac{\sigma a}{T} = \lim_{N_2,N_3\to\infty} \lim_{N_1\to\infty} \frac{1}{N_1} \frac{\Delta F}{T}\,. \tag{4.9}$$

Away from the zero-temperature limit but still in the confined phase, we expect the excitation of additional strings winding around the lattice. All these strings, which might not be minimally thin, have an energy proportional to the extent N_1. Consequently, expanding the volume in the first direction creates a divergent behavior of ΔF such that $\Delta F/(N_1 T)$ stays finite for $N_1 \to \infty$. Hence, the definition of $\sigma(T)$ is expected to stay well-defined away from the zero-temperature limit but it becomes temperature-dependent. In the deconfined phase, thin strings spread and become thick objects. The energy does not increase anymore proportional to the length N_1 such that $\sigma(T) = 0$. The free-energy difference stays finite in the infinite-volume limit because the energy required to impose flux-generating structures becomes negligible. We expect the string tension $\sigma(T)$ to indicate the transition between a confined and deconfined phase:

$$\frac{\sigma a}{T} \begin{cases} > 0, & T < T_{\text{c}} \\ = 0, & T > T_{\text{c}} \end{cases}. \tag{4.10}$$

Importantly, the free-energy difference ΔF diverges in the confined phase, whereas it tends to zero in the deconfined phase. For the ratio $R(\vec{e})$, we therefore expect

$$\lim_{N_1,N_2,N_3\to\infty} R(\vec{e}) = \begin{cases} 0, & T < T_{\text{c}} \\ 1, & T > T_{\text{c}} \end{cases} \tag{4.11}$$

in the infinite-volume limit. For the path-integral formulation of $R(\vec{e})$, this behavior has been demonstrated numerically in [127, 128] for the $(3+1)$-dimensional $\mathrm{SU}(2)$ theory and in [131] for the $(2+1)$-dimensional $\mathrm{SU}(3)$ theory. Unfortunately, there seems to be no numerical results of $R(\vec{e})$ for the $(3+1)$-dimensional $\mathrm{SU}(3)$ theory. However, intuitively, we expect Equation (4.11) to hold. The path integral formulation of $R(\vec{e})$ is identical whether the symmetric or asymmetric transfer operator is used. The symmetric transfer operator,

however, is Hermitian, and, therefore, we can define the Hamiltonian $\hat{T} \propto \mathrm{e}^{-\hat{H}}$ ($a_4 = 1$). The argument of a degenerate ground state becomes applicable to the path integral of $R(\vec{e})$. For fixed temporal extent N_4, we have $\hat{T}^{N_4} \propto \mathrm{e}^{-N_4\hat{H}}$, and the observed phase transition with respect to $R(\vec{e})$ ([127, 128, 131]) is a function of the bare coupling g_0 related to the temperature $T = (a(g_0)N_4)^{-1}$ by the lattice spacing $a(g_0)$ which is determined via the chosen renormalization scheme. In this case, the condensation to thin strings happens at sufficiently large couplings g_0 when $g_0 > g_\mathrm{c}$ is larger than the critical coupling g_c. It is important to state that there are no direct results which determine the sectors $\mathcal{H}_{\{e\}}$ to which the ground states belong. The above mechanism is merely a physical description whose consequences are verified numerically to the degree discussed. Of course, when we take the continuum limit of $R(\vec{e})$, be it the quantum-mechanical or the path integral formulation, we would fix the physical extents of the system when renormalizing the theory. Then, in the confined phase, the string condensation is given by

$$R(\vec{e}) \propto A_{23} \exp\left(-\frac{\sigma L_1}{T}\right)$$

A_{23} the physical surface of S^*_{23}. The string tension is then defined as

$$\sigma = \lim_{A_{23}\to\infty} \lim_{L_1\to\infty} \frac{1}{L_1} \Delta F$$

in the continuum limit.

Another approach of classifying the confinement-deconfinement transition is the insertion of center-magnetic fluxes. Consider a 't Hooft loop $\mathcal{C}^*$ with its minimal surface S^* such that $\mathcal{C}^* = \partial S^*$. The loop $\mathcal{C}^*$ and the surface S^* are defined on the dual spatial lattice. The 1-chain $d_1 = DS^*$ which is dual to S^* gives the expectation value $M(\mathcal{C}^*, k) = I(d_1, \mathrm{e}^{\frac{2\pi}{3}\mathrm{i}k})$ depending only on the 't Hooft loop $\mathcal{C}^*$ and the imposed twist $k \in \mathbb{Z}_3$. The expectation value $M(\mathcal{C}^*, 1)$ is interpreted to describe the insertion of a line $\mathcal{C}^*$ of center-magnetic flux. The free-energy difference of imposing such a line of center-magnetic flux is then $\Delta F = -T \ln M(\mathcal{C}^*, 1)$. The confined phase and deconfined phase are now classified by the behavior of the 't Hooft loop [22, 111, 113, 118, 122]:

$$\frac{\Delta F}{T} \propto \begin{cases} P(\mathcal{C}^*), & T < T_\mathrm{c} \\ A(\mathcal{C}^*), & T > T_\mathrm{c} \end{cases}$$

in the infinite-volume limit if the loops are chosen large enough. Here, $P(\mathcal{C}^*)$ describes the perimeter of the loop $\mathcal{C}^*$ and $A(\mathcal{C}^*)$ the surface of S^*, i.e. the number of plaquettes enclosed by $\mathcal{C}^*$. Similar, one can define an ensemble with a maximal 't Hooft loop. Consider the spatial lattice with equal extents $N = N_i, i \in \{1, 2, 3\}$. The 't Hooft loop $\mathcal{C}^* = R^*_{0,23}$ is set to be a rectangle $R^*_{0,23}$ attached to the origin 0 of the dual lattice on the 23-plane. The rectangle extends l links into each direction. It becomes a maximal 't Hooft loop if we set $l = N$. The expectation value $M(R^*_{0,23}, 1)$ is equivalent to the ratio

$$\frac{Z(\vec{k})}{Z(0)} = M(R^*_{0,23}, 1), \quad \vec{k} = (1, 0, 0)$$

for the maximal 't Hooft loop [122, 124, 127, 128]. Interpreted as a 1-chain, the maximal 't Hooft loop $\mathcal{C}^* = 0$ is zero because for every link $\langle i, j\rangle$ the link $\langle j, i\rangle$ is also part of the 1-chain $\mathcal{C}^*$. Therefore, the maximal 't Hooft loop encloses the surface S^*_{23} which consistently does not possess a boundary: $\partial S^*_{23} = 0$. The free-energy difference ΔF of a maximal 't Hooft loop $R^*_{0,23}$ measures therefore the free energy of introducing temporal twists with $\vec{k} = (1, 0, 0)$. The string tension $\sigma_*(T)$ of the temporal interface $\vec{k} = (1, 0, 0)$, denoted the dual string tension, is defined as ([124])

$$\sigma_* a^2 = -\lim_{N\to\infty} \frac{1}{N^2} \ln M(R^*_{0,23}, 1)\,.$$

Analogously to Equation (4.10), the confined and deconfined phase is expected to be indicated by the dual string tension $\sigma_*(T)$:

$$\sigma_* a^2 \begin{cases} > 0, & T > T_\mathrm{c} \\ = 0, & T < T_\mathrm{c} \end{cases}. \tag{4.12}$$

A consequence of Equation (4.12) is the singular behavior of the free-energy difference $\Delta F/T \to \infty$, $N \to \infty$ in the deconfined phase. In the confined phase, the free-energy difference is assumed to stay finite. We define the ratio $R_*(\vec{k}) = Z(\vec{k})/Z(0)$ which indicates the confinement-deconfinement transition dual to the ratio $R(\vec{e})$:

$$R_*(\vec{k}) = \begin{cases} 0, & T > T_\mathrm{c} \\ 1, & T < T_\mathrm{c} \end{cases}$$

in the infinite volume limit $N \to \infty$. The path integral formulation of $\sigma_*(T)$ and $R_*(\vec{k})$ have been investigated in [121, 122, 124, 126–128] for $(3+1)$-dimensional SU(2) theory, in [131, 138, 139] for $(2+1)$-dimensional SU(3) theory and in [140, 141] for $(3+1)$-dimensional SU(3) theory.

4.2 Fixed quark number ensembles

We are now ready to present the first main result of this thesis. We construct an ensemble in which the net-quark number N_V in a spatial subvolume V of the lattice is fixed to a value $N_V \neq 0 \mod 3$. To define such an ensemble, we first need a notion of local quark and antiquark numbers associated with sites of the spatial lattice. The transfer-matrix formulation naturally provides such a notion. We can define quark- and antiquark-number operators associated with a site i:

$$(\hat{N}^\sigma_\mathrm{q})_{i,a} = (\hat{\xi}^\sigma_\mathrm{q})^\dagger_{i,a}(\hat{\xi}^\sigma_\mathrm{q})_{i,a} \qquad \text{and} \qquad (\hat{N}^\sigma_{\bar{\mathrm{q}}})_{i,a} = (\hat{\xi}^\sigma_{\bar{\mathrm{q}}})^\dagger_{i,a}(\hat{\xi}^\sigma_{\bar{\mathrm{q}}})_{i,a}\,.$$

Hence, the total quark- and antiquark number at a site i are

$$\hat{N}_{\mathrm{q},i} = \sum_{a,\sigma}(\hat{N}^\sigma_\mathrm{q})_{i,a} \qquad \text{and} \qquad \hat{N}_{\bar{\mathrm{q}},i} = \sum_{a,\sigma}(\hat{N}^\sigma_{\bar{\mathrm{q}}})_{i,a}\,.$$

Consider now a simultaneous eigenstate $|\psi\rangle \in \mathcal{H}_\mathrm{phys}$ of all operators $\hat{N}_{\mathrm{q},i}$ and $\hat{N}_{\bar{\mathrm{q}},i}$: $\hat{N}_{\mathrm{q},i}|\psi\rangle = N_{\mathrm{q},i}|\psi\rangle$ and $\hat{N}_{\bar{\mathrm{q}},i}|\psi\rangle = N_{\bar{\mathrm{q}},i}|\psi\rangle$ with $N_{\mathrm{q},i}, N_{\bar{\mathrm{q}},i} \in \{0, \ldots, 6\}$. For

the eigenstate $|\psi\rangle$, it is well-defined to say that the site i is occupied with $N_{\mathrm{q},i}$ quarks and $N_{\bar{\mathrm{q}},i}$ antiquarks.

The net-quark number operator $\hat{N}_V$ for the subvolume V is now given by

$$\hat{N}_V = \sum_{i \in V} \left[\hat{N}_{\mathrm{q},i} - \hat{N}_{\bar{\mathrm{q}},i} \right] .$$

Consequently, the sectors of fixed net-quark number $N_V = e \mod 3$ with $e \in \mathbb{Z}_3$ are defined as

$$\mathcal{H}_V(e) = \overline{\mathrm{span} \Big\{ \, |\psi\rangle \in \mathcal{H}_{\mathrm{phys}} \, | \, \hat{N}_V \, |\psi\rangle = N_V \, |\psi\rangle \, , \, N_V = e \mod 3 \Big\}} .$$

A state $|\psi\rangle \in \mathcal{H}_V(e)$ is said to have a net-quark number $N_V = e \mod 3$ in the subvolume V in the sense that it can be approximated

$$\lim_{n \to \infty} |\psi_n\rangle = |\psi\rangle \tag{4.13}$$

by a sequence $(|\psi_n\rangle)_{n \in \mathbb{N}_0} \subseteq \mathrm{span}\{\ldots\}$ of states which are finite linear combinations of eigenstates of $\hat{N}_V$ with the constraint $N_V = e \mod 3$. Because $\mathcal{H}_V(e) \subseteq \mathcal{H}_{\mathrm{phys}}$ is a Hilbert space, we can define the projection operator $\hat{P}_V(e)$ which projects onto $\mathcal{H}_V(e)$.

Naively, we might be tempted to define the ensemble with fixed net-quark number $N_V = e \mod 3$ by just taking the trace over $\mathcal{H}_V(e)$:

$$Z(N_V =_3 e) = \mathrm{tr} \left(\mathrm{e}^{\beta \mu \hat{N}} \mathrm{e}^{-\beta \hat{H}} \hat{P}_V(e) \hat{P}_0 \right) ,$$

where $a =_3 b$ is a short-hand notation for $a = b \mod 3$. However, this partition function does not describe the ensemble of a quantum-mechanical system with states having a net-quark number $N_V =_3 e$ because actually the Hamiltonian $\hat{H}$ cannot be restricted to $\mathcal{H}_V(e)$. A quantum-mechanical system only described by states from $\mathcal{H}_V(e)$ under the dynamics of $\hat{H}$ is not possible. The Hamiltonian $\hat{H}$ does not commute with the projection operator $\hat{P}_V(e)$, $[\hat{P}_V(e), \hat{H}] \neq 0$, and in general we have to expect an initial state $|\psi_0\rangle \in \mathcal{H}_V(e)$ to be driven out of the sector $\mathcal{H}_V(e)$ after some time $t > 0$:

$$|\psi(t)\rangle = \mathrm{e}^{-\mathrm{i}t\hat{H}} \, |\psi_0\rangle \notin \mathcal{H}_V(e) \, . \tag{4.14}$$

Intuitively, this corresponds to the fact that the dynamics are blind towards our arbitrary choice of the subvolume V. For example ([90]), assume a state $|\psi\rangle \in \mathcal{H}_V(e)$ which also happens to be a simultaneous eigenstate of all operators $\hat{N}_{\mathrm{q},i}$ and $\hat{N}_{\bar{\mathrm{q}},i}$. In general, the dynamics governed by $\hat{H}$ will create additional non-vanishing contributions $|\varphi\rangle \in \mathcal{H}_V(e')$ from the other sectors $\mathcal{H}_V(e')$ with $e' \neq e$. Decomposing the sector $\mathcal{H}_V(e')$ into sectors of all possible eigenvalues of $\hat{N}_{\mathrm{q},i}$ and $\hat{N}_{\bar{\mathrm{q}},i}$, $|\varphi\rangle$ can necessarily only be made of contributions from sectors with particle-number configurations $(N'_{\mathrm{q},i}, \overline{N}'_{\mathrm{q},i})$ which differ from the configuration $(N_{\mathrm{q},i}, \overline{N}_{\mathrm{q},i})$ of $|\psi\rangle$ because $\mathcal{H}_V(e')$ is orthogonal to $\mathcal{H}_V(e)$. Therefore, $|\varphi\rangle$ is a superposition of states with particle configurations $(N'_{\mathrm{q},i}, \overline{N}'_{\mathrm{q},i})$ where the

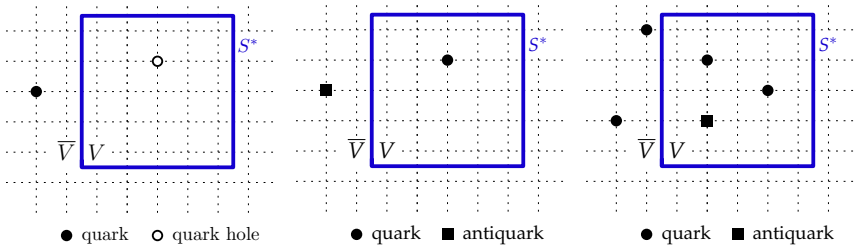

(a) quark-quark-hole pair (b) quark-antiquark pair (c) hadronic structure

Figure 4.7: Illustration of relative changes of the particle-number configuration of some state $|\psi\rangle$ which happens to be an simultaneous eigenstate of all operators $\hat{N}_{\mathrm{q},i}$ and $\hat{N}_{\bar{\mathrm{q}},i}$. The dynamics (4.14) create contributions from sectors with different net-quark number N_V modulo three in general. Exemplary scenarios: (a): a quark moves from V into the complement $\overline{V}$ leaving behind a particle hole in V, (b): a quark-antiquark pair is created between the volume V and $\overline{V}$ and (c): a more complicated hadronic structure is created between both volumes.

net-quark number modulo three is reshuffled between the volume V and its complement $\overline{V}$ relative to the initial configurations $(N_{\mathrm{q},i}, \overline{N}_{\mathrm{q},i})$. Different mechanisms are possible. Quarks and antiquarks can be moved between the volume V and its complement $\overline{V}$, or a quark-antiquark pair or other hadronic structures can be created (destroyed) between both volumes. A schematic illustration is given in Figure 4.7. The only constraint is the conservation of the total net-quark number $N = 0 \mod 3$ up to a multiple of three due to gauge invariance. Because the richness of the QCD dynamics includes the movement, creation and destruction of fermions between different spatial sites, the sector $\mathcal{H}_V(e)$ cannot be left invariant for an arbitrary subvolume V. The interaction has no way of knowing which volume V has been chosen.

Recall that the construction of 't Hooft's center-electric flux ensembles $Z_{\mathrm{el.}}(\vec{e})$ does not possess such a problem because the projection operator $\hat{P}(S^*_{mn}, e)$ projecting onto the sector $\mathcal{H}(S^*_{mn}, e)$ of fixed center-electric flux $e \in \mathbb{Z}_3$ through the surface S^*_{mn} commutes with the Hamiltonian $\hat{H}$: $[\hat{P}(S^*_{mn}, e), \hat{H}] = 0$. The center-electric fluxes winding around a direction can be deformed by the dynamics but are overall stable in their total flux which they generate through the surface S^*_{mn}. However, also the pure gauge theory is not aware of the exact form of the chosen interface. We are free to deform S^*_{mn} into any other shape by means of Gauss's law.

To be able to define $Z(N_V =_3 e)$ correctly, we must make the dynamics aware of the interface d_1 between the volume V and its complement $\overline{V}$, i.e. the 1-chain of links connecting both volumes. On the dual lattice, the volume $V^* = DV$ is the 3-chain of all cubes containing sites of V, which formally is a 0-chain, and the surface of V^* is $S^* = \partial V^*$ such that $d_1 = DS^*$. To make the dynamics aware of the interface d_1, we have to modify the dynamics such that we replace the Hamiltonian $\hat{H}$ with a new Hamiltonian $\hat{H}'$. The modified Hamiltonian $\hat{H}'$ must be gauge-invariant, and the modification should only be made locally at the interface d_1. Such a modification is interpreted as the

insertion of a membrane forbidding changes of net-quark numbers between V and $\overline{V}$ which are not a multiple of three. Then, the correct partition function $Z(N_V =_3 e)$ reads

$$Z(N_V =_3 e) = \mathrm{tr}\left(\mathrm{e}^{\beta\mu\hat{N}}\mathrm{e}^{-\beta\hat{H}'}\hat{P}_V(e)\hat{P}_0\right). \tag{4.15}$$

The total net-quark number operator $\hat{N}$ is not modified however because $[\hat{N}, \hat{P}_V(e)] = 0$. To see this, we first note that $[\hat{N}, \hat{N}_V] = 0$. There exists a sequence $(|\psi_n\rangle)_{n\in\mathbb{N}_0}$ as in Equation (4.13) for a state $|\psi\rangle \in \mathcal{H}_V(e)$. Because $|\psi_n\rangle$ is a linear combination of eigenstates of $\hat{N}_V$ and $[\hat{N}, \hat{N}_V] = 0$, we have $\hat{N}|\psi_n\rangle \in \mathrm{span}\{\ldots\}$. $\hat{N}|\psi_n\rangle$ is a sequence that if it converges its limit value lies in the closure of $\mathrm{span}\{\ldots\}$: $\mathcal{H}_V(e) = \overline{\mathrm{span}\{\ldots\}}$. By continuity of $\hat{N}$, $\hat{N}|\psi_n\rangle$ indeed converges to $\hat{N}|\psi\rangle$. Consequently, $\hat{N}|\psi\rangle \in \mathcal{H}_V(e)$.

How do we construct $\hat{H}'$ correctly and derive the corresponding path integral? To this end, we need to make the connection with center charges and center-electric fields. Remember that Equation (3.18) implies the decomposition of the physical Hilbert space $\mathcal{H}_{\mathrm{phys}}$ into sectors $\mathcal{H}_{\{q,e\}}$ of flux-tube configurations $\{q, e\}$. We can measure the total center-electric charge q_V of a flux-tube configuration $\{q, e\}$ in the subvolume V:

$$q_V = \sum_{i\in V} q_i\,. \tag{4.16}$$

Classifying the flux-tube configurations based on their value $q_V =_3 e$, we can write

$$\mathcal{H}_{\mathrm{phys}} = \mathcal{H}_{q_V=_30} \oplus \mathcal{H}_{q_V=_31} \oplus \mathcal{H}_{q_V=_32}$$

with

$$\mathcal{H}_{q_V=_3e} = \bigoplus_{\substack{\{q,e\}_{\mathrm{phys}}\\ q_V=_3e}} \mathcal{H}_{\{q,e\}}\,.$$

A state $|\psi\rangle \in \mathcal{H}_{q_V=_3e}$ has a well-defined center charge for the subvolume V because

$$\hat{Q}_V^z|\psi\rangle = z^e|\psi\rangle$$

with the total center-charge operator

$$\hat{Q}_V^z = \prod_{i\in V}\hat{Q}_i^z$$

of V. This classification of the Hibert space $\mathcal{H}_{\mathrm{phys}}$ into the total center charge of the subvolume V is essentially based on the same ideas as in [87–89, 106]. Here, we have adapted the concept to our specific transfer-matrix construction via the sectors of flux-tube configurations $\{q, e\}$. Now, we can establish the fact that a state with total center charge $q_V =_3 e$ of the subvolume V is also a state with net-quark number $N_V =_3 e$ because quarks and antiquarks are sources of center charge as implied by Equation (3.12) and (3.13). In our formalism, this means

$$\mathcal{H}_{q_V=_3e} = \mathcal{H}_V(e)\,. \tag{4.17}$$

The proof of this statement is straightforward. Consider $|\psi\rangle \in \mathcal{H}_V(e)$. Then, we have a sequence $(|\psi\rangle_n)_{n\in\mathbb{N}_0}$ as in Equation (4.13). For each $|\psi_n\rangle$, we have

$$|\psi_n\rangle = \sum_{k=1}^{m_n} |\psi_{nk}\rangle$$

with eigenstates $|\psi_{nk}\rangle$ of $\hat{N}_V$ and $N_V =_3 e$: $\hat{N}_V |\psi_{nk}\rangle = N_V |\psi_{nk}\rangle$. Now, such an eigenstate $|\psi_{nk}\rangle$ can be written as

$$|\psi_{nk}\rangle = \sum_m \sum_{\alpha_1,\ldots,\alpha_m} f_{\alpha_1,\ldots,\alpha_m}(U) \otimes \hat{\xi}^\dagger_{\alpha_1} \ldots \hat{\xi}^\dagger_{\alpha_m} |0\rangle \ .$$

Because $|\psi_{nk}\rangle$ is an eigenstate of $\hat{N}_V$ with eigenvalue $N_V =_3 e$, only fermionic particle states with net-quark number $N_V =_3 e$ occur in the expansion of $|\psi_{nk}\rangle$, i.e. the net number of creation operators of quarks and antiquarks associated with sites of the volume V must be e up to a multiple of three. Hence, we have

$$\hat{Q}^z_V |\psi_{nk}\rangle = \left(\sum_{i\in V} \hat{Q}_i\right) |\psi_{nk}\rangle = z^{N_V} |\psi_{nk}\rangle = z^e |\psi_{nk}\rangle$$

if we employ Equation (3.12) and (3.13). Therefore,

$$\hat{Q}^z_V |\psi_n\rangle = z^e |\psi_n\rangle$$

by linearity of $\hat{Q}^z_V$, and

$$\hat{Q}^z_V |\psi\rangle = z^e |\psi\rangle$$

by continuity of $\hat{Q}^z_V$. This shows $\mathcal{H}_V(e) \subseteq \mathcal{H}_{q_V=_3 e}$. Now, assume $|\psi\rangle \in \mathcal{H}_{q_V=_3 e}$. If we diagonalize $\mathcal{H}_{\text{phys}}$ into an orthonormal basis $\{|\psi_k\rangle\}$ of $\hat{N}_V$ eigenstates, we have

$$|\psi\rangle = \sum_{k=1}^{\infty} \alpha_k |\psi_k\rangle$$

with $\hat{N}_V |\psi_k\rangle = N_{V,k} |\psi_k\rangle$. Now,

$$\hat{Q}^z_V |\psi_k\rangle = z^{N_{V,k}} |\psi_k\rangle$$

because $|\psi_k\rangle$ is from the Fock-space sector with a net number $N_{V,k}$ of creation operators, and Equation (3.12) and (3.13) imply a factor z and $z^\dagger$ for each quark- or antiquark-creation operator. Consequently,

$$\hat{Q}^z_V |\psi\rangle = \sum_{k=1}^{\infty} z^{N_{V,k}} \alpha_k |\psi_k\rangle = z^e |\psi\rangle \ .$$

However, the basis vectors $|\psi_k\rangle$ are pairwise orthogonal, and the last equivalence can only be given if

$$z^{N_{V,k}} = z^e$$

for all k. This is only the case if $N_{V,k} =_3 e$ for all k which readily implies that $|\psi\rangle \in \mathcal{H}_V(e)$. This shows that $\mathcal{H}_V(e) \subseteq \mathcal{H}_{q_V=_3 e}$ concluding the proof.

This connection between the net-quark number operator $\hat{N}_V$ and the center-electric charge operator $\hat{Q}^z_V$ allows to reformulate our problem of constructing

an ensemble of fixed net-quark number to the equivalent problem of constructing an ensemble of fixed center charge $q_V =_3 e$ of the subvolume V. We denote the projection operator onto $\mathcal{H}_{q_V=_3 e}$ as $\hat{P}_{q_V}(e)$ which obviously fulfills $\hat{P}_{q_V}(e) = \hat{P}_V(e)$. Because $\hat{Q}_V^z$ is a representation of the center $\mathbb{Z}_3$, the projection operator $\hat{P}_{q_V}(e)$ can explicitly be written as

$$\hat{P}_{q_V}(e) = \frac{1}{3} \sum_{z \in \mathbb{Z}_3} z^{-e} \hat{Q}_V^z \,.$$

For a flux-tube configuration $\{q, e\}$, the total center-electric flux ϕ_{S^*} which flows through the surface S^* of the dual volume V^* is

$$\phi_{S^*} = \sum_{\langle i,j \rangle \in d_1} e_{\langle i,j \rangle} \,. \tag{4.18}$$

Due to the $\mathbb{Z}_3$-Gauss law (3.17), we have

$$q_V = -\phi_{S^*} \mod 3 \,, \tag{4.19}$$

and, therefore, we actually have

$$\mathcal{H}_{q_V=_3 e} = \mathcal{H}_{\phi_{S^*}=_3 -e} = \bigoplus_{\substack{\{q,e\}_{\text{phys}} \\ \phi_{S^*}=_3 -e}} \mathcal{H}_{\{q,e\}} \,.$$

A formal proof can be made by showing $\hat{P}_{q_V}(e) = \hat{P}_{\phi_{S^*}}(-e)$ where $\hat{P}_{\phi_{S^*}}(e)$ is the projection operator onto $\mathcal{H}_{\phi_{S^*}=_3 e}$:

$$\begin{aligned}
\hat{P}_{q_V}(e) &= \frac{1}{3} \sum_{z \in \mathbb{Z}_3} z^{-e} \hat{Q}_V^z = \frac{1}{3} \sum_{z \in \mathbb{Z}_3} z^{-e} \prod_{i \in V} \hat{Q}_i^z \\
&= \frac{1}{3} \sum_{z \in \mathbb{Z}_3} z^{-e} \prod_{i \in V} \prod_{j \sim i} \hat{E}_{\langle i,j \rangle}^{z^{-1}} = \frac{1}{3} \sum_{z \in \mathbb{Z}_3} z^{-e} \prod_{\langle i,j \rangle \in d_1} \hat{E}_{\langle i,j \rangle}^{z^{-1}} \\
&= \frac{1}{3} \sum_{z \in \mathbb{Z}_3} z^{e} \prod_{\langle i,j \rangle \in d_1} \hat{E}_{\langle i,j \rangle}^{z} = \frac{1}{3} \sum_{z \in \mathbb{Z}_3} z^{e} \hat{\phi}_{S^*}^z \\
&= \hat{P}_{S^*}(-e) \,,
\end{aligned}$$

Here, the $\mathbb{Z}_3$-Gauss law (3.15) is used in the second line, and we have defined the center-electric flux operator $\hat{\phi}_{S^*}^z = \prod_{\langle i,j \rangle \in d_1} \hat{E}_{\langle i,j \rangle}^z$ of the surface S^*. Hence, we have shown further that the problem of constructing the ensemble of fixed net-quark number is equivalent to constructing an ensemble of fixed center-flux through the surface S^* of the volume V^*. This connection between net-quark number and center-electric flux through S^* has been first described by [106].

To explicitly see that the dynamics do not leave the sector $\mathcal{H}_V(e)$ invariant, we consider the asymmetric transfer operator $\hat{T}$ and some state $f(U) \otimes |\psi_{\text{F}}\rangle \in \mathcal{H}$. The asymmetric transfer operator acts as

$$\hat{T}(f(U) \otimes |\psi_{\text{F}}\rangle) = \int \mathcal{D}\tilde{U}\, S(U, \tilde{U}) T_{\text{G}}(\tilde{U}) T_{\text{F}}(\tilde{U}) (f(\tilde{U}) \otimes |\psi_{\text{F}}\rangle) \,.$$

Therefore, we can write

$$\hat{\phi}^z_{S^*}\hat{T}(f(U)\otimes|\psi_{\mathrm{F}}\rangle) = \int \mathcal{D}\tilde{U}\, S(U^z,\tilde{U})T_{\mathrm{G}}(\tilde{U})T_{\mathrm{F}}(\tilde{U})(f(\tilde{U})\otimes|\psi_{\mathrm{F}}\rangle)\,,$$

Here U^z denotes the gauge configuration U with all links $\langle i,j\rangle \in d_1$ of the interface d_1 twisted appropriately:

$$U^z_{\langle i,i+\hat{k}\rangle} = \begin{cases} z^\dagger U_{\langle i,i+\hat{k}\rangle}, & \langle i,i+\hat{k}\rangle \in d_1 \\ zU_{\langle i,i+\hat{k}\rangle}, & \langle i+\hat{k},i\rangle \in d_1 \end{cases}. \tag{4.20}$$

Interchanging the order of $\hat{\phi}^z_{S^*}$ and $\hat{T}$ and using the left-invariance of the Haar measure, we have

$$\hat{T}\hat{\phi}^z_{S^*}(f(U)\otimes|\psi_{\mathrm{F}}\rangle) = \int \mathcal{D}\tilde{U}\, S(U,\tilde{U}^{z^{-1}})T_{\mathrm{G}}(\tilde{U}^{z^{-1}})T_{\mathrm{F}}(\tilde{U}^{z^{-1}})(f(\tilde{U})\otimes|\psi_{\mathrm{F}}\rangle)$$

The interface d_1 is the dual of the surface S^* which implies that $T_{\mathrm{G}}(\tilde{U}^{z^{-1}}) = T_{\mathrm{G}}(\tilde{U})$ because every plaquette which contains a link $l \in d_1$ also contains some other link $l' = \langle i,j\rangle$ with $\langle j,i\rangle \in d_1$. The link l imposes the twist $z^\dagger$ whereas l' imposes the twist z. Both twists cancel each other. In summary, $\hat{\phi}^z_{S^*}\hat{T}$ acts via the integral kernel

$$S(U^z,\tilde{U})T_{\mathrm{G}}(\tilde{U})T_{\mathrm{F}}(\tilde{U})\,,$$

and $\hat{T}\hat{\phi}^z_{S^*}$ acts via the integral kernel

$$S(U^z,\tilde{U})T_{\mathrm{G}}(\tilde{U})T_{\mathrm{F}}(\tilde{U}^{z^{-1}})\,.$$

Therefore, the presence of the fermionic part $T_{\mathrm{F}}(\tilde{U})$ prevents the commutator $[\hat{\phi}^z_{S^*},\hat{T}] \neq 0$ and also $[\hat{P}_{S^*}(e),\hat{T}] \neq 0$ to vanish because both fermionic parts are not identical: $T_{\mathrm{F}}(\tilde{U}^{z^{-1}}) \neq T_{\mathrm{F}}(\tilde{U})$. Consistently to the construction of 't Hooft's center-electric flux ensembles, however, $[\hat{\phi}^z_{S^*},\hat{T}] = 0$ in the absence of the fermionic part.

We construct the Hamiltonian $\hat{H}'$ by first modifying the asymmetric transfer-matrix operator $\hat{T}$. By virtue of the Euclidean time continuum $a_4 \to 0$, we then get the corresponding modified Hamiltonian $\hat{H}'$. As it is also desired for $\hat{H}'$, the modified transfer operator $\hat{T}'$ is constructed under the following constraints. First, $\hat{T}'$ should be gauge-invariant, second, $\hat{T}'$ emerges from $\hat{T}$ by local modifications at the interface d_1 and, third, $\hat{T}'$ should leave the sector $\mathcal{H}_{\phi_{S^*}=_3-e} = \mathcal{H}_V(e)$ invariant independently of the choice e. The latter importantly means that $\hat{T}'$ is aware of the interface d_1 but not of which flux $\phi_{S^*} =_3 -e$ flows through the surface S^*. For example, this excludes the naive ansatz

$$\hat{T}'\,|\psi\rangle = \hat{P}_{S^*}(-e)\hat{T}\,|\psi\rangle \in \mathcal{H}_{\phi_{S^*}=-e}$$

which only leaves the sector $\mathcal{H}_{\phi_{S^*}=-e}$ invariant. As described above, the membrane at d_1 should forbid changes of net-quark numbers between V and $\overline{V}$ which are not a multiple of three. The membrane is in this sense some kind of topological property imprinted into the interaction and changing the way in which fermions interact between V and $\overline{V}$. Choosing a sector $\mathcal{H}_V(e)$,

however, merely reflects the choice in which initial state the system is prepared. Therefore, $Z(N_V =_3 e)$ describes an ensemble of fixed net-quark number $N_V =_3 e$ because an observer will only observe states from the sector $\mathcal{H}_V(e)$.

The construction of an ensemble with fixed net-quark number $N_V =_3 e$ can be reformulated to the equivalent problem of constructing an ensemble of fixed center flux $\phi_{S^*} =_3 -e$ as we have seen above. As part of this reformulation the center-flux operator $\hat{\phi}^z_{S^*}$ emerges naturally. The operator $\hat{\phi}^z_{S^*}$ consists of center-electric flux operators $\hat{E}^z_{\langle i,j\rangle}$ with links $\langle i,j\rangle \in d_1$ which are only part of the interface d_1. The operator $\hat{\phi}^z_{S^*}$ only affects gauge variables at the interface d_1. In this sense, $\hat{\phi}^z_{S^*}$ only affects the interface d_1 locally. Hence, $\hat{\phi}^z_{S^*}$ is a natural candidate to modify the dynamics at the surface S^*. We guess the following modified operator $\hat{T}'$:

$$\hat{T}' = \frac{1}{3}\sum_{z\in Z_3} \hat{\phi}^z_{S^*}\hat{T}\hat{\phi}^{z^{-1}}_{S^*}\,.$$

To confirm that $\hat{T}'$ emerges from $\hat{T}$ by only including modifications of the interaction at the interface d_1, we compute the integral kernel $K'(U,\tilde{U})$ of $\hat{T}'$ explicitly:

$$K'(U,\tilde{U}) = \frac{1}{3}\sum_{z\in Z_3} S(U^{z^{-1}},\tilde{U})T_{\mathrm{G}}(\tilde{U})T_{\mathrm{F}}(\tilde{U}^{z^{-1}})\,.$$

It is obvious that only gauge variables which are part of the interface d_1 are affected by the modification. In this sense, the modifications are locally restricted to the interface d_1. Also, $\hat{T}'$ is gauge-invariant because $\hat{\phi}^z_{S^*}$ and $\hat{T}$ are gauge-invariant. The sector $\mathcal{H}_V(e)$ is invariant under the application of the operator $\hat{T}'$: $[\hat{P}_V(e),\hat{T}'] = 0$. To this end, consider $|\psi\rangle \in \mathcal{H}_{\phi_{S^*}=_3 -e}$. We have

$$\hat{T}'\,|\psi\rangle = \frac{1}{3}\sum_{z\in Z_3}\hat{\phi}^z_{S^*}\hat{T}\hat{\phi}^{z^{-1}}_{S^*}\,|\psi\rangle = \frac{1}{3}\sum_{z\in Z_3} z^e\hat{\phi}^z_{S^*}\hat{T}\,|\psi\rangle = \hat{P}_{S^*}(-e)\hat{T}\,|\psi\rangle\,. \tag{4.21}$$

Therefore, $\hat{T}'\,|\psi\rangle \in \mathcal{H}_{\phi_{S^*}=_3 -e} = \mathcal{H}_V(e)$.

Finally, it remains to show that $\hat{T}'$ has a well-defined Euclidean time continuum with a Hamiltonian $\hat{H}'$. Introducing the lattice spacings into the transfer operator $\hat{T}_{a_4}$ gives the modified transfer operator $\hat{T}'_{a_4}$ which depends on the lattice spacing a_4. Hence, we write

$$(\mathcal{N}(a_4)\hat{T}'_{a_4})^{N_4} = \left(\frac{1}{3}\sum_{z\in Z_3}\hat{\phi}^z_{S^*}(\mathcal{N}(a_4)\hat{T}_{a_4})\hat{\phi}^{z^{-1}}_{S^*}\right)^{N_4}.$$

For sufficiently small a_4, we have

$$(\mathcal{N}(a_4)\hat{T}'_{a_4})^{N_4} = \left(\mathbb{1} - a_4\left[\frac{1}{3}\sum_{z\in Z_3}\hat{\phi}^z_{S^*}\hat{H}\hat{\phi}^{z^{-1}}_{S^*}\right] + \mathcal{O}(a_4^2)\right)^{N_4} \tag{4.22}$$

which defines the Euclidean time continuum as

$$\lim_{N_4\to\infty}(\mathcal{N}(a_4)\hat{T}'_{a_4=\beta/N_4})^{N_4} = \mathrm{e}^{-\beta\hat{H}'}$$

with

$$\hat{H}' = \frac{1}{3} \sum_{z \in Z_3} \hat{\phi}^z_{S^*} \hat{H} \hat{\phi}^{z^{-1}}_{S^*} \,. \tag{4.23}$$

Importantly, $\hat{H}'$ is Hermitian because $(\hat{\phi}^z_{S^*})^\dagger = \hat{\phi}^{z^{-1}}_{S^*}$, and $\hat{H}$ is Hermitian. The interpretation of $\hat{H}'$ as a Hamiltonian is well-defined. Furthermore, the derivation of Equation (4.22) uses the simple, but crucial, property

$$\mathbb{1} = \frac{1}{3} \sum_{z \in Z_3} \hat{\phi}^z_{S^*} \mathbb{1} \hat{\phi}^{z^{-1}}_{S^*}$$

which guarantees the manifestation of the identity in the zeroth order term. Otherwise, the Euclidean time continuum would not give a well-defined exponential of the Hamiltonian $\hat{H}'$.

The Hamiltonian $\hat{H}'$ is obviously gauge-invariant, the interaction is only modified at the interface d_1, and the sector $\mathcal{H}_V(e)$ is left invariant by $\hat{H}'$ for all $e \in \mathbb{Z}_3$ because $[\hat{P}_V(e), \hat{T}'] = 0$ which persists in the Euclidean time continuum. Therefore, $\hat{H}'$ restricted to $\mathcal{H}_V(e)$ defines a proper quantum-mechanical system of gauge-invariant states with fixed net-quark number $N_V =_3 e$, and the transfer operator $\hat{T}'_{a_4}$ is the corresponding discretization of $\hat{H}'$ in Euclidean time.

The path integral is computed as it is done for the symmetric and asymmetric transfer operator, see Section 3.2 and 3.3. Comparing with Equation (3.32), we replace the Boltzmann factor $\mathrm{e}^{-\beta \hat{H}'}$ in Equation (4.15) with $\hat{T}'^{N_4}$ introducing the discretization in Euclidean time:

$$Z(N_V =_3 e) = \mathrm{tr} \left(\mathrm{e}^{\beta \mu \hat{N}} (\hat{T}')^{N_4} \hat{P}_{S^*}(-e) \hat{P}_0 \right),$$

where we also have replaced $\hat{P}_V(e)$ with $\hat{P}_{S^*}(-e)$. For any state $|\psi\rangle \in \mathcal{H}$,

$$\hat{P}_{S^*}(-e) \hat{P}_0 |\psi\rangle \in \mathcal{H}_{\phi_{S^*} =_3 -e} \,.$$

Equation (4.21) implies

$$(\hat{T}')^{N_4} \hat{P}_{S^*}(-e) \hat{P}_0 |\psi\rangle = (\hat{P}_{S^*}(-e) \hat{T})^{N_4} \hat{P}_{S^*}(-e) \hat{P}_0 |\psi\rangle \,.$$

Inserting this result into the partition function yields

$$Z(N_V =_3 e) = \mathrm{tr} \left(\mathrm{e}^{\beta \mu \hat{N}} (\hat{P}_{S^*}(-e) \hat{T})^{N_4} \hat{P}_{S^*}(-e) \hat{P}_0 \right).$$

Cyclically shifting the rightmost $\hat{P}_{S^*}(-e)$ to the front and using $\hat{P}^2_{S^*}(-e) = \hat{P}_{S^*}(-e)$, we arrive at

$$Z(N_V =_3 e) = \mathrm{tr} \left(\mathrm{e}^{\beta \mu \hat{N}} \hat{P}_0 (\hat{P}_{S^*}(-e) \hat{T})^{N_4} \right).$$

We replace every projection operator $\hat{P}_{S^*}(-e)$ with its representation

$$\hat{P}_{S^*}(-e) = \frac{1}{3} \sum_{z \in Z_3} z^e \hat{\phi}^z_{S^*}$$

and get

$$Z(N_V =_3 e) = \frac{1}{3^{N_4}} \sum_{\{z_\tau \in Z_3\}} \left[\prod_{\tau=0}^{N_4-1} z_\tau^{-e} \right] \mathrm{tr} \left(\mathrm{e}^{\beta\mu \hat{N}} \hat{P}_0 \prod_{\tau=0}^{N_4-1} \left[\hat{\phi}_{S^*}^{z_\tau^{-1}} \hat{T} \right] \right),$$

where we implicitly made the transformation $z_\tau \to z_\tau^{-1}$, and the product of the operators $\hat{\phi}_{S^*}^{z_\tau^{-1}} \hat{T}$ is defined to be ordered from left to right for increasing τ:

$$\prod_{\tau=0}^{N_4-1} \left[\hat{\phi}_{S^*}^{z_\tau^{-1}} \hat{T} \right] = \left[\hat{\phi}_{S^*}^{z_0^{-1}} \hat{T} \right] \cdot \left[\hat{\phi}_{S^*}^{z_1^{-1}} \hat{T} \right] \cdot \ldots \cdot \left[\hat{\phi}_{S^*}^{z_{N_4-1}^{-1}} \hat{T} \right].$$

The integral kernel $K(U^{z_\tau^{-1}}, \tilde{U})$ of the operator $\hat{\phi}_{S^*}^{z_\tau^{-1}} \hat{T}$ is given by the integral kernel $K(U, \tilde{U})$ of the asymmetric transfer operator, but the gauge configuration U in the first argument is twisted according to Equation (4.20):

$$K(U^{z_\tau^{-1}}, \tilde{U}) = S(U^{z_\tau^{-1}}, \tilde{U}) T_\mathrm{G}(\tilde{U}) T_\mathrm{F}(\tilde{U}).$$

The choice of the asymmetric transfer operator $\hat{T}$ unfolds its full purpose here. The influence of the center operators $\hat{\phi}_{S^*}^{z}$ is restricted to the timelike plaquettes only. Especially, the fermionic parts remain unchanged. The total action of the path integral derived further below retains the form of the Wilson plaquette action (2.3) and the Hasenfratz-Karsch action (2.4). Only certain timelike plaquettes of the gauge action are twisted.

By following the steps in Section 3.3, the derivation of the path integral results in Equation (3.36) with the integral kernels $K(U_\tau, U_{\tau+1})$ replaced by the twisted kernels $K(U_\tau^{z_\tau^{-1}}, U_{\tau+1})$ and the sum taken over all possible twist configurations $\{z_\tau \in Z_3\}$:

$$\begin{aligned} Z(N_V =_3 e) = \frac{1}{3^{N_4}} \sum_{\{z_\tau \in Z_3\}} \left[\prod_{\tau=0}^{N_4-1} z_\tau^{-e} \right] \int \mathcal{D}U \mathcal{D}\Omega \mathcal{D}\bar{\xi} \mathcal{D}\xi \, \mathrm{e}^{-\bar{\xi}\xi} \\ \langle \mathrm{e}^{\beta\mu} \xi_\mathrm{q}^{(0)}, \mathrm{e}^{-\beta\mu} \xi_{\bar{\mathrm{q}}}^{(0)} | \, K\Big(U_0^{z_0^{-1}}, U_1, \Omega \Big) \, | \Omega \xi_\mathrm{q}^{(1)}, \xi_{\bar{\mathrm{q}}}^{(1)} \Omega^\dagger \rangle \\ \times \prod_{\tau=1}^{N_4-1} \langle \xi_\mathrm{q}^{(\tau)}, \xi_{\bar{\mathrm{q}}}^{(\tau)} | \, K\Big(U_\tau^{z_\tau^{-1}}, U_{\tau+1} \Big) \, | \xi_\mathrm{q}^{(\tau+1)}, \xi_{\bar{\mathrm{q}}}^{(\tau+1)} \rangle \\ = \frac{1}{3^{N_4}} \sum_{\{z_\tau\}} \left[\prod_{\tau=0}^{N_4-1} z_\tau^{-e} \right] \int \mathcal{D}U \mathcal{D}\bar{\psi} \mathcal{D}\psi \, \mathrm{e}^{S_\mathrm{G}(\{z_\tau\}, U)} \mathrm{e}^{S_\mathrm{F}(U, \bar{\psi}, \psi)}. \end{aligned}$$

The fermionic part remains unchanged, i.e. $S_\mathrm{F}(U, \bar{\psi}, \psi)$ is just the Hasenfratz-Karsch action (2.4). Analogously to the path integral of $\langle \hat{E}_{\langle i,j \rangle} \rangle$ and Equation (4.1), the gauge action $S_\mathrm{G}(\{z_\tau\}, U)$ is the standard plaquette action $S_\mathrm{G}(U)$ with certain timelike plaquettes twisted according to the twist configuration $\{z_\tau\}$:

$$S_\mathrm{G}(\{z_\tau\}, U) = \frac{2}{g_0^2} \sum_{x, \mu<\nu} \mathrm{ReTr} \left(z(p_{x,\mu\nu}) U_{\partial p_{x,\mu\nu}} \right).$$

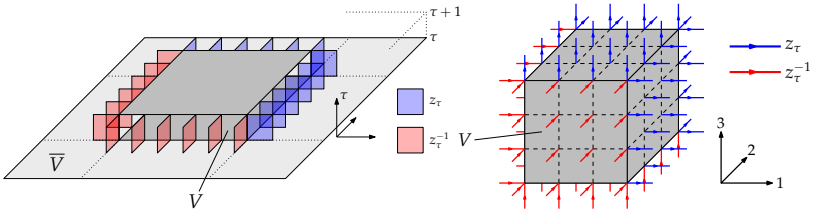

(a) $(2+1)$-dimensions (b) $(3+1)$-dimensions

Figure 4.8: Illustration of the twisted timelike plaquettes of the ensemble $Z(N_V =_3 e)$ in $(2+1)$- and $(3+1)$-dimensions. Figure (a) shows the implementation of twisted timelike plaquettes between the τ-th and $(\tau+1)$-th layer of Euclidean time in $(2+1)$-dimensions. Figure (b) shows the τ-th layer of Euclidean time in $(3+1)$-dimensions. The colored links are the intersections of the twisted timelike plaquettes, which lie between the τ-th and $(\tau+1)$-th layer of time, with the τ-th layer of Euclidean time. The colors represent the twists z_τ and z_τ^{-1}.[†]

The function $z(p_{x,\mu\nu})$ determines the center element with which a plaquette $p_{x,\mu\nu}$ is multiplied:

$$z(p_{(i,\tau),\mu\nu}) = \begin{cases} z_\tau, & \nu = 4, \mu = k, \langle i, i+\hat{k}\rangle \in d_1 \\ z_\tau^{-1}, & \nu = 4, \mu = k, \langle i+\hat{k}, i\rangle \in d_1 \\ 1, & \text{else} \end{cases} .$$

The timelike plaquettes are twisted independently between all subsequent planes of Euclidean time. Consider all timelike plaquettes between the τ-th and $(\tau+1)$-th layer of time and the spatial volume V embedded on the time slice τ. Each timelike plaquette $p_{x,\mu\nu}$ intersecting the τ-th layer of time in the sense that a spatial link $\langle i,j\rangle$ (ignoring the temporal component τ) of the boundary $\partial p_{x,\mu\nu}$ lies on the time layer τ. The function $z(p_{x,\mu\nu})$ twists all timelike plaquettes $p_{x,\mu\nu}$ which border the spatial volume V, i.e. the intersection $\langle i,j\rangle$ of $p_{x,\mu\nu}$ with the time slice τ penetrates the surface S^*:

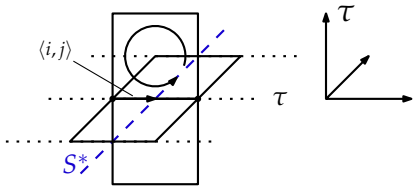

exemplary for $(2+1)$-dimensions. In doing so, the twist configuration $\{z_\tau\}$ dictates the center element $z_\tau \in Z_3$ with which the plaquettes are twisted. A plaquette is twisted with either z_τ or z_τ^{-1} depending on its intersection link $\langle i,j\rangle$: if $\langle i,j\rangle \in d_1$ ($\langle j,i\rangle \in d_1$) is part of the interface d_1, the plaquette is twisted with z_τ (z_τ^{-1}). The twists are illustrated for $(2+1)$- and $(3+1)$-dimensions in Figure 4.8. The $(2+1)$-dimensional case is shown in Figure 4.8a. The time axis is represented by the upwardly directed spatial axis. The plaquettes bordering

[†]Figure (a) is adapted from "FIG. 10" by [90] and used under CC BY 4.0 [142].

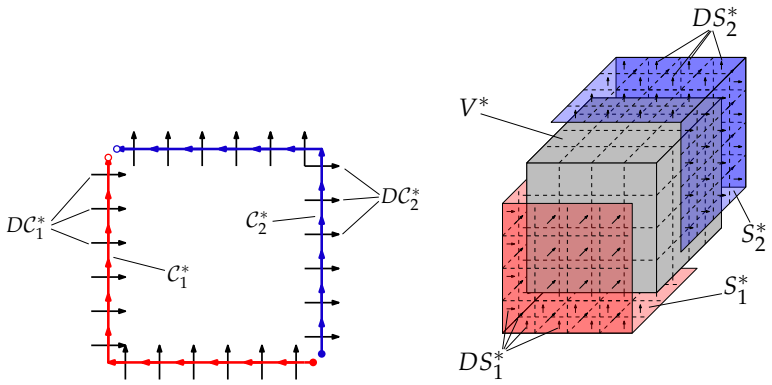

(a) $(2+1)$-dimensions (b) $(3+1)$-dimensions

Figure 4.9: Twists of Figure 4.8 as a result of inserting Dirac strings and Dirac sheets enclosing the spatial subvolume V^* in the τ-th layer of Euclidean time.

and enclosing the volume V are twisted with either the center element z_τ or z_τ^{-1}. The $(3+1)$-dimensional case is shown in Figure 4.8b. Here, only one layer of time is illustrated, and the intersection links $\langle i,j\rangle$ are shown. The colors indicate the twists of the timelike plaquettes.

To make the connection with 't Hooft's center-electric flux ensembles and the topological objects of Section 4.1, we use the twisted ensembles

$$Z(\{z_\tau\}) = \int \mathcal{D}U\mathcal{D}\overline{\psi}\mathcal{D}\psi\, \mathrm{e}^{S_\mathrm{G}(\{z_\tau\},U)}\mathrm{e}^{S_\mathrm{F}(U,\overline{\psi},\psi)} = \mathrm{tr}\left(\mathrm{e}^{\beta\mu\hat{N}}\hat{P}_0\prod_{\tau=0}^{N_4-1}\left[\hat{\phi}_{S^*}^{z_\tau^{-1}}\hat{T}\right]\right). \tag{4.24}$$

The path integral of $Z(\{z_\tau\})$ is computed by inserting the center-flux operator $\hat{\phi}_{S^*}^{z_\tau^{-1}}$ for each time layer τ. The operator $\hat{\phi}_{S^*}^{z}$ is just the product of center-electric flux operators $\hat{E}_{\langle i,j\rangle}^{z}$:

$$\hat{\phi}_{S^*}^{z} = \prod_{\langle i,j\rangle\in d_1}\hat{E}_{\langle i,j\rangle}^{z} = \prod_{\langle i,i+\hat{k}\rangle}\left(\hat{E}_{\langle i,i+\hat{k}\rangle}^{z}\right)^{\alpha_{\langle i,i+\hat{k}\rangle}} \tag{4.25}$$

with the coefficients $\alpha_{\langle i,i+\hat{k}\rangle}\in\{0,-1,1\}$ of the 1-chain d_1. Because d_1 is the dual of the surface S^*, the insertion of $\hat{\phi}_{S^*}^{z_\tau^{-1}}$ into the trace (4.24) is equivalent to the insertion of a Dirac sheet with the twist z_τ^{-1} enclosing the spatial subvolume V^* in the τ-th layer of time. However, we can also absorb all negative coefficients $\alpha_{\langle i,i+\hat{k}\rangle}$ by appropriate replacements $z\to z^{-1}$ in Equation (4.25). Then, $\hat{\phi}_{S^*}^{z} = \hat{\phi}_{S_1^*}^{z^{-1}}\hat{\phi}_{S_2^*}^{z}$ actually decomposes into the product of two separate Dirac sheets S_1^* and S_2^* of opposing twists z^{-1} and z enclosing the volume V^*. The dual DS_i^* of each of theses Dirac sheets is solely made of positively orientated links of the lattice. Contrary to the pure gauge theory, the exact form of a Dirac sheet matters in the presence of dynamical fermions because Gauss's law does not manifest itself in the identity (4.4) and subsequently in the equivalence of surfaces which are deformed relative to each other by adding boundless cubes on the dual lattice (Figure 4.3). Physically, it makes a difference which

subvolume V is chosen. The two Dirac sheets are illustrated in Figure 4.9 for $(2+1)$- and $(3+1)$-dimensions. In the former case, the sheets are actually strings.

Now, we can describe the construction of the ensemble $Z(N_V =_3 e)$ in the terminology of Section 4.1. For every twist configuration $\{z_\tau\}$, we define the twisted ensemble $Z(\{z_\tau\})$ by enclosing the dual subvolume V^* with two Dirac sheets S_1^* and S_2^* in each layer of Euclidean time, as it is depicted in Figure 4.9. In every layer τ, the twists are chosen as z_τ for S_1^* and z_τ^{-1} for S_2^*. This gives the twisted ensemble $Z(\{z_\tau\})$. To get $Z(N_V =_3 e)$, we just have to take the discrete Fourier transform over all twisted ensembles $Z(\{z_\tau\})$. Hence, there are two steps involved. First, the stack of twisted Dirac sheets in Euclidean time is inserted, and then the sum over all possible twists is taken.

Comparing with Section 4.1, 't Hooft's center-electric flux ensembles are defined by inserting the Dirac sheets S_{23}^*, S_{13}^* and S_{12}^* in one layer of time only. Though, we can analogously to $Z(N_V =_3 e)$ insert the Dirac sheets S_{mn}^* in each layer of Euclidean time such that

$$Z_{\text{el.}}(\vec{e}) = \frac{1}{3^{3N_4}} \sum_{\{\vec{k}_\tau \in \mathbb{Z}_3^3\}} \prod_{\tau=0}^{N_4-1} \left[\exp\left(-\frac{2\pi \mathrm{i}}{3}\, \vec{e}\cdot\vec{k}_\tau \right) \right] Z(\{\vec{k}_\tau\})$$

and

$$Z(\{\vec{k}_\tau\}) = \int \mathcal{D}U\mathcal{D}\overline{\psi}\mathcal{D}\psi\, \mathrm{e}^{S_{\mathrm{G}}(\{\vec{k}_\tau\},U)}\,,$$

where $S_{\mathrm{G}}(\{\vec{k}_\tau\},U)$ imposes the Dirac sheets with twist $\vec{k}_\tau$ in each layer of time τ. The equivalence is guaranteed because we can just repeat the construction of $Z(N_V =_3 e)$ with the modified transfer operator

$$\hat{T}' = \frac{1}{3^3} \sum_{z_1,z_2,z_3 \in \mathrm{Z}_3} \hat{E}^{z_1}(S_{23}^*)\hat{E}^{z_2}(S_{13}^*)\hat{E}^{z_3}(S_{12}^*)\, \hat{T}\, \hat{E}^{z_3^{-1}}(S_{12}^*)\hat{E}^{z_2^{-1}}(S_{13}^*)\hat{E}^{z_1^{-1}}(S_{23}^*)$$

in the absence of dynamical fermions. However, because $[\hat{E}^z(S_{mn}^*),\hat{T}] = 0$, actually $\hat{T}' = \hat{T}$. Therefore, we can just replace $\hat{T}$ with $\hat{T}'$ in the derivation of $Z_{\text{el.}}(\vec{e})$ which gives the path integral

$$\begin{aligned} Z_{\text{el.}}(\vec{e}) =& \frac{1}{3^{3N_4}} \sum_{\{\vec{k}_\tau \in \mathbb{Z}_3^3\}} \prod_{\tau=0}^{N_4-1} \left[\exp\left(-\frac{2\pi \mathrm{i}}{3}\, \vec{e}\cdot\vec{k}_\tau \right) \right] \\ & \times \mathrm{tr}\left(\hat{P}_0 \prod_{\tau=0}^{N_4-1} \left[\hat{E}^{z_1(\vec{k}_\tau)}(S_{23}^*)\hat{E}^{z_2(\vec{k}_\tau)}(S_{13}^*)\hat{E}^{z_3(\vec{k}_\tau)}(S_{12}^*)\hat{T} \right] \right) \end{aligned} \tag{4.26}$$

with $z_i(\vec{k}) = \exp(\frac{2\pi \mathrm{i}}{3} k_i)$. We clearly notice the insertion of the Dirac sheets into each layer of time. Because the operators $\hat{E}^z(S_{mn}^*)$ commute with $\hat{T}$, we can shift all Dirac sheets to the front of the product. This amounts to collapsing the stack of sheets in direction of time to exactly one layer of time. Then, we have the temporally twisted ensembles with the total twist

$$\exp\left(-\frac{2\pi \mathrm{i}}{3}\, k_i \right) = \prod_{\tau=0}^{N_4-1} z_i(\vec{k}_\tau)$$

defining the overall twist vector $\vec{k}$ such that

$$Z_{\text{el.}}(\vec{e}) = \frac{1}{3^{3N_4}} \sum_{\vec{k}\in\mathbb{Z}_3^3} N(\vec{k}) \exp\left(-\frac{2\pi \mathrm{i}}{3} \vec{e}\cdot\vec{k} \right) Z(\vec{k}) \,,$$

where $Z(\vec{k})$ are the temporally twisted ensembles and $N(\vec{k})$ counts the number of twist configurations $\{\vec{k}_\tau\}$ with $\vec{k}_0 +_3 \ldots +_3 \vec{k}_{N_4-1} = \vec{k}$. For a fixed vector $\vec{k}$, we have $N(\vec{k}) = 3^{3N_4-3}$. This is because $N(\vec{k}) = N(\vec{k} +_3 \vec{a})$ is actually translation invariant under a shift $\vec{a} \in \mathbb{Z}_3^3$. Therefore all 3^{3N_4} combinations of twist configurations $\{\vec{k}_\tau\}$ are evenly distributed among the 3^3 possible vectors $\vec{k}$: $N(\vec{k}) = 3^{3N_4-3}$. Equation (4.8) and (4.26) are equivalent because we can collapse the Dirac sheets from all layers to only one layer of time. This is an alternative interpretation of the difference between the construction of $Z(N_V =_3 e)$ and $Z_{\text{el.}}(\vec{e})$: $[\hat{\phi}^z_{S^*}, \hat{T}] \neq 0$ prohibits the collapse of Dirac sheets to one layer of time only, whereas $[\hat{E}^z(S^*_{mn}), \hat{T}] = 0$ allows it.

Continuum limit

Finally, some remarks for the continuum limit are in order. To formulate the continuum limit of fixed net-quark number ensembles, we would not fix the lattice subvolume V to a specific extent, but rather we fix a physical subvolume $V_{\text{phys}} = a^3 V$ with fixed physical extents in the spatial directions. Otherwise, by only fixing V, the physical subvolume V_{phys} would actually shrink to zero when approaching the continuum $a \to 0$. This also applies to the quantum-mechanical formulation because, as we have discussed in Chapter 3, the path integral at maximal anisotropy $\xi \to \infty$ and fixed a becomes equivalent to the quantum-mechanical formulation.

Path-integral dualization

As a cross check, we like to emphasize another possibility to construct the ensemble $Z(N_V =_3 e)$. Instead of using the transfer-matrix formulation, we use the dualization scheme described in [107, 108] which reformulates the path integral in terms of Abelian dual variables and provides, like the transfer-matrix formulation, a concept of local net-quark numbers allowing the definition of $Z(N_V =_3 e)$.

However, we do not engage in the full dualization scheme as depicted by [107, 108]. We only consider the dualization of the fermionic part, i.e. we introduce dual variables replacing the Grassmann generators and formally integrate out all gauge variables such that the partition function becomes a sum over fermionic dual variables only. The derivation is completely analogous to [107, 108]. Here, we use Wilson fermions instead of staggered fermions.

Recall the Hasenfratz-Karsch action (2.4):

$$S_{\text{F}}(U, \overline{\psi}, \psi) = \kappa \sum_{x,\mu} \left[\overline{\psi}_x \Lambda^+_{x,\mu} \psi_{x+\hat{\mu}} + \overline{\psi}_{x+\hat{\mu}} \Lambda^-_{x,\mu} \psi_x \right] - \sum_x \overline{\psi}_x \psi_x \,.$$

The matrices are defined as

$$\Lambda^{+}_{x,\mu} = ((1-\delta_{\mu,4}) + \mathrm{e}^{+a_4\mu}\delta_{\mu,4})(1-\gamma_\mu)U_{\langle x,x+\hat{\mu}\rangle}\,,$$
$$\Lambda^{-}_{x,\mu} = ((1-\delta_{\mu,4}) + \mathrm{e}^{-a_4\mu}\delta_{\mu,4})(1+\gamma_\mu)U^{\dagger}_{\langle x,x+\hat{\mu}\rangle}\,,$$

and we naturally understand them to be embedded in a color and Dirac space. The path integral is

$$Z = \int \mathcal{D}U\mathcal{D}\overline{\psi}\mathcal{D}\psi\, \mathrm{e}^{S_{\mathrm{G}}(U)}\mathrm{e}^{S_{\mathrm{F}}(U,\overline{\psi},\psi)}\,.$$

The dualization of the fermionic part is simply an expansion of the Boltzmann factor $\mathrm{e}^{S_{\mathrm{F}}(U,\overline{\psi},\psi)}$ in orders of the Grassmann bilinears $\overline{\psi}^{\omega}_{x}\psi^{\omega'}_{y}$, where $\omega = (a,\alpha)$ summarizes the color and Dirac indices. Bilinears $\overline{\psi}^{\omega}_{x}\psi^{\omega'}_{y}$ commute pairwise, and therefore we can decompose the exponential $\mathrm{e}^{S_{\mathrm{F}}(U,\overline{\psi},\psi)}$ into the product of exponentials:

$$\mathrm{e}^{S_{\mathrm{F}}(U,\overline{\psi},\psi)} = \left[\prod_{x,\omega}\exp\left(-\overline{\psi}^{\omega}_{x}\psi^{\omega}_{x}\right)\right]\left[\prod_{x,\mu,\omega,\omega'}\exp\left(\kappa\overline{\psi}^{\omega}_{x}(\Lambda^{+}_{x,\mu})_{\omega\omega'}\psi^{\omega'}_{x+\hat{\mu}}\right)\right]$$
$$\times\left[\prod_{x,\mu,\omega,\omega'}\exp\left(\kappa\overline{\psi}^{\omega}_{x+\hat{\mu}}(\Lambda^{-}_{x,\mu})_{\omega\omega'}\psi^{\omega'}_{x}\right)\right]\,.$$

Every exponential is expanded in orders of the Grassmann bilinears, and such an expansion always ends with the first order because the second and higher orders include squares or higher powers of a Grassmann number which vanish due to the anti-commuting nature of the numbers:

$$\prod_{x,\omega}\exp\left(-\overline{\psi}^{\omega}_{x}\psi^{\omega}_{x}\right) = \prod_{x,\omega}\sum_{k^{\omega\omega}_{xx}=0}^{1}\left(-\overline{\psi}^{\omega}_{x}\psi^{\omega}_{x}\right)^{k^{\omega\omega}_{xx}}$$
$$\prod_{x,\mu,\omega,\omega'}\exp\left(\kappa\overline{\psi}^{\omega}_{x}(\Lambda^{+}_{x,\mu})_{\omega\omega'}\psi^{\omega'}_{x+\hat{\mu}}\right)$$
$$= \prod_{x,\mu,\omega,\omega'}\sum_{k^{\omega\omega'}_{x,x+\hat{\mu}}=0}^{1}\left(\kappa\cdot(\Lambda^{+}_{x,\mu})_{\omega\omega'}\overline{\psi}^{\omega}_{x}\psi^{\omega'}_{x+\hat{\mu}}\right)^{k^{\omega\omega'}_{x,x+\hat{\mu}}}$$
$$\prod_{x,\mu,\omega,\omega'}\exp\left(\kappa\overline{\psi}^{\omega}_{x+\hat{\mu}}(\Lambda^{-}_{x,\mu})_{\omega\omega'}\psi^{\omega'}_{x}\right)$$
$$= \prod_{x,\mu,\omega,\omega'}\sum_{k^{\omega\omega'}_{x+\hat{\mu},x}=0}^{1}\left(\kappa\cdot(\Lambda^{-}_{x,\mu})_{\omega\omega'}\overline{\psi}^{\omega}_{x+\hat{\mu}}\psi^{\omega'}_{x}\right)^{k^{\omega\omega'}_{x+\hat{\mu},x}}$$

The exponents $k^{\omega\omega'}_{xy} \in \{0,1\}$ are the fermionic dual variables. Only three kinds of dual variables exist: $k^{\omega\omega'}_{xx}$, $k^{\omega\omega'}_{x,x+\hat{\mu}}$ and $k^{\omega\omega'}_{x+\hat{\mu},x}$. Inserting the expansions into the Boltzmann factor $\mathrm{e}^{S_{\mathrm{F}}(U,\overline{\psi},\psi)}$ and shifting the sums in front of the products,

we arrive at the representation

$$\begin{aligned} \mathrm{e}^{S_{\mathrm{F}}(U,\overline{\psi},\psi)} = \sum_{\{k\}} \Bigg[\prod_{x,\omega} \Big(-\overline{\psi}_x^{\omega} \psi_x^{\omega} \Big)^{k_{xx}^{\omega\omega}} \Bigg] \Bigg[\prod_{x,\mu,\omega,\omega'} \Big(\kappa \cdot (\Lambda_{x,\mu}^{+})_{\omega\omega'} \overline{\psi}_x^{\omega} \psi_{x+\hat{\mu}}^{\omega'} \Big)^{k_{x,x+\hat{\mu}}^{\omega\omega'}} \Bigg] \\ \times \Bigg[\prod_{x,\mu,\omega,\omega'} \Big(\kappa \cdot (\Lambda_{x,\mu}^{-})_{\omega\omega'} \overline{\psi}_{x+\hat{\mu}}^{\omega} \psi_x^{\omega'} \Big)^{k_{x+\hat{\mu},x}^{\omega\omega'}} \Bigg] \end{aligned} ,$$

where the sum is taken over all possible configurations $\{k\}$ of dual variables. Now, we can insert this result into the path integral Z, combine the factors $\mathrm{e}^{\pm a_4 \mu}$ into a common exponential and integrate formally over all gauge variables:

$$\begin{aligned} Z = \sum_{\{k\}} W(\{k\}) \exp\Big(a_4 \mu \sum_x (n_x - \overline{n}_x) \Big) \int \mathcal{D}\overline{\psi} \mathcal{D}\psi \\ \times \Bigg[\prod_{x,\omega} \Big(-\overline{\psi}_x^{\omega} \psi_x^{\omega} \Big)^{k_{xx}^{\omega\omega}} \Bigg] \Bigg[\prod_{x,\mu,\omega,\omega'} \Big(\overline{\psi}_x^{\omega} \psi_{x+\hat{\mu}}^{\omega'} \Big)^{k_{x,x+\hat{\mu}}^{\omega\omega'}} \Big(\overline{\psi}_{x+\hat{\mu}}^{\omega} \psi_x^{\omega'} \Big)^{k_{x+\hat{\mu},x}^{\omega\omega'}} \Bigg] \end{aligned} . \tag{4.27}$$

The function $W(\{k\})$ includes the integration over all gauge variables and the plaquette action $S_{\mathrm{G}}(U)$,

$$n_x = \sum_{\omega,\omega'} k_{x,x+\hat{4}}^{\omega\omega'} \qquad \text{and} \qquad \overline{n}_x = \sum_{\omega,\omega'} k_{x+\hat{4},x}^{\omega\omega'} .$$

In this form it is evident that a configuration $\{k\}$ determines which Grassmann generators occur. Also, the integral over the Grassmann numbers is non-zero if and only if every generator occurs exactly once. Therefore, certain $\{k\}$ have zero contribution to the partition function and are unphysical in this sense. The integral over the generators manifests itself in a constrain on the sets of configurations $\{k\}$. This implies rules for diagrammatically representing physical configurations $\{k\}$ [107, 108]. In our case, the rules are as follows. A product $\overline{\psi}_x^{\omega} \psi_y^{\omega'}$ between the nearest-neighbor sites x and y is represented by an arrow. The arrow starts at x and terminates at y. The starting point, therefore, represents always a Grassmann generator $\overline{\psi}_x^{\omega}$, whereas the end point represents a generator $\psi_y^{\omega'}$. If an arrow is pointed in a positive direction then the corresponding dual variable $k_{x,x+\hat{\mu}}^{\omega\omega'} = 1$ is set to one. Similar, an arrow pointing in a negative lattice direction indicates $k_{x+\hat{\mu},x}^{\omega\omega'} = 1$. We represent a pair $(\overline{\psi}_x^{\omega}, \psi_x^{\omega})$ by an open circle placed at the site x. Arrows start and end at these open circles. An on-site variable $k_{xx}^{\omega\omega} = 1$ is indicated by filling the open circle of the pair $(\overline{\psi}_x^{\omega}, \psi_x^{\omega})$. Because a configuration $\{k\}$ is physical if and only if every generator occurs exactly once, there are only two diagrammatical possibilities: either one arrow starts and one arrows ends in an open circle or the circle is filled:

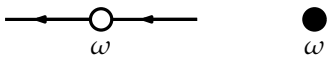

Therefore, a physical configuration $\{k\}$ decomposes into a set of closed loops which consist of distinct arrows or one filled circle. The latter is considered a loop of zero length.

Using the dualization scheme, we can construct the ensemble $Z(N_V =_3 e)$. First, we observe that the number of arrows entering and leaving a site must be identical due to the diagrammatic rules:

$$\sum_{\mu,\omega,\omega'} \left(k^{\omega\omega'}_{x-\hat{\mu},x} - k^{\omega\omega'}_{x,x-\hat{\mu}} + k^{\omega\omega'}_{x+\hat{\mu},x} - k^{\omega\omega'}_{x,x+\hat{\mu}} \right) = 0 \,. \tag{4.28}$$

for every site x. Second, the variables n_x and $\overline{n}_x$ are interpreted as the quark number and antiquark number at the spacetime point x, and the local net-quark number is defined as $N_x = n_x - \overline{n}_x$. This interpretation is due to the occurrence of the variables in the exponential

$$\exp\left(a_4 \mu \sum_x (n_x - \overline{n}_x) \right)$$

in Equation (4.27). In the usual sense, the total net-quark number N of the grand-canonical ensemble is identified via the factor $\mathrm{e}^{\beta\mu N}$, where β is the inverse temperature. Therefore, if we write

$$\mathrm{e}^{\beta\mu N} = \exp\left(a_4 \mu \sum_x (n_x - \overline{n}_x) \right) = \exp\left(\beta\mu \frac{a_4}{\beta} \sum_x (n_x - \overline{n}_x) \right),$$

we identify

$$N = \frac{1}{N_4} \sum_x (n_x - \overline{n}_x) \,.$$

As it is pointed out in [108], only closed fermion loops winding around the time direction contribute to N. Assuming the interpretation of n_x and $\overline{n}_x$ as local particle numbers at a certain place and time, the timelike parts of closed loops describe the propagation of quarks and antiquarks in direction of Euclidean time. Therefore, if a quark or antiquark propagates through all layers of time and persists at all times, it contributes to the total net-quark number N. Otherwise it just fluctuates into existence, is destroyed at a later point of time and does not contribute to N. An example of a fermion loop winding around the time direction is given in Figure 4.10. The loop describes the propagation of a quark starting at $\tau = 0$ till τ_0. At τ_0, a quark-antiquark pair is created such that one quark and the antiquark annihilate one time step later. The remaining quark propagates further closing the loop. In total, one quark persists at all times.

Next, Equation (4.28) and the definition of the local net-quark number N_x allow to establish a local continuity equation, i.e. the change of net-quark number at a spatial site i between two layers of time $\tau - 1$ and τ must equal the outgoing quark-number current on the τ-th layer of time. To derive the

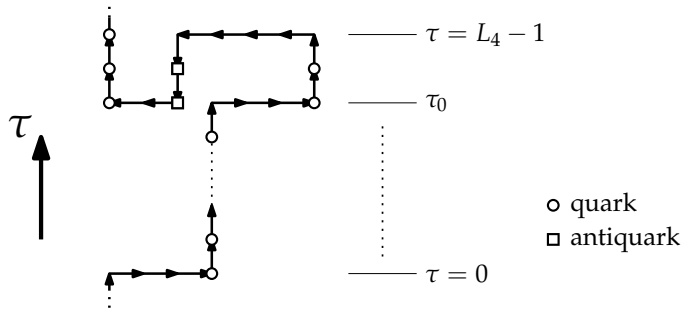

Figure 4.10: Illustration of a closed fermion loop which contributes one quark to the total net-quark number N. With the interpretation of n_x and $\overline{n}_x$ as local quark and antiquark numbers, the shown fermion loop describes the propagation of one quark from $\tau = 0$ till τ_0. At τ_0, a quark-antiquark pair is created. One time step later, one quark and the antiquark annihilate such that only one quark persists closing the loop.

continuity equation, we split Equation (4.28) into temporal and spatial parts:

$$\sum_{\mu,\omega,\omega'} \left(k^{\omega\omega'}_{x-\hat{\mu},x} - k^{\omega\omega'}_{x,x-\hat{\mu}} + k^{\omega\omega'}_{x+\hat{\mu},x} - k^{\omega\omega'}_{x,x+\hat{\mu}} \right)$$
$$= N_{x-\hat{4}} - N_x + \sum_{k=1}^{3} \sum_{\omega,\omega'} \left(k^{\omega\omega'}_{x-\hat{k},x} - k^{\omega\omega'}_{x,x-\hat{k}} + k^{\omega\omega'}_{x+\hat{k},x} - k^{\omega\omega'}_{x,x+\hat{k}} \right).$$

Therefore, Equation (4.28) implies

$$\Delta_4 N_x = \sum_{k=1}^{3} \sum_{\omega,\omega'} \left(k^{\omega\omega'}_{x-\hat{k},x} - k^{\omega\omega'}_{x,x-\hat{k}} + k^{\omega\omega'}_{x+\hat{k},x} - k^{\omega\omega'}_{x,x+\hat{k}} \right)$$

with $\Delta_4 N_x = N_x - N_{x-\hat{4}}$. We define the quark-number current by

$$j_{x,x+\hat{k}} = \sum_{\omega\omega'} \left(k^{\omega\omega'}_{x,x+\hat{k}} - k^{\omega\omega'}_{x+\hat{k},x} \right)$$

which measures the net-number of arrows pointing from x to $x + \hat{k}$ in the spatial direction $k \in \{1, 2, 3\}$. Hence, the continuity equation reads

$$\Delta_4 N_x = -\sum_{k=1}^{3} \left(j_{x,x+\hat{k}} - j_{x-\hat{k},x} \right). \tag{4.29}$$

Defining the total net-quark number $N_\tau = \sum_i N_{(i,\tau)}$ in the τ-th layer of time, the continuity equation implies

$$\Delta_4 N_\tau = \sum_i \Delta_4 N_{(i,\tau)} = -\sum_i \sum_{k=1}^{3} \left(j_{(i,\tau),(i+\hat{k},\tau)} - j_{(i-\hat{k},\tau),(i,\tau)} \right) = 0$$

on the spatial torus. Therefore, the total net-quark number N is actually $N = N_\tau$ for all $\tau \in \{0, \ldots, N_4 - 1\}$. It is therefore not necessary to consider all

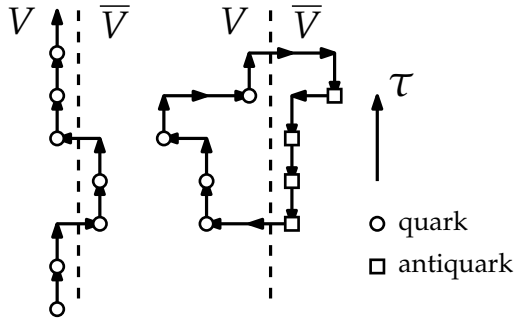

Figure 4.11: Examples of changes of the net-quark number $q_{V,\tau}$ at different times due to fermion loops. Left, a quark propagates in time and hops out of and back into the volume V. Right, a quark-antiquark pair is created at the interface between V and $\overline{V}$ and destroyed at a later point of time.†

layers of time, but it is enough to consider N_τ of some arbitrary and fixed layer τ of time:

$$\mathrm{e}^{\beta\mu N} = \mathrm{e}^{\beta\mu N_\tau} .$$

Being able to consider only one layer τ of time, we further verify the notion of $N_{(i,\tau)}$ as the local net-quark number at site i because the sum over all spatial sites i gives the total net-quark number.

Now consider some fixed layer τ of time. We define the net-quark number of the spatial subvolume V as

$$N_{V,\tau} = \sum_{i \in V} N_{(i,\tau)} .$$

The continuity equation implies

$$\Delta_4 N_{V,\tau} = \sum_i \Delta_4 N_{(i,\tau)} = - \sum_{\langle x,y \rangle \in (d_1,\tau)} j_{x,y} = -\Phi_{S^*,\tau} .$$

with the interface d_1 of the volume V, i.e. $d_1 = DS^*$ and $S^* = \partial V^*$. The notation (d_1, τ) indicates the interface d_1 embedded on the τ-th layer of time. In general, the value $\Phi_{S^*,\tau} \neq 0$, therefore, $N_{V,\tau}$ can be different for different times τ. This is just the manifestation of the fact which we have already worked out in the transfer-matrix formulation. The interaction is blind towards our choice of the subvolume V. If we fix the quark number $N_{V,\tau_0} =_3 e$ at some time τ_0, it might change at a later or earlier point of time. Changes of the net-quark number between V and $\overline{V}$ due to fermion loops are illustrated in Figure 4.11.

Consequently, it is not enough to fix the net-quark number $N_{V,\tau_0} =_3 e$ at one point τ_0 in time, but we again have to fix it at all times: $N_{V,\tau} =_3 e$ for all $\tau \in \{0, \ldots, N_4 - 1\}$. In this sense, a dual configuration $\{k\}$ describes a state of fixed net-quark number $N_V =_3 e$. The ensemble $Z(N_V =_3 e)$ is constructed by inserting the constrain

$$\prod_{\tau=0}^{N_4-1} \delta(N_{V,\tau} =_3 e)$$

†The figure is adapted from "FIG. 11" by [90] and used under CC BY 4.0 [142].

into Equation (4.27):

$$Z(N_V =_3 e) = \sum_{\{k\}} W(\{k\}) \int \mathcal{D}\overline{\psi}\mathcal{D}\psi \left[\prod_\tau \mathrm{e}^{a_4\mu N_\tau}\right]\left[\prod_\tau \delta(N_{V,\tau} =_3 e)\right] \times \left[\prod_{x,\omega}\left(-\overline{\psi}_x^\omega \psi_x^{\omega'}\right)^{k_{xx}^{\omega\omega}}\right]\left[\prod_{x,\mu,\omega,\omega'}\left(\overline{\psi}_x^\omega \psi_{x+\hat{\mu}}^{\omega'}\right)^{k_{x,x+\hat{\mu}}^{\omega\omega'}}\left(\overline{\psi}_{x+\hat{\mu}}^\omega \psi_x^{\omega'}\right)^{k_{x+\hat{\mu},x}^{\omega\omega'}}\right].$$

Next, we reformulate the constraints such that we can undo the dualization and derive the path integral as an integral over the fermionic and gauge variables. To this end, we use the identity

$$\delta(N_{V,\tau} =_3 e) = \frac{1}{3}\sum_{z_\tau \in Z_3} z_\tau^{N_{V,\tau}-e}$$

which implies

$$\left[\prod_\tau \mathrm{e}^{a_4\mu N_\tau}\right]\left[\prod_\tau \delta(N_{V,\tau} =_3 e)\right] = \frac{1}{3^{N_4}}\sum_{\{z_\tau\}}\left[\prod_\tau z_\tau^{-e}\right]\left[\prod_\tau \left(\mathrm{e}^{a_4\mu}\right)^{N_{\overline{V},\tau}}\left(\mathrm{e}^{a_4\mu} z_\tau\right)^{N_{V,\tau}}\right].$$

Therefore, the ensemble $Z(N_V =_3 e)$ is

$$Z(N_V =_3 e) = \frac{1}{3^{N_4}}\sum_{\{z_\tau\}}\left[\prod_\tau z_\tau^{-e}\right] Z(\{z_\tau\})$$

with the twisted ensembles

$$Z(\{z_\tau\}) = \sum_{\{k\}} W(\{k\}) \int \mathcal{D}\overline{\psi}\mathcal{D}\psi \left[\prod_\tau \left(\mathrm{e}^{a_4\mu}\right)^{N_{\overline{V},\tau}}\left(\mathrm{e}^{a_4\mu} z_\tau\right)^{N_{V,\tau}}\right]\left[\prod_{x,\omega}\dots\right]\left[\prod_{x,\mu,\omega,\omega'}\dots\right].$$

The twisted ensemble $Z(\{z_\tau\})$ has a similar form as Equation (4.27). The difference lies in the multiplication of the factors $\mathrm{e}^{a_4\mu N_{(i,\tau)}}$ with the center elements if i lies in the volume V. Undoing the dualization steps, which yield Equation (4.27), for $Z(\{z_\tau\})$ gives the path integral

$$Z(\{z_\tau\}) = \int \mathcal{D}U\mathcal{D}\overline{\psi}\mathcal{D}\psi\, \mathrm{e}^{S_\mathrm{G}(U)}\mathrm{e}^{S_\mathrm{F}(\{z_\tau\},U,\overline{\psi},\psi)}.$$

The fermion action $S_\mathrm{F}(\{z_\tau\}, U, \overline{\psi}, \psi)$ is the Hasenfratz-Karsch action (2.4) but with modified hopping terms in direction of time

$$S_\mathrm{F}(\{z_\tau\}, U, \overline{\psi}, \psi) = \kappa\sum_{x,\mu}\left[\overline{\psi}_x \Gamma^+_{x,\mu}\psi_{x+\hat{\mu}} + \overline{\psi}_{x+\hat{\mu}}\Gamma^-_{x,\mu}\psi_x\right] - \sum_x \overline{\psi}_x\psi_x,$$

where

$$\Gamma^\pm_{x,\mu} = \begin{cases} z_\tau^{\pm 1}\Lambda^\pm_{(i,\tau),4}, & i \in V \text{ and } \mu = 4 \\ \Lambda^\pm_{x,\mu}, & \text{else} \end{cases}.$$

All timelike hops with spatial components in the volume V are multiplied by the center elements z_τ or z_τ^{-1}depending on whether timelike hops are forward or backward directed.

In this form, the only modifications are done in the fermion action but recall that only the gauge part $S_\mathrm{G}(\{z_\tau\}, U)$ has been modified in the transfer-matrix construction. However, we actually derived the same twisted ensemble here because we can shift all center dependence from $S_\mathrm{F}(\{z_\tau\}, U, \overline{\psi}, \psi)$ into $S_\mathrm{G}(U)$. To this end, we use the left-invariance of the Haar measure. We substitute all timelike gauge variables with

$$U_{\langle x, x+\hat{4}\rangle} \longrightarrow \begin{cases} z_\tau^{-1} U_{\langle x, x+\hat{4}\rangle}, & x = (i, \tau) \text{ and } i \in V \\ U_{\langle x, x+\hat{4}\rangle}, & \text{else} \end{cases} .$$

This removes the center elements from the fermion action and moves the center dependence into the plaquette action. Between two layers of time τ and $\tau + 1$, only the timelike plaquettes are twisted with z_τ such that we get $S_\mathrm{G}(\{z_\tau\}, U)$ as in the case of the transfer-matrix formulation. This is because the twists can only influence plaquettes with timelike gauge variables having spatial components in V. These are either plaquettes which have two or one temporal links with components in V. In the former case, the overall twist of the plaquette is one because one timelike link points in positive and one in negative direction. The positively orientated gauge variable is multiplied with z_τ^{-1}, whereas the negatively orientated variable is multiplied with z_τ. In the latter case, one gauge variable of the plaquette is twisted with $z_\tau^{\pm 1}$ which implies an overall twist with $z_\tau^{\pm 1}$. These kind of plaquettes $p_{x,\mu\nu}$ are exactly those which border the spatial volume V.

Chapter 5

Percolation in QCD

In the last chapter, we have used the decomposition of the physical Hilbert space $\mathcal{H}_{\text{phys}}$ into sectors $\mathcal{H}_{\{q,e\}}$ of flux-tube configurations $\{q, e\}$ to construct the ensembles $Z(N_V =_3 e)$ of fixed net-quark numbers. In this chapter, we use the transfer-matrix formalism to construct a notion of confinement and deconfinement based on the percolation of flux-tube configurations. Our notion is gauge-invariant and can be defined as an observable on the lattice. Similar to the fixed net-quark number ensembles and 't Hooft's center-electric flux ensemble, the observable is formulated as a sum over ensembles of twisted plaquettes, where we again leverage the properties of the asymmetric transfer-matrix formulation to shift all twists into the purge gauge part only. The percolating phase of flux-tube configurations, i.e. the phase of infinitely large center-electric structures, is then identified with the deconfined phase whereas we identify the non-percolating phase of only local center-electric structures as the confined phase. Because a percolation transition is of geometric nature only and does not rely on a non-analytic behavior of the free energy density, our notion also applies to all parameters of the theory which especially includes the presence of dynamical quarks. The idea of interpreting confinement and deconfinement in QCD as a consequence of percolation was put forward by Satz [28]. We complete the idea of Satz by explicitly stating a gauge-invariant notion of percolation based on flux-tube configurations in full QCD. The incentive of understanding the confinement-deconfinement transition by means of percolating flux-tube configurations goes back to works of Patel [29]. At the end, in this chapter, we suggest the correct combination of both ideas to fully define a notion of confinement and deconfinement in QCD. In Section 5.1, we discuss the basic properties of percolation. Afterwards, in Section 5.2, we discuss Satz's ([28]) and Patel's ([29]) ideas as a preparation for the actual formulation of percolation in full QCD which is then discussed in Section 5.3. We also demonstrate that a percolation transition based on our notion consistently implies the $\mathbb{Z}_3$-transition in the case of infinitely heavy quarks and make a conjecture about the phase diagram of QCD based on what we expect from our notion of confinement.

5.1 The phenomena of percolation

Percolation is the phenomena of a system undergoing a geometric phase transition between a phase of locally finite spatial structures to a phase of infinitely large ones. This is admittedly a very broad and vague definition, because what is meant by spatial structures depends on the system in question. Let us start with an intuitive example before we turn our focus onto a more rigorous consideration which provides the basis for this chapter. We refer to [143] for a more detailed account of percolation theory in general.

Consider some non-conducting and sufficiently large plate, for example made of wood or stone, and some very fine metal flakes which are shaped like disks of the same radius r and evenly spread over the surface of the plate. Two opposite edges of the plate are assumed to be coated with a thin layer of metal. The density of the metal disks is then $\sigma = N/A$, where N is the total number of flakes and A is the plate's surface. We now ask the question whether the two opposite edges of the plate are electrically connected if a voltage is applied between them. If the density σ is very low, the disks do not overlap and there are large gaps between them. Therefore, there is no path of overlapping metal flakes which acts as a conductor between both sides. No current is going to flow from one side of the plate to the other side. However, increasing the density σ, chunks of overlapping flakes will form because we just throw more metal disks onto the plate. The size of these chunks increases with increasing density σ. The probability of having one large chunk connecting both sides of the plate is near one above a critical point $\sigma > \sigma_c$. The system undergoes a phase transition between a phase in which all chunks of overlapping flakes are finite ($\sigma < \sigma_c$) to a phase in which an infinitely large chunk exists ($\sigma > \sigma_c$). This is an example of continuum percolation and the threshold σ_c is known to be

$$\sigma_c = \frac{\eta_c}{\pi r^2}$$

with the critical filling factor $\eta_c = 1.12808737(6)$ for the above disk model [144].

Bond percolation

To demonstrate the key concepts of percolation and percolation transitions in a more rigorous way, we consider a simple non-trivial example: bond percolation in two spatial dimensions.

Consider a two-dimensional lattice of extent N in all directions and free boundary conditions. We define the bond variables $b_{\langle i,j\rangle} \in \{0,1\}$ which, contrary to links, are undirected: $b_{\langle i,j\rangle} = b_{\langle j,i\rangle}$. We interpret a bond variable as a line drawn between the sites i and j if $b_{\langle i,j\rangle} = 1$. A configuration $\{b\}$ of bond variables is therefore a configuration of lines. Two sites i and j are said to be connected if and only if there exists a path

$$\mathcal{C} = \langle i, a_1\rangle + \langle a_1, a_2\rangle + \ldots + \langle a_n, j\rangle$$

along which all bond variables $b_l = 1$, $l \in \mathcal{C}$ are set, i.e. i and j are connected by at least one path of lines. Trivially, each site i is connected with itself by

definition. A bond configuration decomposes into regions called clusters. A cluster is a maximal set of sites which are pairwise connected, and all bonds which are set and incident to the sites are defined to be part of the cluster.

We now consider an ensemble of bond configurations, i.e. a probability measure $P(\{b\})$ determining the frequency with which a configuration is perceived by an observer. In standard bond percolation, each bond variable $b_{\langle i,j\rangle}$ is set independently with the probability p:

$$P(\{b\}) = p^{n_1}(1-p)^{n_0}\,,$$

where n_1 (n_0) is the number of links with $b_{\langle i,j\rangle} = 1$ ($b_{\langle i,j\rangle} = 0$).

Making the connection with the example of continuum percolation, consider the spanning probability $R_1(p, N)$ to observe a path which connects one edge of the lattice with an opposite edge in a fixed direction. How large is $R_1(p, N)$? For any finite lattice $N < \infty$, this probability is always larger than zero as long $p > 0$ because every bond configuration $\{b\}$ has a non-zero probability $P(\{b\})$. However, the system undergoes a percolation transition at $p = p_c = 0.5$ [145]. The spanning probability $R_1(p, N)$ tends to zero for any $p < p_c$ and to one for any $p > p_c$ if $N \to \infty$. Below the percolation threshold, it becomes unlikely, and above, it becomes almost certain to observe a spanning cluster which connects both edges of the lattice. Spanning clusters are also referred to as percolating clusters [143].

In Figure 5.1, the spanning probability $R_1(p, N)$ is shown for different extents N. The results are obtained by Monte-Carlo computations where random bond configurations $\{b\}$ are generated and tested to whether a configuration has a path connecting both sides of the lattice in the first direction. Clearly, the formation of the step function can be observed at $p_c = 0.5$ for the infinite volume limit $N \to \infty$. The different curves cross at the common value $R_1(p_c, N \to \infty)$ for sufficiently large N. In general, $R_1(p, N)$ has a scaling behavior near the critical point p_c if N is sufficiently large:

$$R_1(p, N) = \Phi\Big(A \cdot (p - p_c)N^{\frac{1}{\nu}}\Big)$$

with the critical exponent $\nu = 4/3$ [143], the non-universal metric factor A and the scaling function Φ [143, 146, 147]. This behavior is universal in the sense that the scaling function Φ only depends on the dimension, the boundary condition and the aspect ratio [146, 147]. The scaling behavior is insensitive to whether bond or site percolation or a different lattice geometry is chosen. All non-universal behavior is incorporated into the metric factor A [148–150]. Therefore the crossing probability

$$R_1(p_c, N \to \infty) = \Phi(0)$$

is universal in the same sense.

As an example, spanning clusters are illustrated in Figure 5.2 for $N = 64$. For $p = 0.4$, it is unlikely to observe a spanning cluster, for $p = p_c = 0.5$, spanning clusters are observed, but they are typically not filling the whole space, and, for $p = 0.6$ it is almost certain to observe a spanning cluster which also contains most points of the lattice.

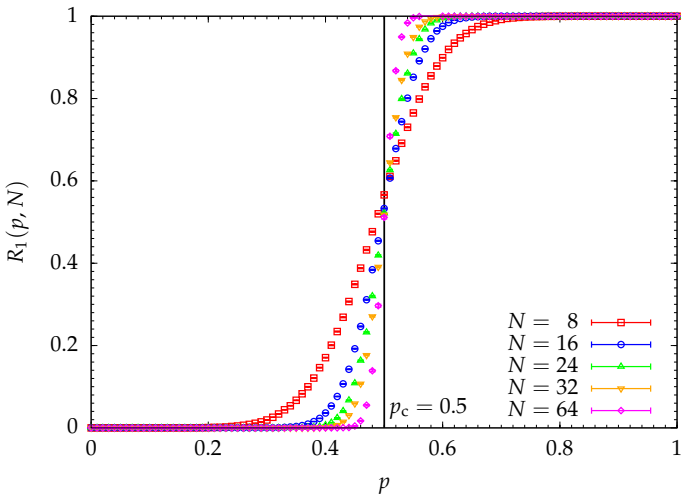

Figure 5.1: Spanning probability $R_1(p, N)$ for bond percolation in two dimensions on a $N \times N$ square lattice. The black line indicates the percolation threshold $p_c = 0.5$ which is analytically known [145].

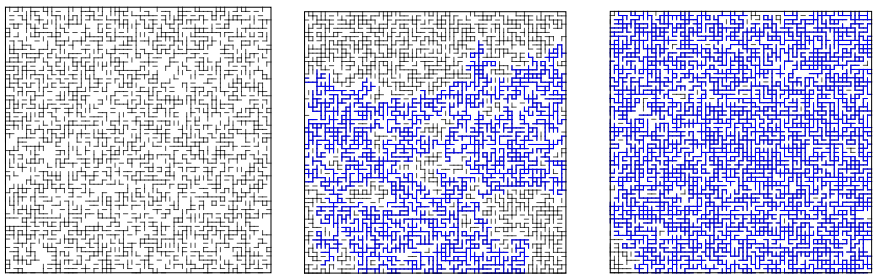

(a) $p = 0.4$ (b) $p = p_c = 0.5$ (c) $p = 0.6$

Figure 5.2: Illustration of bond configurations $\{b\}$ randomly generated with different probabilities p on a $N = 64$ lattice. The blue lines indicate a spanning cluster connecting the left and right side of the lattice.

A percolation transition also exists in three dimensions – the case that we are most interested in. However, the percolation threshold $p_c = 0.24881182(10)$ and the critical exponent $\nu^{-1} = 1.1410(15)$ are different [151].

Other kinds of spanning probabilities can be defined in general. For example, we could consider the probability $R_0(p, N)$ of observing a spanning cluster which percolates in only one direction, or we could also define the probability $R_2(p, N)$ of observing a spanning cluster which spans in all directions [147, 152]. Later on, we will also consider the probability $R(p, N)$ of observing a spanning cluster which percolates in at least one direction. Different notions of the spanning probability influence the universal scaling function Φ but the general behavior of the spanning probability remains the same – the formation of a step function at the percolation transition p_c.

5.2 Percolation in QCD

Satz ([28]) put forward the idea to understand the phase of confinement and deconfinement by the phenomena of percolation. He based his argument on the following analogy. Spin systems typically undergo a phase transition due to a spontaneous symmetry breaking of the underlying discrete symmetry group G (e.g. $\mathbb{Z}_n$). The breaking of the symmetry is defined in the limit of vanishing external field $h \to 0^+$, where the symmetry under G is restored. Because the symmetry is explicitly broken for $h > 0$, there exists a critical value $h_c \geq 0$ such that the phase transition vanishes once $h > h_c$. Satz compared this situation to QCD where we have a spontaneous symmetry breaking of the center symmetry $\mathbb{Z}_3$ in the limit of infinite quark masses $m_q \to \infty$. As we discussed in Section 2.4, however, the phase transition vanishes towards finite quark masses m_q because the center symmetry is explicitly broken by the presence of dynamical fermions. Hence, the quark mass in QCD acts inversely compared to the external field in spin systems. The notion of confinement and deconfinement based on the Polyakov loop breaks down for sufficiently small masses m_q.

He furthered the analogy by comparing to the phenomena of the Kertész line ([153]) in the two-dimensional Ising model. Percolation and spontaneous symmetry breaking both describe a phase transition in a thermodynamic system. However, percolation is a geometric phase transition, where the distribution of geometric objects is considered. Spontaneous symmetry breaking yields a phase transition in the usual sense. The transition is a non-analytic behavior of the free energy density. In the two-dimensional Ising model both notions coincide if clusters are defined by randomly setting bond variables with the probability $p = 1 - \mathrm{e}^{-2J/T}$ between neighboring sites of equally aligned spins (site-bond clusters) [154]. Here, J is the usual coupling between nearest-neighbor sites in the Ising model. Then the onset of percolation is identical to the critical temperature T_c of the symmetry breaking transition, and the percolation transition lies in the universality class of the two-dimensional Ising model [154–156]. The Ising model loses its criticality for $h > 0$. However, the percolation transition persists for all external fields h but with different threshold temperatures $T_c(h)$, and the universality class is given by bond percolation in two dimensions [157]. The function $T_c(h)$ is the Kertész line. If $h \to \infty$, all spins are aligned in the same direction and the bonds are set randomly with the probability p. The transition reduces to standard bond percolation with the critical value

$$T_c = \frac{2J}{\ln((1 - p_c)^{-1})},$$

where p_c is the percolation threshold of two-dimensional percolation. Satz concluded his analogy by suggesting that a Kertész line might also be given in the case of QCD if the correct notion of clusters is defined. The percolation transition along the Kertész line would allow to sharply distinguish between a confined and deconfined phase at all quark masses m_q of the theory.

Fortunato and Satz tried to formulate a suitable site-bond picture in QCD by considering effective Polyakov-loop theories where the Polyakov loop $L_{\vec{x}}$ takes the role of the spin in the site-bond picture [156, 158–160]. Other existing

approaches of describing confinement by the phenomena of percolation are percolation of center vortices [114, 161–170] and center clusters [171–180]. The percolation of center vortices indeed coincide with the transition of the pure gauge theory but is not gauge-invariant because it includes a certain gauge and center projection. Center clusters are gauge-invariant because they are defined by local Polyakov loops $L_{\vec{x}}$. However, similar to the site-bond picture, a choice of a parameter δ is involved which only chooses sites where the phase value of $L_{\vec{x}}$ clearly favors a specific center element [171, 177]. Taking the continuum limit then requires to make the parameter $\delta(a)$ depend on the lattice spacing a and relate the cluster sizes to a fixed physical scale d_{phys} at low temperatures [174, 177]. For $\mathrm{SU}(3)$, the onset of percolation then coincide with the spontaneous symmetry breaking transition in the continuum limit [173, 174, 177]. Nevertheless, this is not the case for pure $\mathrm{SU}(4)$-gauge theory [176]. The symmetry transition does not coincide with an onset of percolation in the continuum limit.

It is one of the main results of this thesis to suggest an inherently gauge-invariant notion of percolation filling the missing puzzle piece in Satz's understanding of confinement. As it turns out, our notion is not only gauge-invariant but also does not rely on any additional parameter or arbitrary scale setting. Consistent with the understanding of a Kertész line, we show that the percolation transition and the symmetry breaking transition coincide in the limit of infinite quark masses. We essentially use Patel's original idea ([29]) to understand the confinement-deconfinement transition by percolation of flux-tube configurations and show that it can be implemented gauge-invariantly in full Lattice QCD. Patel interpreted deconfinement and confinement by whether electric-flux tubes and charges subject to Gauss's law are forming infinite (percolating) networks or not. He proposed a classical flux-tube model on the lattice which phenomenologically reflects this understanding. Chapter 6 is devoted to the discussion of the flux-tube model. The essential part of the flux-tube model is, however, the state space being given by flux-tube configurations similar to the flux-tube configurations $\{q, e\}$ of Chapter 3. Because the physical Hilbert space $\mathcal{H}_{\text{phys}}$ decomposes into sectors of flux-tube configurations $\{q, e\}$, we straightforwardly can define a notion of percolation based on the configurations $\{q, e\}$. This is done in detail in the next section. The non-percolating phase reflects a phase in which only local objects like hadrons exist marking the confined phase whereas the percolating phase is a phase of infinitely large gauge-invariant structures of charges and fluxes which we interpret as the deconfined phase.

During the authoring of this thesis, it was noted that a similar definition of confinement has been put forward in [181, 182] for a $\mathbb{Z}_2$-lattice gauge theory with a local $\mathbb{Z}_2$-Gauss law. However, it is worthwhile to stress again that the understanding of confinement and deconfinement as a percolation of electric fluxes has essentially been put forward firstly by Patel [29] and that we have already suggested a possible connection between the center-electric fluxes in full QCD, Patel's ([29]) and Satz's ([28]) ideas in the conclusion of our work in [90]. Additionally, in this thesis, we present a construction for full QCD, derive the path integral for the spanning probability and show the connection

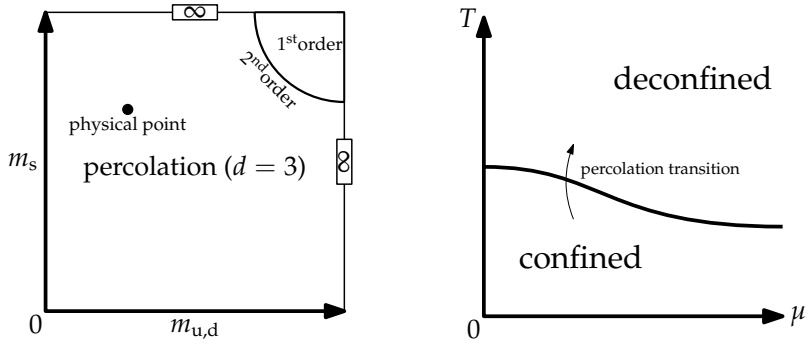

(a) Columbia plot ($N_f = 2 + 1, \mu = 0$). (b) QCD-phase diagram (μ-T plane).

Figure 5.3: Conjecture of the confinement-deconfinement transition.

between the percolation transition and the $\mathbb{Z}_3$-transition in pure gauge theory.

Before we dive into the formal construction, we end this section with a somewhat bold conjecture for the QCD-phase diagram with respect to confinement. The concept of the Kertész line might translate to the Columbia plot shown in Figure 5.3a. At the upper right corner, where confinement is given by the spontaneous symmetry breaking transition of the center group $\mathbb{Z}_3$, the percolation transition coincide with the first-order transition. For finite but sufficiently large quark masses, the first-order transition persists till it ends in a second-order line. We expect the percolation transition also to persist and to coincide with the first- and second-order transitions such that the percolation transition lies in the same universality class as the $\mathbb{Z}_3$ transition. Once the quark masses are small enough, the non-analytic behavior of the free energy density vanishes and the system is described by a crossover behavior. However, the percolation transition persists still marking a confined and deconfined phase, but, because is not related anymore to any other thermodynamic transition, we expect the universality class to be just given by three dimensional bond percolation. The three dimensions reflect the three spatial dimensions because flux-tube configurations $\{q, e\}$ are spatial objects. What does the conjecture imply? Confinement is generally defined by percolation and the understanding of it in the infinite-quark mass limit is just a special case where we can replace the notion of percolation by a $\mathbb{Z}_3$ transition. Furthermore, we note that the concept of color confinement is still given because the sectors of flux-tube configurations $\{q, e\}$ are inherently defined on the physical Hilbert space $\mathcal{H}_{\text{phys}}$ which is made of colorless states. Color confinement is therefore given at all parameters independent of whether the system is confined or deconfined. The chiral-phase transition is not included in this picture of confinement because we suspect the Kertész line not to coincide with the behavior of the chiral condensate. This is because we do not have any evidence of a mechanism which relates the chiral condensate, which is the expectation value of local fields, with the non-local concept of flux-tube percolation. In contrast, we explicitly demonstrate the connection between percolation and the $\mathbb{Z}_3$ transition in the next section. Furthermore, in the infinite-coupling limit of Lattice QCD, the condensate exhibits a transition despite the system being

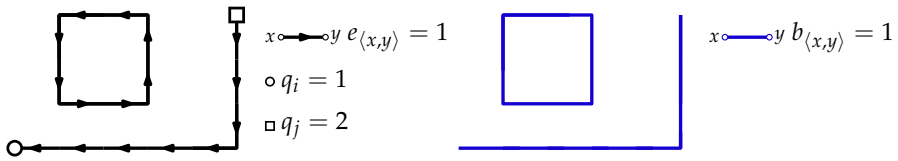

Figure 5.4: Bond configuration $B(\{q, e\})$ (right) derived from the flux-tube configuration $\{q, e\}$ (left) of Figure 3.2.

described only by on-site hadronic contributions [183]. As we discuss in the next section, only having on-site hadronic contributions translates to a vanishing spanning probability for all system sizes. There is no spatial extent of the quark-gluon matter. The system is permanently confined despite the presence of a chiral transition. If our notion of confinement and chiral phase transitions are not associated with each other, we also cannot expect any relation in the μ-T plane of the QCD-phase diagram. Hence, a suspected first-order transition of the chiral condensate terminating at a critical end point does not necessarily indicate a transition between a confined (hadronic matter) and deconfined phase (quark-gluon plasma). We expect a percolation line dividing the plane in a confined low-temperature and deconfined high-temperature region. This might be given by a curve as shown in Figure 5.3b. Of course, we have no knowledge about the form of the transition line and whether it ends at some finite μ_c at $T = 0$.

5.3 Percolation of flux-tube configurations

We are now ready to describe the percolation of flux-tube configurations in Lattice QCD with Wilson fermions. Remember from Equation (3.18) that the physical Hilbert space $\mathcal{H}_{\text{phys}}$ of the transfer-matrix formulation decomposes into sectors of flux-tube configurations $\{q, e\}$:

$$\mathcal{H}_{\text{phys}} = \bigoplus_{\{q,e\}_{\text{phys}}} \mathcal{H}_{\{q,e\}} \,.$$

When is a flux-tube configuration $\{q, e\}$ percolating? To this end, we are interested in the spatial distribution of the center-electric fluxes because they describe the connectivity between spatial sites. We define the function $B(\{q, e\})$ which derives a bond configuration $\{b\}$ from the flux-tube configuration $\{q, e\}$:

$$b_{\langle i,j\rangle} = \begin{cases} 1, & e_{\langle i,j\rangle} \neq 0 \\ 0, & e_{\langle i,j\rangle} = 0 \end{cases}$$

A bond $b_{\langle i,j\rangle}$ is set if and only if the center-electric flux $e_{\langle i,j\rangle} \neq 0$ is non-vanishing. In this sense, the function $B(\{q, e\})$ reduces a flux-tube configurations $\{q, e\}$ to its spatial information. The mapping is illustrated in Figure 5.4. We say that the flux-tube configuration $\{q, e\}$ is percolating if and only if its corresponding bond configuration $B(\{q, e\})$ is percolating. However, some care must be taken because, contrary to Section 5.1, the spatial lattice has periodic boundary conditions, and it is not obvious what is meant by a percolating bond configuration

$\{b\}$. Here, we define a bond configuration $\{b\}$ to percolate in a specific lattice direction $\vec{k}$ if it spans along the whole direction, i.e. it connects all pairs of subsequent planes which are orthogonal to $\hat{k}$ along a path of set bonds. This definition is similar to the ones used by [177, 184, 185] for example.

Now, we can classify all flux-tube configurations depending on whether they percolate. We denote with $\mathcal{R}_1$ ($\overline{\mathcal{R}}_1$) the set of all flux-tube configurations which are (not) percolating in the first direction. Therefore, the physical Hilbert space decomposes into sectors of percolating and non-percolating configurations:

$$\mathcal{H}_{\text{phys}} = \mathcal{H}_{\mathcal{R}_1} \oplus \mathcal{H}_{\overline{\mathcal{R}}_1}$$

with

$$\mathcal{H}_{\mathcal{R}_1} = \bigoplus_{\{q,e\}\in\mathcal{R}_1} \mathcal{H}_{\{q,e\}} \qquad \text{and} \qquad \mathcal{H}_{\overline{\mathcal{R}}_1} = \bigoplus_{\{q,e\}\in\overline{\mathcal{R}}_1} \mathcal{H}_{\{q,e\}}$$

Naturally, we define the spanning probability R_1 as the probability of observing a percolating flux-tube configuration $\{q,e\}$:

$$R_1(T,\mu) = \frac{1}{Z}\,\text{tr}\left(\mathrm{e}^{\beta\mu\hat{N}}\mathrm{e}^{-\beta\hat{H}}\hat{P}_{\mathcal{R}_1}\hat{P}_0\right),$$

where $\hat{P}_{\mathcal{R}_1}$ projects onto the sector $\mathcal{H}_{\mathcal{R}_1}$.

In the terminology of bond percolation, the grand-canonical ensemble yields a probability measure of flux-tube configurations $P(\{q,e\})$ from which a probability measure $P(\{b\})$ of bond configurations is inferred. However, we are not faced with standard bond percolation, where $P(\{b\})$ decomposes into independent probability measures of bonds, but with the more general case of correlated percolation. The infinite-volume limit of R_1 is

$$R_{1,\infty}(T,\mu) = \lim_{N\to\infty} R_1(T,\mu),$$

where we assume a finite lattice spacing $a > 0$ and equal extents N in all spatial directions. Consider some fixed chemical potential μ. The system undergoes a percolation transition if there exists a critical temperature T_c such that

$$R_{1,\infty}(T,\mu) = \begin{cases} 1, & T > T_\text{c} \\ 0, & T < T_\text{c} \end{cases}$$

Following the understanding of Satz ([28]) and Patel ([29]) , we identify the confined phase with the non-percolating phase and the deconfined phase with the percolating phase. This is in accordance with the intuitive idea of confinement as a manifestation of local hadronic objects only and deconfinement as a phase of delocalized quark-gluon matter.

Pure gauge theory

Indeed it is possible to show that the spontaneous $\mathbb{Z}_3$-symmetry breaking of the pure gauge theory can be seen as a consequence of a percolation transition.

To be more precise, if a percolation transition at temperature T_c exists, it implies under mild assumptions Equation (4.11) for the ratio

$$R(\vec{e}) = \frac{Z_{\text{el.}}(\vec{e})}{Z_{\text{el.}}(0)}$$

of center-electric flux ensembles, which has been discussed in Chapter 4. The spontaneous symmetry breaking is probed by $R(\vec{e})$ due to the thinning mechanism of color-electric fluxes in the confined phase.

We show that a percolation transition at T_c implies the behavior of $R(\vec{e})$ in the pure gauge case under mild assumptions. To this end, we make one key observation: only percolating clusters can create a non-vanishing center-electric flux through some surface S^*_{mn} which winds around the directions m and n of the spatial torus. This property is a consequence of the local $\mathbb{Z}_3$-Gauss law which enforces non-trivial center-electric fluxes $e_{\langle i,j\rangle} \neq 0$ to form closed loops. For a configuration $\{e\}$ to create a non-trivial center flux through a surface S^*_{mn}, it necessarily needs to include a path $\mathcal{C}$ of non-trivial flux variables $e_{\langle i,j\rangle} \neq 0$ which winds around the lattice in the direction orthogonal to the m-n-plane. Clusters which do not wind in said direction either do not penetrate the surface S^*_{mn} or penetrate it multiple times such that the net-center flux created through S^*_{mn} is zero. Note that there are configurations $\{e\}$ which percolate but do not wind around the torus. A configuration $\{e\}$ winds around the torus if its bond configuration $\{b\} = B(\{e\})$ includes a path $\mathcal{C}$ which is not null-homotopic, i.e. $\mathcal{C}$ cannot be deformed continuously into a point, see for example [186] concerning the notion of winding clusters. Requiring for the existence of a cluster connecting all pairs of subsequent planes orthogonal to a direction $\vec{k}$ is therefore a less strict definition of percolation.

Assume $\vec{e} = (1,0,0)$ for simplicity. Consider the finite system with extent N. We define the probabilities

$$r_{\vec{w}} = \frac{Z_{\text{el.}}(\vec{w})}{Z} = \frac{1}{Z}\,\text{tr}\left(\hat{P}(S^*_{23}, w_1)\hat{P}(S^*_{13}, w_2)\hat{P}(S^*_{12}, w_3)\mathrm{e}^{-\beta\hat{H}}\hat{P}_0\right)$$

of observing flux-tube configurations creating the center-electric fluxes $\vec{w} = (w_1, w_2, w_3)$ through the surfaces S^*_{23}, S^*_{13} and S^*_{12} respectively. Due to our key observation, all flux-tube configurations $\{e\}$ which generate a flux $w_1 \neq 0$ through S^*_{23} must belong to $\mathcal{R}_1$: $\{e\} \in \mathcal{R}_1$. Therefore, we get

$$\hat{P}_{\mathcal{R}_1} = \sum_{w_1=1,2}\sum_{w_2,w_3} \hat{P}(S^*_{23}, w_1)\hat{P}(S^*_{13}, w_2)\hat{P}(S^*_{12}, w_3) + \hat{P}_{\mathcal{M}_1}\,,$$

where $\mathcal{M}_1 \subseteq \mathcal{R}_1$ contains all flux-tube configurations of $\mathcal{R}_1$ which do not belong to sectors with $w_1 = 1,2$. This implies a sum rule for the spanning probability $R_1(T)$:

$$R_1(T) = \sum_{w_1=1,2}\sum_{w_2,w_3} r_{\vec{w}} + r_1 \tag{5.1}$$

with the probability $r_1 = \langle \hat{P}_{\mathcal{M}_1}\rangle$. A configuration which is part of $\mathcal{M}_1$ percolates in the first direction but does not create any flux through S^*_{23} ($w_1 = 0$). We further classify the configurations in $\mathcal{M}_1$ by their fluxes w_2 and w_3 through the

surfaces S_{13}^* and S_{12}^*. This gives us the decomposition of r_1 into the probabilities $r_{1,(w_2,w_3)}$ of having a flux-tube configuration $\{e\}$ which percolates in the first direction and generates the fluxes w_2 and w_3 in the other directions:

$$r_1 = \sum_{w_2,w_3} r_{1,(w_2,w_3)} \,.$$

The probability $\overline{R}_1(T) = 1 - R_1(T)$ of observing no percolating cluster in the first direction can be decomposed analogously. We classify the flux-tube configurations $\{e\} \in \overline{\mathcal{R}}_1$ by their fluxes w_2 and w_3 which they generate through the surfaces S_{13}^* and S_{12}^*. There are no configurations in $\overline{\mathcal{R}}_1$ which create a non-trivial flux $w_1 \neq 0$ because all these configurations are included in $\mathcal{R}_1$. We have the probabilities $r_{0,(w_2,w_3)}$ of observing a non-percolating configuration which generates the fluxes w_2 and w_3:

$$\overline{R}_1(T) = \sum_{w_2,w_3} r_{0,(w_2,w_3)} \,. \tag{5.2}$$

These definitions imply

$$\begin{aligned} \frac{Z_{\text{el.}}(\vec{e})}{Z} &= r_{\vec{w}=(1,0,0)} \,, \\ \frac{Z_{\text{el.}}(0)}{Z} &= r_{1,(0,0)} + r_{0,(0,0)} \,. \end{aligned}$$

The ratio $R(\vec{e})$ is written as

$$R(\vec{e}) = \frac{r_{\vec{w}=(1,0,0)}}{r_{1,(0,0)} + r_{0,(0,0)}} \,.$$

We now assume the existence of a percolation transition at T_c and make the assumptions

$$\lim_{N\to\infty} r_{0,(0,0)} > 0$$

in the confined phase and

$$\lim_{N\to\infty} r_{\vec{w}=(1,0,0)} = \lim_{N\to\infty} r_{1,(0,0)}$$

in the deconfined phase.

In the confined phase, $\lim_{N\to\infty} R_1(T) = 0$ implies $r_{\vec{w}=(1,0,0)} \to 0$ and $r_{1,(0,0)} \to 0$ for $N \to \infty$ due to Equation (5.1):

$$R_1(T) = \sum_{w_1=1,2} \sum_{w_2,w_3} r_{\vec{w}} + r_1 \longrightarrow 0, \quad N \to \infty$$

and therefore $r_{\vec{w}} \to 0$ and $r_1 \to 0$ because $r_{\vec{w}}, r_1 \geq 0$. Because $r_{0,(0,0)}$ is assumed to stay non-zero in the infinite-volume limit, we have

$$\lim_{N\to\infty} R(\vec{e}) = \lim_{N\to\infty} \frac{\overbrace{r_{\vec{w}=(1,0,0)}}^{\to 0}}{\underbrace{r_{1,(0,0)}}_{\to 0} + \underbrace{r_{0,(0,0)}}_{\to c>0}} = 0 \,.$$

In the deconfined phase, $R_1(T) \to 1$ and $\overline{R}_1(T) \to 0$ for $N \to \infty$. Now, the sum rule (5.2) implies $r_{0,(0,0)} \to 0$ and

$$\lim_{N\to\infty} R(\vec{e}) = \lim_{N\to\infty} \frac{\overbrace{r_{\vec{w}=(1,0,0)}}^{\to d}}{\underbrace{r_{1,(0,0)}}_{\to d} + \underbrace{r_{0,(0,0)}}_{\to 0}} = \frac{d}{d} = 1\,,$$

where the second assumption is used.

What is the physical motivation for the above assumptions? In the confined phase, the assumption

$$\lim_{N\to\infty} r_{0,(0,0)} > 0$$

just tells us that the probability of observing a non-percolating configuration $\{e\}$ which happens to create also no flux along the other directions is non-zero in the infinite-volume limit. We expect this because otherwise we would only observe configurations which are non-percolating in the first direction but percolating in at least one other direction. However, there is no special distinction between the directions, and therefore the spanning probabilities for the second and third direction should also vanish. We actually have $\vec{w} = 0$ in the confined phase. This implies

$$\lim_{N\to\infty} r_{0,(0,0)} = 1$$

because $\lim_{N\to\infty} r_{0,(w_2,w_3)} = 0$ if $w_2 \neq 0$ or $w_3 \neq 0$, and $\lim_{N\to\infty} \overline{R}_1(T) = 1$ in Equation (5.2).

The sum rule (5.1) gives us

$$R_1(T) = \sum_{w_1=1,2} \sum_{w_2,w_2} r_{\vec{w}} + r_1 \longrightarrow 1$$

in the infinite-volume limit and the deconfined phase because we only observe percolating configurations. Furthermore, we have

$$r_{\vec{w}=(0,w_2,w_3)} = r_{1,(w_2,w_3)} + \underbrace{r_{0,(w_2,w_3)}}_{\to 0} \longrightarrow \lim_{N\to\infty} r_{1,(w_2,w_3)}\,. \tag{5.3}$$

The observed zero-flux $w_1 = 0$ configurations are always percolating which allows us to write Equation (5.1) as

$$\sum_{\vec{w}} \lim_{N\to\infty} r_{\vec{w}} = 1\,.$$

Then the second assumption is implied by the assumption that all probabilities $\lim_{N\to\infty} r_{\vec{w}}$ are identical because

$$\lim_{N\to\infty} r_{\vec{w}} = \frac{1}{3^3}\,.$$

gives

$$\lim_{N\to\infty} r_{\vec{w}=(1,0,0)} = \lim_{N\to\infty} r_{\vec{w}=(0,0,0)} = \lim_{N\to\infty} r_{1,(0,0)}\,,$$

where we used Equation (5.3) for the last equal sign. The probability $r_{\vec{w}}$ is invariant under changing the sign of the components in $\vec{w}$:

$$r_{(w_1,w_2,w_3)} = r_{(w_1',w_2',w_3')}$$

with $w_k' = (-1)^{n_k} w_k$ and $n_k \in \mathbb{N}_0$. Only the vanishing or non-vanishing of a center flux w_k is relevant. This is shown in Appendix A.1. Hence, the question of whether $\lim_{N\to\infty} r_{\vec{w}}$ are equally distributed is a question of whether the probabilities of observing flux-tube configurations which generate zero or a non-zero flux in a specific direction k through the surface S^*_{mn} are identical. In the confined case, the answer is no. The probability of observing a non-zero flux $w_k \neq 0$ goes to zero in the infinite-volume limit because flux-tube configurations $\{e\}$ with $w_k \neq 0$ are necessarily percolating in the k-th direction. These configurations are suppressed. In the deconfined phase, we only observe percolating configurations and therefore configurations with non-zero $w_k \neq 0$ are not suppressed anymore. Comparing to standard bond percolation (see for example Figure 5.2), we expect the percolating phase to be dominated by configurations with one large bond configuration $\{b\} = B(\{e\})$ nearly occupying the whole space. We expect all kind of space-filling flux-tube configurations $\{e\}$, some creating a net flux $w_k \neq 0$ in a direction k and some creating no net flux $w_k = 0$. There is no reason to believe in a favoring towards configurations with a particular net flux w_k in the k-th direction. A favoring of some w_k would require some non-local mechanism which ensures the space-filling configurations to wind around the directions of the spatial volume in a particular way.

Note that the above arguments are also valid under a renormalization scheme when we replace the infinite-volume limits with the continuum limit followed by a infinite-volume limit as long as all probabilities in question possess a continuum limit. The main arguments of the proof are namely based on the sum rules which are valid at any intermediate step of the continuum and infinite-volume limit.

Path-integral formulation

As we have done in Chapter 3, especially Section 3.3, the path integral of $R_1(T,\mu)$ is obtained by discretizing Euclidean time with the replacement

$$\mathrm{e}^{-\beta\hat{H}} \longrightarrow \left(\mathcal{N}(a_4)\hat{T}_{a_4=\beta/N_4}\right)^{N_4},$$

where $\hat{T}_{a_4}$ is again chosen to be the asymmetric transfer operator and $\beta = 1/T$ is the inverse temperature. Therefore, the discretized version of $R_1(T,\mu)$ reads

$$R_1(T,\mu) = \frac{1}{Z}\,\mathrm{tr}\left(\mathrm{e}^{\beta\mu\hat{N}}\hat{T}_{a_4}^{N_4}\hat{P}_{\mathcal{R}_1}\hat{P}_0\right). \tag{5.4}$$

The path integral is then computed along the same steps as presented in Section 3.2 and 3.3.

However, similar to the ensemble $Z(N_V = e \mod 3)$ in Section 4.2, we have to incorporate the projection operator $\hat{P}_{\mathcal{R}_1}$ appropriately. To this end,

we formulate $\hat{P}_{\mathcal{R}_1}$ as a sum over center-electric flux operators $\hat{E}^z_{\langle i,j\rangle}$ on $\mathcal{H}_{\text{phys}}$. Together with the choice of the asymmetric transfer operator, the influence of $\hat{P}_{\mathcal{R}_1}$ is again restricted to twisting only plaquettes in the pure gauge action. The fermionic part remains unchanged. The sector $\mathcal{H}_{\mathcal{R}_1}$ of percolating flux-tube configurations is just the direct sum over all sectors $\mathcal{H}_{\{q,e\}}$ with flux-tube configurations $\{q,e\} \in \mathcal{R}_1$ which percolate as defined for the spanning probability in question. Therefore, the projection operator $\hat{P}_{\mathcal{R}_1}$ can also be written as a sum over the projection operator $\hat{P}_{\{q,e\}}$ which maps onto the sector $\mathcal{H}_{\{q,e\}}$:

$$\hat{P}_{\mathcal{R}_1} = \sum_{\{q,e\}\in\mathcal{R}_1} \hat{P}_{\{q,e\}}\,.$$

Because all center operators $\hat{E}^z_{\langle i,j\rangle}$ and $\hat{Q}^z_i$ commute pairwise, we can actually project on a sector $\mathcal{H}_{\{q,e\}}$ by projecting subsequently onto the sectors $\mathcal{H}_i^{q_i}$ and $\mathcal{H}^{e_{\langle i,i+\hat{k}\rangle}}_{\langle i,i+\hat{k}\rangle}$ for all sites i and links $\langle i, i+\hat{k}\rangle$:

$$\hat{P}_{\{q,e\}} = \left[\prod_i \hat{P}_i(q_i)\right]\left[\prod_{\langle i,i+\hat{k}\rangle} \hat{P}_{\langle i,i+\hat{k}\rangle}(e_{\langle i,i+\hat{k}\rangle})\right].$$

Replacing the operators on the right-hand side by their Fourier transforms (3.16) over the center Z_3 gives

$$\hat{P}_{\{q,e\}} = \frac{1}{3^{4N_\mathrm{s}}}\sum_{\{z\}} z^{-\{q,e\}}\left[\prod_i \hat{Q}_i^{z_i}\right]\left[\prod_{\langle i,i+\hat{k}\rangle} \hat{E}^{z_{\langle i,i+\hat{k}\rangle}}_{\langle i,i+\hat{k}\rangle}\right] \tag{5.5}$$

with the short-hand notation

$$z^{-\{q,e\}} = \left[\prod_i z_i^{-q_i}\right]\left[\prod_{\langle i,i+\hat{k}\rangle} z^{-e_{\langle i,i+\hat{k}\rangle}}_{\langle i,i+\hat{k}\rangle}\right]$$

and the Z_3-spin configuration $\{z\}$ assigning a spin $z_i \in \mathrm{Z}_3$ and $z_{\langle i,j\rangle} = z^{-1}_{\langle j,i\rangle} \in \mathrm{Z}_3$ at every site i and link $\langle i,j\rangle$. This result allows us to replace the projection operator $\hat{P}_{\mathcal{R}_1}$ with a sum over center operators $\hat{Q}^z_i$ and $\hat{E}^z_{\langle i,j\rangle}$. Nevertheless, this is not the desired final form because we like to formulate $\hat{P}_{\mathcal{R}_1}$ as a sum of center-electric flux operators only. Because Equation (5.4) takes the trace over the physical Hilbert space $\mathcal{H}_{\text{phys}}$, the projection operator $\hat{P}_{\mathcal{R}_1}$ acts solely on gauge-invariant states. In this case, a center-charge operator $\hat{Q}^z_i$ can be replaced with the flux operators $\hat{E}^z_{\langle i,j\rangle}$ $(j \sim i)$ due to the $\mathbb{Z}_3$-Gauss law (3.15):

$$\hat{P}_{\mathcal{R}_1} = \frac{1}{3^{4N_\mathrm{s}}}\sum_{\{q,e\}\in\mathcal{R}_1}\sum_{\{z\}} z^{-\{q,e\}}\left[\prod_i\prod_{j\sim i} \hat{E}^{z_i^{-1}}_{\langle i,j\rangle}\right]\left[\prod_{\langle i,i+\hat{k}\rangle} \hat{E}^{z_{\langle i,i+\hat{k}\rangle}}_{\langle i,i+\hat{k}\rangle}\right] \tag{5.6}$$

on $\mathcal{H}_{\text{phys}}$. The spanning probability $R_1(T,\mu)$ is therefore just a linear combination

$$R_1 = \frac{1}{3^{4N_\mathrm{s}}}\sum_{\{q,e\}\in\mathcal{R}_1}\sum_{\{z\}} z^{-\{q,e\}}\left\langle\left[\prod_i\prod_{j\sim i} \hat{E}^{z_i^{-1}}_{\langle i,j\rangle}\right]\left[\prod_{\langle i,i+\hat{k}\rangle} \hat{E}^{z_{\langle i,i+\hat{k}\rangle}}_{\langle i,i+\hat{k}\rangle}\right]\right\rangle$$

of expectation values over center-electric flux operators. The path integrals of these expectation values are similar to the path integral of $I(d_1, z)$ with a 1-chain d_1 and twist $z \in Z_3$ from Section 4.1. However, here, the expectation values are even more general because the result is not determined by only one center element $z \in Z_3$ but by the spin configuration $\{z\}$. Despite this difference, the derivation of the path integral follows the same line of argument and is basically not different to the path-integral formulation of the simple expectation value $\langle \hat{E}^z_{\langle i,j \rangle} \rangle$ discussed in Section 3.3 and 4.1. The crucial part of the derivation is that we can just repeat the computations of Chapter 3, especially Section 3.2 and 3.3, in obtaining the Lattice QCD path integral of the partition function Z, but we have to incorporate the influence of the center-electric flux operators onto the first integral kernel $K(U_0, U_1)$ between the zeroth and first layer of Euclidean time. This means, as we have done for $\langle \hat{E}^z_{\langle i,j \rangle} \rangle$, to replace the integral kernel $K(U_0, U_1)$ with the twisted kernel $K(U_0^{\{z\}}, U_1)$, where the gauge variables U_0 in the zeroth layer of time are twisted according to the spin configuration $\{z\}$. Therefore, the path integral results in Equation (3.36), where the center-flux operators are absorbed into the first integral kernel:

$$\begin{aligned}
&\left\langle \left[\prod_i \prod_{j \sim i} \hat{E}^{z_i^{-1}}_{\langle i,j \rangle} \right] \left[\prod_{\langle i, i+\hat{k} \rangle} \hat{E}^{z_{\langle i,i+\hat{k} \rangle}}_{\langle i,i+\hat{k} \rangle} \right] \right\rangle = \\
&\quad \frac{1}{Z} \int \mathcal{D}U \mathcal{D}\Omega \mathcal{D}\overline{\xi} \mathcal{D}\xi \, \mathrm{e}^{-\overline{\xi}\xi} \, \langle \mathrm{e}^{\beta\mu} \xi^{(0)}_{\mathrm{q}}, \mathrm{e}^{-\beta\mu} \xi^{(0)}_{\overline{\mathrm{q}}} | \, K(U_0^{\{z\}}, U_1, \Omega) \, | \Omega \xi^{(1)}_{\mathrm{q}}, \xi^{(1)}_{\overline{\mathrm{q}}} \Omega^\dagger \rangle \, , \\
&\qquad \times \prod_{\tau=1}^{N_4 - 1} \langle \xi^{(\tau)}_{\mathrm{q}}, \xi^{(\tau)}_{\overline{\mathrm{q}}} | \, K(U_\tau, U_{\tau+1}) \, | \xi^{(\tau+1)}_{\mathrm{q}}, \xi^{(\tau+1)}_{\overline{\mathrm{q}}} \rangle
\end{aligned}$$

with the lattice spacing set to $a = a_4 = 1$. Calculating the matrix elements, transforming and condensing everything as in Chapter 3, we arrive at

$$\begin{aligned}
Z(\{z\}) &= \left\langle \left[\prod_i \prod_{j \sim i} \hat{E}^{z_i^{-1}}_{\langle i,j \rangle} \right] \left[\prod_{\langle i, i+\hat{k} \rangle} \hat{E}^{z_{\langle i,i+\hat{k} \rangle}}_{\langle i,i+\hat{k} \rangle} \right] \right\rangle \\
&= \frac{1}{Z} \int \mathcal{D}U \mathcal{D}\overline{\psi} \mathcal{D}\psi \, \mathrm{e}^{S_{\mathrm{G}}(\{z\}, U)} \mathrm{e}^{S_{\mathrm{F}}(U, \overline{\psi}, \psi)}
\end{aligned} \, .$$

The fermionic action $S_{\mathrm{F}}(U, \overline{\psi}, \psi)$ is the Hasenfratz-Karsch action (2.4) and the gauge action $S_{\mathrm{G}}(\{z\}, U)$ is the Wilson plaquette action in which the timelike plaquettes between the zeroth and first layer of Euclidean time are twisted depending on the spin configuration $\{z\}$. Before we state the specific rules of twisting the plaquettes, we should stress the reoccurring theme in this thesis. Whatever we have discussed up until this point, be it the simple expectation value $\langle \hat{E}^z_{\langle i,j \rangle} \rangle$, 't Hooft's center-electric flux ensembles, the values $I(d_1, z)$, the ensembles $Z(N_V = e \mod 3)$ of fixed net-quark number N_V in a subvolume V or the spanning probability $R_1(T, \mu)$, we always have established the corresponding path integral by inserting center-electric flux operators $\hat{E}^z_{\langle i,j \rangle}$ into the computation of the trace. Wherever we have considered dynamical fermions, we have made the tactical choice to use the asymmetric transfer operator. All this has repeatedly gave us a path-integral formulation, where

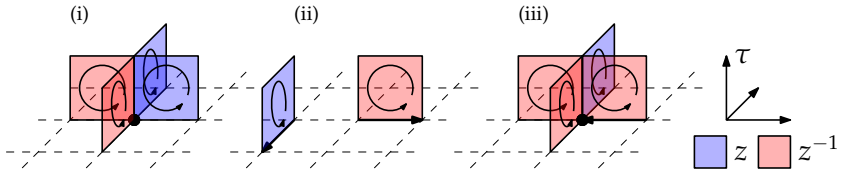

Figure 5.5: Illustration of the three rules for imposing a spin configuration $\{z\}$ in the ensemble $Z(\{z\})$ for $(2+1)$-dimensions. The configuration $\{z\}$ is embedded on the zeroth layer of time. A dot represents the center element $z_i = z$ and an arrow from i to j represents $z_{\langle i,j\rangle} = z$.

the fermionic action remains unchanged, and we only modify the gauge action by twisting timelike plaquettes.

There are three rules for imposing the twists $\{z\}$ in the twisted ensemble $Z(\{z\})$ and, for this purpose, we think of $\{z\}$ to be embedded on the zeroth layer of time: (i) An on-site spin z_i twists any timelike plaquette $p_{x,k4}$ between the zeroth and first layer of time for which the intersection link $\langle j, j+\hat{k}\rangle$ on the zeroth layer of time (ignoring the temporal component τ) is incident to the site i. If such an intersection link $\langle j, j+\hat{k}\rangle$ points away from (into) the site i, the corresponding timelike plaquette $p_{x,k4}$ is twisted with the spin z_i (z_i^{-1}); (ii) A timelike plaquette $p_{x,k4}$ between the zeroth and first layer of time intersecting the zeroth layer of time at the link $\langle i, i+\hat{k}\rangle$ is twisted with $z^{-1}_{\langle i,i+\hat{k}\rangle}$; (iii) If a plaquette is to be twisted by multiple applications of the rules (i) and (ii), the total twist is the product of the separate twists. The rules are illustrated in Figure 5.5 for $(2+1)$-dimensions.

The total path integral of R_1 reads

$$R_1 = \frac{1}{3^{4N_s}} \sum_{\{q,e\}\in\mathcal{R}_1} \sum_{\{z\}} z^{-\{q,e\}} Z(\{z\})\,.$$

Of course, formally, we can write the path integral of the spanning probability R_1 as an ordinary observable of the Lattice QCD path integral such that

$$R_1 = \langle \mathcal{O}(U)\rangle = \frac{1}{Z}\int \mathcal{D}U\mathcal{D}\overline{\psi}\mathcal{D}\psi\, \mathcal{O}(U) \mathrm{e}^{S_G(U)} \mathrm{e}^{S_F(U,\overline{\psi},\psi)}$$

with

$$\mathcal{O}(U) = \frac{1}{3^{4N_s}} \sum_{\{q,e\}\in\mathcal{R}_1} \sum_{\{z\}} z^{-\{q,e\}} \mathrm{e}^{S_G(\{z\},U)-S_G(U)}\,. \tag{5.7}$$

In this form, the gauge-invariance of the path integral is evident because the center elements commute with all elements of the gauge group.

Infinite-coupling limit

A naive consideration for testing further the notion of confinement based on percolation is to consider the infinite-coupling limit $g_0 \to \infty$. We take the limit on a finite lattice such that the Lattice QCD path integral reduces to

$$\lim_{g_0\to\infty} Z = \int \mathcal{D}U\mathcal{D}\overline{\psi}\mathcal{D}\psi\, \mathrm{e}^{S_F(U,\overline{\psi},\psi)} \tag{5.8}$$

because

$$\lim_{g_0\to\infty} \mathrm{e}^{S_\mathrm{G}(U)} = 1\,.$$

This limit is somewhat unphysical; QCD does not possess a proper continuum limit for $g_0 \to \infty$, i.e. we are unable to construct a renormalization scheme in the limit $g_0 \to \infty$ because the continuum limit is taken towards $g_0 \to 0$ due to asymptotic freedom. However, we are free to explore the naive limit $g_0 \to \infty$.

The intuitive understanding is to be in the confined phase if the gauge coupling becomes infinitely large because we expect the quarks to be bounded maximally tightly to each other. There are no spatial distributions of hadronic matter and, therefore, surely also no infinitely large clusters of quark-gluon matter. This intuitive understanding is confirmed further by considering the fact that the partition function (5.8) can be written as a sum over hadronic degrees of freedom [183, 187–189] (and references therein); the mentioned results are for staggered fermions but the reduction to hadronic degrees can also be shown for Wilson fermions as demonstrated in Appendix A.2, where the dualized path integral from Section 4.2 is reduced to configurations of hadronic occupations only at all spacetime points in the infinite-coupling limit. If our notion of confinement based on percolation coincides with the expected behavior in the infinite-coupling limit, we anticipate

$$\lim_{g_0\to\infty} R_1 = 0 \tag{5.9}$$

to vanish for all spatial lattice extents $N > 1$. The system is in a permanent state of confinement for all temperatures, chemical potentials and sizes.

We show Equation (5.9) by taking the infinite-coupling limit for R_1 such that

$$\begin{aligned}
\lim_{g_0\to\infty} R_1 &= \frac{1}{3^{4N_\mathrm{s}}} \sum_{\{q,e\}\in\mathcal{R}_1} \sum_{\{z\}} z^{-\{q,e\}} \frac{1}{\lim_{g_0\to\infty} \mathrm{Z}} \int \mathcal{D}U\mathcal{D}\overline{\psi}\mathcal{D}\psi\, \mathrm{e}^{S_\mathrm{F}(U,\overline{\psi},\psi)} \\
&= \frac{1}{3^{4N_\mathrm{s}}} \sum_{\{q,e\}\in\mathcal{R}_1} \sum_{\{z\}} z^{-\{q,e\}} \\
&= \frac{1}{3^{4N_\mathrm{s}}} \sum_{\{q,e\}\in\mathcal{R}_1} \Bigg[\prod_i \sum_{z\in\mathrm{Z}_3} z^{-q_i}\Bigg] \Bigg[\prod_{\langle i,i+\hat{k}\rangle} \sum_{z\in\mathrm{Z}_3} z^{-e_{\langle i,i+\hat{k}\rangle}}\Bigg]\,,
\end{aligned}$$

where we have factorized the sum over spin-configurations in the last step. For all $\{q,e\} \in \mathcal{R}_1$, there must be at least one $e_{\langle j,j+\hat{k}\rangle} \neq 0$ because $N > 1$. Consequently,

$$\sum_{z\in\mathrm{Z}_3} z^{-e_{\langle j,j+\hat{k}\rangle}} = 0$$

rendering the whole product zero in the above equation. This proves Equation (5.9). The spanning probability of not observing a spanning cluster must consistently be given by

$$\lim_{g_0\to\infty} \overline{R}_1 = 1 - \lim_{g_0\to\infty} R_1 = 1$$

in the infinite coupling limit. Analogous to R_1, we have

$$\lim_{g_0\to\infty} \overline{R}_1 = \frac{1}{3^{4N_\mathrm{s}}} \sum_{\{q,e\}\in\overline{\mathcal{R}}_1} \sum_{\{z\}} z^{-\{q,e\}} \,.$$

All configurations $\{q,e\} \in \overline{\mathcal{R}}_1$ with at least one $e_{\langle i,j\rangle} \neq 0$ again do not contribute because the respective sum over all spin configurations vanishes. The configuration $\{q=0, e=0\}$ is the only flux-tube configuration where all center-electric fluxes are zero and this configuration does not lie in $\mathcal{R}_1$ which is the reason for Equation (5.9). We have

$$\lim_{g_0\to\infty} \overline{R}_1(T,\mu) = \frac{1}{3^{4N_\mathrm{s}}} \sum_{\{z\}} z^{-\{q=0,e=0\}} = \frac{1}{3^{4N_\mathrm{s}}} \sum_{\{z\}} 1 = 1$$

because there are 3^{4N_s} spin configurations $\{z\}$ in total.

Zero-coupling limit

The opposite limit is the zero-coupling limit $g_0 \to 0$. In this limit we expect the system to be deconfined which should give us $R_1 \to 1$ in the infinite-volume limit. To describe this limit, we use Equation (5.7) to write $R_1 = \langle \mathcal{O}(U)\rangle$ as an expectation value. We integrate out the fermionic degrees first such that

$$R_1 = \frac{\langle \mathcal{O}(U) \det M(U)\rangle}{\langle \det M(U)\rangle} \,,$$

where the expectation value is taken relative to the pure gauge theory. In the zero-coupling limit $g_0 \to 0$, the plaquettes $U_{\partial p_{x,\mu\nu}} \approx \mathbb{1}$ get centered around the identity [41, 49]. Now, because $\mathcal{O}(U)$ actually only depends on the plaquettes, we can consider its zeroth-order expansion such that

$$R_1 \longrightarrow \mathcal{O}(U_{\partial p_{\mu\nu}} = \mathbb{1})$$

for $g_0 \to 0$. We have

$$\mathrm{e}^{S_\mathrm{G}(\{z\},U) - S_\mathrm{G}(U)} \longrightarrow \prod_{\langle i,i+\hat{k}\rangle} \exp\left(\frac{6}{g_0^2}\left[\mathrm{Re}\left(z_i z^{-1}_{\langle i,i+\hat{k}\rangle} z^{-1}_{i+\hat{k}}\right) - 1\right]\right).$$

Therefore, in the limit $g_0 \to 0$, the spanning probability is

$$R_1 \to \frac{1}{3^{4N_\mathrm{s}}} \sum_{\{q,e\}\in\mathcal{R}_1} \sum_{\{z\}} z^{-\{q,e\}} \prod_{\langle i,i+\hat{k}\rangle} \exp\left(\frac{6}{g_0^2}\left[\mathrm{Re}\left(z_i z^{-1}_{\langle i,i+\hat{k}\rangle} z^{-1}_{i+\hat{k}}\right) - 1\right]\right).$$

Now, we write $z^{-\{q,e\}} = z^{-\{q,0\}} z^{-\{0,e\}}$ and sum over the spins $z_{\langle i,i+\hat{k}\rangle}$ first such that

$$R_1 \to \frac{1}{3^{4N_\mathrm{s}}} \sum_{\{q,e\}\in\mathcal{R}_1} \sum_{\{z_i\}} z^{-\{q,0\}} \prod_{\langle i,i+\hat{k}\rangle} \sum_{z} z^{e_{\langle i,i+\hat{k}\rangle}} \exp\left(\frac{6}{g_0^2}\left[\mathrm{Re}(z z_i z^{-1}_{i+\hat{k}}) - 1\right]\right).$$

And, therefore, the substitution $z \to z z_i^{-1} z_{i+\hat{k}}$ gives

$$R_1 \to \frac{1}{3^{4N_\mathrm{s}}} \sum_{\{q,e\}\in\mathcal{R}_1} \sum_{\{z_i\}} z^{-\{q,0\}} \prod_{\langle i,i+\hat{k}\rangle} z_i^{-e_{\langle i,i+\hat{k}\rangle}} z_{i+\hat{k}}^{e_{\langle i,i+\hat{k}\rangle}} \sum_z z^{e_{\langle i,i+\hat{k}\rangle}} \mathrm{e}^{6g_0^{-2}(\mathrm{Re}z-1)} .$$

All the on-site spin factors can actually be combined to unity because

$$\left[\prod_{\langle i,i+\hat{k}\rangle} z_i^{-e_{\langle i,i+\hat{k}\rangle}}\right]\left[\prod_{\langle i,i+\hat{k}\rangle} z_{i+\hat{k}}^{e_{\langle i,i+\hat{k}\rangle}}\right] = \prod_i z_i^{-\sum_{j\sim i} e_{\langle i,j\rangle}} = \prod_i z_i^{q_i}$$

which compensates the factor $z^{-\{q,0\}}$. In doing so, we used the Z_3-Gauss law (3.17). Finally the zero-coupling limit reads

$$\lim_{g_0\to 0} R_1 = \frac{1}{3^{4N_\mathrm{s}}} \sum_{\{q,e\}\in\mathcal{R}_1} \sum_{\{z_i\}} 1 = \frac{1}{3^{3N_\mathrm{s}}} \sum_{\{q,e\}\in\mathcal{R}_1} 1$$

because the exponential $\mathrm{e}^{6g_0^{-2}(\mathrm{Re}z-1)} \to 0$ vanishes for any non-trivial twist z in the limit $g_0 \to 0$. For any configuration $\{e\}$ of center-electric fluxes not necessarily fulfilling Gauss's law, there is exactly one configuration of center charges q_i such that $\{q,e\}$ fulfills the Z_3 law:

$$\lim_{g_0\to 0} R_1 = \frac{1}{3^{3N_\mathrm{s}}} \sum_{\{e\}\in\mathcal{R}_1} 1 .$$

This is identical to the spanning probability as obtained by a system where center-electric fluxes $e_{\langle i,j\rangle}$ are set independently with the probability $p(e_{\langle i,j\rangle}) = 1/3$. Therefore, the spanning probability R_1 in the zero-coupling limit is described by standard bond percolation in three dimensions with the bond probability $p_b = 2/3$ which lies over the percolation threshold $p_\mathrm{c} = 0.24881182(10)$ [151]:

$$\lim_{N_\mathrm{s}\to\infty} \lim_{g_0\to 0} R_1 = 1 .$$

Continuum limit

Because our notion of percolation is characterized by the spanning probability $R_1(T,\mu)$ which has its value between zero and one in the quantum-mechanical formulation of the lattice theory and is not a function of the quantum fields, actually $R_1(T,\mu)$ already is the renormalized quantity which can be taken to its continuum value. Any physical renormalization scheme should deliver a real and finite value for $R_1(T,\mu)$ because it is a real and finite value at all parameters. Note that it is not immediately obvious whether $R_1(T,\mu)$ lies in the interval $[0,1]$ in the path-integral formulation. This is because we derived the path integral via the asymmetric and non-hermitian transfer operator. Therefore, the path-integral formulation might very well give us complex values for $R_1(T,\mu)$. However, this is no obstacle because, as we have seen in Chapter 3, renormalizing the path integral at maximal anisotropy $\xi \to \infty$ and fixed spatial lattice spacing a translates the spanning probability expressed as a path integral into the expectation value in the respective quantum-mechanical

system. Because the physical results in the continuum do not depend on the choice of ξ, the path integral renormalized at $\xi = 1$ and $\xi \to \infty$ deliver the same result for $a \to 0$. Therefore, $R_1(T, \mu)$ gives also a number between $[0, 1]$ in or near the continuum if computed with the path integral.

Chapter 6

Flux-tube model

The constructions of fixed-quark number ensembles in Chapter 4 and the notion of confinement based on percolation in Chapter 5 yield path integrals which are practically impossible to compute numerically. An especially hopeless pursuit is the numerical evaluation of the spanning probability in the form of Equation (5.7) because we do not only have to sum over all possible Z_3-spin configurations $\{z\}$, defined on sites and links, but we also have to sum over all possible flux-tube configurations $\{q, e\}$ which percolate in the first direction. Additionally, the evaluation of Equation (5.7) requires the computation of expectation values

$$\exp\left(-\frac{\Delta F}{T}\right) = \left\langle \mathrm{e}^{S_{\mathrm{G}}(\{z\},U)-S_{\mathrm{G}}(U)} \right\rangle$$

relative to the untwisted ensemble Z. These expectation values measure the free energy cost ΔF of inserting twists $\{z\}$ into the ensemble. In principle, we can compute these expectation values with standard Monte-Carlo techniques. However, from the pure gauge theory, it is well-known that the insertion of many non-trivial twists is accompanied with an overlap problem rendering the direct evaluation of the expectation value unfeasible [121, 122, 124, 127]. The fixed-quark number ensembles $Z(N_V =_3 e)$ do not require the summation over flux-tube configurations and only require the insertion of independent twists z_τ for each time layer τ. Therefore, the number of terms in the sum over the twisted ensembles scales like 3^{N_4} and can be kept moderate if we consider small N_4 only. Then, in principle, the algorithm described in [121, 122] might become feasible which circumvents the overlap problem by computing the ratio of ensembles where the ensembles only differ in the twist of one plaquette.

The stated numerical obstacles prevent us from illustrating the analytic concepts of Chapter 4 and 5 with actual numerical result. Therefore, the purpose of this chapter is to divert to a simple model system which shares all necessary features of full QCD such as flux-tube configurations, the $\mathbb{Z}_3$-Gauss law and twisted ensembles. This model is the flux-tube model which was first introduced by Patel ([29]) and investigated further in [190–192]. Originally, Patel introduced the model to give a qualitative mechanism for confinement and deconfinement in QCD. Remember from Chapter 5 that we used Patel's and

Satz's ([28]) ideas to formalize the notion of confinement based on percolation in full QCD.

A flux-tube model is a static system where the state space is a set of flux-tube configurations, and no interaction takes place between the degrees of freedom. As it is the case for the flux-tube configurations $\{q, e\}$ of Chapter 3, the configurations fulfill a local $\mathbb{Z}_3$-Gauss law. In a flux-tube model the (anti-)quark occupation numbers are placed at the sites such that each quark or antiquark contributes its mass m_q to the total energy of the Hamiltonian H. The center-electric fluxes $l_{\langle i,j\rangle}$ are placed at the links $\langle i, j\rangle$ and contribute with their string energy σa to H if $l_{\langle i,j\rangle} \neq 0$. Flux-tube models come in different realizations but here we are especially concerned with the flux-tube model constructed in [90]. Our flux-tube model is motivated by the simultaneous strong-coupling and heavy-quark limit of QCD which is derived in [193–195].

An important feature of flux-tube models is their duality to $\mathbb{Z}_3$-spin systems with nearest-neighbor interaction [191, 192]. It is this very duality which creates the analogy to the concepts of Chapter 4 and Chapter 5. When we define the ensembles of fixed-quark numbers and notion of percolation in the flux-tube model, we can express the same observables in the dual $\mathbb{Z}_3$-spin system, and, as it turns out, the observables in the spin system are of similar structure as the observables in full QCD. The plaquette action is replaced by the nearest-neighbor interaction of spins, the fermionic action is replaced with on-site spin factors $\prod_i Q(z_i)$, we twist the couplings between nearest-neighbor spins instead of twisting timelike plaquettes, and we sum over the twisted ensembles in the same manner.

The flux-tube model presented in Section 6.1 has been published in [90]. The author of this thesis is responsible for its derivation based on the strong-coupling and heavy-quark limit. In Section 6.2, the concepts of Chapter 4 are applied to the flux-tube model, where the numerical results from [90] are presented for which also the author of this thesis is responsible. Finally, in Section 6.3, we numerically investigate the percolation properties of the flux-tube model and demonstrate that the spanning probability of the flux-tube model maps to a twisted $\mathbb{Z}_3$-Potts model similarly to the case of full QCD as presented in Chapter 5.

6.1 Flux-tube model for heavy quarks and strong couplings

Strong-coupling and heavy-quark limit

We consider the strong-coupling and heavy-quark limit of QCD as derived by [193–195]. The limit expands the gauge action around zero inverse coupling $g_0^{-1} = 0$ and zero hopping parameter $\kappa = 0$. This is the simultaneous limit of strong coupling $g_0 \to \infty$ and heavy quarks $am \to \infty$ because the hopping parameter is

$$\kappa = \frac{1}{2am + 8}\,.$$

The expansion is based on writing the Lattice QCD partition function as an integral over the timelike gauge variables:

$$Z = \int \left[\prod_{\langle i,i+\hat{4}\rangle} \mathrm{d}U_{\langle i,i+\hat{4}\rangle} \right] \mathrm{e}^{S_{\mathrm{eff}}} ,$$

where the effective action

$$S_{\mathrm{eff}} = \ln \int \left[\prod_{\langle i,i+\hat{k}\rangle} \mathrm{d}U_{\langle i,i+\hat{k}\rangle} \right] \int \mathcal{D}\overline{\psi}\mathcal{D}\psi \, \mathrm{e}^{S_{\mathrm{G}}(U)+S_{\mathrm{F}}(U,\overline{\psi},\psi)}$$

is derived by integrating out all spatial degrees of freedom ($k \in \{1,2,3\}$). The effective action is expanded by considering the simultaneous strong-coupling expansion of the gauge part and the hopping expansion of the fermionic part. The action is then written as ([194])

$$S_{\mathrm{eff}} = \sum_{i=1}^{\infty} \lambda_i(g_0^{-1},\kappa,N_4) S_i^{\mathrm{s}} - 2\sum_{i=1}^{\infty} \left[h_i(g_0^{-1},\kappa,\mu,N_4) S_i^{\mathrm{a}} + \overline{h}_i(g_0^{-1},\kappa,\mu,N_4)(S_i^{\mathrm{a}})^* \right] ,$$

where the terms S_i^{s} are Z_3-symmetric and the terms S_i^{a} explicitly break the Z_3 symmetry. In the expansion, the terms S_i^{s} and S_i^{a} occur multiple times in general but with different pre-factors depending on g_0^{-1}, κ and N_4. Sorting all expansion terms based on equivalence up to a constant gives then the above expansion with the factors λ_i, h_i and $\overline{h}_i$. The decomposition of S_{eff} into the terms S_i^{s} and S_i^{a} is just an appropriate rearrangement of the underlying expansion such that higher orders i become negligible for small g_0^{-1} and κ.

Here, we are not interested in the technicalities of deriving the expansion but we just use the leading order result of [194] and [195] which reads

$$Z_{\mathrm{eff}} = \int \left[\prod_{\langle i,i+\hat{4}\rangle} \mathrm{d}U_{\langle i,i+\hat{4}\rangle} \right] \left[\prod_{\langle i,i+\hat{k}\rangle} \left(1 + 2\lambda \mathrm{Re}\left(L_i L_{i+\hat{k}}^*\right)\right) \right] \left[\prod_i Q(L_i) \right]$$

with

$$Q(L_i) = (1 + hL_i + h^2 L_i^* + h^3)^2 (1 + \overline{h} L_i^* + \overline{h}^2 L_i + \overline{h}^3)^2$$

at sufficiently small g_0^{-1} and κ. The coefficients h and $\overline{h}$ are given by

$$h(\kappa,\mu,N_4) = (2\kappa \mathrm{e}^{a\mu})^{N_4} = \overline{h}(\kappa,-\mu,N_4) .$$

Apparently, the effective action Z_{eff} is defined on the spatial lattice with the Polyakov loops L_i as the degrees of freedom. We integrate over all timelike links, but because the Polyakov loops L_i are gauge-invariant, we actually can gauge-fix all timelike gauge variables to maximal temporal gauge such that only one gauge variable U_i remains per spatial site which gives

$$Z_{\mathrm{eff}} = \int \left[\prod_i \mathrm{d}U_i \right] \left[\prod_{\langle i,i+\hat{k}\rangle} \left(1 + 2\lambda \mathrm{Re}\left(L_i L_{i+\hat{k}}^*\right)\right) \right] \left[\prod_i Q(L_i) \right]$$

with $L_i = \mathrm{tr}(U_i)$. The temporal extent fully vanishes from the effective theory and only its length N_4 remains as a parameter of the coefficients λ, h and $\overline{h}$.

We write the hopping parameter $\kappa = \frac{1}{2}\mathrm{e}^{-am_\mathrm{q}}$ as the exponential of the constituent quark mass m_q because the pion mass m_π is given by $am_\pi = -2\ln(2\kappa) + \mathcal{O}(\kappa^2)$ in leading order of κ [194, 195]. Therefore, the coefficients h and $\bar{h}$ can be written as

$$h = \exp\left(\frac{\mu - m_\mathrm{q}}{T}\right) \qquad \text{and} \qquad \bar{h} = \exp\left(-\frac{\mu + m_\mathrm{q}}{T}\right). \tag{6.1}$$

In this form, the effective theory still requires integrations over the gauge group SU(3). To simplify and reduce the effective theory to a spin system over the center Z_3 of SU(3) and preserve as many properties as possible, we replace the integrations over SU(3) with a sum over the center Z_3:

$$\int \mathrm{d}U_i\, f(L_i) \longrightarrow \frac{1}{3}\sum_{z_i \in \mathrm{Z}_3} f(z_i)\,.$$

This yields the spin system

$$Z_\mathrm{spin} = \frac{1}{3^{N_\mathrm{s}}}\sum_{\{z\}}\left[\prod_{\langle i,i+\hat{k}\rangle}\left(1 + 2\lambda\mathrm{Re}\left(z_i z^*_{i+\hat{k}}\right)\right)\right]\left[\prod_i Q(z_i)\right]. \tag{6.2}$$

How is this replacement motivated? In the infinite-coupling limit $g_0 \to \infty$, the parameter $\lambda \to 0$ goes to zero such that

$$Z_\mathrm{eff} \longrightarrow \prod_i\left[\int \mathrm{d}U_i\, Q(L_i)\right].$$

The partition function factorizes, and we are left with integrations over the on-site factors $Q(L_i)$:

$$\begin{aligned}\int \mathrm{d}U_i\, Q(L_i) = \int \mathrm{d}U_i \Bigg(&\alpha_{0,0} + \sum_{k=1}^{4}\alpha_{k,0}L_i^k + \sum_{k=1}^{4}\alpha_{0,k}(L_i^*)^k \\ &+\alpha_{1,1}L_i(L_i^*) + \alpha_{2,2}L_i^2(L_i^*)^2 + \sum_{k=2}^{3}\alpha_{k,1}(L_i)^k L_i^* + \sum_{k=2}^{3}\alpha_{1,k}L_i(L_i^*)^k\Bigg)\end{aligned},$$

where $Q(L_i)$ is expanded as a polynomial of orders $L_i^m(L_i^*)^n$, $m, n \in \mathbb{N}_0$; the full expansion is listed in Appendix B.1. The coefficients $\alpha_{i,j}$ are polynomials of orders $h^{n_\mathrm{q}}\bar{h}^{n_{\bar{\mathrm{q}}}}$, $n_\mathrm{q}, n_{\bar{\mathrm{q}}} \in \mathbb{N}_0$. The integral

$$T_{m,n} = \int \mathrm{d}U\, L^m (L^*)^n$$

over Polyakov loops can be computed analytically [196]. Especially, we have $T_{m,n} = 0$ if $m - n \neq 0 \mod 3$. Therefore,

$$Z_i = \int \mathrm{d}U_i\, Q(L_i) = \alpha_{0,0} + \alpha_{3,0}\cdot 1 + \alpha_{0,3}\cdot 1 + \alpha_{1,1}\cdot 1 + \alpha_{2,2}\cdot 2\,,$$

with the integrals over powers $L_i^m(L_i^*)^n$ replaced by the values listed in [196]. The remaining coefficients $\alpha_{i,j}$ are exactly those for which the terms $h^{n_\mathrm{q}}\bar{h}^{n_{\bar{\mathrm{q}}}}$

fulfill $n_{\mathrm{q}} - n_{\overline{\mathrm{q}}} = 0 \mod 3$. We interpret n_{q} ($n_{\overline{\mathrm{q}}}$) as a (anti-)quark number. The on-site partition function Z_i is therefore made of various terms of hadronic contributions $(n_{\mathrm{q}}, n_{\overline{\mathrm{q}}})$, $n_{\mathrm{q}} - n_{\overline{\mathrm{q}}} = 0 \mod 3$. Remember from Section 5.3 that any spatial distribution of hadronic matter seizes to exists in the infinite-coupling limit and that we only have on-site hadronic occupations. We now conduct the replacement (6.1) of the group integration. In this case, we have

$$\begin{aligned} T_{m,n} &= \int \mathrm{d}U\, L^m (L^*)^n \\ &\longrightarrow T'_{m,n} = \frac{1}{3} \sum_{z \in Z_3} z^{m-n} = \begin{cases} 0, & m-n \neq 0 \mod 3 \\ 1, & m-n = 0 \mod 3 \end{cases} . \end{aligned}$$

The sum $T'_{m,n}$ correctly reproduces the property of $T_{m,n}$ for $m - n \neq 0 \mod 3$ but is one for all $m - n = 0 \mod 3$. $T_{m,n}$, however, is not always one because it actually counts the numbers of $\mathrm{SU}(3)$ singlets in the decomposition of $3^m \otimes \overline{3}^n$ into its irreducible representations. This is already the case for the on-site factor Z_i where the group integration gives the factor 2 for $\alpha_{2,2}$. However, Equation 6.1 gives

$$Z_i = \alpha_{0,0} + \alpha_{3,0} \cdot 1 + \alpha_{0,3} \cdot 1 + \alpha_{1,1} \cdot 1 + \alpha_{2,2} \cdot 1 \,,$$

which is wrong about the term $\alpha_{2,2} = h^2\overline{h}^2 + 4h^3\overline{h}^3 + h^4\overline{h}^4$. In summary, the replacement of the group integration by the sum over the center does not reproduce the infinite-coupling limit fully but preserves the property of only having on-site hadronic occupations.

Flux-tube model

As we have seen in Chapter 3, especially Equation (3.17) and (3.18), Lattice QCD can be formulated as a quantum-mechanical system in the transfer-matrix approach with gauge invariance implying the decomposition of the physical Hilbert space $\mathcal{H}_{\mathrm{phys}}$ into sectors $\mathcal{H}_{\{q,e\}}$ of flux-tube configurations $\{q, e\}$ which fulfill a local $\mathbb{Z}_3$-Gauss law. Now, we show that the effective spin system Z_{spin} also preserves the appearance of the $\mathbb{Z}_3$-Gauss law because Z_{spin} can be written as a sum over flux-tube configurations, i.e. Z_{spin} is equivalent to a flux-tube model Z_{flux}. The flux-tube model was originally introduced by Patel ([29]) as a simple model for describing confinement and deconfinement in QCD. Remember from Chapter 5 that we combined Patel's ([29]) and Satz's ([28]) idea to construct the notion of confinement in QCD via the percolation of flux-tube configurations.

In [90], we have described the effective spin system Z_{spin} and defined a flux-tube model Z_{flux} which is equivalent to Z_{spin}. The flux-tube model Z_{flux} is defined on the spatial lattice. The relation between flux-tube models and Z_3-spin systems has been investigated in [191, 192], where similar spin systems as in Equation (6.2) have been considered. The difference between these spin systems and the spin system (6.2) is the choice of the on-site fermionic part $Q(z_i)$. Therefore, they also consider different flux-tube models. However, the basic steps of mapping the flux-tube model to the respective spin system are the same, and we base our calculations on [191, 192]. As discussed further

below, spin systems of the form (6.2) can also be mapped onto a Z_3-Potts model with complex external field. When all these flux-tube models are essentially just a Potts model with an external field, why are we not using the flux-tube models described in [191] and [192]? As it turns out, the (anti-)quark masses, the temperature and the chemical potential of the flux-tube model constructed in [90] are identical to the constituent quark mass m_q, the temperature T and chemical potential μ of the effective spin system (6.2), i.e. we have a direct interpretation of the parameters of $h(m_\mathrm{q}, \mu, T)$ and $\overline{h}(m_\mathrm{q}, \mu, T)$ in the flux-tube model. If we were to use one of the flux-tube models in [191, 192], we could not interpret m_q, T and μ of Equation (6.2) as the corresponding parameters in the respective flux-tube model.

We describe the flux-tube model of [90]. As already mentioned, the model is defined on the spatial lattice. At every site i, we have the occupation numbers

$$n_{i,s} \in \{0, \ldots, 3\} \qquad \text{and} \qquad \overline{n}_{i,s} \in \{0, \ldots, 3\}$$

for quarks and antiquarks with spin $s \in \{\uparrow, \downarrow\}$, and, at every link $\langle i, j\rangle$, a center-electric flux $l_{\langle i,j\rangle} \in \{-1, 0, 1\}$ is defined such that $l_{\langle i,j\rangle} = -l_{\langle j,i\rangle}$. If $l_{\langle i,j\rangle} = 1$, we say that the sites i and j are connected by a flux tube from i to j. The Hamiltonian of the system is given by

$$H(\{n, l\}) = \sigma a \sum_{\langle i, i+\hat{k}\rangle} |l_{\langle i,i+\hat{k}\rangle}| + m_\mathrm{q} \sum_{i,s} \left(n_{i,s} + \overline{n}_{i,s}\right)$$

with the string tension σ, the lattice spacing a and (anti-)quark mass m_q. The flux-tube model is a static system in the sense that there is no interaction between different degrees of freedom. Every occupation number just contributes to the total energy proportionally to its value. A non-trivial center-electric flux $l_{\langle i,i+\hat{k}\rangle} \neq 0$ contributes its string energy σa to the total energy whereas every quark ($n_{i,s}$) or antiquark ($\overline{n}_{i,s}$) adds its mass m_q to the Hamiltonian H. To introduce the local $\mathbb{Z}_3$-Gauss law, we restrict the possible configurations $\{n, l\}$ to those which fulfill

$$\sum_s \left(n_{i,s} - \overline{n}_{i,s}\right) - \sum_{j\sim i} l_{\langle i,j\rangle} = 0 \mod 3 \tag{6.3}$$

at every site i. As it is the case for the flux-tube configurations $\{q, e\}$ of Chapter 3, a configuration $\{n, l\}$ is physical and denoted a flux-tube configuration if and only if it fulfills the local $\mathbb{Z}_3$-Gauss law (6.3) at every site i. Note that antiquarks are negatively counted in Equation (6.3). This is analogous to QCD and the transfer-matrix formulation, where antiquarks contribute negatively to the net-quark number $\hat{N}$ and have a negative center charge (cf. Equation (3.13)). The local net-quark number is given by

$$q_i = \sum_s \left(n_{i,s} - \overline{n}_{i,s}\right)$$

such that the total net-quark number is $q = \sum_i q_i$. The total center flux flowing out of a site i, is $\phi_i = \sum_{j\sim i} l_{\langle i,j\rangle}$. Therefore, Gauss's law reads $q_i - \phi_i =_3 0$, where we again use the short-hand notation $a =_3 b$ for $a = b \mod 3$.

The grand-canonical partition function of the flux-tube model is

$$Z_{\text{flux}} = \sum_{\{n,l\}_{\text{phys}}} \exp\Big(-\beta H(\{n,l\}) + \beta\mu q \Big)$$

with the inverse temperature $\beta = T^{-1}$, and the sum is restricted to flux-tube configurations only, i.e. configurations $\{n,l\}$ which are physical and fulfill the local $\mathbb{Z}_3$-Gauss law (6.3). To show that Z_{flux} is equivalent to Z_{spin}, we commence by writing the partition function Z_{flux} as an unrestricted sum over all possible configurations $\{n,l\}$:

$$Z_{\text{flux}} = \sum_{\{n,l\}} \exp\Big(-\beta H(\{n,l\}) + \beta\mu q \Big) \prod_i \delta_{q_i - \phi_i =_3 0}\,.$$

The product over $\delta_{q_i-\phi_i=_3 0}$ implements Gauss's law, and the transition to Z_3-spins is done by using the identity

$$\delta_{q_i-\phi_i=_3 0} = \frac{1}{3}\sum_{z\in \mathrm{Z}_3} z^{q_i-\phi_i}\,. \tag{6.4}$$

Inserting this equation into the partition function yields

$$Z_{\text{flux}} = \frac{1}{3^{N_{\text{s}}}} \sum_{\{z\}} \sum_{\{n,l\}} \exp\Big(-\beta H(\{n,l\}) + \beta\mu q \Big) \prod_i z_i^{q_i-\phi_i}\,,$$

where $\{z\}$ is a Z_3-spin configuration. To end with a spin system only, we need to explicitly compute the sum over the configurations $\{n,l\}$. This can be achieved by rearranging the terms such that the sum over $\{n,l\}$ factorizes into the product of independent sums over the on-site occupations $\{n\}$ and the center-electric fluxes $\{l\}$:

$$\begin{aligned} Z_{\text{flux}} = \frac{1}{3^{N_{\text{s}}}} \sum_{\{z\}} \Bigg[\sum_{\{l\}} \exp\Bigg(-\beta \sum_{\langle i,i+\hat{k}\rangle} \sigma a |l_{\langle i,i+\hat{k}\rangle}| \Bigg) \prod_i z_i^{-\phi_i} \Bigg] \\ \times \Bigg[\sum_{\{n\}} \exp\Bigg(\sum_{i,s} \beta(\mu - m_{\text{q}}) n_{i,s} - \sum_{i,s} \beta(m_{\text{q}} + \mu)\overline{n}_{i,s} \Bigg) \prod_i z_i^{q_i} \Bigg]\,. \end{aligned}$$

After some simple algebraic manipulations of separating the positively and negatively orientated links (i.e. whether we have a link $\langle i+\hat{k}, i\rangle$ or $\langle i, i+\hat{k}\rangle$) in each ϕ_i and rearranging the factors z_i, we get

$$\begin{aligned} &\sum_{\{l\}} \exp\Bigg(-\beta \sum_{\langle i,i+\hat{k}\rangle} \sigma a |l_{\langle i,i+\hat{k}\rangle}| \Bigg) \prod_i z_i^{-\phi_i} \\ &\quad = \sum_{\{l\}} \exp\Bigg(-\beta \sum_{\langle i,i+\hat{k}\rangle} \sigma a |l_{\langle i,i+\hat{k}\rangle}| \Bigg) \Bigg(\prod_{\langle i,i+\hat{k}\rangle} z_i^{-l_{\langle i,i+\hat{k}\rangle}} \Bigg) \Bigg(\prod_{\langle i,i+\hat{k}\rangle} z_{i+\hat{k}}^{\,l_{\langle i,i+\hat{k}\rangle}} \Bigg)\,. \end{aligned}$$

Evidently, the sum over all center fluxes $\{l\}$ factorizes into the sum over the individual variables $l_{\langle i,i+\hat{k}\rangle}$:

$$\sum_{\{l\}} \exp\left(-\beta \sum_{\langle i,i+\hat{k}\rangle} \sigma a |l_{\langle i,i+\hat{k}\rangle}|\right) \prod_i z_i^{-\phi_i} = \prod_{\langle i,i+\hat{k}\rangle} \sum_{l=-1}^{1} \mathrm{e}^{-\beta\sigma a|l|} (z_i^* z_{i+\hat{k}})^l = \prod_{\langle i,i+\hat{k}\rangle} \left(1 + 2\mathrm{e}^{-\beta\sigma a} \mathrm{Re}(z_i z_{i+\hat{k}}^*)\right) .$$

The nearest-neighbor interaction of Z_{spin} originates from the sum over the center fluxes $\{l\}$, and we identify λ of Equation (6.2) with $\lambda = \mathrm{e}^{-\beta\sigma a}$. We arrive with a similar computation, where we separate the quark $n_{i,s}$ and antiquark numbers $\overline{n}_{i,s}$ of q_i and rearrange the factors z_i, at

$$\sum_{\{n\}} \exp\left(\sum_{i,s} \beta(\mu - m_{\mathrm{q}}) n_{i,s} - \sum_{i,s} \beta(m_{\mathrm{q}} + \mu) \overline{n}_{i,s}\right) \prod_i z_i^{q_i} = \sum_{\{n\}} \left(\prod_{i,s} \mathrm{e}^{\beta(\mu - m_{\mathrm{q}}) n_{i,s}} z_i^{n_{i,s}}\right) \left(\prod_{i,s} \mathrm{e}^{-\beta(m_{\mathrm{q}} + \mu)\overline{n}_{i,s}} z_i^{-\overline{n}_{i,s}}\right) .$$

The sum over the occupation numbers $\{n\}$ factorizes into independent sums over the quark $n_{i,s}$ and antiquark numbers $\overline{n}_{i,s}$:

$$\begin{aligned}
&\sum_{\{n\}} \exp\left(\sum_{i,s} \beta(\mu - m_{\mathrm{q}}) n_{i,s} - \sum_{i,s} \beta(m_{\mathrm{q}} + \mu) \overline{n}_{i,s}\right) \prod_i z_i^{q_i} \\
&\quad = \left(\prod_{i,s} \sum_{n=0}^{3} \mathrm{e}^{\beta(\mu - m) n} z_i^n\right) \left(\prod_{i,s} \sum_{\overline{n}=0}^{3} \mathrm{e}^{-\beta(m+\mu)\overline{n}} z_i^{-\overline{n}}\right) \\
&\quad = \prod_i \left(1 + h z_i + h^2 z_i^* + h^3\right)^2 \left(1 + \overline{h} z_i^* + \overline{h}^2 z_i + \overline{h}^3\right)^2
\end{aligned}$$

which is the on-site fermionic part of Equation (6.2) with h and $\overline{h}$ as in Equation (6.1). This demonstrates that the flux-tube model Z_{flux} is equivalent to the spin system (6.2) with a one-to-one identification of the parameters m_{q}, μ and T.

Potts model

Because the nearest-neighbor spin interaction $\mathrm{Re}(z_i z_{i+\hat{k}}^*)$ occurs in Equation (6.2), we might suspect that the spin system (6.2) can actually be mapped onto a Z_3-Potts model, and, indeed, this is possible. Such a mapping for a spin system similar to (6.2) can be found in [192]. Adapting the steps in [192], the spin system (6.2) is mapped to a nearest-neighbor Potts model

$$Z_{\mathrm{spin}} = \frac{1}{3^{N_{\mathrm{s}}}} \sum_{\{z\}} \exp\left(2\gamma \sum_{\langle i,i+\hat{k}\rangle} \mathrm{Re}\left(z_i z_{i+\hat{k}}^*\right) + \eta \sum_i \mathrm{Re}\, z_i + \mathrm{i}\eta' \sum_i \mathrm{Im}\, z_i + \chi\right)$$

with a complex external field $\eta + \mathrm{i}\eta'$. In our case, the nearest-neighbor coupling γ is written as

$$\gamma = \frac{1}{3} \ln\left(\frac{1 + 2\lambda}{1 - \lambda}\right) \tag{6.5}$$

and the external field $\eta + \mathrm{i}\eta'$ and the constant shift χ are given by

$$\begin{aligned}
\eta &= \frac{2}{3}\ln(a+b+c) - \frac{1}{3}\ln\left[\left(a - \frac{1}{2}(b+c)\right)^2 + \frac{3}{4}(b-c)^2\right], \\
\eta' &= \frac{2}{\sqrt{3}}\arctan\left(\frac{\sqrt{3}(b-c)}{2a-(b+c)}\right), \\
\chi &= \frac{1}{3}\ln(a+b+c) + \frac{1}{3}\ln\left[\left(a - \frac{1}{2}(b+c)\right)^2 + \frac{3}{4}(b-c)^2\right],
\end{aligned}$$

where

$$\begin{aligned}
a = {} & 1 + 4\bar{h}^3 + \bar{h}^6 + 4\bar{h}h + 6\bar{h}^4h + 9\bar{h}^2h^2 + 6\bar{h}^5h^2 + 4h^3 + 16\bar{h}^3h^3 + 4\bar{h}^6h^3 \\
& + 6\bar{h}h^4 + 9\bar{h}^4h^4 + 6\bar{h}^2h^5 + 4\bar{h}^5h^5 + h^6 + 4\bar{h}^3h^6 + \bar{h}^6h^6 \\
b = {} & 3\bar{h}^2 + 2\bar{h}^5 + 2h + 8\bar{h}^3h + 2\bar{h}^6h + 6\bar{h}h^2 + 9\bar{h}^4h^2 + 12\bar{h}^2h^3 + 8\bar{h}^5h^3 \\
& + 3h^4 + 12\bar{h}^3h^4 + 3\bar{h}^6h^4 + 4\bar{h}h^5 + 6\bar{h}^4h^5 + 3\bar{h}^2h^6 + 2\bar{h}^5h^6
\end{aligned}$$

and

$$\begin{aligned}
c = {} & 2\bar{h} + 3\bar{h}^4 + 6\bar{h}^2h + 4\bar{h}^5h + 3h^2 + 12\bar{h}^3h^2 + 3\bar{h}^6h^2 + 8\bar{h}h^3 + 12\bar{h}^4h^3 + 9\bar{h}^2h^4 \\
& + 6\bar{h}^5h^4 + 2h^5 + 8\bar{h}^3h^5 + 2\bar{h}^6h^5 + 2\bar{h}h^6 + 3\bar{h}^4h^6
\end{aligned}.$$

The full derivation is stated in Appendix B.2. The external complex field is a consequence of the on-site fermionic part $Q(z)$ because $Q(z)$ is formulated as

$$Q(z) = \exp\left(\chi + \eta\mathrm{Re}z + \mathrm{i}\eta'\mathrm{Im}z\right).$$

6.2 Quark numbers in the flux-tube model

The state space of the flux-tube model are flux-tube configurations $\{n, l\}$. This immediately allows us to carry over the construction of fixed-quark number ensembles $Z(N_V =_3 e)$ to the flux-tube model. Consider some subvolume V of the spatial lattice, i.e. a collection of sites. The surface S^* of the volume V is $S^* = \partial V^*$ in the terminology of Section 4.2. The interface between the volume V and its complement $\overline{V}$ is $d_1 = DS^*$. Comparing with Section 4.2 and Equation (4.16), (4.18) and (4.19), we define the total net-quark number

$$q_V = \sum_{i \in V} q_i = \sum_{i \in V} \sum_s (n_{i,s} - \overline{n}_{i,s})$$

of the subvolume V, the total flux

$$\phi_{S^*} = \sum_{\langle i,j \rangle \in d_1} l_{\langle i,j \rangle}$$

through the surface S^* and relate both definitions via the $\mathbb{Z}_3$-Gauss law (6.3):

$$q_V = \phi_{S^*} \mod 3.$$

Constructing $Z(N_V =_3 e)$ in QCD, as it is done in Section 4.2, requires two essential ideas. First, the equivalence $\mathcal{H}_{q_V=_3 e} = \mathcal{H}_V(e)$ between the sector $\mathcal{H}_{q_V=_3 e}$ of fixed center charge $q_V =_3 e$ and the sector $\mathcal{H}_V(e)$ of fixed net-quark number $N_V =_3 e$. This identification together with the $\mathbb{Z}_3$-Gauss law allows to establish the equivalence of the ensemble $Z(N_V =_3 e)$ with the ensemble of fixed center-electric flux $\phi_{S^*} =_3 -e$ through the surface S^*. Second, the dynamics have to be modified at the surface S^* which is expressed in the replacement of the Hamiltonian $\hat{H}$ with a modified Hamiltonian $\hat{H}'$. The modification is important because the dynamics of QCD allow the hopping of single quarks and antiquarks between the volumes V and $\overline{V}$ or the creation or annihilation of hadronic structures intersecting the surface S^* and lying partly in both volumes. Such kind of changes have to be suppressed by the dynamics because otherwise states with $N_V \neq e \mod 3$ mix into the ensemble. The necessity of modifying the dynamics is however not present in the flux-tube model because the system is static and the above mechanisms do not exist. It is enough to restrict the partition function to the subset of fixed net-quark numbers $q_V =_3 e$. Furthermore, the identification of the net-quark number N_V and the center charge q_V is trivial in the flux-tube model because the quark and antiquark-occupation numbers are inherently part of the $\mathbb{Z}_3$-Gauss law. The net-quark number q_V of the flux-tube model assumes the same role in Gauss's law as the center charge q_V of Equation (4.19) does in full QCD.

The ensemble of fixed net-quark number $q_V =_3 e$ reads

$$Z_{\text{flux}}(q_V =_3 e) = \sum_{\substack{\{n,l\}_{\text{phys}} \\ q_V=_3 e}} \exp\Big(-\beta H(\{n,l\}) + \beta\mu q \Big),$$

where the sum is restricted to only those flux-tube configurations which fulfill $q_V =_3 e$. We replace the net-quark number q_V with the center-electric flux ϕ_{S^*} by virtue of the $\mathbb{Z}_3$-Gauss law and replace the sum over the flux-tube configurations with the sum over all possible configurations $\{n,l\}$ by explicitly inserting Gauss's law and the constraint $q_V =_3 e$ into the sum:

$$Z_{\text{flux}}(q_V =_3 e) = \sum_{\{n,l\}} \exp\Big(-\beta H(\{n,l\}) + \beta\mu q \Big) \delta_{\phi_{S^*}-e=_3 0} \prod_i \delta_{q_i-\phi_i=_3 0}\,.$$

The ensemble $Z_{\text{flux}}(q_V =_3 e)$ is mapped onto a $\mathbb{Z}_3$-spin system by using again Equation (6.4). However, we apply now the equation also to the constraint $\delta_{\phi_{S^*}-e=_3 0}$. To this end, we introduce

$$s_{\langle i,j\rangle} = \begin{cases} +1, & \langle i,j\rangle \in d_1 \\ -1, & \langle j,i\rangle \in d_1 \\ 0, & \text{otherwise} \end{cases}$$

which allows us to write ϕ_{S^*} as an unrestricted sum over all links $\langle i, i+\hat{k}\rangle$ [90]:

$$\phi_{S^*} = \sum_{\langle i,i+\hat{k}\rangle} s_{\langle i,i+\hat{k}\rangle} l_{\langle i,i+\hat{k}\rangle}\,.$$

This implies

$$\delta_{\phi_{S^*}-e=_3 0} = \frac{1}{3}\sum_z z^{\phi_{S^*}-e} = \frac{1}{3}\sum_z z^{-e} \prod_{\langle i,i+\hat{k}\rangle} z^{s_{\langle i,i+\hat{k}\rangle} l_{\langle i,i+\hat{k}\rangle}} .$$

We follow the steps of deriving Z_{spin} from Z_{flux} to map $Z_{\text{flux}}(q_V =_3 e)$ onto a $\mathbb{Z}_3$-spin system:

$$Z_{\text{flux}}(q_V =_3 e) = \frac{1}{3}\sum_{\{z\}} z^{-e} Z_{S^*}(z)$$

with

$$Z_{S^*}(z) = \frac{1}{3^{N_\text{s}}}\sum_{\{z\}}\left[\sum_{\{l\}} \mathrm{e}^{-\beta\sum_{\langle i,i+\hat{k}\rangle}\sigma a|l_{\langle i,i+\hat{k}\rangle}|}\left(\prod_{\langle i,i+\hat{k}\rangle} z^{s_{\langle i,i+\hat{k}\rangle} l_{\langle i,i+\hat{k}\rangle}}\right)\prod_i z_i^{-\phi_i}\right] \times\left[\sum_{\{n\}}\exp\left(\sum_{i,s}\beta(\mu-m_\text{q})n_{i,s} - \sum_{i,s}\beta(m_\text{q}+\mu)\overline{n}_{i,s}\right)\prod_i z_i^{q_i}\right] .$$

Again, the sums over the fluxes $\{l\}$ and the quark-occupation numbers $\{n\}$ factorize and can be computed separately. In doing so, the fermionic part is the same as in the flux-tube model Z_{flux}. The sum over the fluxes $\{l\}$ is however different due to the constraint $\phi_{S^*} - e =_3 0$ but the computation of the sum is completely analogous to Z_{flux}. We end with a nearest-neighbor interaction where the spin couplings $z_i z_j^*$ along links $\langle i,j\rangle \in d_1$ are twisted by z^{-1}:

$$Z_{S^*}(z) = \frac{1}{3^{N_\text{s}}}\sum_{\{z\}}\left[\prod_{\langle i,i+\hat{k}\rangle}\left(1+2\mathrm{e}^{-\beta\sigma a}\mathrm{Re}\left(z^{-s_{\langle i,i+\hat{k}\rangle}} z_i z^*_{i+\hat{k}}\right)\right)\right]\left[\prod_i Q(z_i)\right] . \quad (6.6)$$

Comparing with full QCD in Section 4.2, we observe the similarity between $Z_{\text{flux}}(q_V =_3 e)$ and $Z(N_V =_3 e)$. We identify $Z_{S^*}(z)$ as the twisted ensemble $Z(\{z_\tau\})$, and notice that both fixed-quark number ensembles are the result of taking the discrete Fourier transform over Z_3. However, because the flux-tube model is static, there are no layers of Euclidean time. The ensemble $Z_{\text{flux}}(q_V =_3 e)$ is conceptually simpler because only one twist z occurs instead of one twist z_τ for each layer of Euclidean time τ.

The advantage of considering the ensemble $Z_{\text{flux}}(q_V =_3 e)$ is evident. We just need to evaluate a Z_3-Potts system which makes all standard Monte-Carlo techniques (e.g. Metropolis algorithm) applicable with the methods being numerically less expensive compared to Monte-Carlo techniques used in Lattice QCD. Additionally, we do not have an exponential increase of independent twists $\{z_\tau\}$ with the number of time layers. The sum over all possible twists is independent of the model parameters and consists of only three terms. Unfortunately, as we are going to see further below, the overlap problem due to the insertion of twists at the interface d_1 and which we have explained in the introduction of this chapter still persists. It is however mild enough, and we can to a certain and limited degree compute the ensemble relative to the untwisted spin system without relying on the algorithm of [121, 122].

We present the numerical results of [90] in the following.

One-dimensional chain

The flux-tube model can be defined in any number of spatial dimensions $d \geq 1$. We consider the case $d = 1$ as a simple example. The one-dimensional lattice with periodic boundary conditions is a one-dimensional chain of length $N \in \mathbb{N}_0 \backslash \{0\}$. To study the ensemble $Z_{\text{flux}}(q_V =_3 e)$, we have to make a choice of how V is defined. We take V to divide the chain into the two halves

$$V = \left\{0, \ldots, \frac{N}{2} - 1\right\} \qquad \text{and} \qquad \overline{V} = \left\{\frac{N}{2}, \ldots, N-1\right\} :$$

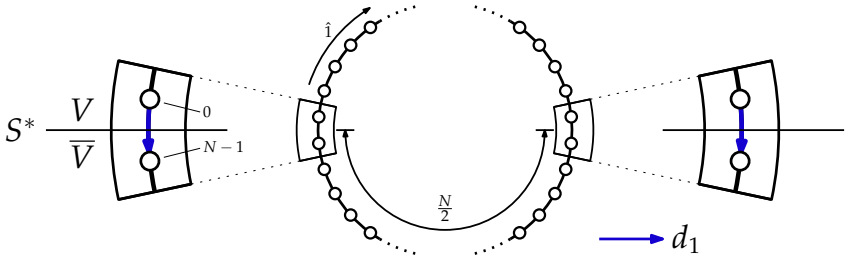

This of course requires N to be even. The one-dimensional chain allows to either evaluate the partition function $Z_{\text{flux}}(q_V =_3 e)$ analytically for sufficiently small N or to use the well-known transfer-matrix approach of one-dimensional spin systems which reformulates the partition function as a chain of matrix multiplications, see for example [197] and [198]. The latter then allows in principle to compute arbitrary large chains in polynomial time because the number of matrix multiplications scales proportional to N. However, some care must be taken because of numerical inaccuracy occurring for large chains of matrix multiplications. To use the transfer-matrix approach, we use the results of the previous section and express the on-site fermionic part as

$$Q(z) = \exp\left(\chi + \eta \text{Re}z + \text{i}\eta' \text{Im}z\right)$$

via the parameters η, η' and χ. The full transfer-matrix formulation is stated in Appendix B.3.

We first discuss the total-net quark number $\langle q \rangle$ as a function of the chemical potential μ/m_{q} for the unrestricted ensemble Z_{flux} and the fixed-quark number ensemble $Z_{\text{flux}}(q_V =_3 1)$. To this end, the parameters $\sigma a/m_{\text{q}} = 0.3$, $T/m_{\text{q}} = 0.1$ and $N = 6$ are chosen. The results are shown in Figure 6.1.

Because the temperature is a tenth of the quark mass m_{q}, we are in the low-temperature regime and can observe the formation of step-like functions. In the zero-temperature limit, only those states persist for which the energy $\Delta = H - \mu q$ is minimal ($\Delta = \Delta_{\text{min}}$) because the states of the system are weighted by the Boltzmann factor $\text{e}^{-\Delta/T}$ and any state with $\Delta > \Delta_{\text{min}}$ is suppressed relative to a state with Δ_{min}. Why do we observe plateaus of finite size? This is because the state space is discrete and, therefore, we only have a finite number of possible energies Δ_i. The parameter space $\mu/m_{\text{q}} \in \mathbb{R}$ decomposes,

$$\overline{\bigcup_{i=1}^{n} (\mu_i/m_{\text{q}}, \mu_{i+1}/m_{\text{q}})} = \mathbb{R}\,,$$

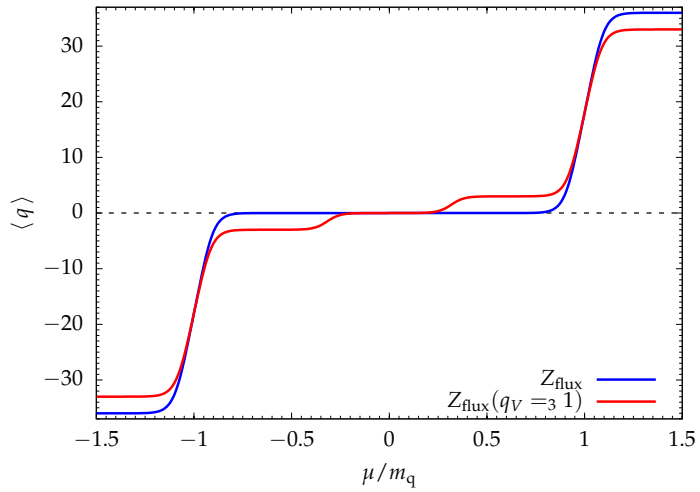

Figure 6.1: Results from [90] for the total net-quark number $\langle q \rangle$ of the ensembles Z_{flux} and $Z_{\text{flux}}(q_V =_3 1)$ with $\sigma a/m_{\text{q}} = 0.3$, $T/m_{\text{q}} = 0.1$ and $N = 6$ as a function of μ/m_{q}.[†]

into n intervals $(\mu_i/m_{\text{q}}, \mu_{i+1}/m_{\text{q}})$, $\mu_i \in [-\infty, \infty]$. On each such interval, one function Δ_i is minimal among all possible energies and therefore only states with Δ_i are observed. Changing the net-quark number q yields a different slope and energies which are consequently larger than the minimal value in the interval. Hence, the net-quark number q is constant within each of the intervals. These are the observed plateaus of Figure 6.1.

The flux-tube model Z_{flux} has three plateaus in the zero-temperature limit. The net-quark number $\langle q \rangle$ vanishes between $\mu = -m_{\text{q}}$ and $\mu = m_{\text{q}}$ because the energy $\Delta = H - \mu q$ is minimized by the empty lattice and by the empty lattice only. Any non-trivial flux-tube configuration gives larger energies. To see this, note that

$$\Delta = (m_{\text{q}} - \mu) n_{\text{q}} + (m_{\text{q}} + \mu) \overline{n}_{\text{q}} + \sigma a u \,,$$

where n_{q} ($\overline{n}_{\text{q}}$) is the total (anti-)quark number and u is the number of non-zero flux variables $l_{\langle i,j \rangle} \neq 0$. The empty lattice has $\Delta = 0$. For $\mu \geq 0$, Δ can only reach zero if $\mu \geq m_{\text{q}}$ because only then $(m_{\text{q}} - \mu) n_{\text{q}}$ becomes negative whereas all other terms remain positive, no matter how large μ is chosen. Once $\mu > m_{\text{q}}$, the state with maximally saturated quark numbers $n_{\text{q}} = 6N$, no antiquarks $\overline{n}_{\text{q}} = 0$ and no non-zero fluxes $u = 0$ minimizes Δ because then the slope of Δ is maximal and the ordinate minimal. This is exactly what is shown in Figure 6.1. Once $\mu/m_{\text{q}} > 1$, $\langle q \rangle$ jumps to the maximal saturated state with $q = 36$. The same argument holds for $\mu \leq 0$ but with the roles of n_{q} and $\overline{n}_{\text{q}}$ exchanged. The situation now changes when the net-quark number $q_V =_3 1$ is fixed. Additional plateaus occur for the intervals $\mu/m_{\text{q}} \in (1/3, 1)$ and $\mu/m_{\text{q}} \in (-1, -1/3)$. We again have a vanishing net-quark number $\langle q \rangle = 0$ in

[†]The figure is adapted from "FIG. 4" by [90] and used under CC BY 4.0 [142].

the interval $\mu/m_\mathrm{q} \in (-1/3, 1/3)$. However, compared to Z_flux, the system is not described by the empty lattice because the constraint $q_V =_3 1$ necessarily requires a non-vanishing flux through the surface S^*. The system is described by a quark-antiquark pair condensing at the surface S^* with the (anti-)quark residing in V ($\overline{V}$). Gauss's law is then maintained by a non-vanishing flux-tube variable $l_{\langle x,y\rangle} = 1$ where $\langle x, y\rangle$ is one of the interface links. All other occupation numbers and flux variables are zero.

Assume $\mu > 0$ without loss of generality. If $\mu/m_\mathrm{q} > 1/3$, a new plateau occurs because now the energy Δ is minimized not by a mesonic state ($\mathrm{q}\overline{\mathrm{q}}$) but by a baryonic state (qqq), i.e. it is energetically more preferable if the antiquark is replaced by two quarks. This is because the energy difference between both states is given by

$$\Delta(\mathrm{qqq}) - \Delta(\mathrm{q}\overline{\mathrm{q}}) = m_\mathrm{q} - 3\mu$$

such that $\Delta(\mathrm{qqq})$ becomes smaller than $\Delta(\mathrm{q}\overline{\mathrm{q}})$ once $\mu > m_\mathrm{q}/3$. If the chemical potential is increased even further, the plateau of maximal saturation occurs again for $\mu > m_\mathrm{q}$. However, remember that the flux through S^* cannot vanish due to the constraints put on the system. Therefore, the maximal saturation in this case means $q = n_\mathrm{q} = 33$ such that two quark holes in V and one quark hole in $\overline{V}$ are connected by one non-vanishing flux variable $l_{\langle x,y\rangle} = 1$ of the interface, i.e. a baryonic hole condenses at the surface S^*.

Depending on the chemical potential, we can enforce the condensation of either mesonic or baryonic states at the inferface S^* in the zero-temperature limit. In principle, we might expect this intuitive mechanism also in the full theory and $d = 3$. Note, however, that the meson or baryon can condense along the whole surface S^* in higher-spatial dimensions.

The condensation mechanism can also be illustrated by considering a longer chain and computing the local net-quark numbers $\langle q_i\rangle$. This is shown in Figure 6.2 for $N = 20$ and $\sigma a/m_\mathrm{q} = 0.3$. We can observe the condensation of a meson at the surface S^* in Figure 6.2a when the zero-temperature limit is approached. There are two choices for the meson determined by which interface link $\langle x, y\rangle \in d_1 = DS^*$ the quark-antiquark pair is connected. This is the reason for the local net-quark number approaching $\langle q_i\rangle = 0.5$ ($\langle q_i\rangle = -0.5$) at $i = 0$ and $i = 9$ ($i = 10$ and $i = 19$). When the temperature is increased, higher energetic excitations become possible and the mesonic state dissolves. Analogously, we observe the formation of a baryon in Figure 6.2b. Here the local net-quark number converges to $\langle q_i\rangle = 0.5$ ($\langle q_i\rangle = 1$) at $i = 0$ and $i = 9$ ($i = 10$ and $i = 19$). Finally, Figure 6.2c shows the condensation of a baryonic hole at the surface S^*.

Free-energy difference

We, now, consider the three dimensional case $d = 3$. We define the volumes V and $\overline{V}$ by halving the first direction with planes orthogonal to the direction as we have done for the one-dimensional chain. Hence, a site $i = (i_1, i_2, i_3) \in V$ lies in V if and only if $i_1 \in \{0, \dots N_1/2 - 1\}$.

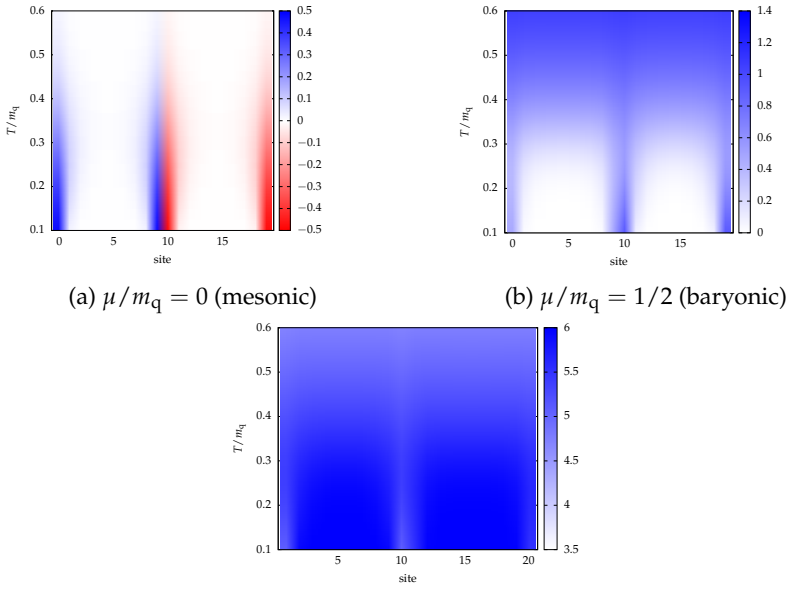

(a) $\mu/m_q = 0$ (mesonic)

(b) $\mu/m_q = 1/2$ (baryonic)

(c) $\mu/m_q = 3/2$ (saturation)

Figure 6.2: Results from [90] for the local net-quark number $\langle q_i \rangle$ in the ensemble $Z_{\text{flux}}(q_V =_3 1)$. The parameters are chosen as $N = 20$ and $\sigma a/m_q = 0.3$.[†]

Similar to the string tension σ defined in Equation (4.9), we consider the free-energy difference

$$\Delta F_\infty = \lim_{N_1 \to \infty} \left[-\frac{1}{\beta} \ln \left(\frac{Z_{\text{flux}}(q_V =_3 1)}{Z_{\text{flux}}(q_V =_3 0)} \right) \right]$$

between the ensembles $Z_{\text{flux}}(q_V =_3 1)$ and $Z_{\text{flux}}(q_V =_3 0)$. With the first direction taken to its infinite-volume limit, ΔF_∞ becomes a function of N_2 and N_3 which are identically chosen for both ensembles and, for our purposes, are assumed equal.

Because the analytic approach of the one-dimensional chain is not feasible in higher dimensions, we use ΔF_∞ to gain some insights about the three dimensional case. We consider the high- and low-temperature expansion of ΔF_∞ [90]. If $\beta > 0$ is sufficiently small (high-temperature limit), the free-energy difference ΔF at finite N_1 can be expanded as

$$\Delta F = -\frac{1}{\beta} \ln \left(\frac{M_1}{M_0} \right) + \frac{\alpha_1}{M_1} - \frac{\alpha_0}{M_0} + \mathcal{O}(\beta) \,,$$

where

$$\alpha_e = \sum_{\{n,l\}_{\text{phys}}} (H - \mu q) \delta_{\phi_{S^*} - e =_3 0}$$

and

$$M_e = Z_{\text{flux}}(q_V =_3 e, \beta = 0) \,.$$

[†]The figure is adapted from "FIG. 5" by [90] and used under CC BY 4.0 [142].

The ratio M_1/M_0 is known analytically and reads

$$\frac{M_1}{M_0} = \frac{1 + 4^{-4N_\mathrm{s}} - 2 \cdot 4^{-2N_\mathrm{s}}}{1 + 4 \cdot 4^{-4N_\mathrm{s}} + 4 \cdot 4^{-2N_\mathrm{s}}}$$

which converges to one if $N_1 \to \infty$ because then $N_\mathrm{s} \to \infty$. The other ratios can also be computed explicitly such that

$$\frac{\alpha_e}{M_e} = 2\sigma a N_\mathrm{s} + \frac{6m_\mathrm{q} N_\mathrm{s} + \mathcal{O}(N_\mathrm{s} \cdot 4^{-2N_\mathrm{s}})}{1 + \mathcal{O}(4^{-2N_\mathrm{s}})} .$$

This means that the difference between both fractions

$$\frac{\alpha_1}{M_1} - \frac{\alpha_0}{M_0} \longrightarrow 0$$

approaches zero for $N_\mathrm{s} \to \infty$. Therefore, the free-energy difference ΔF_∞ has the high-temperature expansion $\Delta F_\infty = \mathcal{O}(\beta)$ because the orders smaller than one vanish for $N_1 \to \infty$. The free-energy difference ΔF_∞ vanishes for very large temperatures. Both ensembles become identical for high temperatures. Why are we not considering the free-energy difference relative to the unrestricted ensemble Z_flux? As it turns out, the free-energy difference ΔF_∞ would then diverge in the infinite-temperature limit because the fraction $M_1/M \to 3$ with $M = Z_\mathrm{flux}(\beta = 0)$ tends to a value different to one in the limit $N_1 \to \infty$ which means that the β^{-1} term would not vanish. The derivation of the high-temperature expansion is not difficult but somehow cumbersome and therefore not mentioned in [90]. Nevertheless, we include it in Appendix B.4 for the sake of completeness.

The low-temperature expansion, i.e. $\beta \to \infty$, is given by reordering the terms of the partition functions based on their energies $\Delta = H - \mu q$. We write $\Delta_e^{(0)} < \Delta_e^{(1)} < \ldots$ for the energies of $Z_\mathrm{flux}(q_V =_3 e)$ [90]. Then the free-energy difference ΔF can be written relative to the states with energies $\Delta_e^{(0)}$:

$$\Delta F = (\Delta_1^{(0)} - \Delta_0^{(0)}) - \frac{1}{\beta} \ln \left(\frac{N_1^{(0)} + N_1^{(1)} \mathrm{e}^{-\beta(\Delta_1^{(1)} - \Delta_1^{(0)})} + \ldots}{N_0^{(0)} + N_0^{(1)} \mathrm{e}^{-\beta(\Delta_0^{(1)} - \Delta_0^{(0)})} + \ldots} \right) .$$

The factor $N_e^{(i)}$ is the multiplicity of the energy $\Delta_e^{(i)}$, i.e. the number of states with said energy. Assuming the convergence of both terms in the limit $N_1 \to \infty$, we have

$$\Delta F_\infty = \lim_{N_1 \to \infty} (\Delta_1^{(0)} - \Delta_0^{(0)}) + \mathcal{O}\left(\frac{1}{\beta}\right) .$$

We can again state the expansion explicitly up to a certain point by computing the multiplicities $N_e^{(i)}$ and energies $\Delta_e^{(i)}$. However, this a laborious combinatorical task, and was done in [90] for the one-dimensional chain up to the orders $N_e^{(1)}$ and for $d = 3$ only up to the orders $N_e^{(0)}$. Because the derivations of the multiplicities for the the one-dimensional chain are somewhat cumbersome, they are not directly mentioned in [90]. They are nevertheless listed in Appendix B.5.

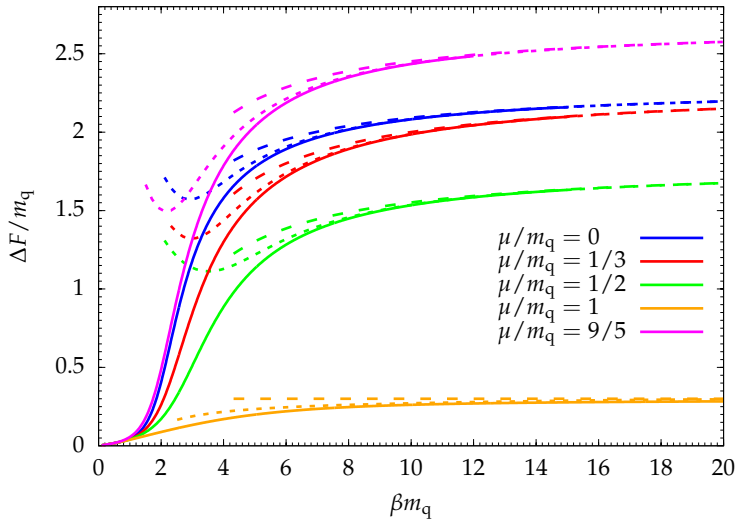

Figure 6.3: Results from [90] for the free-energy difference ΔF of a one-dimensional chain with $\sigma a/m_q = 0.3$ for various chemical potentials μ/m_q. The size of the chain is $N = 64$ which approximates the infinite-volume limit $N \to \infty$. The long-dashed line shows the low-temperature expansion including only the ground states. The short-dashed lines shows the expansion including the first excitations.[†]

We compute the free-energy difference ΔF_∞ for the one-dimensional chain by approximating $N \to \infty$ with $N = 64$. The results from [90] are shown in Figure 6.3 depending on various chemical potentials. The solid lines are the numerical results obtained via the transfer-matrix approach, whereas the dashed lines represent the low-temperature expansions. The long-dashed lines represent the expansion to the lowest order $\Delta_e^{(0)}$ and $N_e^{(0)}$ which only includes the ground states. The short-dashed lines represent the expansion up to the order $\Delta_e^{(1)}$ and $N_e^{(1)}$. The ground state expansions asymptotically approach the numerical results and continue them for $\beta m_q \to \infty$. When adding the first excitations, this behavior is obviously improved in the sense that the expansion approximates the numerical results more precisely at lower inverse temperatures βm_q and approaches the same asymptotic values in the zero-temperature limit. The numerical results suggest that the low-temperature expansion are a valid continuation of the curves for ΔF_∞ and that we can henceforth determine the asymptotic values ΔF_∞ by means of the low-temperature expansion. We have

$$\lim_{\beta\to\infty} \Delta F_\infty = \Delta_1^{(0)} - \Delta_0^{(0)} = \begin{cases} 2m_q + \sigma a, & \mu \le \frac{m_q}{3} \\ 3|m_q - \mu| + \sigma a, & \mu > \frac{m_q}{3} \end{cases}$$

for the one-dimensional chain [90]. The free-energy difference just reflects the condensation of a hadronic state at the surface S^* relative to an ensemble with no flux through S^*. For $\mu \le m_q/3$, the empty chain constitutes $\Delta_0^{(0)} = 0$.

[†]The figure is adapted from "FIG. 6" by [90] and used under CC BY 4.0 [142].

Then, we actually just have $\Delta F_\infty = \Delta_1^{(0)}$ which is given by the energy of the mesonic state condensing at S^* if $\mu < m_\mathrm{q}/3$ and the mesonic or baryonic state condensing at S^* if $\mu = m_\mathrm{q}/3$. In the plateau region $\mu/m_\mathrm{q} \in (1/3, 1)$ we still have $\Delta_0^{(0)} = 0$ and the free-energy difference is just the energy of one condensed baryonic state at S^*. Finally, ΔF_∞ is the energy to create an baryonic hole in the fully occupied chain for $\mu/m_\mathrm{q} > 1$.

Three-dimensional lattice

To numerical compute the three-dimensional lattice, we rely on a simple Metropolis algorithm for the equivalent Potts model. The twisted action of the Potts model is given by

$$S_k(\{z\}) = 2\gamma \sum_{\langle i, i+\hat{k}\rangle} \mathrm{Re}\big(u^{-k s_{\langle i,i+\hat{k}\rangle}} z_i z_{i+\hat{k}}^*\big) + \eta \sum_i \mathrm{Re}\, z_i + \mathrm{i}\eta' \sum_i \mathrm{Im}\, z_i$$

with $u = \mathrm{e}^{\frac{2\pi}{3}\mathrm{i}}$. We consider vanishing chemical potential $\mu = 0$. In this case, the action is real and $\eta' = 0$. The free energy is formulated relative to the untwisted ensembles $\langle \bullet \rangle_0$ ($k = 0$) such that ([90])

$$\Delta F = \frac{1}{\beta} \ln \left(\frac{1 - \frac{1}{2}\big(\langle \mathrm{e}^{S_1 - S_0}\rangle_0 + \langle \mathrm{e}^{S_2 - S_0}\rangle_0\big)}{1 + \langle \mathrm{e}^{S_1 - S_0}\rangle_0 + \langle \mathrm{e}^{S_2 - S_0}\rangle_0} \right).$$

The computation of the expectation value $\langle \mathrm{e}^{S_k - S_0}\rangle_0$ becomes numerically difficult in the low temperature region because of the overlap problem when inserting many non-trivial twist. Nevertheless, it is still possible to reasonably compute the free energy ΔF for certain parameters. The numerical results of [90] are shown in Figures 6.4a, 6.4b and 6.4c with the free energy computed for various values of $\sigma a/m_\mathrm{q}$.

The difference to the one-dimensional chain is mainly that ΔF depends on the area $A = N_2 N_3$. The low-temperature expansion is computed to the order $N_1^{(0)}$ and $N_0^{(0)}$ and shown as dashed lines in Figure 6.4a and 6.4b. The coefficients are given by

$$\begin{aligned} N_1^{(0)} &= 4 \cdot 2A = 8A\,, \\ N_0^{(0)} &= 1\,. \end{aligned}$$

The factor $N_1^{(0)} = 8A$ is the ground state multiplicity of $Z_\mathrm{flux}(q_V =_3 1)$ which is given by a quark-antiquark pair condensating at the surface S^* where the quark and the antiquark are connected by one flux tube only and the quark lies in V whereas the antiquark lies in $\overline{V}$. There are four different quark-occupation numbers for a quark-antiquark pair connected by the same flux tube. Furthermore each pair can be placed with its flux tube at any of the $2A$ links of the interface $d_1 = DS^*$. The free-energy difference is therefore expanded as

$$\Delta F = (\Delta_1^{(0)} - \Delta_0^{(0)}) - \frac{1}{\beta} \ln(8A)\,.$$

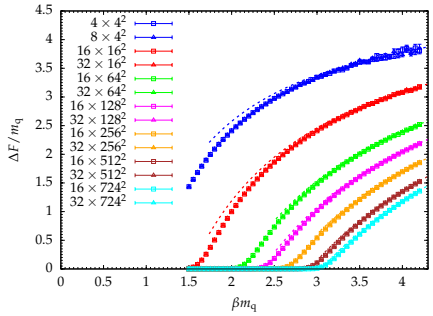

(a) $\sigma a/m_q = 3$.

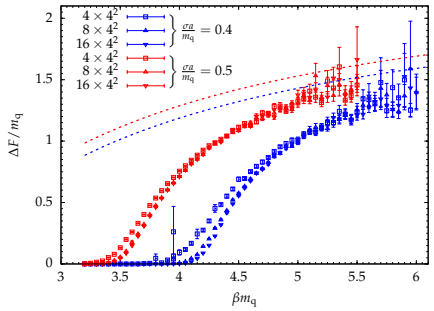

(b) ΔF for $\sigma a/m_q = 0.4$ and $\sigma a/m_q = 0.3$

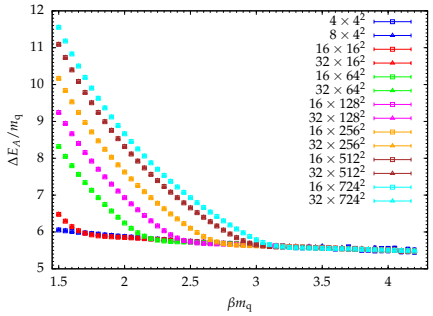

(c) ΔE_A for the results of Figure 6.4a

Figure 6.4: Numerical results of the free-energy difference ΔF and the energy ΔE_A for the three-dimensional flux-tube model. Results are taken from [90]. The dashed lines represent the low temperature expansion of ΔF including only $N_1^{(0)}$ and $N_0^{(0)}$.†

The numerical results and the expansion suggest that the free-energy difference actually vanishes for $A \to \infty$. To understand the reason behind this, recall that ΔF measure the free-energy difference between the ensembles $Z_{\text{flux}}(q_V =_3 1)$ and $Z_{\text{flux}}(q_V =_3 0)$. Both ensembles become thermodynamically equivalent. At large temperatures, this is due to the occurrence of all kinds of thermal excitations forming large spatial structures such that whether additional center charges are placed in V and $\overline{V}$ becomes insignificant relative to the background of flux-tube configurations with $q_V =_3 0$. At low temperatures, when the expansion is valid, the free-energy difference decreases because the multiplicity $8A$ of the quark-antiquark pair creates an increase in the entropic difference ΔS if we identify $\Delta F = \Delta E - \beta^{-1}\Delta S$. Only when we increase A sufficiently large, the combinatorical factors $N_e^{(i)}$ of higher order terms become significant guaranteeing $\Delta F \to 0$ for $A \to \infty$ with ΔF remaining strictly positive. This can be seen best if we remove the entropic contribution

†Figures are adapted from "FIG. 7", "FIG. 8" and "FIG. 9" by [90] and used under CC BY 4.0 [142].

of the quark-antiquark pairs from ΔF and define

$$\Delta E_A = \Delta F + \frac{1}{\beta} \ln(8A)$$

which is shown in Figure 6.4c.

The phenomena of condensating hadronic structures at low temperatures can also be noticed in the N_1-dependence of ΔF. Comparing Figure 6.4a with Figure 6.4b, we notice that ΔF does not visibly depend on N_1 for the larger string tension $\sigma a / m_{\mathrm{q}}$. However, a slight dependence can be observed for the smaller string tensions. Larger string tensions make large hadronic structures energetically more expensive. Therefore the typical diameter d of a hadronic structure forming at the surface S^* and enforcing the flux through S^* becomes smaller for increasing string tension. If $N_1 \gg d$ exceeds this typical size, the interfaces separate and become decorrelated.

6.3 Percolation in the flux-tube model

The state space of the flux-tube model is given by flux-tube configurations $\{n, l\}$ which fulfill the $\mathbb{Z}_3$-Gauss law (6.3) at every site i. Hence, completely analogous to full QCD, we can define the notion of percolation by considering whether the non-vanishing flux tubes $l_{\langle i,j \rangle} \neq 0$ form percolating structures. Adapting therefore the definition of Section 5.3, we divide the state space of the flux-tube model into the set $\mathcal{R}_1$ of flux-tube configurations which percolate in the first direction and the set $\overline{\mathcal{R}}_1$ of configurations which do not percolate in the first direction. The spanning probability R_1 reads

$$R_1 = \frac{1}{Z_{\mathrm{flux}}} \sum_{\{n,l\} \in \mathcal{R}_1} \exp\Big(- \beta H(\{n,l\}) + \beta \mu q \Big) .$$

We show that evaluating R_1 and mapping it onto its dual $\mathbb{Z}_3$-spin system gives an observable analogous to Equation (5.7) of full QCD. However, we twist the Potts couplings of the spin system instead of timelike plaquettes. But the rules of inserting the twists are similar.

The set $\mathcal{R}_1$ is determined by the spatial structure of the non-vanishing flux tubes $l_{\langle i,j \rangle} \neq 0$ and the induced bond configurations $B(\{n,l\})$. The center charge q_i at a site can be written as

$$q_i =_3 \sum_s \left(n_{i,s} - \overline{n}_{i,s} \right)$$

with $q_i \in \mathbb{Z}_3$. Therefore, we can identify a flux-tube configuration $\{n,l\}$ with a flux-tube configuration $\{q,e\}$ by setting $e_{\langle i,j \rangle} = l_{\langle i,j \rangle}$. A flux-tube configuration $\{q,e\}$ describes an equivalence class $[\{q,e\}]$ of all flux-tube configurations $\{n,l\}$ with the same center fluxes $e_{\langle i,j \rangle}$ and the same on-site center charges q_i. We use the notion of percolation as in Section 5.3 for $\{q,e\}$ and denote the set of percolating flux-tube configurations $\{q,e\}$ as $[\mathcal{R}_1]$. Hence, the set $\mathcal{R}_1$ decomposes into sectors of flux-tube configurations $\{q,e\}$:

$$\mathcal{R}_1 = \bigcup_{\{q,e\} \in [\mathcal{R}_1]} [\{q,e\}] .$$

The spanning probability R_1 reads

$$R_1 = \frac{1}{Z_{\text{flux}}} \sum_{\{q,e\}\in[\mathcal{R}_1]} \sum_{\{n,l\}\in[\{q,e\}]} \exp\Big(-\beta H(\{n,l\}) + \beta\mu q \Big)$$
$$= \frac{1}{Z_{\text{flux}}} \sum_{\{q,e\}\in[\mathcal{R}_1]} \sum_{\{n,l\}} \delta_{\{n,l\}\in[\{q,e\}]} \exp\Big(-\beta H(\{n,l\}) + \beta\mu q \Big) .$$

We can project onto an equivalence class $[\{q,e\}]$ via

$$\delta_{\{n,l\}\in[\{q,e\}]} = \frac{1}{3^{4N_s}} \sum_{\{z\}} z^{-\{q,e\}} \left[\prod_i z_i^{\sum_s (n_{i,s}-\overline{n}_{i,s})} \right] \left[\prod_{\langle i,i+\hat{k}\rangle} z_{\langle i,i+\hat{k}\rangle}^{l_{\langle i,i+\hat{k}\rangle}} \right] .$$

Using Gauss's law, we replace the sum over the on-site net-quark number by the sum over incident center fluxes:

$$\delta_{\{n,l\}\in[\{q,e\}]} = \frac{1}{3^{4N_s}} \sum_{\{z\}} z^{-\{q,e\}} \left[\prod_i z_i^{\sum_{j\sim i} l_{\langle i,j\rangle}} \right] \left[\prod_{\langle i,i+\hat{k}\rangle} z_{\langle i,i+\hat{k}\rangle}^{l_{\langle i,i+\hat{k}\rangle}} \right] .$$

The function $\delta_{\{n,l\}\in[\{q,e\}]}$ fulfills the same purpose as the projection operator $\hat{P}_{\{q,e\}}$ from Section 5.3 and is of similar structure as $\hat{P}_{\{q,e\}}$ in Equation (5.5). Replacing $\delta_{\{n,l\}\in[\{q,e\}]}$ with the above identity gives

$$R_1 = \frac{1}{3^{4N_s}} \sum_{\{q,e\}\in[\mathcal{R}_1]} \sum_{\{z\}} z^{-\{q,e\}} Z_{\text{flux}}(\{z\}) ,$$

where

$$Z_{\text{flux}}(\{z\}) = \left\langle \left[\prod_i z_i^{\sum_{j\sim i} l_{\langle i,j\rangle}} \right] \left[\prod_{\langle i,i+\hat{k}\rangle} z_{\langle i,i+\hat{k}\rangle}^{l_{\langle i,i+\hat{k}\rangle}} \right] \right\rangle .$$

Computing the expectation value and mapping it onto the $\mathbb{Z}_3$-Potts system follows the same steps as in deriving $Z_{\text{flux}}(q_V =_3 e)$ in Section 6.2. However, we do not twist the Potts couplings at an interface d_1 but at every link $\langle i,j\rangle$ based on the twist configuration $\{z\}$:

$$Z_{\text{flux}}(\{z\}) = \frac{Z_{\text{flux}}^{-1}}{3^{N_s}} \sum_{\{u\}} \left[\prod_{\langle i,i+\hat{k}\rangle} \Big(1 + 2\mathrm{e}^{-\beta\sigma a} \mathrm{Re}\big(z(\{z\}) \cdot u_i u_{i+\hat{k}}^* \big) \Big) \right] \left[\prod_i Q(u_i) \right] .$$

Here $z(\{z\}) \in \mathrm{Z}_3$ imposes the twists based on the twist configuration $\{z\}$. There are three rules: (i) An on-site spin z_i twists all couplings $u_j u_{j+\hat{k}}^*$ with links $\langle j, j+\hat{k}\rangle$ incident to the site i. If such an link points away from (into) the site i, the coupling is twisted with z_i^{-1} (z_i). (ii) A coupling $u_i u_{i+\hat{k}}^*$ is twisted with the spin $z_{\langle i,i+\hat{k}\rangle}^{-1}$. (iii) If a coupling $u_i u_{i+\hat{k}}^*$ is to be twisted by multiple applications of the rules (i) and (ii), the total twist is the product of the separate twists. Clearly, these are the same rules that we derived in Section 5.2 for QCD but adapted to the $\mathbb{Z}_3$-Potts model. We arrive at the same result as in QCD. To determine the spanning probability R_1, we can just sum over all possible twisted ensembles $Z_{\text{flux}}(\{z\})$ and percolating flux-tube configurations $\{q,e\}$.

Unfortunately, the direct evaluation of $Z_{\text{flux}}(\{z\})$ is still not practical. The simplicity of the flux-tube model, however, opens the possibility to determine the spanning probability by directly probing the flux-tube configurations. To this end, we just need to generate flux-tube configurations $\{n, l\}$ with the Boltzmann weight $\mathrm{e}^{-\beta H(\{n,l\})+\beta\mu q}$.

Worm algorithm

Fortunately, there is already an algorithm which allows to sample the state space of the flux-tube model according to the Boltzman weight. The worm algorithm generates configurations by updating the degrees of freedom with a simple Metropolis step but does so along paths of flux tubes which are either closed or terminate at sites where the quark-occupation numbers have been changed [199–203]. This is because updating a quark occupation or a flux tube by a Metropolis step will break Gauss's law in general. The algorithm updates variables till the initial violation of Gauss's law is fixed. Here, we base our implementation on the algorithm described in [200–203]. We adapt the algorithm accordingly and use a modification of the proof shown in [204] to guarantee detailed balance and ergodicity. Our implementation of the worm algorithm is stated in Appendix B.6. The spanning probability R_1 is then determined by counting the numbers N_1 of flux-tube configurations $\{n, l\}$ percolating in the first direction and divide N_1 by the total number of generated configurations:

$$R_1 \approx \frac{N_1}{N} .$$

In the following, we do not consider the spanning probability R_1. We use the probability R of observing a flux-tube configuration which percolates in at least one direction.

Fully-dynamic connectivity problem

We face the problem to test whether a flux-tube configuration $\{n, l\}$ percolates. In its core this reduces to the problem of determining the connection of two sites via a path of set bonds in the induced bond configuration $B(\{n, l\})$. The bond configuration is just a graph of edges and vertices. The edges are the set bonds and the vertices are the sites. To test whether a configuration percolates in a direction $\hat{k}$, we have to determine whether there exists a path of set bonds along which all planes orthogonal to the direction $\hat{k}$ are connected. However, the situation is complicated by the fact that the induced bond configuration changes in general when the flux-tube configuration is updated. This means that the connectivity information of the graph potentially changes with every update step. We need to maintain the connectivity information between vertices every time an edge is added or removed from the graph. This problem is known as the fully-dynamic connectivity problem. Efficient solutions to this problem exist and we choose to adapt the algorithm described in [205]. We denote a solution to the problem as a FDC-algorithm. The idea of the algorithm is described in Appendix B.7. Notably, in a another setting of identifying

clusters in a Potts model, the algorithm was employed by [206] which is our initial incentive to also use it for the flux-tube model.

Assume some flux-tube configuration $\{n, l\}$ and its induced bond configuration $\{b\} = B(\{n, l\})$. The FDC-algorithm is used to also maintain the cluster decomposition of $\{b\}$. We test whether a cluster of $\{b\}$ percolates in a given direction $\hat{k}$. We start with a plane orthogonal to $\hat{k}$ and sweep over all sites of the plane. For each site, we check whether it is part of the cluster and if so whether it is incident with a bond in positive k-direction connecting the plane with its nearest-neighbor plane. If we do not find a site which is part of the cluster and incident with a bond in positive k-direction, we must conclude that the cluster is not percolating in that direction. If we find a site with these properties, we jump to the next plane in the positive k-direction and conduct the same test again. If and only if bonds of the cluster exist between every pair of subsequent planes, the cluster is percolating in the k-direction. A bond configuration is therefore percolating in the direction $\hat{k}$ if there exists at least one cluster which percolates. To determine the spanning probability R, we test whether a flux-tube configuration $\{n, l\}$ is percolating in at least one direction.

Spanning probability

We consider the flux-tube model parametrized by the parameters $\beta\sigma a$ and $\sigma a / m_{\mathrm{q}}$ at vanishing chemical potential $\mu = 0$. For fixed $\beta\sigma a$, this accounts to changing the quark mass m_{q}. We vary the inverse temperature $\beta\sigma a$ at fixed $\sigma a / m_{\mathrm{q}}$. The infinite-mass case is then reached at $\sigma a / m_{\mathrm{q}} = 0$. This set up allows us to explore the phase diagram of the flux-tube model and compare it to the conjectured behavior of the Columbia plot from Section 5.2, however, only with one quark mass. We are going to see that the flux-tube model seems to be a simple model which exhibits exactly the behavior conjectured for QCD. The quark mass acts inversely to the external field of the dual $\mathbb{Z}_3$-Potts model. The percolation transition coincides with the thermal first-order transition at infinite quark masses persisting till the second-order critical endpoint of the three dimensional $\mathbb{Z}_3$-Potts model is reached. For even lighter masses, when the free-energy density of the $\mathbb{Z}_3$-Potts model becomes analytical and the transition is smoothed to a crossover, the percolation transition of the flux-tube model still persists marking a confined and deconfined phase.

Here, we consider four cases: $\sigma a / m_{\mathrm{q}} = 0$, $\sigma a / m_{\mathrm{q}} = 3/4$, $\sigma a / m_{\mathrm{q}} = 6$ and $\sigma a / m_{\mathrm{q}} \to \infty$. Before we dive into the numerical results, we shortly discuss the phase diagram of the $\mathbb{Z}_3$-Potts model with real external field $\eta \geq 0$. We are concerned with this case because the mapping between the flux-tube model parameters and the parameters of the Potts model gives a vanishing imaginary field $\eta' = 0$ if $\mu = 0$.

When $\eta = 0$, the $\mathbb{Z}_3$-Potts model undergoes a first-order transition breaking the $\mathbb{Z}_3$-symmetry spontaneously at the critical point $2\gamma_{\mathrm{c}} = 0.36708(2)$ [71]. The inverse of Equation (6.5) then gives the parameter $(\beta\sigma a)_{\mathrm{Potts}}$ in the flux-tube model. The first-order transition persists for non-vanishing external fields $\eta < \eta_{\mathrm{c}}$ with the critical line $(2\gamma_{\mathrm{c}}(\eta), \eta)$ ending in the critical endpoint $(2\gamma_{\mathrm{c}}, \eta_c)_{\mathrm{Ising}}$ [207]. The endpoint lies in three-dimensional Ising universality class and is

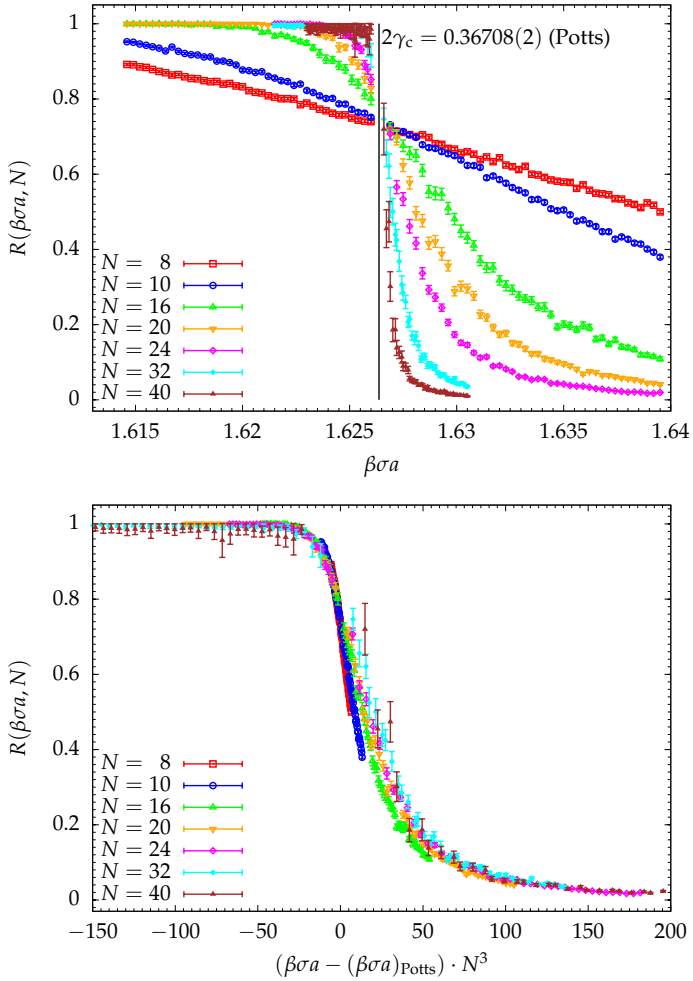

Figure 6.5: Top, the spanning probability $R(\beta\sigma a, N)$ for $\sigma a / m_q = 0$ as a function of $\beta\sigma a$. Bottom, the same results but scaled according to the critical point $(\beta\sigma a)_{\text{Potts}}$ and the critical exponent $\nu^{-1} = 3$.

given by $(2\gamma_c, \eta_c)_{\text{Ising}} = (0.366253(13), 0.0005167(67))$ [207]. For any $\eta > \eta_c$ the transition vanishes, and the Potts model only exhibits a crossover behavior.

In general, if we assume the first-order behavior to be the consequence of a renormalization fix point in the sense of Nienhuis and Nauenberg [208], we expect a volume dependence of the finite-size scaling law for the singular part f_s of the free-energy density near the critical point:

$$f_s(T, N) = N^{-d} \Phi\left(A \cdot (T - T_c) N^{\frac{1}{\nu}} \right)$$

with the spatial dimension $d = 3$, the critical temperature T_c, a universal function Φ, the non-universal metric factor A and the critical exponent $\nu^{-1} = 3$. Such a volume dependence is numerically observed for the $\mathbb{Z}_3$-Potts model

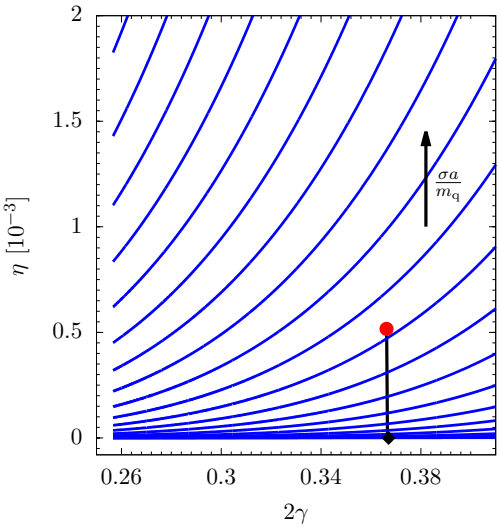

Figure 6.6: Map between the flux-tube parameters $(\beta\sigma a, \sigma a/m_q)$ and the Potts parameters $(2\gamma, \eta)$. Curves of constant $\sigma a/m_q$ depending on $\beta\sigma a$ are shown. The curves are traversed from the right to left for increasing $\beta\sigma a$. The square dot is the critical point ([71]) of the first-order transition at $\eta = 0$. The red point is the Ising critical end point [207]. The linear curve is the approximation to the first-order line with the slope as reported in [207].

[71, 209–211]. We do not further the discussion about the reason of the volume dependence because only its existence is relevant for us.

Let us start with the numerical results for $\sigma a/m_q = 0$. The spanning probability $R(\beta\sigma a, N)$ is shown in Figure 6.5 for various lattice extents N of the three dimensional system. Numerically, $\sigma a/m_q = 0$ is reached by just setting the quark mass to a very large value and starting the simulation with all occupation numbers set to zero. It practically becomes nearly impossible that a quark or antiquark is added to the system. In Figure 6.5 (top), we observe the formation of a step-like function if the lattice sizes are increased. The formation of a step function in the limit $N \to \infty$ is what we expect in the presence of a percolation transition. In the same figure, the black vertical line indicates the critical point $2\gamma_c$ of the Potts model at zero external field mapped to the corresponding parameter $(\beta\sigma a)_{\text{Potts}}$ in the flux-tube model. The step function seems to form at the vertical line which indicates that a percolation transition takes place at $(\beta\sigma a)_{\text{Potts}}$. Additionally, we also expect the universality class of the percolation transition not to be given anymore by bond percolation but by the volume dependence characteristical for the first-order transition. This is confirmed in Figure 6.5 (bottom) where the spanning probability R is shown as a function of $(\beta\sigma a - (\beta\sigma a)_{\text{Potts}}) \cdot N^3$. The curves approximately collapse on a common curve which is expected if the spanning probability is to be described by a scaling behavior

$$R(\beta\sigma a, N) = \Phi\left(A \cdot (\beta\sigma a - (\beta\sigma a)_{\text{Potts}}) N^{\frac{1}{\nu}}\right)$$

with $\nu = 1/3$, the universal function Φ, which differs from the function Φ further above, and a non-universal metric factor A if N is sufficiently large. The numerical results therefore suggest that the flux-tube model indeed exhibits a percolation transition at infinite quark masses which coincides with the critical point and universal behavior of the first-order transition of the $\mathbb{Z}_3$-Potts model.

For our further considerations, we map horizontal lines in the $(\beta\sigma a, \sigma a/m_\mathrm{q})$-parameter plane of the flux-tube model onto the corresponding curves on the parameter plane $(2\gamma, \eta)$ of the Potts model. The mapping is shown in Figure 6.6. The blue curves are the mapped horizontal lines. They are traversed from right to left for increasing $\beta\sigma a$. Additionally, we include an approximation of the first-order line of the Potts model based on the results of [71] and [207]. An important implication of this mapping is that the curves do not intersect the first-order line of the Potts model once $\sigma a/m_\mathrm{q}$ is sufficiently large. In other words, we are guaranteed not to hit any singular behavior of the Potts model. In this case, our conjecture implies the percolation transition to still persists along the horizontal lines in the $(\beta\sigma a, \sigma a/m_\mathrm{q})$ plane but, because there is no other non-analytic behavior due to the free-energy density, the transition lies in the universality class of bond percolation.

The first-order line is not intersected for $\sigma a/m_\mathrm{q} = 3/4$, and we show the results for $\sigma a/m_\mathrm{q} = 3/4$ in Figure 6.7. The top figure again shows the formation of a step function for increasing lattice extents N. However, the formation is not as prominent as for $\sigma a/m_\mathrm{q} = 0$. To confirm the existence of the percolation transition further and its universality class, we scale the results according the critical exponent $\nu^{-1} = 1.1410(15)$ ([151]) of bond percolation in three dimensions. The only problem we face is fixing the critical transition point $(\beta\sigma a)_\mathrm{c}$. We just tune $(\beta\sigma a)_\mathrm{c}$ without any specific systematics such that the scaled functions tend to lie on one curve for large N. We found $(\beta\sigma a)_\mathrm{c} \approx 1.776$ with the scaled functions as shown in the bottom figure. Indeed, the curves tend to collapse onto one common curve for increasing lattice extents N. The results are consistent with the existence of a percolation transition lying in the universality class of standard bond percolation in three dimensions.

Next, we consider the limit $\sigma a/m_\mathrm{q} \to \infty$. This case is reached by setting the quark mass to zero when running the worm algorithm. The results are shown in Figure 6.8. Additionally, the left figure includes interpolated numerical results for standard bond percolation in three dimensions shown as solid lines. The probability p of setting a bond is mapped to $\beta\sigma a$ via Equation (6.7). We see that the flux-tube results match the standard bond percolation results within the stated errors. It is important to keep in mind that our flux-tube model does not exactly reduce to standard bond percolation at zero quark masses. The Boltzmann weights for the quarks and antiquarks drop out of the partition function when $m_\mathrm{q} = 0$. However, the quarks and antiquarks are still relevant for the $\mathbb{Z}_3$-Gauss law. The partition function is then given by

$$Z_\mathrm{flux} = \sum_{\{l\}} \mathcal{N}(\{l\})(1 + 2\mathrm{e}^{-\beta\sigma a})^{3N_\mathrm{s}} \,,$$

where $\mathcal{N}(\{l\})$ is the number of all flux-tube configurations $\{n, l\}$ with the same configuration $\{l\}$ of flux variables. Only if $\mathcal{N}(\{l\}) = \mathcal{N}(\{l'\})$ for all

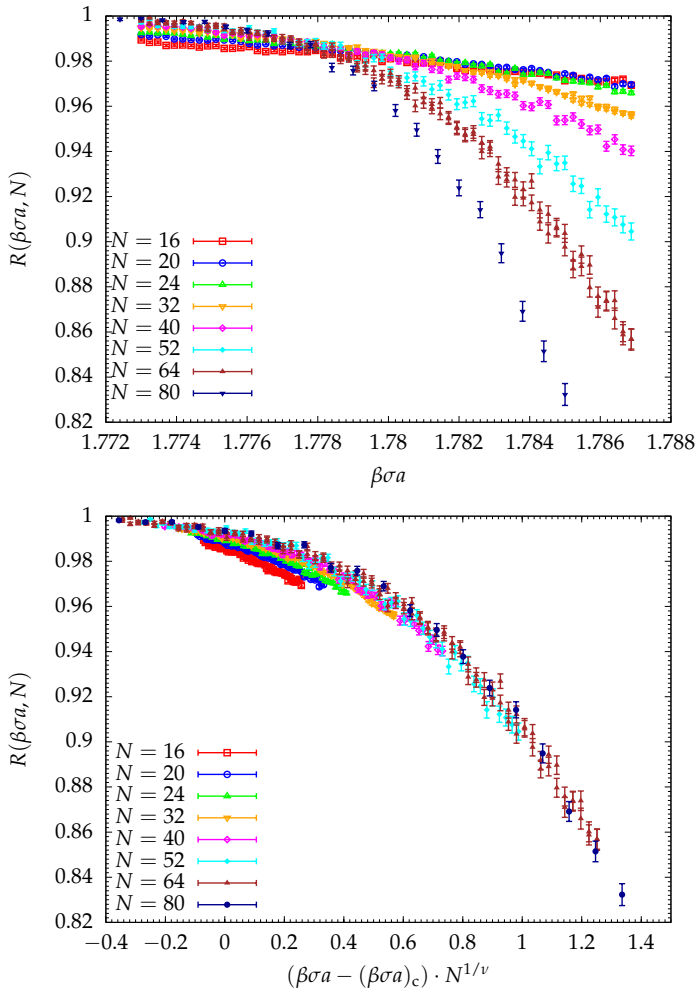

Figure 6.7: Top, the spanning probability $R(\beta\sigma a, N)$ for $\sigma a / m_q = 3/4$ as a function of $\beta\sigma a$. Bottom, the same results but scaled according to the critical exponent $\nu^{-1} = 1.1410(15)$ ([151]) and the estimated critical point $(\beta\sigma a)_c \approx 1.776$.

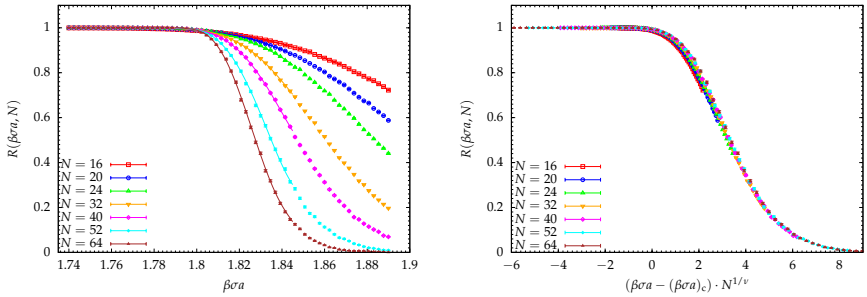

Figure 6.8: Left, the spanning probability $R(\beta\sigma a, N)$ for $\sigma a/m_q \to \infty$ as a function of $\beta\sigma a$. Right, the same results but scaled according to the critical exponent $\nu^{-1} = 1.1410(15)$ ([151]) and the critical point $(\beta\sigma a)_c \approx 1.7981$ determined by mapping the critical probability $p_c = 0.24881182(10)$ ([151]) for bond percolation onto $(\beta\sigma a)_c$ via the inverse of Equation (6.7). The solid lines are interpolated results of standard bond percolation in three dimensions.

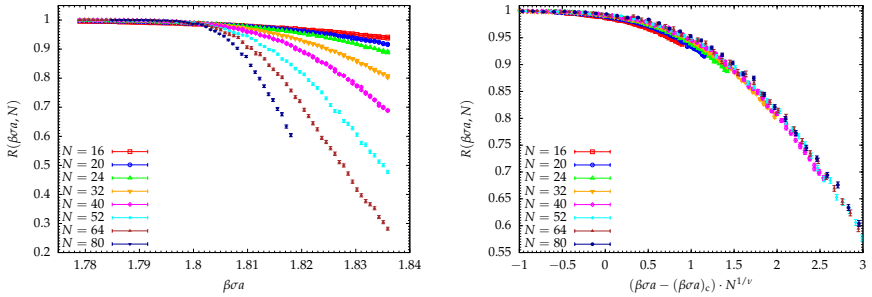

Figure 6.9: Left, the spanning probability $R(\beta\sigma a, N)$ for $\sigma a/m_q = 6$ as a function of $\beta\sigma a$. Right, the same results but scaled according to the critical exponent $\nu^{-1} = 1.1410(15)$ ([151]) and the critical point $(\beta\sigma a)_c \approx 1.7981$ determined by mapping the critical probability $p_c = 0.24881182(10)$ ([151]) for bond percolation onto $(\beta\sigma a)_c$ via the inverse of Equation (6.7).

$\{l\}$ and $\{l'\}$, the partition function reduces to the case of bond variables set independently with the probability

$$p(b_{\langle i,j\rangle} = 1) = \frac{2e^{-\beta\sigma a}}{1 + 2e^{-\beta\sigma a}}\,. \tag{6.7}$$

Gauss's law dictates the required net-quark number modulo three at a specific site i for a fixed configuration $\{l\}$. If q_i has to equal $0 \mod 3$, there are 86 possibilities to do so by choosing the on-site occupation numbers. There are 85 possibilities for the cases $q_i = 1, 2 \mod 3$ respectively. This difference in the number of combinations prevents the partition function to decompose into the case of standard bond percolation because $\mathcal{N}(\{l\}) \neq \mathcal{N}(\{l'\})$ in general. Nevertheless, the numerical results of the flux-tube model match within the stated errors with the numerical results of standard bond percolation. This does not allow us to distinguish whether the flux-tube model reproduces exactly the standard bond percolation case in the infinite-volume limit or

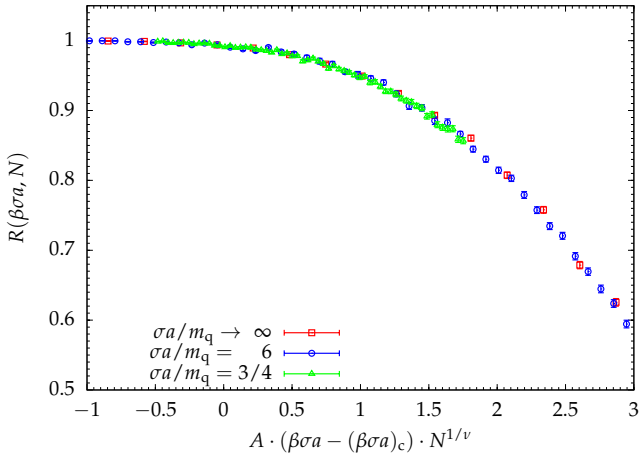

Figure 6.10: $R(\beta\sigma a, N)$ as a function of $A \cdot (\beta\sigma a - (\beta\sigma a)_c)N^{1/\nu}$. The data points are taken from the $N = 64$ curves of Fig. 6.7, 6.8 and 6.9. The factor is $A = 1$ for the zero-mass case and $\sigma a/m = 6$ and $A = 1.4$ for $\sigma a/m = 3/4$.

the results only match approximately with the deviations not recognizable within the given uncertainties. Figure 6.8 (right) shows the scaled results according to the critical exponent ν^{-1} of bond percolation in three dimensions and $(\beta\sigma a)_c \approx 1.7981$ determined by the inverse of Equation (6.7) applied to the percolation threshold $p_c = 0.24881182(10)$ ([151]). As expected, the curves visibly collapse on a common curve for large N.

The case $\sigma a/m_q = 6$ is shown in Figure 6.9. It still approximate the zero-mass case because the curves coincide with the curves of Figure 6.8 within the stated errors. Hence, the right plot represents the scaling with the same critical values as for the zero-mass case. The curves collapse on each other for large N.

The concept of the non-universal metric factors gives another possibility to test whether above cases $\sigma a/m_q = 3/4$, $\sigma a/m_q = 6$ and $\sigma a/m_q \to \infty$ are described by the same universality class [184]. If we consider the spanning probabilities as a function of $A \cdot (\beta\sigma a - (\beta\sigma a)_c)N^{1/\nu}$ with the respective critical values $(\beta\sigma a)_c$ and some constant $A \in \mathbb{R}$, and we set $A = 1$ for $\sigma a/m \to \infty$ then we should be able to collapse the functions for the different $\sigma a/m$ onto one function by choosing the values of A appropriately. This is demonstrated in Fig. 6.10. We exclusively use the $N = 64$ results from Fig. 6.7, 6.9 and 6.8. We have chosen $A = 1$ for $\sigma a/m = 6$ and $A = 1.4$ for $\sigma a/m = 3/4$. All curves seem to collapse onto each other. The important result is the non-trivial factor $A = 1.4$ for $\sigma a/m = 3/4$ which demonstrates further that this case belongs into the same universality class as the other cases despite $\sigma a/m = 3/4$ not approximating the zero-mass case at all.

We have to make a final remark. Certain data points were created with a version of the worm algorithm which was not implemented entirely as it was intended. This has essentially implemented a worm algorithm for which the adapted proof of [204] is not directly applicable. To be more precise we are specifically talking about the results for $N = 80$ of Figure 6.7, $N = 52$, $N = 64$

and $N = 80$ of Figure 6.9. All other results were computed with the correct implementation for which the proof holds. By comparing, the results of the correct implementation with the incorrect implementation for smaller lattices, we were not able to observe any deviations outside the stated errors. Therefore, a possible breaking of the Markov chain properties does not seem to be severe and therefore we accept the results of the incorrect implementation. The reader might verify this by himself. We have included the comparisons in the figures. For Fig. 6.7, we have included the data points by the incorrect implementation for $N = 32$ and $N = 64$. For Fig. 6.9, we included the data points by the incorrect implementation for $N = 16, 20, 24, 32, 40$.

The Ising critical point has also been investigated but unfortunately the results were not conclusive and plagued with the occurrence of random data points lying significantly away from the curves. It is unclear why these difficulties occur and we suspect some ergodicity problem at the Ising critical endpoint. This has to be investigated further.

In summary, the flux-tube model is shown to undergo a percolation transition in the universality class of the first-order Potts transition at infinite quark masses. Furthermore, the percolation transition persist in the crossover region where the free-energy density is analytical. The universality class then reduces to standard bond percolation. This complements the picture drawn by Patel [29, 190, 212] and can be seen as a proof of concept that flux-tube configurations can give rise to sharp transitions even at light quark masses. This allows an unambiguous definition of confinement and deconfinement at all parameters. We are unaware of any direct investigation of the percolation properties for $\mathbb{Z}_3$ flux-tube models at low quark masses, i.e. the crossover region of the equivalent Potts model, in existing literature. For example [213] mention the possibility of a percolation transition at light quark masses but does not show any further investigation or evidence of it. Contrary, even Patel only describes the smoothing of the percolation transition towards light quark masses despite the fact that he noticed that his flux-tube model reduces to pure bond percolation at zero quark masses [190]. In [191] it is argued against a percolation transition at low quark masses.

Chapter 7

Conclusion

As we have described in the introduction, we have presented two main results in this thesis: the construction of a fixed quark-number ensemble $Z(N_V = e \mod 3)$ which fixes the net-quark number to values $N_V = e \mod 3$ in a spatial subvolume V and the notion of confinement based on the percolation of center-electric fluxes. We have utilized the transfer-matrix formulation describing Lattice QCD with Wilson fermions as a quantum-mechanical system on the spatial lattice. The quantum-mechanical description has the advantage of giving an intuitive understanding of what is meant with the net-quark number in a subvolume V and naturally gives rise to the decomposition of the physical state space into sectors of flux-tube configurations. We have leveraged the properties of the asymmetric transfer operator and the local Z_3-Gauss law to restrict the path integrals to only twisting timelike plaquettes with center elements $z \in Z_3$, analogous to the case of 't Hooft's center-electric flux ensembles. The fermionic action remains unchanged. Furthermore, our formulations are inherently gauge-invariant. Especially, the spanning probability which distinguishes the percolating and non-percolating phase, can be formulated as a gauge-invariant observable on the lattice. We have shown, under rather mild assumptions, that a percolation transition indeed gives rise to the confinement-deconfinement transition at infinite quark masses. This transition can in principle survive at physical quark masses because percolation does not rely on a singular behavior of the free-energy density. Our main conjecture is then that QCD at the physical point and vanishing chemical potential exhibits a genuine transition which is not based on the non-analytic behavior of the free-energy density but rather on the percolation of center-electric fluxes. The percolation transition is in the same universality class as bond percolation in three spatial dimensions. Such a transition would allow the unambiguous distinction between a confined phase below and a deconfined phase above the critical temperature T_c. If such a transition exists, it would of course be also interesting to know where T_c lies relative to the crossover transition of QCD.

The picture drawn above remains, except for the pure gauge case, speculative because, unfortunately, as we have discussed in Chapter 6, both of our main results, as they stand, are highly impractical to compute on the lattice. We had to resort to the simple flux-tube model which is motivated by the strong-coupling and heavy-quark limit of QCD. The flux-tube model is dual

to a Z_3-Potts model and shares with QCD the decomposition of its state space into flux-tube configurations which fulfill a local Z_3-Gauss law. The spanning probability can also be formulated in the spin system and gives an observable of similar form as in Lattice QCD. Instead of twisting timelike plaquettes, we have to twist the couplings between Potts spins. Therefore, the flux-tube model serves as a very simple system reduced to the bare features necessary for discussing our notion of confinement numerically. Indeed we have seen, that the percolation transition coincides with the first-order transition of the equivalent Z_3-Potts model and seems to also share its volume scaling $\nu^{-1} = 3$. At low quark masses, we have seen that the percolation transition persists and lies in the universality class of bond percolation. The results indicate a Kertész line in the sense of Satz ([28]) for the flux-tube model and demonstrate that the percolation of center-electric flux structures can indeed give rise to the notion of confinement as conjectured for QCD.

Further, in favor of our conjecture, we like to point to a recent study of the percolation of center vortices presented in [170] published right before the finishing of this thesis. Their numerical studies indicate a loss of percolation for the center vortices at roughly two times ($T \approx 2T_c$) the crossover temperature T_c of the chiral transition, i.e. the finding suggest that full QCD has a second transition at larger temperatures representing a deconfinement transition. Of course, it would be interesting to know, if the center-electric fluxes exhibit a phase transition in full QCD, whether the percolation transition then coincides with the percolation of center vortices.

Appendix A

Supplementary considerations for Chapter 5

A.1 Reflection invariance of center-electric fluxes

We show that the probability

$$r_{\vec{w}} = \frac{Z_{\text{el.}}(\vec{w})}{Z} = \frac{1}{Z}\,\text{tr}\left(\hat{P}(S^*_{23}, w_1)\hat{P}(S^*_{13}, w_2)\hat{P}(S^*_{12}, w_3)\mathrm{e}^{-\beta\hat{H}}\hat{P}_0\right)$$

is invariant under changes of signs in the components of $\vec{w}$:

$$r_{(w_1,w_2,w_3)} = r_{(w_1',w_2',w_3')} \tag{A.1}$$

with $w_k' = (-1)^{n_k} w_k$ and $n_k \in \mathbb{N}_0$. Only the vanishing or non-vanishing of a center flux w_k is relevant. Physically, a change of the sign in front of a component w_k is the result of mirroring the system at the coordinate plane orthogonal to the direction $\vec{k}$. Changing the sign of a component in $\vec{w}$ yields a change of the flux direction but not its length. The number of different directions due to changes in signs depends on how many components of $\vec{w}$ are non-zero. If k components are non-zero, then there are 2^k directions. The three possible cases with non-zero flux $\vec{w}$ are shown in Figure A.1. The arrows indicate the possible directions if one of the arrows is the actual $\vec{w}$. We see that any two directions can be mapped onto each other by consecutive reflections at coordinate planes. To prove Equation (A.1) and without loss of generality, it

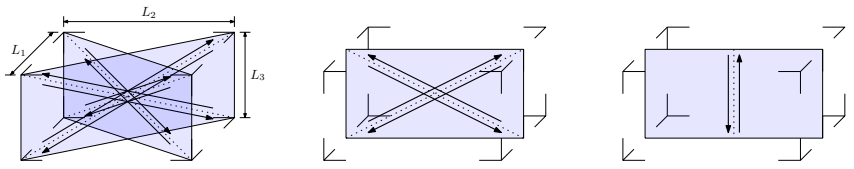

(a) all w_i are non-zero (b) two w_i are non-zero (c) only one w_i is non-zero

Figure A.1: Illustration of all possible directions which are a result of changing the signs of the components of a center flux $\vec{w}$.

is enough to show

$$r_{(w_1,w_2,w_3)} = r_{(-w_1,w_2,w_3)} \tag{A.2}$$

because the proof is the same for the other components.

We first consider the path integral formulation of $r_{(w_1,w_2,w_3)}$ and discretize Euclidean time such that

$$r_{(w_1,w_2,w_3)} = \lim_{N_4\to\infty} \frac{1}{Z} \operatorname{tr}\left(\hat{P}(S_{23}^*, w_1)\hat{P}(S_{13}^*, w_2)\hat{P}(S_{12}^*, w_3)\left(\hat{T}_{a_4=\beta/N_4}\right)^{N_4}\hat{P}_0\right),$$

where the asymmetric or symmetric transfer operator from Chapter 3 is used. Remember that we are concerned with the pure gauge theory, where dynamical fermions are absent. Therefore, the choice of the transfer operator does not matter. The path integral formulation of $r_{(w_1,w_2,w_3)}$ is given by the path integral of Z and $Z_{\text{el.}}(\vec{w})$. The former has been derived in Chapter 3 and the latter has been derived in Section 4.1. The ensemble Z is just the usual path integral with the Wilson plaquette action, and the ensemble $Z_{\text{el.}}(\vec{w})$ is given by the discrete Fourier transform over the temporally twisted ensembles $Z(\vec{k})$ as stated in Equation (4.8):

$$Z_{\text{el.}}(\vec{w}) = \frac{1}{3^3}\sum_{\vec{k}\in\mathbb{Z}_3^3} \exp\left(-\frac{2\pi\mathrm{i}}{3}\,\vec{w}\cdot\vec{k}\right) Z(\vec{k})\,.$$

We show Equation A.1 for the path integral formulation. Equation (A.1) is then obtained by taking the continuum limit in the direction of Euclidean time.

We define the reflection operator

$$\Theta x = \Theta(x_1, x_2, x_3, x_4) = (-x_1, x_2, x_3, x_4)$$

which is similar to the usual time reflection operator (see for example [48]) but applied to the spatial direction. Taking a negative coordinate is to be interpreted on the spatial torus. We count the sites relative to the origin in negative direction with respect to the periodic boundary conditions, e.g.

$$\Theta(1, x_2, x_3, x_4) = (-1, x_2, x_3, x_4) = (N_1 - 1, x_2, x_3, x_4)\,.$$

We apply the transformation to the path integral such that the gauge variables are transformed according to

$$U_{\langle x,y\rangle} \longrightarrow U_{\langle \Theta x, \Theta y\rangle}\,,$$

and we write $\Theta U = \{\ldots, U_{\langle \Theta x, \Theta(x+\hat{k})\rangle}, \ldots\}$. For all links which do not point in the first direction, this accounts to permuting them along the first direction with each other. Therefore, plaquettes which do not have any links pointing in the first direction are mapped onto other plaquettes of the same kind. Gauge variables in the first direction are mapped to gauge variables pointing into the opposite direction. Hence, plaquettes containing links pointing in the first direction are mapped onto plaquettes of the same kind but with opposite orientation. This is illustrated in Figure A.2 for spatial plaquettes.

The total transformation is just a permutation of gauge variables, where we take the adjoint for some of the gauge variables. Permuting the variables

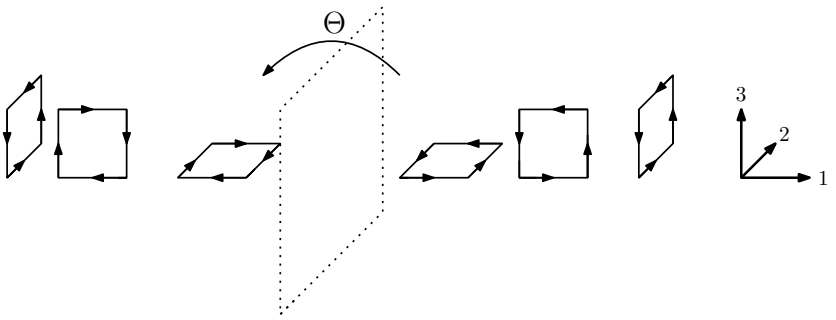

Figure A.2: Spatial plaquettes under the reflection operator Θ. Plaquettes with links in the first direction change their orientation.

is essentially just a renaming of the integration variables, and the Haar measure is invariant under the substitution $U_{\langle x,y\rangle} \to U^\dagger_{\langle x,y\rangle}$. Substituting a gauge configuration U with ΘU does not change the partition function:

$$Z(\vec{k}) = \int \mathcal{D}U \, \mathrm{e}^{S_\mathrm{G}(\vec{k},\Theta U)} \,,$$

where $S_\mathrm{G}(\vec{k}, U)$ is the action twisting the timelike plaquettes between the zeroth and first layer according to the Dirac sheets S^*_{mn}, i.e. the plaquettes are twisted by $z_s = \mathrm{e}^{\frac{2\pi}{3}\mathrm{i}k_s}$ if they intersect the zeroth layer at the interface links $d^{(s)}_1 = DS^*_{nm}$ of the sheet. The reflection operator Θ maps in a one-to-one fashion a plaquette $\partial p_{x,\mu\nu}$ onto a plaquette $\partial p_{x',\mu\nu}$ and changes the orientation of all plaquettes which have spatial links pointing in the first direction. Therefore, all terms of the form $\mathrm{ReTr}(U_{\partial p_{x,\mu\nu}})$ in $S_\mathrm{G}(\vec{k}, U)$ are replaced with $\mathrm{ReTr}(U_{\partial p_{x',\mu\nu}})$:

$$\mathrm{ReTr}(U_{\partial p_{x,\mu\nu}}) \longrightarrow \mathrm{ReTr}(U_{\partial p_{x',\mu\nu}})$$

because the orientation of the plaquette does not matter when the trace is taken. However, if a twist is involved and the orientation is changed, we have the replacement

$$\mathrm{ReTr}(zU_{\partial p_{x,\mu\nu}}) \longrightarrow \mathrm{ReTr}(z^\dagger U_{\partial p_{x',\mu\nu}})$$

This replacement only applies to the timelike links involved in the twists of the Dirac sheet S^*_{23} because only $d^{(1)}_1$ consists of links pointing in the first direction. Therefore, our substitution gives us the replacement

$$S_\mathrm{G}((k_1,k_2,k_3),\Theta U) \longrightarrow S_\mathrm{G}((-k_1,k_2,k_3),U)$$

and

$$Z(k_1,k_2,k_3) = Z(-k_1,k_2,k_3)\,.$$

We remark that the operator Θ shifts the twist to different positions. However, the exact positions of the twists are insignificant for the path integral which justifies the above replacement of the action.

Inserting this result into the computation of $Z_{\mathrm{el.}}(\vec{w})$, we get

$$Z_{\mathrm{el.}}(\vec{w}) = \frac{1}{3^3} \sum_{\vec{k}\in\mathbb{Z}_3^3} \exp\left(-\frac{2\pi\mathrm{i}}{3}\,\vec{w}\cdot(k_1,k_2,k_3)\right) Z(-k_1,k_2,k_3)$$

and

$$Z_{\text{el.}}(\vec{w}) = \frac{1}{3^3} \sum_{\vec{k}\in\mathbb{Z}_3^3} \exp\left(-\frac{2\pi \mathrm{i}}{3}\, \vec{w}\cdot(-k_1,k_2,k_3)\right) Z(k_1,k_2,k_3)$$

after the substitution $k_1 \to -k_1$. We end with the desired result:

$$Z_{\text{el.}}(w_1,w_2,w_3) = Z_{\text{el.}}(-w_1,w_2,w_3)\,.$$

A.2 Infinite-coupling limit for Wilson fermions

In Section 5.3 of Chapter 5, we based the intuitive understanding of quarks and antiquarks being maximally tightly bound on writing the infinite-coupling path integral (5.8) as a sum over hadronic degrees of freedom only. To this end, we cited multiple references [183, 187–189] (and references therein) in which the infinite-coupling limit is explicitly computed as a sum over hadronic degrees of freedom. However, the results are based on staggered fermions. We use Wilson fermions, and, therefore, the purpose of this appendix is to show that the same interpretation holds in the case of Wilson fermions. We cannot duplicate the computations of [188] for the case of Wilson fermions due to the complication of having Dirac indices additional to the color indices. Nevertheless, we adapt the considerations in [108] and use the dualized path integral from Section 4.2 to write the infinite-coupling limit as sums over products of integrals of the form ([214])

$$I = \int \mathrm{d}U\, U_{a_1b_1}\dots U_{a_nb_n} U^\dagger_{\bar{a}_1\bar{b}_1}\dots U^\dagger_{\bar{a}_{\overline{n}}\bar{b}_{\overline{n}}}$$

Then, similar to [188] but more general, the computation of the integral I is done based on the considerations of [214] which gives us the constraint $n-\overline{n}=0 \mod 3$ for non-vanishing $I\neq 0$. This immediately implies that the local quark and antiquark numbers n_x and $\overline{n}_x$ from Section 4.2 indeed fulfill $n_x-\overline{n}_x = 0 \mod 3$. The net-quark number at all spacetime points must be a multiple of three. All spacetime points have hadronic occupations only.

Dualized path integral at infinite-coupling

Consider the dualization of the Lattice QCD partition function from Section 4.2 which is given by Equation (4.27):

$$Z = \sum_{\{k\}} W(\{k\}) \exp\left(a_4\mu \sum_x (n_x-\overline{n}_x)\right) \int \mathcal{D}\overline{\psi}\mathcal{D}\psi\big[\dots\big]_{\{k\}}$$

with the configuration $\{k\}$ of fermionic dual variables. The integration over gauge variables is included in the weight

$$W(\{k\}) = \int \mathcal{D}U\, \mathrm{e}^{S_{\mathrm{G}}(U)} \prod_{x,\mu,a,b,\alpha,\beta} \Big(\kappa\cdot(1-\gamma_\mu)_{\alpha\beta}(U_{\langle x,x+\hat{\mu}\rangle})_{ab}\Big)^{k^{(a,\alpha)(b,\beta)}_{x,x+\hat{\mu}}} \times \Big(\kappa\cdot(1+\gamma_\mu)_{\alpha\beta}(U^\dagger_{\langle x,x+\hat{\mu}\rangle})_{ab}\Big)^{k^{(a,\alpha),(b,\beta)}_{x+\hat{\mu},x}}\,.$$

The gauge action vanishes in the infinite-coupling limit, and we have

$$\lim_{g_0\to\infty} W(\{k\}) = \prod_{x,\mu}\Bigg[\prod_{a,b,\alpha,\beta}\Big(\kappa\cdot(1-\gamma_\mu)_{\alpha\beta}\Big)^{k^{(a,\alpha)(b,\beta)}_{x,x+\hat{\mu}}}\Big(\kappa\cdot(1+\gamma_\mu)_{\alpha\beta}\Big)^{k^{(a,\alpha),(b,\beta)}_{x+\hat{\mu},x}}\Bigg]$$
$$\times\Bigg[\int \mathrm{d}U_{\langle x,x+\hat{\mu}\rangle}\prod_{a,b,\alpha,\beta}(U_{\langle x,x+\hat{\mu}\rangle})^{k^{(a,\alpha)(b,\beta)}_{x,x+\hat{\mu}}}_{ab}(U^\dagger_{\langle x,x+\hat{\mu}\rangle})^{k^{(a,\alpha),(b,\beta)}_{x+\hat{\mu},x}}_{ab}\Bigg]$$

Therefore, the weight $W(\{k\})$ is a product of integrals of the form I in the infinite-coupling limit. An integral of the kind I has the property $n-\overline{n}=0 \mod 3$ if I is non-vanishing. This is explicitly shown further below. The weight $\lim_{g_0\to\infty} W(\{k\})$ can only be non-vanishing if

$$\sum_{\omega,\omega'}\Big[k^{\omega\omega'}_{x,x+\hat{\mu}}-k^{\omega\omega'}_{x+\hat{\mu},x}\Big]=0 \mod 3$$

for all links $\langle x,x+\hat{\mu}\rangle$. This especially applies to timelike links such that

$$n_x-\overline{n}_x=\sum_{\omega,\omega'}\Big[k^{\omega\omega'}_{x,x+\hat{4}}-k^{\omega\omega'}_{x+\hat{4},x}\Big]=0 \mod 3$$

because

$$n_x=\sum_{\omega,\omega'}k^{\omega\omega'}_{x,x+\hat{4}} \qquad \text{and} \qquad \overline{n}_x=\sum_{\omega,\omega'}k^{\omega\omega'}_{x+\hat{4},x}\,.$$

by definition. This is the desired result. We only have hadronic occupations at all spacetime points.

To explicitly see that $n-\overline{n}=0 \mod 3$ is a necessity for $I\neq 0$, we consider the general rules of computing I as worked out in [214], where the condition $n-\overline{n}=0 \mod 3$ is essentially also mentioned. The integral I can be written as a sum over derivatives at $J=0$ of the functional ([214])

$$F(J)=\int \mathcal{D}U\,\exp\Big(\mathrm{tr}(J\cdot U)\Big)=\sum_{k=0}^{\infty}a_k(\det J)^k \tag{A.3}$$

where $J\in\mathbb{C}^{n\times n}$ and $a_k\in\mathbb{R}$. To be more specific, we have the derivative

$$U_{a_i,b_i}\longrightarrow\frac{\partial}{\partial J_{a_ib_i}}$$

for each U_{a_i,b_i} and the derivative

$$U^\dagger_{\bar{a}_i,\bar{b}_i}\longrightarrow\frac{1}{2}\sum_{p,p',q,q'}\varepsilon_{\bar{a}_i,p,p'}\varepsilon_{\bar{b}_i,q,q'}\frac{\partial}{\partial J_{pq}}\frac{\partial}{\partial J_{p'q'}}$$

for each $U^\dagger_{\bar{a}_i,\bar{b}_i}$ such that

$$I=\Bigg(\Bigg[\prod_{i=1}^{n}\frac{\partial}{\partial J_{a_ib_i}}\Bigg]\Bigg[\prod_{i=1}^{\overline{n}}\Bigg(\frac{1}{2}\sum_{p,p',q,q'}\varepsilon_{\bar{a}_i,p,p'}\varepsilon_{\bar{b}_i,q,q'}\frac{\partial}{\partial J_{pq}}\frac{\partial}{\partial J_{p'q'}}\Bigg)\Bigg]F(J)\Bigg)_{J=0}\,.$$

Appendix A. Supplementary considerations for Chapter 5

The determinant $\det J$ is

$$\det J = \frac{1}{3!} \sum_{i_1,i_2,i_3} \sum_{j_1,j_2,j_3} \varepsilon_{i_1,i_2,i_3} \varepsilon_{j_1,j_2,j_3} J_{i_1 j_1} J_{i_2 j_2} J_{i_3 j_3} \,.$$

The integral I can only be non-vanishing if the derivatives applied to the right-hand side of Equation (A.3) yield a non-zero expression which does not depend on J. This can only be achieved if the number of derivatives involved in the computation of I is a multiple of three because otherwise there are always one or two derivatives which are applied to some $\det J$ such that two or one matrix element J_{ij} remains. We need three derivatives for each $\det J$ to fully transform every $J_{i_k j_k}$ to a Kronecker delta such that $\det J$ becomes a function independent of J. Every factor $U^\dagger_{\bar{a}_i \bar{b}_i}$ contributes two derivatives whereas every U_{a_i,b_i} contributes one derivative to the computation of I. Hence, the total number of derivatives involved is $n + 2\overline{n}$, and I can only be non-vanishing if $n + 2\overline{n} = 0 \mod 3$. This condition is, however, equivalent to $n - \overline{n} = 0 \mod 3$.

Appendix B

Supplementary considerations for Chapter 6

B.1 Power expansion of $Q(L)$

The expansion of $Q(L)$ in powers of $L^m L^n$ is given by

$$
\begin{aligned}
&Q(L) = \\
&\left(1 + 2h^3 + h^6 + 2\overline{h}^3 + 4h^3\overline{h}^3 + 2h^6\overline{h}^3 + h^6 + 2h^3\overline{h}^6 + h^6\overline{h}^6\right) \\
&+\Big(2h + 2h^4 + 2\overline{h}^2 + 4h^3\overline{h}^2 + 2h^6\overline{h}^2 \\
&\qquad + 4h\overline{h}^3 + 4h^4\overline{h}^3 + 2\overline{h}^5 + 4h^3\overline{h}^5 + 2h^6\overline{h}^5 + 2h\overline{h}^6 + 2h^4\overline{h}^6\Big)L \\
&+\left(h^2 + 4h\overline{h}^2 + 4h^4\overline{h}^2 + 2h^2\overline{h}^3 + \overline{h}^4 + 2h^3\overline{h}^4 + h^6\overline{h}^4 + 4h\overline{h}^5 + 4h^4\overline{h}^5 + h^2\overline{h}^6\right)L^2 \\
&+\left(2h^2\overline{h}^2 + 2h\overline{h}^4 + 2h^4\overline{h}^4 + 2h^2\overline{h}^5\right)L^3 + h^2\overline{h}^4L^4 \\
&+\Big(2h^2 + 2h^5 + 2\overline{h} + 4h^3\overline{h} + 2h^6\overline{h} \\
&\qquad + 4h^2\overline{h}^3 + 4h^5\overline{h}^3 + 2\overline{h}^4 + 4h^3\overline{h}^4 + 2h^6\overline{h}^4 + 2h^2\overline{h}^6 + 2h^5\overline{h}^6\Big)L^* \\
&+\left(h^4 + 4h^2\overline{h} + 4h^5\overline{h} + \overline{h}^2 + 2h^3\overline{h}^2 + h^6\overline{h}^2 + 2h^4\overline{h}^3 + 4h^2\overline{h}^4 + 4h^5\overline{h}^4 + h^4\overline{h}^6\right)(L^*)^2 \\
&+\left(2h^4\overline{h} + 2h^2\overline{h}^2 + 2h^5\overline{h}^2 + 2h^4\overline{h}^4\right)(L^*)^3 + h^4\overline{h}^2(L^*)^4 \\
&+\Big(2h^3 + 4h\overline{h} + 4h^4\overline{h} + 4h^2\overline{h}^2 + 4h^5\overline{h}^2 \\
&\qquad + 2\overline{h}^3 + 8h^3\overline{h}^3 + 2h^6\overline{h}^3 + 4h\overline{h}^4 + 4h^4\overline{h}^4 + 4h^2\overline{h}^5 + 4h^5\overline{h}^5 + 2h^3\overline{h}^6\Big)LL^* \\
&+\left(2h^2\overline{h} + 4h^3\overline{h}^2 + 4h\overline{h}^3 + 4h^4\overline{h}^3 + 4h^2\overline{h}^4 + 2h^5\overline{h}^4 + 4h^3\overline{h}^5\right)L^2L^* \\
&+\left(2h^2\overline{h}^3 + 2h^3\overline{h}^4\right)L^3L^* \\
&+\left(4h^3\overline{h} + 2h\overline{h}^2 + 4h^4\overline{h}^2 + 4h^2\overline{h}^3 + 4h^5\overline{h}^3 + 4h^3\overline{h}^4 + 2h^4\overline{h}^5\right)L(L^*)^2 \\
&+\left(h^2\overline{h}^2 + 4h^3\overline{h}^3 + h^4\overline{h}^4\right)L^2(L^*)^2 \\
&+\left(2h^3 + 2h^4\overline{h}^3\right)L(L^*)^3
\end{aligned}
$$

B.2 Equivalence between Equation (6.2) and the Z_3-Potts model

We derive the mapping from Equation (6.2) to a $\mathbb{Z}_3$-Potts model based on the mapping described in [192]. First, we determine the coupling parameter γ such that

$$1 + 2\lambda \mathrm{Re}(z_i z_{i+\hat{k}}^*) = \mathrm{e}^{2\gamma \mathrm{Re}(z_i z_{i+\hat{k}}^*)}$$

Because $z_i z_{i+\hat{k}}^* \in \mathrm{Z}_3$, we actually have the equations

$$1 + 2\lambda \mathrm{Re}\, z = \mathrm{e}^{2\gamma \mathrm{Re}\, z}$$

for all $z \in \mathrm{Z}_3$. The real part $\mathrm{Re}\, z$ of z can only assume the values $\mathrm{Re}\, z \in \{-\frac{1}{2}, 1\}$. Therefore, we have two equations

$$\begin{aligned} 1 + 2\lambda &= \mathrm{e}^{2\gamma}\,, \\ 1 - \lambda &= \mathrm{e}^{-\gamma}\,. \end{aligned}$$

Dividing the first equation with the second equation, we get

$$\frac{1 + 2\lambda}{1 - \lambda} = \mathrm{e}^{3\gamma}$$

which implies

$$\gamma = \frac{1}{3} \ln \left(\frac{1 + 2\lambda}{1 - \lambda} \right).$$

The on-site fermionic part $Q(z)$ is mapped to the complex external field $\eta + \mathrm{i}\eta'$ and χ by solving the equations

$$Q(z) = \left(1 + hz + h^2 z^* + h^3\right)^2 \left(1 + \overline{h} z^* + \overline{h}^2 z + \overline{h}^3\right)^2 = \exp\left(\chi + \eta \mathrm{Re} z + \mathrm{i}\eta' \mathrm{Im} z\right).$$

for all $z \in \mathrm{Z}_3$. First, we expand $Q(z)$ and sort the terms such that

$$Q(z) = a + bz + cz^*\,,$$

where

$$\begin{aligned} a = {} & 1 + 4\overline{h}^3 + \overline{h}^6 + 4\overline{h}h + 6\overline{h}^4 h + 9\overline{h}^2 h^2 + 6\overline{h}^5 h^2 + 4h^3 + 16\overline{h}^3 h^3 + 4\overline{h}^6 h^3 \\ & + 6\overline{h}h^4 + 9\overline{h}^4 h^4 + 6\overline{h}^2 h^5 + 4\overline{h}^5 h^5 + h^6 + 4\overline{h}^3 h^6 + \overline{h}^6 h^6 \\ b = {} & 3\overline{h}^2 + 2\overline{h}^5 + 2h + 8\overline{h}^3 h + 2\overline{h}^6 h + 6\overline{h}h^2 + 9\overline{h}^4 h^2 + 12\overline{h}^2 h^3 + 8\overline{h}^5 h^3 \\ & + 3h^4 + 12\overline{h}^3 h^4 + 3\overline{h}^6 h^4 + 4\overline{h}h^5 + 6\overline{h}^4 h^5 + 3\overline{h}^2 h^6 + 2\overline{h}^5 h^6 \end{aligned}$$

and

$$\begin{aligned} c = {} & 2\overline{h} + 3\overline{h}^4 + 6\overline{h}^2 h + 4\overline{h}^5 h + 3h^2 + 12\overline{h}^3 h^2 + 3\overline{h}^6 h^2 + 8\overline{h}h^3 + 12\overline{h}^4 h^3 + 9\overline{h}^2 h^4 \\ & + 6\overline{h}^5 h^4 + 2h^5 + 8\overline{h}^3 h^5 + 2\overline{h}^6 h^5 + 2\overline{h}h^6 + 3\overline{h}^4 h^6 \end{aligned}.$$

Hence, we have to solve the equations

$$a + bz + cz^* = \exp\left(\chi + \eta \mathrm{Re} z + \mathrm{i}\eta' \mathrm{Im} z\right)$$

for all $z \in Z_3$. Because $z \in \left\{1, -\frac{1}{2} + \mathrm{i}\frac{\sqrt{3}}{2}, -\frac{1}{2} - \mathrm{i}\frac{\sqrt{3}}{2}\right\}$, we have

$$\begin{aligned} a + b + c &= \mathrm{e}^{\chi+\eta} \\ a - \frac{1}{2}(b+c) + \mathrm{i}\frac{\sqrt{3}}{2}(b-c) &= \mathrm{e}^{\chi - \frac{1}{2}\eta + \mathrm{i}\frac{\sqrt{3}}{2}\eta'} \\ a - \frac{1}{2}(b+c) - \mathrm{i}\frac{\sqrt{3}}{2}(b-c) &= \mathrm{e}^{\chi - \frac{1}{2}\eta - \mathrm{i}\frac{\sqrt{3}}{2}\eta'} \end{aligned}$$

The first equation implies $\chi + \eta = \ln(a+b+c)$. Multiplying the second and third equation, we get

$$\left(a - \frac{1}{2}(b+c)\right)^2 + \frac{3}{4}(b-c)^2 = \mathrm{e}^{2\chi-\eta}$$

which implies

$$\ln\left[\left(a - \frac{1}{2}(b+c)\right)^2 + \frac{3}{4}(b-c)^2\right] = 2\chi - \eta\,.$$

Therefore, we have

$$\begin{aligned} \chi &= \frac{1}{3}\ln\left[a+b+c\right] + \frac{1}{3}\ln\left[\left(a - \frac{1}{2}(b+c)\right)^2 + \frac{3}{4}(b-c)^2\right] \\ \eta &= \frac{2}{3}\ln\left[a+b+c\right] - \frac{1}{3}\ln\left[\left(a - \frac{1}{2}(b+c)\right)^2 + \frac{3}{4}(b-c)^2\right] \end{aligned}$$

Finally, dividing the second equation by the third equation gives

$$\frac{a - \frac{1}{2}(b+c) + \mathrm{i}\frac{\sqrt{3}}{2}(b-c)}{a - \frac{1}{2}(b+c) - \mathrm{i}\frac{\sqrt{3}}{2}(b-c)} = \mathrm{e}^{\mathrm{i}\sqrt{3}\eta'}\,.$$

This implies

$$\eta' = \frac{2}{\sqrt{3}}\arctan\left(\frac{\sqrt{3}(b-c)}{2a-(b+c)}\right)\,.$$

B.3 Transfer-matrix formulation for one-dimensional chains

We describe the transfer-matrix formulation of $Z_{S^*}(z)$ for the one-dimensional chain. The twisted ensemble of Equation (6.6) is written as

$$Z_{S^*}(z) = \frac{1}{3^{N_\mathrm{s}}}\sum_{\{z\}}\left[\prod_{\langle i,i+1\rangle}\left(1 + 2\mathrm{e}^{-\beta\sigma a}\mathrm{Re}\left(z^{-s_{\langle i,i+1\rangle}} z_i z_{i+1}^*\right)\right)\right] \times \left[\prod_i \mathrm{e}^{\eta\mathrm{Re}\,z_i + \mathrm{i}\eta'\mathrm{Im}\,z_i + \chi}\right]\,.$$

On the one-dimensional chain of length N, the fermionic part is equivalent to

$$\begin{aligned} &\prod_i \mathrm{e}^{\eta\mathrm{Re}\,z_i + \mathrm{i}\eta'\mathrm{Im}\,z_i + \chi} \\ &\quad = \mathrm{e}^{N\chi}\prod_i \exp\left(\frac{\eta}{2}[\mathrm{Re}\,z_i + \mathrm{Re}\,z_{i+1}] + \mathrm{i}\frac{\eta'}{2}[\mathrm{Im}\,z_i + \mathrm{Im}\,z_{i+1}]\right)\,. \end{aligned}$$

Therefore, because the system is one-dimensional, we can write

$$Z_{S^*}(z) = \frac{\mathrm{e}^{N\chi}}{3^{N_\mathrm{s}}} \sum_{\{z\}} \prod_{i=0}^{N-1} \left(1 + 2\mathrm{e}^{-\beta\sigma a} \mathrm{Re}\left(z^{-s_{\langle i,i+1\rangle}} z_i z_{i+1}^*\right)\right) \\ \times \exp\left(\frac{\eta}{2}[\mathrm{Re}\, z_i + \mathrm{Re}\, z_{i+1}] + \mathrm{i}\frac{\eta'}{2}[\mathrm{Im}\, z_i + \mathrm{Im}\, z_{i+1}]\right)$$

This gives

$$Z_{S^*}(z) = \frac{\mathrm{e}^{N\chi}}{3^{N_\mathrm{s}}} \sum_{\{z\}} \prod_{i=0}^{N-1} F(z_i, z_{i+1})$$

with

$$F(z_i, z_{i+1}) = \left(1 + 2\mathrm{e}^{-\beta\sigma a} \mathrm{Re}\left(z^{-s_{\langle i,i+1\rangle}} z_i z_{i+1}^*\right)\right) \\ \times \exp\left(\frac{\eta}{2}[\mathrm{Re}\, z_i + \mathrm{Re}\, z_{i+1}] + \mathrm{i}\frac{\eta'}{2}[\mathrm{Im}\, z_i + \mathrm{Im}\, z_{i+1}]\right).$$

A specific variable z_{i+1} only occurs in the i-th factor $F(z_i, z_{i+1})$ and in the $(i+1)$-th factor $F(z_{i+1}, z_{i+2})$. Therefore, we have

$$Z_{S^*}(z) = \frac{\mathrm{e}^{N\chi}}{3^{N_\mathrm{s}}} \sum_{\{z'\}_1} \left(\sum_{z_1} F(z_0, z_1) F(z_1, z_2)\right) \prod_{i=2}^{N-1} F(z_i, z_{i+1}),$$

where $\{z'\}_1$ excludes the spin z_1. If we have

$$Z_{S^*}(z) = \frac{\mathrm{e}^{N\chi}}{3^{N_\mathrm{s}}} \sum_{\{z'\}_n} I_n(z_0, z_{n+1}) \prod_{i=n+1}^{N-1} F(z_i, z_{i+1})$$

where $\{z'\}_n$ now excludes all spins $z_1, \ldots, z_n$ and

$$I_n(z_0, z_{n+1}) = \sum_{z_n} I_{n-1}(z_0, z_n) F(z_n, z_{n+1})$$

with

$$I_1(z_0, z_2) = \sum_{z_1} F(z_0, z_1) F(z_1, z_2),$$

we get the next step

$$Z_{S^*}(z) = \frac{\mathrm{e}^{N\chi}}{3^{N_\mathrm{s}}} \sum_{\{z'\}_{n+1}} \underbrace{\left(\sum_{z_{n+1}} I_n(z_0, z_{n+1}) F(z_{n+1}, z_{n+2})\right)}_{=I_{n+1}(z_0, z_{n+2})} \prod_{i=n+2}^{N-1} F(z_i, z_{i+1}) \\ = \frac{\mathrm{e}^{N\chi}}{3^{N_\mathrm{s}}} \sum_{\{z'\}_{n+1}} I_{n+1}(z_0, z_{n+2}) \prod_{i=n+2}^{N-1} F(z_i, z_{i+1}).$$

Therefore, the partition function can be formulated over the recursively defined function $I_{N-1}(z_0, z_0)$:

$$Z_{S^*}(z) = \frac{\mathrm{e}^{N\chi}}{3^{N_\mathrm{s}}} \sum_{z_0} I_{N-1}(z_0, z_0).$$

Defining the matrices

$$M_{kl}(z,i) = \left(1 + 2\mathrm{e}^{-\beta\sigma a}\mathrm{Re}\left(z^{-s_{\langle i,i+1\rangle}}u^k u^{-l}\right)\right) \times \exp\left(\frac{\eta}{2}[\mathrm{Re}\,u^k + \mathrm{Re}\,u^l] + \mathrm{i}\frac{\eta'}{2}[\mathrm{Im}\,u^k + \mathrm{Im}\,u^l]\right)$$

with $k,l \in \{0,1,2\}$ and $u = \mathrm{e}^{\frac{2\pi}{3}\mathrm{i}}$ gives

$$I_1(z_0,z_2) = \sum_r M_{kr}(z,0)M_{rl}(z,1) = (M(z,0)M(z,1))_{kl}\,,$$

where $z_0 = u^k$ and $z_2 = u^l$. Furthermore,

$$I_n(z_0,z_{n+1}) = \sum_r I_{n-1}(z_0,u^r)M_{rl}(z,n) \quad \text{and} \quad z_{n+1} = u^l$$

This implies that $I_{N-1}(z_0,z_0)$ is just a chain of matrix multiplications:

$$I_{N-1}(z_0,z_0) = \Big[M(z,0)\dots M(z,N-1)\Big]_{ll}\,.$$

Hence, the partition function reads

$$\begin{aligned} Z_{S^*}(z) &= \frac{\mathrm{e}^{N\chi}}{3^{N_\mathrm{s}}}\sum_l \Big[M(z,0)\dots M(z,N-1)\Big]_{ll} \\ &= \frac{\mathrm{e}^{N\chi}}{3^{N_\mathrm{s}}}\,\mathrm{tr}\Big[M(z,0)\dots M(z,N-1)\Big] \end{aligned}$$

which is the desired form of the partition function formulated as a chain of matrix multiplications. Due to our choice of V, twists only occur at the two links

$$\langle 0,N-1\rangle \quad \text{and} \quad \left\langle \frac{N}{2}-1,\frac{N}{2}\right\rangle\,.$$

Therefore, $z = 1$ for most matrices $M(z,i)$ which also implies that these matrices are independent of i. We write $M = M(1,i)$ and have

$$Z_{S^*}(z) = \frac{\mathrm{e}^{N\chi}}{3^{N_\mathrm{s}}}\,\mathrm{tr}\left[M^{\frac{N}{2}-1}M\left(z,\frac{N}{2}-1\right)M^{\frac{N}{2}-1}M\Big(z,N-1\Big)\right]$$

B.4 High-temperature expansion of ΔF

We state the detailed computation of the high-temperature expansion in [90]. To derive the high-temperature expansion of ΔF, we note that the partition functions $Z_{\mathrm{flux}}(q_V =_3 e)$ and Z_{flux} only differ based on which set M of flux-tube configurations $\{n,l\}$ is used for the sum of the respective partition function. Therefore, we have

$$Z_M = \sum_{\{n,l\}\in M} \mathrm{e}^{-\beta\Delta(\{n,l\})}$$

with $\Delta(\{n,l\}) = H - \mu q$. Expanding the partition function Z_M with respect to the parameter β gives

$$\begin{aligned} Z_M = \sum_{\{n,l\}\in M} \mathrm{e}^{-\beta\Delta(\{n,l\})} &= \sum_{n=0}^{\infty} \frac{(-1)^n}{n!}\beta^n \left(\sum_{\{n,l\}\in M} \Delta^n(\{n,l\}) \right) \\ &= M - N_1\beta + \frac{N_2}{2}\beta^2 - \frac{N_3}{6}\beta^3 + \mathcal{O}(\beta^4)\,, \end{aligned}$$

where

$$N_k = \sum_{\{n,l\}\in M} \Delta^k(\{n,l\})$$

and

$$M = \sum_{\{n,l\}\in M} 1\,.$$

This implies

$$\begin{aligned} -\frac{1}{\beta}\ln(Z_M) &= -\frac{1}{\beta}\ln\left(M - N_1\beta + \frac{N_2}{2}\beta^2 - \frac{N_3}{6}\beta^3 + \mathcal{O}(\beta^4)\right) \\ &= -\frac{1}{\beta}\ln\left(M\left(1 - \frac{N_1}{M}\beta + \frac{N_2}{2M}\beta^2 - \frac{N_3}{6M}\beta^3 + \mathcal{O}(\beta^4)\right)\right) \\ &= -\frac{1}{\beta}\ln M - \frac{1}{\beta}\ln\Bigg(1 \underbrace{- \frac{N_1}{M}\beta + \frac{N_2}{2M}\beta^2 - \frac{N_3}{6M}\beta^3 + \mathcal{O}(\beta^4)}_{=x}\Bigg)\,. \\ &= -\frac{1}{\beta}\ln M - \frac{1}{\beta}\left(x - \frac{x^2}{2} + \frac{x^3}{3} + \mathcal{O}(x^4)\right) \\ &= -\frac{1}{\beta}\ln M - \frac{1}{\beta}\Bigg(- \frac{N_1}{M}\beta + \left(\frac{N_2}{2M} - \frac{N_1^2}{2M^2}\right)\beta^2 \\ &\qquad\qquad + \left(\frac{N_1N_2}{2M^2} - \frac{N_3}{6M} - \frac{N_1^3}{3M^3}\right)\beta^3 + \mathcal{O}(\beta^4)\Bigg) \\ &= -\frac{1}{\beta}\ln M + \frac{N_1}{M} - \left(\frac{N_2}{2M} - \frac{N_1^2}{2M^2}\right)\beta - \left(\frac{N_1N_2}{2M^2} - \frac{N_3}{6M} - \frac{N_1^3}{3M^3}\right)\beta^2 + \mathcal{O}(\beta^3) \end{aligned}$$

Therefore, we have

$$\begin{aligned} \Delta F &= -\frac{1}{\beta}\ln Z_{\text{flux}}(q_V =_3 1) - \frac{1}{\beta}\ln Z_{\text{flux}}(q_V =_3 0) \\ &= -\frac{1}{\beta}\ln\left(\frac{M_1}{M_0}\right) + \frac{\alpha_1}{M_1} - \frac{\alpha_0}{M_0} + \mathcal{O}(\beta) \end{aligned}$$

with $\alpha_e = \sum_{\{n,l\}\in M_e} \Delta(\{n,l\})$. We compute M_e and α_e by mapping both sums onto their respective Potts formulation as it is done for the flux-tube model in Chapter 6.

The value of M_e is given by

$$\begin{aligned} M_e &= Z_{\text{flux}}(q_V =_3 e, \beta = 0) = \sum_{\{n,l\}} \delta_{\phi_{S^*} - e =_3 0} \prod_i \delta_{q_i - \phi_i =_3 0} \\ &= \frac{1}{3^{N_s}} \frac{1}{3} \sum_z z^{-e} \sum_{\{z\}} \sum_{\{n,l\}} z^{\phi_{S^*}} \prod_i z_i^{q_i - \phi_i} \\ &= \frac{16^{N_s}}{3^{N_s}} \frac{1}{3} \sum_z z^{-e} \sum_{\{z\}} \left(\prod_i (1 + \operatorname{Re} z_i)^4 \right) \prod_{\langle i, i+\hat{k} \rangle} \left(1 + 2\operatorname{Re}(z^{-s_{\langle i,i+\hat{k}\rangle}} z_i z_{i+\hat{k}}^*) \right) , \end{aligned}$$

where $s_{\langle i,j \rangle}$ is defined as in Section 6.2. Using the identity

$$1 + 2\operatorname{Re}\left(u^{-n} u^m u^k\right) = \begin{cases} 3, & m + k =_3 n \\ 0, & \text{otherwise} \end{cases}$$

with $u = \mathrm{e}^{\frac{2\pi}{3}\mathrm{i}}$, the product over all links is non-vanishing only if all spins within the volume V and $\overline{V}$ are respectively identical denoting them with z_V and $z_{\overline{V}}$. Because both volumes are connected by the interface d_1 of links, the spins z_V and $z_{\overline{V}}$ cannot be independent and must fulfill the relation $z^{-1} z_V = z_{\overline{V}}$. Hence, we get

$$\begin{aligned} M_e &= \frac{16^{N_s} \cdot 3^{3N_s}}{3^{N_s}} \frac{1}{3} \sum_z z^{-e} \sum_{z_V} (1 + \operatorname{Re}(z_V))^{4N_V} (1 + \operatorname{Re}(z^{-1} z_V))^{4N_{\overline{V}}} \\ &= \frac{16^{N_s} \cdot 3^{3N_s}}{3^{N_s}} \frac{1}{3} \sum_{m=0}^{2} \sum_{k=0}^{2} u^{-me} (1 + \operatorname{Re}(u^k))^{4N_V} (1 + \operatorname{Re}(u^{-m} u^k))^{4N_{\overline{V}}} \end{aligned}$$

with N_V ($N_{\overline{V}}$) the number of sites in the volume V ($\overline{V}$). Hence, the ratio reduces to

$$\begin{aligned} M_e = \frac{16^{N_s} \cdot 3^{3N_s}}{3^{N_s}} \frac{1}{3} \Bigg(& 2^{4N_V} 2^{4N_{\overline{V}}} + \left(\frac{1}{2}\right)^{4N_V} \left(\frac{1}{2}\right)^{4N_{\overline{V}}} + \left(\frac{1}{2}\right)^{4N_V} \left(\frac{1}{2}\right)^{4N_{\overline{V}}} \\ & + u^{-e} 2^{4N_V} \left(\frac{1}{2}\right)^{4N_{\overline{V}}} + u^{-e} \left(\frac{1}{2}\right)^{4N_V} \left(\frac{1}{2}\right)^{4N_{\overline{V}}} + u^{-e} \left(\frac{1}{2}\right)^{4N_V} 2^{4N_{\overline{V}}} \\ & + u^{-2e} 2^{4N_V} \left(\frac{1}{2}\right)^{4N_{\overline{V}}} + u^{-2e} \left(\frac{1}{2}\right)^{4N_V} \left(\frac{1}{2}\right)^{4N_{\overline{V}}} + u^{-2e} \left(\frac{1}{2}\right)^{4N_V} 2^{4N_{\overline{V}}} \Bigg) \end{aligned}$$

which implies

$$\begin{aligned} M_e = \frac{16^{N_s} \cdot 3^{3N_s}}{3^{N_s}} \frac{2^{4N_s}}{3} \Bigg(& 1 + 2 \cdot 4^{-4N_s} \\ & + u^{-e} (4^{-4N_s} + 4^{-4N_V} + 4^{-4N_{\overline{V}}}) \\ & + u^{-2e} (4^{-4N_s} + 4^{-4N_V} + 4^{-4N_{\overline{V}}}) \Bigg) \end{aligned} .$$

This gives the ratio

$$\frac{M_e}{M_0} = \frac{1 + 2 \cdot 4^{-4N_s} + u^{-e} (4^{-4N_s} + 2 \cdot 4^{-2N_s}) + u^{-2e} (4^{-4N_s} + 2 \cdot 4^{-2N_s})}{1 + 4 \cdot 4^{-4N_s} + 4 \cdot 4^{-2N_s}}$$

if we set $N_V = N_{\overline{V}} = N_\mathrm{s}/2$. For $e = 1$, we have

$$\frac{M_1}{M_0} = \frac{1 + 4^{-4N_\mathrm{s}} - 2 \cdot 4^{-2N_\mathrm{s}}}{1 + 4 \cdot 4^{-4N_\mathrm{s}} + 4 \cdot 4^{-2N_\mathrm{s}}}$$

because $u^{-1} + u^{-2} = 2\mathrm{Re}(u^{-1}) = -1$.

We proceed with the mapping of α_e to its corresponding Potts formulation:

$$\begin{aligned}
\alpha_e &= \sum_{\{n,l\}} \Delta(\{n,l\}) \delta_{\phi_{S^*} - e =_3 0} \prod_i \delta_{q_i - \phi_i = 0 \mod 3} \\
&= \sum_{\{n,l\}} \Bigg(\sum_{i,s} \left[(m_\mathrm{q} - \mu) n_{i,s} + (m_\mathrm{q} + \mu) \overline{n}_{i,s} \right] \\
&\qquad\qquad + \sigma a \sum_{\langle i, i+\hat{k} \rangle} |l_{\langle i, i+\hat{k} \rangle}| \Bigg) \delta_{\phi_{S^*} - e =_3 0} \prod_i \delta_{q_i - \phi_i =_3 0} \\
&= \frac{1}{3} \frac{1}{3^{N_\mathrm{s}}} \sum_z z^{-e} \sum_{\{z\}} \Bigg[\underbrace{\sum_{\{n,l\}} \sum_{i,s} (m_\mathrm{q} - \mu) n_{i,s} z^{\phi_{S^*}} \prod_j z_j^{q_j - \phi_j}}_{\text{(i)}} \\
&\quad + \underbrace{\sum_{\{n,l\}} \sum_{i,s} (m_\mathrm{q} + \mu) \overline{n}_{i,s} z^{\phi_{S^*}} \prod_j z_j^{q_j - \phi_j}}_{\text{(ii)}} + \underbrace{\sigma a \sum_{\{n,l\}} \sum_{\langle i, i+\hat{k} \rangle} |l_{\langle i, i+\hat{k} \rangle}| z^{\phi_{S^*}} \prod_j z_j^{q_j - \phi_j}}_{\text{(iii)}} \Bigg]
\end{aligned}$$

We evaluate expression (i) and (ii) by using the identity

$$\sum_{\{l\}} z^{\phi_{S^*}} \prod_j z_j^{-\phi_j} = \prod_{\langle i, i+\hat{k} \rangle} \left(1 + 2\mathrm{Re}(z^{-s_{\langle i, i+\hat{k} \rangle}} z_i z_{i+\hat{k}}^*) \right).$$

Expression (i) is

$$\begin{aligned}
\text{(i)} &= \left(\sum_{\{n\}} \sum_{i,s} (m_\mathrm{q} - \mu) n_{i,s} \prod_j z_j^{q_j} \right) \left(\sum_{\{l\}} z^{\phi_{S^*}} \prod_j z_j^{-\phi_j} \right) \\
&= \left(\sum_{\{n\}} \sum_{i,s} (m_\mathrm{q} - \mu) n_{i,s} \prod_j z_j^{q_j} \right) \prod_{\langle i, i+\hat{k} \rangle} \left(1 + 2\mathrm{Re}(z^{-s_{\langle i, i+\hat{k} \rangle}} z_i z_{i+\hat{k}}^*) \right) \\
&= \left[(m_\mathrm{q} - \mu) \sum_{i,s} \left(\sum_{n_{i,s}=0}^{3} n_{i,s} z_i^{n_{i,s}} \right) \left(\prod_{\substack{(j,s') \\ \neq (i,s)}} \sum_{n_{j,s'}=0}^{3} z_j^{n_{j,s'}} \right) \left(\prod_{j,s'} \sum_{\overline{n}_{j,s'}=0}^{3} z_j^{-\overline{n}_{j,s'}} \right) \right] \\
&\quad \times \prod_{\langle i, i+\hat{k} \rangle} \left(1 + 2\mathrm{Re}(z^{-s_{\langle i, i+\hat{k} \rangle}} z_i z_{i+\hat{k}}^*) \right) \\
&= \left[(m_\mathrm{q} - \mu) \sum_{i,s} \left(3 + z_i + 2 z_i^{-1} \right) (2 + 2\mathrm{Re} z_i) \prod_{(j,s') \neq (i,s)} \left(2 + 2\mathrm{Re} z_j \right)^2 \right] \prod_{\langle i, i+\hat{k} \rangle} \cdots \\
&= \left[2(m_\mathrm{q} - \mu) \sum_i \left(3 + z_i + 2 z_i^{-1} \right) (2 + 2\mathrm{Re} z_i)^3 \prod_{j \neq i} \left(2 + 2\mathrm{Re} z_j \right)^4 \right] \prod_{\langle i, i+\hat{k} \rangle} \cdots .
\end{aligned}$$

Analogously, expression (ii) reads

$$\text{(ii)} = \left[2(m+\mu)\sum_i \left(3 + 2z_i + z_i^{-1}\right)(2+2\text{Re}z_i)^3 \prod_{j\neq i}(2+2\text{Re}z_j)^4\right] \prod_{\langle i,i+\hat{k}\rangle} \dots .$$

The next step is to sum expression (i) and (ii) over all twists and spin configurations, where we again us the fact that the sum over all spin configurations reduces to a sum over all spins z_V for the volume V. Expression (i) gives

$$\sum_z z^{-e} \sum_{\{z\}} \text{(i)} = 2\cdot 3^{3N_\text{s}}(m_\text{q}-\mu)N_V \cdot \text{(a)} + 2\cdot 3^{3N_\text{s}}(m_\text{q}-\mu)N_{\overline{V}} \cdot \text{(b)}$$

with

$$\begin{aligned}
&\text{(a)} = \\
&\sum_{m,k=0}^{2} u^{-me}(3+u^k+2u^{-k})(2+2\text{Re}(u^k))^{4N_V-1}(2+2\text{Re}(u^{-m}u^k))^{4N_{\overline{V}}} \\
&= 4^{4N_\text{s}}\Bigg(\frac{3}{2} + 3\cdot 4^{-4N_\text{s}} + 3\cdot 4^{-4N_{\overline{V}}}\text{Re}(u^{-e}) \\
&\quad + 2\cdot 4^{-4N_\text{s}}\text{Re}(u^{-e}(3+u^*+2u)) + 2\cdot 4^{-4N_V}\text{Re}(u^{-e}(3+2u^*+u))\Bigg)
\end{aligned}$$

and

$$\begin{aligned}
&\text{(b)} = \\
&\sum_{m,k=0}^{2} u^{-me}(3+u^{-m}u^k+2u^m u^{-k})(2+2\text{Re}(u^{-m}u^k))^{4N_{\overline{V}}-1}(2+2\text{Re}(u^k))^{4N_V} \\
&= 4^{4N_\text{s}}\Bigg(\frac{3}{2} + 3\cdot 4^{-4N_\text{s}} + 3\cdot 4^{-4N_V}\text{Re}(u^{-e}) \\
&\quad + 2\cdot 4^{-4N_\text{s}}\text{Re}(u^{-e}(3+2u^*+u)) + 2\cdot 4^{-4N_{\overline{V}}}\text{Re}(u^{-e}(3+u^*+2u))\Bigg)
\end{aligned}$$

Expression (ii) gives

$$\sum_z z^{-e} \sum_{\{z\}} \text{(ii)} = 2\cdot 3^{3N_\text{s}}(m_\text{q}+\mu)N_V \cdot \text{(c)} + 2\cdot 3^{3N_\text{s}}(m_\text{q}+\mu)N_{\overline{V}} \cdot \text{(d)}$$

with

$$\begin{aligned}
&\text{(c)} = \\
&\sum_{m,k=0}^{2} u^{-me}(3+2u^k+u^{-k})(2+2\text{Re}(u^k))^{4N_V-1}(2+2\text{Re}(u^{-m}u^k))^{4N_{\overline{V}}} \\
&= 4^{4N_\text{s}}\Bigg(\frac{3}{2} + 3\cdot 4^{-4N_\text{s}} + 3\cdot 4^{-4N_{\overline{V}}}\text{Re}(u^{-e}) \\
&+ 2\cdot 4^{-4N_\text{s}}\text{Re}(u^{-e}(3+2u^*+u)) + 2\cdot 4^{-4N_V}\text{Re}(u^{-e}(3+u^*+2u))\Bigg)
\end{aligned}$$

and

$$
\begin{aligned}
&\text{(d)} = \\
&\sum_{m,k=0}^{2} u^{-me}(3+2u^{-m}u^{k}+u^{m}u^{-k})(2+2\mathrm{Re}(u^{-m}u^{k}))^{4N_{\overline{V}}-1}(2+2\mathrm{Re}(u^{k}))^{4N_V} \\
&= 4^{4N_\mathrm{s}}\Bigg(\frac{3}{2}+3\cdot 4^{-4N_\mathrm{s}}+3\cdot 4^{-4N_V}\mathrm{Re}(u^{-e}) \\
&+2\cdot 4^{-4N_\mathrm{s}}\mathrm{Re}(u^{-e}(3+u^{*}+2u))+2\cdot 4^{-4N_{\overline{V}}}\mathrm{Re}(u^{-e}(3+2u^{*}+u))\Bigg)
\end{aligned}
$$

We put everything together, choose $N_V = N_{\overline{V}} = N_\mathrm{s}/2$ and order everything appropriately:

$$
\begin{aligned}
&\sum_z z^{-e}\sum_{\{z\}}\text{(i)}+\sum_z z^{-e}\sum_{\{z\}}\text{(ii)} \\
&\quad= 4\cdot 3^{3N_\mathrm{s}}\cdot m_\mathrm{q}\cdot N_\mathrm{s}\cdot 4^{4N_\mathrm{s}}\Bigg(\frac{3}{2}+3\cdot 4^{-4N_\mathrm{s}}+3\cdot 4^{-2N_\mathrm{s}}\mathrm{Re}(u^{-e}) \\
&\qquad\quad+\Big[4^{-4N_\mathrm{s}}+4^{-2N_\mathrm{s}}\Big]\Big[\mathrm{Re}(u^{-e}(3+u^{*}+2u))+\mathrm{Re}(u^{-e}(3+2u^{*}+u))\Big]\Bigg) \\
&\quad= 4\cdot 3^{3N_\mathrm{s}}\cdot m_\mathrm{q}\cdot N_\mathrm{s}\cdot 4^{4N_\mathrm{s}}\Bigg(\frac{3}{2}+\mathcal{O}(4^{-2N_\mathrm{s}})\Bigg).
\end{aligned}
$$

Therefore, the fermionic part of α_e is

$$
\begin{aligned}
\beta_e &= \frac{1}{3}\frac{1}{3^{N_\mathrm{s}}}\Bigg(\sum_z z^{-e}\sum_{\{z\}}\text{(i)}+\sum_z z^{-e}\sum_{\{z\}}\text{(ii)}\Bigg) \\
&= 2\cdot m_\mathrm{q}\cdot 3^{2N_\mathrm{s}}\cdot 4^{4N_\mathrm{s}}\Bigg(N_\mathrm{s}+\mathcal{O}(N_\mathrm{s}\cdot 4^{-2N_\mathrm{s}})\Bigg)
\end{aligned}
$$

and, consequently,

$$
\begin{aligned}
\frac{\beta_e}{M_e} &= \frac{2\cdot m_\mathrm{q}\cdot 3^{2N_\mathrm{s}}\cdot 4^{4N_\mathrm{s}}\cdot 3^{N_\mathrm{s}}\cdot 3}{16^{N_\mathrm{s}}\cdot 3^{3N_\mathrm{s}}\cdot 2^{4N_\mathrm{s}}}\frac{N_\mathrm{s}+\mathcal{O}(N_\mathrm{s}\cdot 4^{-2N_\mathrm{s}})}{1+\mathcal{O}(4^{-2N_\mathrm{s}})} \\
&= 6m_\mathrm{q}\cdot\frac{N_\mathrm{s}+\mathcal{O}(N_\mathrm{s}\cdot 4^{-2N_\mathrm{s}})}{1+\mathcal{O}(4^{-2N_\mathrm{s}})}.
\end{aligned}
$$

It remains to evaluate expression (iii):

$$
\begin{aligned}
\text{(iii)} &= \Bigg(\sum_{\{l\}}\sum_{\langle i,i+\hat{k}\rangle}|l_{\langle i,i+\hat{k}\rangle}|z^{\phi_{S^*}}\prod_j z_j^{-\phi_j}\Bigg)\Bigg(\sum_{\{n\}}\prod_j z_j^{q_j}\Bigg) \\
&= \Bigg[\sum_{\langle i,i+\hat{k}\rangle}2\mathrm{Re}\left(z^{S_{\langle i,i+\hat{k}\rangle}}z_i^{*}z_{i+\hat{k}}\right)\prod_{\substack{\langle j,j+\hat{m}\rangle \\ \neq\langle i,i+\hat{k}\rangle}}\left(1+2\mathrm{Re}\left(z^{S_{\langle j,j+\hat{m}\rangle}}z_j^{*}z_{j+\hat{m}}\right)\right)\Bigg] \\
&\qquad\times\prod_i(2+2\mathrm{Re}\,z_i)^4
\end{aligned}
$$

This implies

$$\sum_z z^{-e} \sum_{\{z\}} (\text{iii}) \\ = 6N_\text{s} \cdot 3^{3N_\text{s}-1} 16^{N_\text{s}} 2^{4N_\text{s}} \left(1 + 2 \cdot 4^{-4N_\text{s}} + 2\text{Re}(u^{-e})(4^{-4N_\text{s}} + 4^{-4N_V} + 4^{-4N_{\overline{V}}})\right) .$$

The flux-tube part of α_e is then given by

$$\gamma_e = \frac{1}{3} \frac{1}{3^{N_\text{s}}} \sum_z z^{-e} \sum_{\{z\}} (\text{iii}) = 2N_\text{s} M_e \cdot \sigma a$$

which yields

$$\frac{\gamma_e}{M_e} = 2N_\text{s} \cdot \sigma a$$

Finally, we have

$$\frac{\alpha_e}{M_e} = \frac{\beta_e + \gamma_e}{M_e} = 2\sigma a N_\text{s} + \frac{6m_\text{q} N_\text{s} + \mathcal{O}(N_\text{s} \cdot 4^{-2N_\text{s}})}{1 + \mathcal{O}(4^{-2N_\text{s}})} .$$

B.5 Low-temperature expansion of ΔF

We supplement the results of [90] by explicitly stating the derivation of the low-temperature expansion for the one-dimensional chain. We derive the energies $\Delta_e^{(0)}$ and $\Delta_e^{(1)}$ and the multiplicities $N_e^{(0)}$ and $N_e^{(1)}$ for $e = 0, 1$. We do so by assuming without loss of generality $\mu \geq 0$ and considering the intervals $\mu/m_\text{q} \in [0, 1/3)$, $\mu/m_\text{q} = 1/3$, $\mu/m_\text{q} \in (1/3, 1)$, $\mu/m_\text{q} = 1$ and $\mu/m_\text{q} > 1$ separately. Any energy $\Delta = H - \mu q$ can be expressed in the form

$$\Delta = (n_\text{q} + \overline{n}_\text{q}) m_\text{q} - \mu q + u \cdot \sigma a$$

where $u \in \mathbb{N}_0$ and $q = 3k$, $k \in \mathbb{Z}$. q is the net-quark number of the whole chain. Furthermore, we use the notation $(n_{i,\uparrow}, n_{i,\downarrow})$ ($[\overline{n}_{i,\uparrow}, \overline{n}_{i,\downarrow}]$) for a pair of (anti-)quark occupation numbers.

$\frac{\mu}{m_\text{q}} \in \left[0, \frac{1}{3}\right)$

$\Delta_1^{(0)}$**:** We distinguish the case $q = 0$ and $q \neq 0$. If $q = 0$, the energy is minimized by a mesonic state made of one quark in V, one antiquark in $\overline{V}$ and exactly one flux-tube variable $l_{\langle i,j \rangle} = 1$ of the interface d_1 is set and generates the required flux $e = 1$ through S^*. The mesonic state is therefore given by $n_\text{q} + \overline{n}_\text{q} = 2$, $u = 1$. Diagrammatically,

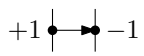

with the charges represented at the end points. The interface link is represented by an arrow between two horizontal lines. Obviously all other states with $q = 0$ have larger energies. If $q = 3k > 0$, we have

$$2m_\text{q} + \sigma a \leq \left(1 - \frac{1}{3}\right) q m_\text{q} + u\sigma a < (n_\text{q} + \overline{n}_\text{q}) m_\text{q} - \mu q + u\sigma a$$

showing that any state with $q = 3k > 0$ has energies Δ which are larger than the mesonic state. If $q = -3k < 0$, the inequality reads

$$2m_\mathrm{q} + \sigma a < \underbrace{(n_\mathrm{q} + \overline{n}_\mathrm{q})}_{\geq 3} m_\mathrm{q} + \sigma a \leq (n_\mathrm{q} + \overline{n}_\mathrm{q}) m_\mathrm{q} - \mu q + u\sigma a$$

because $-\mu q \geq 0$. All negative charge states have an energy strictly larger than the mesonic state.

We conclude

$$\Delta_1^{(0)} = 2m_\mathrm{q} + \sigma a\,.$$

The diagram has a multiplicity of $D = 2 \cdot 2 = 4$ because we have two possibilities for the quark and antiquark occupation respectively: $(1,0), (0,1)$ and $[1,0], [0,1]$. Furthermore, there are two interface links at which we can place the mesonic state:

$$N_1^{(0)} = 2 \cdot D = 8$$

$\Delta_1^{(1)}$**:** The next larger energy level relative to $\Delta_1^{(0)}$ depends on the relations between the string tension σa, the quark mass m_q and the chemical potential μ. If $q = 0$, the next larger energy relative to $\Delta_1^{(0)}$ is given by

$$\Delta_1^{(1)} = \begin{cases} 2m_\mathrm{q} + 2\sigma a, & \sigma a / m_\mathrm{q} \leq 2 \\ 4m_\mathrm{q} + \sigma a, & \sigma a / m_\mathrm{q} > 2 \end{cases}.$$

The first case is a mesonic state with two flux tubes and the second case is a state with one meson at the interface and one on-site meson placed at any site of the lattice. Diagrammatically, the first case corresponds to

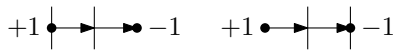

Each diagram has a multiplicity of $D = 4$ and can be placed at either link of S^*. This gives the total multiplicity $\gamma_1 = 4 \cdot 2 \cdot 2 = 16$. In the second case, there are 4 possibilities to place a meson at an empty site. If the site is already occupied by one quark, we have 6 possibilities:

$$\begin{array}{lll} (2,0)[1,0] & (0,2)[1,0] & (1,1)[1,0] \\ (2,0)[0,1] & (0,2)[0,1] & (1,1)[0,1] \end{array}$$

We analogously have 6 possibilities if the site is occupied with an antiquark. The total multiplicity of the second case, consequently, reads

$$\gamma_2 = 2 \cdot ((N-2) \cdot 4 \cdot 4 + 6 \cdot 2 + 6 \cdot 2) = 32(N-2) + 48\,.$$

If $q = 3k$ with $k > 0$, the minimal energy is given by a baryonic state at the interface S^* because

$$\begin{aligned} 3\left(1 - \frac{\mu}{m_\mathrm{q}}\right) m_\mathrm{q} + \sigma a \leq \underbrace{\left(1 - \frac{\mu}{m_\mathrm{q}}\right)}_{>0} q m_\mathrm{q} + \sigma a \\ \leq (n_\mathrm{q} + \overline{n}_\mathrm{q}) m_\mathrm{q} - \mu q + u\sigma a \end{aligned}.$$

The energy of a baryonic state is larger than the minimal energy $\Delta_1^{(0)}$ and is therefore also a suitable candidate for $\Delta_1^{(1)}$. If $q = -3k$ with $k > 0$, the minimal energy is given by an anti-baryonic state at the interface S^* because

$$\begin{aligned} 3\left(1+\frac{\mu}{m_\mathrm{q}}\right)m_\mathrm{q}+\sigma a &\leq \left(1+\frac{\mu}{m_\mathrm{q}}\right)|q|m_\mathrm{q}+\sigma a \\ &\leq (n_\mathrm{q}+\overline{n}_\mathrm{q})m_\mathrm{q}-\mu q+u\sigma a \end{aligned} .$$

For $\mu \geq 0$, the energy of an antibaryonic state is always larger than $\Delta_1^{(0)}$ and, therefore, the antibaryonic state is also a suitable candidate for the energy $\Delta_1^{(1)}$. Diagrammatically, the (anti-)baryonic state corresponds to

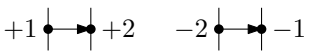

The (anti-)quark can be arranged in two ways. The two (anti-)quarks can be arranged with three possibilities: $(2,0),(0,2),(1,1)$. Hence, a (anti-)baryonic diagram has the multiplicity of $D = 6$. S^* has two links. Therefore, we have

$$\gamma_3 = 2 \cdot 6 = 12$$

for (anti-)baryonic states. We need to distinguish between multiple cases in which either the mesonic, baryonic or anti-baryonic states realize $\Delta_1^{(1)}$. Firstly, let us decide between baryonic and mesonic states. Assume $\sigma a/m_\mathrm{q} \leq 2$. The conditions read

$$2m+2\sigma a \lessgtr 3\left(1-\frac{\mu}{m}\right)m+\sigma a$$

which are given if and only if

$$\frac{\sigma a}{m_\mathrm{q}} \lessgtr 1-3\frac{\mu}{m_\mathrm{q}}$$

Assume $\sigma a/m_\mathrm{q} > 2$. The conditions are

$$4m_\mathrm{q}+\sigma a \lessgtr 3\left(1-\frac{\mu}{m_\mathrm{q}}\right)m_\mathrm{q}+\sigma a$$

which is given if and only if

$$4 \lessgtr 3\left(1-\frac{\mu}{m_\mathrm{q}}\right) .$$

This is however only true for $>$. Hence, only the baryonic state contributes for $\sigma a/m_\mathrm{q} > 2$. If $\mu > 0$, then the energy of an anti-baryonic sate is evidently always larger than the corresponding baryonic state. Only in the case $\mu = 0$, the baryonic and antibaryonic state have the same energy and we have to include the multiplicities of the anti-baryonic states.

We can summarize the above results:

$$\Delta_1^{(1)} = \begin{cases} 2m_\mathrm{q} + 2\sigma a\,, & \sigma a/m_\mathrm{q} \leq 2\,,\ \sigma a/m_\mathrm{q} \leq 1 - 3\frac{\mu}{m_\mathrm{q}} \\ 3m_\mathrm{q} - 3\mu + \sigma a\,, & \sigma a/m_\mathrm{q} \leq 2\,,\ \sigma a/m_\mathrm{q} > 1 - 3\frac{\mu}{m_\mathrm{q}} \\ 3m_\mathrm{q} - 3\mu + \sigma a\,, & \sigma a/m_\mathrm{q} > 2 \end{cases}$$

$$N_1^{(1)} = \begin{cases} \gamma_1\,, & \sigma a/m_\mathrm{q} < 2\,,\ \sigma a/m_\mathrm{q} < 1 - 3\frac{\mu}{m_\mathrm{q}} \\ \gamma_1 + \gamma_3 + \gamma_3\delta_{\mu,0}\,, & \sigma a/m_\mathrm{q} < 2\,,\ \sigma a/m_\mathrm{q} = 1 - 3\frac{\mu}{m_\mathrm{q}} \\ \gamma_3 + \gamma_3\delta_{\mu,0}\,, & \sigma a/m_\mathrm{q} < 2\,,\ \sigma a/m_\mathrm{q} > 1 - 3\frac{\mu}{m_\mathrm{q}} \\ \gamma_3 + \gamma_3\delta_{\mu,0}\,, & \sigma a/m_\mathrm{q} = 2 \\ \gamma_3 + \gamma_3\delta_{\mu,0}\,, & \sigma a/m_\mathrm{q} > 2 \end{cases}$$

$$= \begin{cases} 16\,, & \sigma a/m_\mathrm{q} < 2\,,\ \sigma a/m_\mathrm{q} < 1 - 3\frac{\mu}{m_\mathrm{q}} \\ 28 + 12\delta_{\mu,0}\,, & \sigma a/m_\mathrm{q} < 2\,,\ \sigma a/m_\mathrm{q} = 1 - 3\frac{\mu}{m_\mathrm{q}} \\ 12 + 12\delta_{\mu,0}\,, & \sigma a/m_\mathrm{q} < 2\,,\ \sigma a/m_\mathrm{q} > 1 - 3\frac{\mu}{m_\mathrm{q}} \\ 12 + 12\delta_{\mu,0}\,, & \sigma a/m_\mathrm{q} = 2 \\ 12 + 12\delta_{\mu,0}\,, & \sigma a/m_\mathrm{q} > 2 \end{cases}$$

$$= \begin{cases} 16\,, & \sigma a/m_\mathrm{q} < 2\,,\ \sigma a/m_\mathrm{q} < 1 - 3\frac{\mu}{m_\mathrm{q}} \\ 28 + 12\delta_{\mu,0}\,, & \sigma a/m_\mathrm{q} < 2\,,\ \sigma a/m_\mathrm{q} = 1 - 3\frac{\mu}{m_\mathrm{q}} \\ 12 + 12\delta_{\mu,0}\,, & \sigma a/m_\mathrm{q} < 2\,,\ \sigma a/m_\mathrm{q} > 1 - 3\frac{\mu}{m_\mathrm{q}} \\ 12 + 12\delta_{\mu,0}\,, & \sigma a/m_\mathrm{q} \geq 2 \end{cases}$$

$\Delta_0^{(0)}$: The flux through S^* has to be zero. Obviously, the empty chain fulfills this constrain. It remains to show that any other configuration has an energy strictly larger than the empty chain. If $q = 0$, then a non-empty chain ($n_\mathrm{q} + \overline{n}_\mathrm{q} > 0$ or $u > 0$) has a strictly positive energy. If $q \neq 0$,

$$0 < \left(1 \mp \frac{\mu}{m_\mathrm{q}}\right) |q| m_\mathrm{q} + u\sigma a \leq (n_\mathrm{q} + \overline{n}_\mathrm{q}) m_\mathrm{q} - \mu q + u\sigma a\,.$$

Hence, the empty chain is indeed the only chain minimizing the energy: $\Delta_0^{(0)} = 0$ and $N_0^{(0)} = 1$.

$\Delta_0^{(1)}$: Because we have the constrain of no flux through S^*, a configuration with a single on-site meson is admissible. This configuration has the energy

$$\Delta_0^{(1)} = 2m_\mathrm{q}\,.$$

For $q = 0$, any other state is either the empty chain or a state with strictly more energy:

$$2m_\mathrm{q} < (n_\mathrm{q} + \overline{n}_\mathrm{q}) m_\mathrm{q} + u\sigma a$$

because either $(n_\mathrm{q} + \overline{n}_\mathrm{q}) = 2$ and $u > 0$ or $(n_\mathrm{q} + \overline{n}_\mathrm{q}) > 2$. For $q > 0$, we have

$$\begin{aligned} 2m_\mathrm{q} \leq 3 \cdot \left(1 - \frac{1}{3}\right) m + u\sigma a \leq \left(1 - \frac{1}{3}\right) q m_\mathrm{q} + u\sigma a \\ < (n_\mathrm{q} + \overline{n}_\mathrm{q}) m_\mathrm{q} - \mu q + u\sigma a \end{aligned}$$

which implies that all positive charge configurations have a energy strictly larger than $\Delta_0^{(1)}$. For $q < 0$,

$$2m_\mathrm{q} < \underbrace{(n_\mathrm{q} + \overline{n}_\mathrm{q})}_{\geq 3} m_\mathrm{q} + u\sigma a \leq (n_\mathrm{q} + \overline{n}_\mathrm{q})m_\mathrm{q} - \mu q + u\sigma a\,.$$

Hence, we conclude that the mesonic states are indeed the states of the first excitation relative to $\Delta_0^{(0)}$. Each meson can be arranged with four possibilities at a site and we have N sites: $\Delta_0^{(1)} = 2m_\mathrm{q}$, $N_0^{(1)} = 4N$.

$\frac{\mu}{m_\mathrm{q}} = \frac{1}{3}$

$\Delta_1^{(0)}$**:** We again have at least one flux tube at the interface S^*. For $q = 0$, the states with the lowest energy are the mesonic sates

$$+1 \bullet\!\!\rightarrow\!\!\bullet\, -1$$

with energy $2m_\mathrm{q} + \sigma a$. For $q > 0$, we have

$$2m_\mathrm{q} + \sigma a = 3m_\mathrm{q} - \frac{1}{3}\cdot 3m_\mathrm{q} + \sigma a \leq (n_\mathrm{q} + \overline{n}_\mathrm{q})m_\mathrm{q} - \frac{1}{3}m_\mathrm{q} q + u\sigma a\,.$$

Hence, the baryonic states

$$+1 \bullet\!\!\rightarrow\!\!\bullet\, +2$$

of lowest energy have the same energy as the mesonic states of lowest energy. For $q < 0$,

$$2m_\mathrm{q} + \sigma a < \left(1 + \frac{1}{3}\right)|q| m_\mathrm{q} + \sigma a \leq (n_\mathrm{q} + \overline{n}_\mathrm{q})m_\mathrm{q} + \frac{1}{3}m_\mathrm{q}|q| + u\sigma a\,.$$

Any state with negative net-quark number has a strictly larger energy than the mesonic states of lowest energy. We conclude

$$\begin{aligned}\Delta_1^{(0)} &= 2m_\mathrm{q} + \sigma a \\ N_1^{(0)} &= 2\cdot(\underbrace{4}_{\text{mesonic}} + \underbrace{6}_{\text{baryonic}}) = 20\end{aligned}$$

$\Delta_1^{(1)}$**:** We consider the first excitations of the mesonic and baryonic states which results in states with $q = 0$ or $q > 0$. There are three possibilities. We can either add exactly one flux tube, one on-site meson or one on-site baryon:

1. Adding one flux tube to the mesonic states of $\Delta_1^{(0)}$ gives

$$\Delta_1^{(1)} = 2m_\mathrm{q} + 2\sigma a$$

with the multiplicity $\gamma_1 = 16$.

2. Adding one on-site meson to the mesonic states of $\Delta_1^{(0)}$ gives

$$\Delta_1^{(1)} = 4m_q + \sigma a$$

with the multiplicity $\gamma_2 = 32(N-2) + 48$.

3. Adding one on-site baryon to the mesonic states of $\Delta_1^{(0)}$ gives

$$\Delta_1^{(1)} = 4m_q + \sigma a\,.$$

There are 4 possibilities to add an on-site baryon to an empty site:

$$(3,0) \quad (0,3) \quad (2,1) \quad (1,2)$$

There are 3 possibilities to add an on-site baryon to a site already occupied by one quark:

$$(3,1) \quad (1,3) \quad (2,2)$$

There are 8 possibilities to add an on-site baryon to a site already occupied by one antiquark:

$$\begin{array}{cccc} (3,0)[1,0] & (0,3)[1,0] & (2,1)[1,0] & (1,2)[1,0] \\ (3,0)[0,1] & (0,3)[0,1] & (2,1)[0,1] & (1,2)[0,1] \end{array}$$

The mesonic diagram

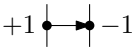

has the multiplicity $D = 4$. The total multiplicity for adding an on-site baryon to a mesonic state is consequently

$$\gamma_3 = 2 \cdot (D \cdot 4 \cdot (N-2) + 3 \cdot 2 + 2 \cdot 8) = 32(N-2) + 12 + 32$$

4. Adding a flux tube to a bayronic state of $\Delta_1^{(0)}$ gives the energy

$$\Delta_1^{(1)} = 2m_q + 2\sigma a\,.$$

There a three possible diagrams

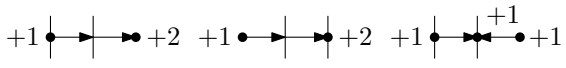

for adding one flux tube to a baryonic state. The first two diagrams have both a multiplicity of 6. The third diagram has a multiplicity of 8. Therefore,

$$\gamma_4 = 2 \cdot (6 + 6 + 8) = 40$$

5. Adding an on-site meson to a baryonic state of $\Delta_1^{(0)}$ gives the energy

$$\Delta_1^{(1)} = 4m_q + \sigma a\,.$$

The baryonic diagram

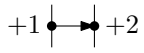

has a multiplicity of $D = 6$. There are 4 possibilities to add a meson to an empty site, 6 possibilities to add it to a site which is already occupied by a quark and 8 possibilities to add it to a site which is already occupied by two quarks. The total multiplicity reads

$$\gamma_5 = 2 \cdot (6 \cdot 4 \cdot (N-2) + 6 \cdot 3 + 8 \cdot 2) = 48(N-2) + 68\,.$$

6. Adding an on-site baryon to a baryonic state of $\Delta_1^{(0)}$ gives the energy

$$\Delta_1^{(1)} = 4m_\mathrm{q} + \sigma a\,.$$

There are 4 possibilities to add an on-site baryon to an empty site, 3 possibilities to add it to a site already occupied by one quark and 2 possibilities to add it to a site already occupied by two quarks ($(3,2)$ and $(2,3)$). Hence, we have

$$\gamma_6 = 2 \cdot (6 \cdot 4 \cdot (N-2) + 3 \cdot 3 + 2 \cdot 2) = 48(N-2) + 26\,.$$

If $q < 0$, the states of lowest energy are antibaryonic states

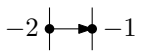

with the energy $3m_\mathrm{q} + \frac{1}{3} \cdot 3m_\mathrm{q} + \sigma a = 4m_\mathrm{q} + \sigma a$. If the first excitations for $q = 0$ and $q > 0$ are indeed given by $\Delta_1^{(1)} = 4m_\mathrm{q} + \sigma a$, we have to also add the multiplicity of the antibaryonic states which is given by $\gamma_7 = 2 \cdot 6 = 12$. In summary, we have

$$\Delta_1^{(1)} = \begin{cases} 2m_\mathrm{q} + 2\sigma a, & \sigma a/m_\mathrm{q} \leq 2 \\ 4m_\mathrm{q} + \sigma a, & \sigma a/m_\mathrm{q} > 2 \end{cases}$$

$$N_1^{(1)} = \begin{cases} \gamma_1 + \gamma_4, & \sigma a/m_\mathrm{q} < 2 \\ \sum_{i=1}^{7} \gamma_i, & \sigma a/m_\mathrm{q} = 2 \\ \gamma_2 + \gamma_3 + \gamma_5 + \gamma_6 + \gamma_7, & \sigma a/m_\mathrm{q} > 2 \end{cases}$$

$$= \begin{cases} 56, & \sigma a/m_\mathrm{q} < 2 \\ 160(N-2) + 254, & \sigma a/m_\mathrm{q} = 2 \\ 160(N-2) + 198, & \sigma a/m_\mathrm{q} > 2 \end{cases}$$

$\Delta_0^{(0)}$: Here, we have, again, only one state: the empty chain. Hence, $\Delta_0^{(0)} = 0$ and $N_0^{(0)} = 1$.

$\Delta_0^{(1)}$: For $q = 0$, we again have all configurations with one meson at an arbitrary site. For $q > 0$, the states with one baryon at an arbitrary site have the same energy as the states with a single on-site meson. All other states in

both regions have a strictly larger energy. Especially all negative charge states also have strictly larger energies. Therefore, we conclude:

$$\Delta_0^{(1)} = 2m_\mathrm{q}\,,$$
$$N_0^{(1)} = 4N + 4N = 8N\,.$$

$\frac{\mu}{m_\mathrm{q}} \in \left(\frac{1}{3}, 1\right)$

$\Delta_1^{(0)}$**:** The states with lowest energies fulfilling the constraints are the mesonic states

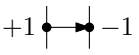

for $q = 0$ and the baryonic states

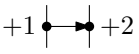

for $q > 0$. We have

$$2m_\mathrm{q} + \sigma a > \underbrace{3\left(1 - \frac{\mu}{m_\mathrm{q}}\right)}_{<2} + \sigma a = 3m_\mathrm{q} - 3\mu + \sigma a\,.$$

Hence, the baryonic states have a strictly smaller energy than the mesonic states. All states with $q < 0$ have a strictly larger energy than the lowest energy states with $q > 0$. Therefore,

$$\Delta_1^{(0)} = 3m_\mathrm{q} - 3\mu + \sigma a\,,$$
$$N_1^{(0)} = 2 \cdot 6 = 12$$

$\Delta_1^{(1)}$**:** There are two possibilities for the first excitation of a baryonic state:

1. Adding a flux tube to a baryonic state of $\Delta_1^{(0)}$ gives the energy

   $$\Delta_1 = 3m_\mathrm{q} - 3\mu + 2\sigma a$$

   There are three diagrams

   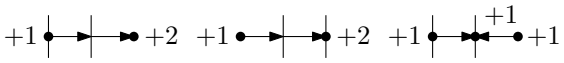

   for which the total multiplicity has been computed further above: $\gamma_1 = 40$.
2. Adding an on-site baryon to a baryonic state of $\Delta_1^{(0)}$ gives the energy

   $$\Delta_2 = 6m_\mathrm{q} - 6\mu + \sigma a\,.$$

   The total multiplicity has been computed further above:

   $$\gamma_2 = 48(N-2) + 26\,.$$

The mesonic states of lowest energy $\Delta_3 = 2m_q + \sigma a$ have a multiplicity of $\gamma_3 = 8$. The anti-baryonic states of lowest energy $\Delta_4 = 3m_q + 3\mu + \sigma a$ have a multiplicity of $\gamma_4 = 6$. We have to decide which of the four candidates of $\Delta_1^{(1)}$ are realized at which parameters:

1. Consider
$$\Delta_1 \lessgtr \Delta_2$$
which is equivalent to
$$\frac{\sigma a}{m_q} \lessgtr 3\left(1 - \frac{\mu}{m_q}\right).$$

2. Consider $\Delta_1 \lessgtr \Delta_3$ which is equivalent to
$$3\left(1 - \frac{\mu}{m_q}\right) \lessgtr 2 - \frac{\sigma a}{m_q}.$$

3. Consider $\Delta_1 \lessgtr \Delta_4$ which is equivalent to
$$\frac{\sigma a}{m_q} \lessgtr 6\frac{\mu}{m_q}$$

4. Consider $\Delta_2 \lessgtr \Delta_3$ which is equivalent to
$$\frac{2}{3} \lessgtr \frac{\mu}{m_q}$$

5. Consider $\Delta_2 \lessgtr \Delta_4$ which is equivalent to
$$\frac{1}{3} \lessgtr \frac{\mu}{m_q}.$$
This implies $\Delta_2 < \Delta_4$.

6. Consider $\Delta_3 \lessgtr \Delta_4$ which is equivalent to
$$-\frac{1}{3} \lessgtr \frac{\mu}{m_q}.$$
This implies $\Delta_3 < \Delta_4$.

Because $\Delta_4 > \Delta_2$ and $\Delta_4 > \Delta_3$, Δ_4 cannot constitute $\Delta_1^{(1)}$. We have to determine the minimum between the energies Δ_1, Δ_2 and Δ_3. We have

We get

$$\Delta_1^{(1)} = \begin{cases} 2m_\mathrm{q} + \sigma a, & 2 - \frac{\sigma a}{m_\mathrm{q}} \leq 3(1 - \frac{\mu}{m_\mathrm{q}}),\ \sigma a/m_\mathrm{q} \leq 3(1 - \frac{\mu}{m_\mathrm{q}}) \\ 3m_\mathrm{q} - 3\mu + 2\sigma a, & 2 - \frac{\sigma a}{m_\mathrm{q}} > 3(1 - \frac{\mu}{m_\mathrm{q}}),\ \sigma a/m_\mathrm{q} \leq 3(1 - \frac{\mu}{m_\mathrm{q}}) \\ 2m_\mathrm{q} + \sigma a, & \frac{\mu}{m_\mathrm{q}} \leq \frac{2}{3},\ \sigma a/m_\mathrm{q} > 3(1 - \frac{\mu}{m_\mathrm{q}}) \\ 6m_\mathrm{q} - 6\mu + \sigma a, & \frac{\mu}{m_\mathrm{q}} > \frac{2}{3},\ \sigma a/m_\mathrm{q} > 3(1 - \frac{\mu}{m_\mathrm{q}}) \end{cases}$$

$$N_1^{(1)} = \begin{cases} 8 & 2 - \frac{\sigma a}{m} < 3\left(1 - \frac{\mu}{m}\right), \sigma a/m < 3\left(1 - \frac{\mu}{m}\right) \\ 48 & 2 - \frac{\sigma a}{m} = 3\left(1 - \frac{\mu}{m}\right), \sigma a/m < 3\left(1 - \frac{\mu}{m}\right) \\ 40 & 2 - \frac{\sigma a}{m} > 3\left(1 - \frac{\mu}{m}\right), \sigma a/m < 3\left(1 - \frac{\mu}{m}\right) \\ 8 & 2 - \frac{\sigma a}{m} < 3\left(1 - \frac{\mu}{m}\right), \sigma a/m = 3\left(1 - \frac{\mu}{m}\right) \\ 48(N-2) + 74 & 2 - \frac{\sigma a}{m} = 3\left(1 - \frac{\mu}{m}\right), \sigma a/m = 3\left(1 - \frac{\mu}{m}\right) \\ 48(N-2) + 66 & 2 - \frac{\sigma a}{m} > 3\left(1 - \frac{\mu}{m}\right), \sigma a/m = 3\left(1 - \frac{\mu}{m}\right) \\ 8 & \frac{\mu}{m} < \frac{2}{3}, \sigma a/m > 3\left(1 - \frac{\mu}{m}\right) \\ 48(N-2) + 34 & \frac{\mu}{m} = \frac{2}{3}, \sigma a/m > 3\left(1 - \frac{\mu}{m}\right) \\ 48(N-2) + 26 & \frac{\mu}{m} > \frac{2}{3}, \sigma a/m > 3\left(1 - \frac{\mu}{m}\right) \end{cases}$$

$\Delta_0^{(0)}$: Because $0 < \mu < m_\mathrm{q}$, the lowest energy state for the zero-flux ensemble is still the empty chain: $\Delta_0^{(0)} = 0$ and $N_0^{(0)} = 1$.

$\Delta_0^{(1)}$: The first excitation is given by states with one on-site meson for $q = 0$, one on-site baryon for $q > 0$ and one on-site anti-baryon for $q < 0$. Inserting a baryon costs strictly less than a meson or an anti-baryon. Hence, we have found the first excitation. An on-site baryon can be arranged in four possible ways at a site:

$$\Delta_0^{(1)} = 3m_\mathrm{q} - 3\mu\,,$$
$$N_0^{(1)} = 4N\,.$$

$\frac{\mu}{m_\mathrm{q}} = 1$

$\Delta_1^{(0)}$: We need at least one flux tube. Obviously, we can minimize the energy by considering configurations made of exactly one flux tube and no antiquarks. The number of quarks becomes irrelevant because their insertion or removal costs zero energy. Hence, the lowest energy states fulfilling the constrains are given by one flux tube located at a link of S^* and all other sites occupied by any valid on-site configuration with the occupation numbers: 0, 3, 6.

We have the diagram

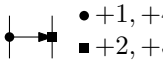

We can arrange the quark numbers in the following way

$$\begin{array}{lll} (1,0) & (0,1) & \\ (3,1) & (1,3) & (2,2) \\ (2,0) & (0,2) & (1,1) \\ (3,2) & (2,3) & \end{array}$$

The multiplicity of the diagram is $D = 5 \cdot 5 = 25$.

An on-site occupation can be arranged in the following ways.

$$\begin{array}{llll} & (0,0) & & \\ (3,0) & (0,3) & (2,1) & (1,2) \\ (3,3) & & & \end{array}$$

Hence, there are 6 possibilities per site. S^* has two links. We conclude

$$\begin{aligned} \Delta_1^{(0)} &= \sigma a\,, \\ N_1^{(0)} &= 6^{N-2} \cdot 25 \cdot 2\,. \end{aligned}$$

$\Delta_1^{(1)}$**:** It is only possible to increase the energy in two ways. We either add one additional flux tube or we add one antiquark. Adding a flux tube costs σa. Adding an antiquark costs $2m_\mathrm{q}$. Hence, we distinguish between the cases $\sigma a/m_\mathrm{q} < 2$, $\sigma a/m_\mathrm{q} = 2$ and $\sigma a/m_\mathrm{q} > 2$.

We compute the multiplicities for the different cases. If we add only one flux tube, we have following diagrams

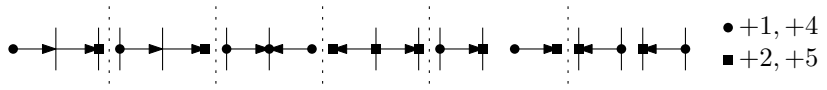

The first and second diagram have both a multiplicity of $D_1 = D_2 = 25$. The third and fourth diagram have both a multiplicity of $D_3 = D_4 = 5^3 = 125$. The fifth diagram has the multiplicity

$$D_5 = 25 \cdot 2 \cdot 25(N-4) = 1250 \cdot (N-4)$$

The last diagram has the multiplicity $D_6 = 25 \cdot 25 = 625$. The total multiplicity for adding a flux tube is, now, just given by

$$\begin{aligned} \gamma_1 &= 2 \cdot D_1 \cdot 6^{N-2} + 2 \cdot D_2 \cdot 6^{N-2} + 2 \cdot D_3 \cdot 6^{N-3} \\ &\qquad + 2 \cdot D_4 \cdot 6^{N-3} + 2 \cdot D_5 \cdot 6^{N-4} + D_6 \cdot 6^{N-4} \\ &= (2 \cdot D_1 + 2 \cdot D_2) \cdot 6^{N-2} \\ &\qquad + (2 \cdot D_3 + 2 \cdot D_4) \cdot 6^{N-3} + (2 \cdot D_5 + D_6) \cdot 6^{N-4} \\ &= (2 \cdot 25 + 2 \cdot 25) \cdot 6^{N-2} \\ &\qquad + (2 \cdot 125 + 2 \cdot 125) \cdot 6^{N-3} + (2 \cdot 1250(N-4) + 625) \cdot 6^{N-4} \\ &= 100 \cdot 6^{N-2} + 500 \cdot 6^{N-3} + (2500(N-4) + 625) \cdot 6^{N-4} \end{aligned}$$

If we add only one antiquark, we can either place it at a site which is not incident to any flux tube or we can place it at one of the two sites incident with the flux tube. In the former case, we place the antiquark with two possibilities. The possible quark occupations are, then, just $+1$ and $+4$. There are again five possibilities to create any valid quark occupation. Hence, we have $2 \cdot 5 = 10$ possibilities and together with the other sites:

$$\gamma_2 = 2 \cdot (N-2) \cdot 25 \cdot 10 \cdot 6^{N-3} = (N-2) \cdot 500 \cdot 6^{N-3}$$

In the latter case, we have the diagrams

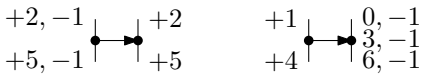

In the left diagram, there are five ways to arrange the quarks at either site and two ways to arrange the antiquark. The left diagram has the multiplicity $F_1 = 2 \cdot 5 \cdot 5 = 50$. There are five ways to create a quark occupation with $+1$ or $+4$. There are six ways to create a quark occupation with $+0$,$+3$ or $+6$. Hence the right diagram has the multiplicity $F_2 = 5 \cdot (2 \cdot 6) = 60$. In total, we have

$$\gamma_3 = 2 \cdot F_1 \cdot 6^{N-2} + 2 \cdot F_2 \cdot 6^{N-2} = 2(F_1 + F_2) \cdot 6^{N-2} = 220 \cdot 6^{N-2}$$

for the latter case.

We summarize the above:

$$\Delta_1^{(1)} = \begin{cases} \sigma a, & 2\sigma a \leq 2m_\mathrm{q} \\ 2m_\mathrm{q}, & \sigma a > 2m_\mathrm{q} \end{cases}$$

$$N_1^{(1)} = \begin{cases} \gamma_1, & \sigma a < 2m_\mathrm{q} \\ \gamma_1 + \gamma_2, & \sigma a = 2m_\mathrm{q} \\ \gamma_2, & \sigma a > 2m_\mathrm{q} \end{cases}$$

$$= \begin{cases} 100 \cdot 6^{N-2} + 500 \cdot 6^{N-3} + (2500(N-4) + 625) \cdot 6^{N-4}, & \sigma a < 2m \\ 100 \cdot 6^{N-2} + 500 \cdot 6^{N-3} & \\ \quad + (2500(N-4) + 625) \cdot 6^{N-4} + (N-2) \cdot 500 \cdot 6^{N-3}, & \sigma a = 2m_\mathrm{q} \\ (N-2) \cdot 500 \cdot 6^{N-3}, & \sigma a > 2m_\mathrm{q} \end{cases}$$

$$= \begin{cases} 100 \cdot 6^{N-2} + 500 \cdot 6^{N-3} + (2500(N-4) + 625) \cdot 6^{N-4}, & \sigma a < 2m_\mathrm{q} \\ 100 \cdot 6^{N-2} + (N-1) \cdot 500 \cdot 6^{N-3} & \\ \quad + (2500(N-4) + 625) \cdot 6^{N-4} \quad , & \sigma a = 2m_\mathrm{q} \\ (N-2) \cdot 500 \cdot 6^{N-3}, & \sigma a > 2m_\mathrm{q} \end{cases}$$

$\Delta_0^{(0)}$**:** Here, we minimize the energy by the configurations with no flux tube and no antiquarks. Hence, we only have on-site occupations and, therefore,

$$\Delta_0^{(0)} = 0$$
$$N_0^{(0)} = 6^N$$

$\Delta_0^{(1)}$: The first excitation can be achieved by either adding one flux tube or one antiquark. Hence, we distinguish again the cases $\sigma a/m_\mathrm{q} < 2$, $\sigma a/m_\mathrm{q} = 2$ and $\sigma a/m_\mathrm{q} > 2$.

Placing a flux tube means that, we have the following diagram

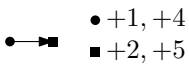

The diagram has a multiplicity of 25. It can occur at any link except for the links of S and in both orientations. Hence,

$$\gamma_1 = 2 \cdot 25 \cdot (N-2) \cdot 6^{N-1} = 50(N-2) \cdot 6^{N-2}$$

Adding an antiquark at a site is possible as long as we create an on-site net occupation number of either 0, 3 or 6. We have the possibilities to occupy the site with 1 or 4 quarks. The antiquark can be occupied with two possibilities and we have five possibilities for the quarks. This implies 10 possibilities for an antiquark at a site: $\gamma_2 = 6^{N-1} \cdot 10 \cdot N$

In total:

$$\begin{aligned}
\Delta_0^{(1)} &= \begin{cases} \sigma a, & \sigma a \leq 2m_\mathrm{q} \\ 2m_\mathrm{q}, & \sigma a > 2m_\mathrm{q} \end{cases} \\
N_0^{(1)} &= \begin{cases} \gamma_1, & \sigma a < 2m_\mathrm{q} \\ \gamma_1 + \gamma_2, & \sigma a = 2m_\mathrm{q} \\ \gamma_2, & \sigma a > 2m_\mathrm{q} \end{cases} \\
&= \begin{cases} 50(N-2) \cdot 6^{N-2}, & \sigma a < 2m_\mathrm{q} \\ 50(N-2) \cdot 6^{N-1} + 6^{N-1} \cdot 10 \cdot N, & \sigma a = 2m_\mathrm{q} \\ 6^{N-1} \cdot 10 \cdot N, & \sigma a > 2m_\mathrm{q} \end{cases}
\end{aligned}$$

$\frac{\mu}{m_\mathrm{q}} > 1$

$\Delta_1^{(0)}$: Again, we need one flux tube to ensure the constrains. Now, the insertion of quarks even decreases the energy. The minimal energy which could be achieved without any restriction is nothing else than a lattice fully occupied with quarks and without any flux tubes or antiquarks. This is the configuration we work relative to. The general form is

$$\begin{aligned}
\Delta &= -(6N-r)\underbrace{(\mu - m_\mathrm{q})}_{>0} + \overline{n}_\mathrm{q}(m_\mathrm{q} + \mu) + u\sigma a \\
&= -6N(\mu - m_\mathrm{q}) + r(\mu - m_\mathrm{q}) \\
&\qquad + \overline{n}_\mathrm{q}(\mu + m_\mathrm{q}) + u\sigma a > -6N \cdot (\mu - m_\mathrm{q}) = \Delta_\mathrm{min}
\end{aligned}$$

with $u \geq 1, r \geq 1$. Now, to ensure the $\mathbb{Z}_3$-Gauss law, we have to remove the minimal amount of quarks and add the minimal amount of antiquarks. We have multiple possibilities:

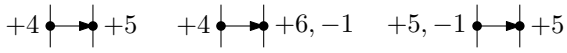

The first diagram increases Δ_{min} by $3(\mu - m_{\text{q}}) + \sigma a = 3\mu - 3m_{\text{q}} + \sigma a$. The second and third diagram remove two quarks and add one antiquark. This increases Δ_{min} by $2(\mu - m_{\text{q}}) + (\mu + m_{\text{q}}) + \sigma a = 3\mu - m_{\text{q}} + \sigma a$. Hence, the first diagram is the state of lowest energy compatible with the constrains. At a site, four quarks can be arranged like

$$(3,1) \quad (1,3) \quad (2,2)$$

and five quarks can be arranged like

$$(3,2) \quad (2,3)$$

The multiplicity of the first diagram is $D = 3 \cdot 2 = 6$. Hence, $N_1 = 2 \cdot D = 12$:

$$\begin{aligned} \Delta_1^{(0)} &= \Delta_{\text{min}} + 3(\mu - m_{\text{q}}) + \sigma a \\ N_1^{(0)} &= 12 \end{aligned}$$

$\Delta_1^{(1)}$**:** We take Δ_{min} and insert one flux tube at a link of S^*. From there on, we have to create a valid configuration. The energetically minimal way would be to remove three quarks. Nevertheless, we search for the first excitation. Hence, the next minimal possibilities are to remove two quarks and add one antiquark or to remove three quarks and add one flux tube. We have

$$\Delta_1^{(1)} = \begin{cases} \Delta_{\text{min}} + 3(\mu - m_{\text{q}}) + 2\sigma a, \sigma a \leq 2m_{\text{q}} \\ \Delta_{\text{min}} + 2(\mu - m_{\text{q}}) + (\mu + m_{\text{q}}) + \sigma a, \sigma a > 2m_{\text{q}} \end{cases}$$

If $\sigma a < 2m_{\text{q}}$, we have the diagrams

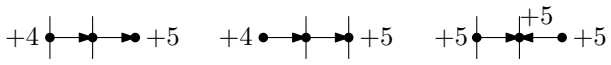

The first two diagrams have a multiplicity of $D_1 = D_2 = 6$. The third diagram has a multiplicity of $D_3 = 2^3 = 8$. This gives

$$\gamma_1 = 2 \cdot D_1 + 2 \cdot D_2 + 2 \cdot D_3 = 40$$

If $\sigma a > 2$,, we have the diagrams

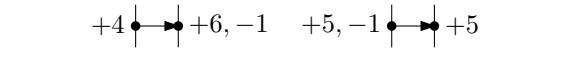

The first diagram has the multiplicity $F_1 = 3 \cdot 2 = 6$ and the second diagram has the multiplicity $F_2 = 4 \cdot 2 = 8$. Therefore,

$$\gamma_2 = 2F_1 + 2F_2 = 12 + 16 = 28\,.$$

We conclude

$$\Delta_1^{(1)} = \begin{cases} \Delta_{\min} + 3(\mu - m_{\mathrm{q}}) + 2\sigma a, & \sigma a \leq 2m_{\mathrm{q}} \\ \Delta_{\min} + 2(\mu - m_{\mathrm{q}}) + (\mu + m_{\mathrm{q}}) + \sigma a, & \sigma a > 2m_{\mathrm{q}} \end{cases}$$

$$N_1^{(1)} = \begin{cases} \gamma_1, & \sigma a < 2m_{\mathrm{q}} \\ \gamma_1 + \gamma_2, & \sigma a = 2m_{\mathrm{q}} \\ \gamma_2, & \sigma a > 2m_{\mathrm{q}} \end{cases} = \begin{cases} 40, & \sigma a < 2m_{\mathrm{q}} \\ 68, & \sigma a = 2m_{\mathrm{q}} \\ 28, & \sigma a > 2m_{\mathrm{q}} \end{cases}$$

$\Delta_1^{(0)}$**:** Here, we just have $\Delta_1' = \Delta_{\min}$ and $N_0^{(0)} = 1$

$\Delta_0^{(1)}$**:** Here, we just have all combinations where we remove one baryon from $\Delta_{\min}$. At a site where we remove a baryon only three quarks remain with the multiplicity of four: $(3,0), (0,3), (2,1), (1,2)$. In total, we have

$$\Delta_0^{(1)} = \Delta_{\min} + 3(\mu - m_{\mathrm{q}})$$
$$N_0^{(1)} = 4N$$

B.6 Worm algorithm

We describe the worm algorithm for our flux-tube model presented in Section 6.1. We use a modified algorithm which is based on [200–203]. The worm algorithm updates a flux-tube configuration fulfilling the local $\mathbb{Z}_3$-Gauss law by changing the local quark numbers or the flux-tube variables. The resulting configuration also fulfills the local $\mathbb{Z}_3$-Gauss law. For the purpose of the algorithm's formulation, we take the antiquark numbers to be negative $\overline{n}_{i,s} \in \{-3, \ldots, 0\}$ such that the net-quark number at a site reads

$$q_i = \sum_s (n_{i,s} + \overline{n}_{i,s})$$

instead of

$$q_i = \sum_s (n_{i,s} - \overline{n}_{i,s}) \ .$$

The update procedure is shown in Figure B.1. For the moment, let us ignore the initial and final sweeps changing the quark sector and the possibility of cyclic changes in the first step. The algorithm starts at some random site x_0 of the spatial lattice where it decides to either change an occupation number or a flux-tube variable by a random value $w \in \{-1, 1\}$. Such a change is accepted with the standard Metropolis acceptance probability. Changes in occupation numbers which would exceed the maximal or minimal possible values are always rejected. Adding w to a flux-tube variable is always treated as a $\mathbb{Z}_3$-addition.

If the change at the site x_0 is accepted, the local $\mathbb{Z}_3$-Gauss law becomes violated at the site because if Gauss's law was initially given, we either have

$$q_{x_0} + w \neq \sum_{j \sim x_0} l_{\langle j, x_0 \rangle} \mod 3$$

in the case of a modified occupation number or

$$q_{x_0} \neq (l_{\langle x_0, j \rangle} +_3 w) + \sum_{\substack{j' \sim x_0 \\ j \neq j'}} l_{\langle x_0, j' \rangle} \mod 3$$

in the case of modified flux tube variable $l_{\langle x_0, j \rangle}$. Hence, the algorithm has to continue changing flux-tube variables and occupation numbers till Gauss's law is restored. To achieve this, the algorithm moves to another site, imposes some changes, moves to the next site impose changes there and so on till it reaches the original site x_0 and either changes an occupation number by $-w$ or a flux-tube variable $l_{\langle j, x_0 \rangle}$ incident to x_0 by w. This final change restores Gauss's law at x_0. On the way to x_0, all violations of Gauss's law at other sites $x \neq x_0$ are immediately compensated in the next step of the algorithm.

Unfortunately this update procedure is not enough because it does not allow any changes in the total net-quark number. The algorithm is stuck in the quark-number sector $q = 3k, k \in \mathbb{Z}$ of the initial configuration because whenever an occupation number is changed by a value w at a site i, a corresponding occupation number is changed by $-w$ at some other site j. Therefore, we have to add additional update steps which can change the quark-number sector. We allow therefore cyclic changes of occupation numbers, i.e. transitions from $0 \to 3$, $3 \to 0$, $0 \to -3$ and $-3 \to 0$, in the first step of an update procedure. Such kind of changes are essentially the insertion or removal of a baryon or anti-baryon at the site x_0. Additionally, the algorithm randomly proposes to insert such baryons or anti-baryons at N_s randomly chosen sites in the beginning and end of the update procedure if it is possible.

Detailed balance

We, now, prove the detailed balance property for our worm algorithm. The proof is based on the proof given in [204]. One update step is a sequence of smaller steps taken by the algorithm to generate the next configuration. Such a sequence is generally of the form

$$\gamma = \left(\prod_{i=1}^{p \leq N_\mathrm{s}} [y_i, n_{y_i}^{\pm 3}] \right), x_0, \langle x_0, x_1 \rangle, (x_1, n_1^+), (x_2, n_2^-), \langle x_2, x_3 \rangle, x_3, \langle x_3, x_4 \rangle,$$
$$\ldots, \langle x_n, x_0 \rangle, x_0, \left(\prod_{i=1}^{m \leq N_\mathrm{s}} [\tilde{y}_i, n_{\tilde{y}_i}^{\pm 3}] \right),$$

or

$$\gamma = \left(\prod_{i=1}^{p \leq N_\mathrm{s}} [y_i, n_{y_i}^{\pm 3}] \right), (x_0, n_0^{\pm 3})_w, \left(\prod_{i=1}^{m \leq N_\mathrm{s}} [\tilde{y}_i, n_{\tilde{y}_i}^{\pm 3}] \right)$$

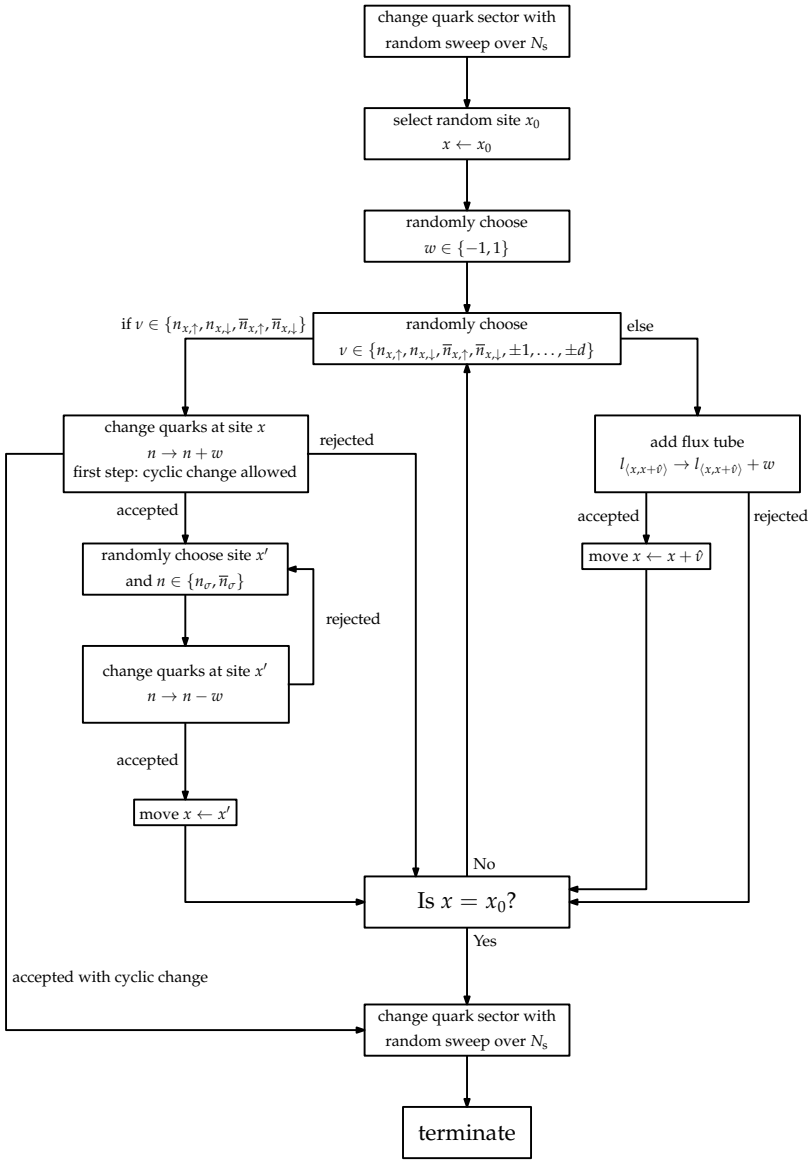

Figure B.1: One update step of the worm algorithm.

where the product is to be interpreted as

$$\left(\prod_{i=1}^{p\leq|\Lambda_d|}[y_i,n_{y_i}^{\pm 3}]\right)=[y_1,n_{y_1}^{\pm 3}],\ldots,[y_k,n_{y_k}^{\pm 3}]\,.$$

The different parts of a sequence are

1. $(x,\langle x,y\rangle,y)_w$ for updating the flux-tube variable $l_{\langle x,y\rangle}$ by adding w,
2. $(x,n^+)_w$ for updating a (anti-)quark number variable n at a site x by adding the value w,
3. $(x,n^-)_w$ for updating a (anti-)quark number variable n at a site x by adding the value $-w$,
4. $(x,n^{\pm 3})_w$ for updating a (anti-)quark number variable n at a site x by adding the value w and inducing a cyclic change of the quark number, i.e. a transition of the form $0\to 3$, $0\to -3$, $-3\to 0$ or $3\to 0$ and
5. $[x,n^{\pm 3}]$ for updating a (anti-)quark number variable n at a site x by adding the value ± 3. This step can only happen at the beginning or end of the update procedure.

We use following rules to concatenate successive steps:

$$\begin{aligned}(x,\langle x,y\rangle,y)_w,(y,\langle y,z\rangle,z)_w &\longrightarrow (x,\langle x,y\rangle,y,\langle y,z\rangle,z)_w\,,\\ (x,\langle x,y\rangle,y)_w,(y,n^{\pm})_w &\longrightarrow (x,\langle x,y\rangle,(y,n^{\pm}))_w\,,\\ (x,n^{\pm})_w,(x,\langle x,y\rangle,y)_w &\longrightarrow ((x,n^{\pm}),\langle x,y\rangle,y)_w\,.\end{aligned}$$

Furthermore, we might drop the subscript w if it is not explicitly needed. An update sequence γ has a time dependence $\gamma(t)$ giving the t-th step of the sequence, e.g. $\gamma(t)=(x,\langle x,y\rangle,y)_w$. Excluding the initial and final sweeps, we have the inner part of a sequence denoted by $\gamma_w(t)\,,t\in\{p+1,\ldots,t_{\max}+p\}$. The initial and final updates are stated as $\gamma_{\mathrm{B}}(i)\,,i\in\{1,\ldots,p\}$ and $\gamma_{\mathrm{E}}(i)\,,i\in\{t_{\max}+1,\ldots,t_{\max}+p+m\}$. We denote with Θ the set of all possible sequences γ of the algorithm. There is also an empty sequence $\lambda=\{\}$ where no changes are made. Also, we can have sequences without the inner part $\gamma_w(t)$, initial or final updates.

For each $\gamma\in\Theta$, we define the inverse sequence γ^{-1} by

$$\begin{aligned}\gamma^{-1}=&\left(\prod_{i=m}^{1}[\tilde{y}_i,n_{\tilde{y}_i}^{\mp 3}]\right),x_0,\langle x_0,x_n\rangle,\\ &\ldots,\langle x_4,x_3\rangle,x_3,\langle x_3,x_2\rangle,(x_2,n_2^+),(x_1,n_1^-),\langle x_1,x_0\rangle,x_0,\left(\prod_{i=p}^{1}[y_i,n_{y_i}^{\mp 3}]\right)\end{aligned}$$

or

$$\gamma^{-1}=\left(\prod_{i=m}^{1}[\tilde{y}_i,n_{\tilde{y}_i}^{\mp 3}]\right),(x_0,n_0^{\pm 3})_{-w},\left(\prod_{i=p}^{1}[y_i,n_{y_i}^{\mp 3}]\right)\,.$$

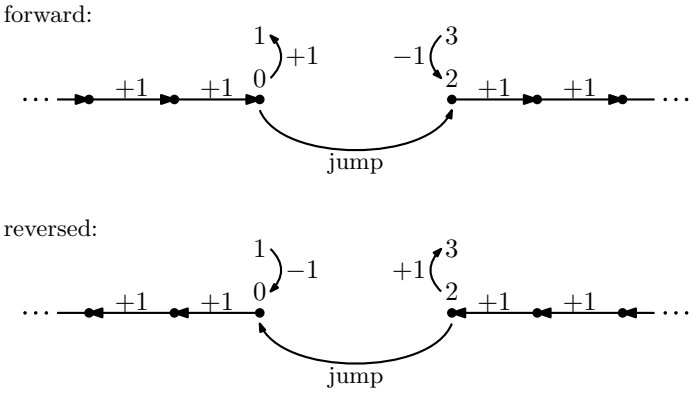

Figure B.2: Illustration of a sequence $\gamma_w(t)$ and its reverse $\gamma_w^{-1}(t)$.

The inverse λ^{-1} of the empty sequence λ is just the empty sequence itself: $\lambda^{-1} = \lambda$. Along a sequence $\gamma_w(t)$ the algorithm updates a path of flux-tube variables and jumps from a site i to another site j if the occupation number has been changed at i. This is the reason why the algorithm is denoted a worm algorithm. The algorithm inserts worms along which flux-tube variables are updated. The inverse sequence $\gamma_w^{-1}(t)$ follows the sequence $\gamma_w(t)$ in reverse direction and adds the same value w to the flux-tube variables as in the forward direction. The reverse path $\gamma_w^{-1}(t)$ is illustrated in Figure B.2.

An update step transforms a flux-tube configuration Γ into a configuration Γ' with the probability $P(\Gamma \to \Gamma')$. If $P(\Gamma \to \Gamma') > 0$ then their exists a sequence γ which can transform Γ into Γ'. The inverse sequence γ^{-1} transforms Γ' into Γ and, therefore, $P(\Gamma' \to \Gamma) > 0$. For $P(\Gamma \to \Gamma') > 0$, the detailed balance property reads

$$\frac{P(\Gamma \to \Gamma')}{P(\Gamma' \to \Gamma)} = \frac{P(\Gamma')}{P(\Gamma)} \,.$$

If this holds for all $P(\Gamma \to \Gamma') > 0$ then the stationary condition

$$\sum_{\Gamma} P(\Gamma \to \Gamma') P(\Gamma) = P(\Gamma')$$

is obviously fulfilled. The transition probability $P(\Gamma \to \Gamma')$ can be written as

$$P(\Gamma \to \Gamma') = \sum_{\gamma \in \Theta} P_\gamma(\Gamma \to \Gamma') \,,$$

where $P_\gamma(\Gamma \to \Gamma')$ is the probability that the algorithm takes the path γ and yields the transition from Γ to Γ'. Consequently, $P_\gamma(\Gamma \to \Gamma') = 0$ if γ does not give the transition $\Gamma \to \Gamma'$. To prove the detailed balance property for $P(\Gamma \to \Gamma') > 0$ it is sufficient to prove

$$\frac{P_\gamma(\Gamma \to \Gamma')}{P_{\gamma^{-1}}(\Gamma' \to \Gamma)} = \frac{P(\Gamma')}{P(\Gamma)} \tag{B.1}$$

for all $P_\gamma(\Gamma \to \Gamma') > 0$. This is because if Equation (B.1) holds, we can write

$$\underbrace{\sum_\gamma P_\gamma(\Gamma \to \Gamma')}_{=P(\Gamma\to\Gamma')} = \frac{P(\Gamma')}{P(\Gamma)} \sum_\gamma P_{\gamma^{-1}}(\Gamma' \to \Gamma)\,.$$

The inverse map $\bullet^{-1}$ is a bijective map from Θ to Θ, therefore, we have

$$\sum_\gamma P_{\gamma^{-1}}(\Gamma' \to \Gamma) = \sum_\gamma P_\gamma(\Gamma' \to \Gamma) = P(\Gamma' \to \Gamma)$$

which yields the detailed balance property

$$P(\Gamma \to \Gamma') = \frac{P(\Gamma')}{P(\Gamma)} P(\Gamma' \to \Gamma)\,.$$

We, now, prove Equation (B.1). For the empty sequence λ, we have

$$\frac{P_\lambda(\Gamma \to \Gamma)}{P_\lambda(\Gamma \to \Gamma)} = 1 = \frac{P(\Gamma)}{P(\Gamma)}$$

because there is no other possibility. The empty sequence always creates a transition from Γ to Γ itself. Consider some non-empty sequence $\gamma \neq \lambda$ with $P_\gamma(\Gamma \to \Gamma') > 0$. We have

$$P_\gamma(\Gamma \to \Gamma') = \left(\prod_{t=1}^{p} p(\Gamma_{t-1}, \gamma_\mathrm{B}(t))\right) \left(\prod_{t=p+1}^{t_\mathrm{max}+p} p(\Gamma_{t-1}, \gamma_w(t))\right) \times \left(\prod_{t=t_\mathrm{max}+p+1}^{t_\mathrm{max}+p+m} p(\Gamma_{t-1}, \gamma_\mathrm{E}(t))\right)$$

where the sequence Γ_t represents the intermediate configuration after the t-th update step. We define $\Gamma_0 = \Gamma$ and $\Gamma_{t_\mathrm{max}+p+m} = \Gamma'$. The probability $p(\Gamma_{t-1}, \gamma(t))$ is the probability that the algorithm takes the step $\gamma(t)$ on the configuration Γ_{t-1}. For our algorithm, $p(\Gamma_{t-1}, \gamma(t))$ has the general form

$$\begin{aligned} p(\Gamma_{t-1}, \gamma(t)) &= \underbrace{\left(\sum_{n=0}^{\infty} p_\mathrm{rej.}^n(\Gamma_{t-1}, \gamma(t))\right)}_{\text{all possible trajectories of rejection}} \varrho(\Gamma_{t-1}, \gamma(t)) \\ &= \frac{1}{1 - p_\mathrm{rej.}(\Gamma_{t-1}, \gamma(t))} \varrho(\Gamma_{t-1}, \gamma(t)) \end{aligned}$$

with $p_\mathrm{rej.}(\Gamma, \gamma_\mathrm{B}(t)) = p_\mathrm{rej.}(\Gamma, \gamma_\mathrm{E}(t)) = 0$, $p_\mathrm{rej.}(\Gamma, \gamma_w(p+1)) = 0$ and the probability $\varrho(\Gamma_{t-1}, \gamma(t))$ of accepting the step $\gamma(t)$. There is one exception to this form and that is for the first step of the inner sequence if it is not empty:

$$p(\Gamma_{t-1}, \gamma_w(p+1)) = \frac{1}{2} \varrho(\Gamma_{t-1}, \gamma_w(p+1))\,.$$

The factor $\frac{1}{2}$ considers the random choice $w = \pm 1$ for the inner sequence.

The probability $p_{\text{rej.}}(\Gamma_{t-1}, \gamma(t))$ is the total probability that a change to Γ_{t-1} by any possible step is rejected. Because once the algorithm is at some point $x \neq x_0$, it has to try to update local variables of x till it succeeds because otherwise Gauss's law will not be restored. Hence before $\gamma(t)$ was accepted, the algorithm might had rejected n different proposals before. Let us formulate $p(\Gamma, \gamma(t))$ for all steps:

$\gamma(t) = (x, \langle x, x+\hat{\mu}\rangle, x+\hat{\mu})_w\,, \mu \in \{\pm 1, \ldots, \pm d\}$**:** The acceptance probability is

$$\varrho(\Gamma_{t-1}, \gamma(t)) = \frac{1}{2d+4} \min\left(1, \frac{\mathrm{e}^{-\beta\sigma|l^{(t-1)}_{\langle x,x+\hat{\mu}\rangle}+3w|}}{\mathrm{e}^{-\beta\sigma|l^{(t-1)}_{\langle x,x+\hat{\mu}\rangle}|}}\right).$$

If $p_{\text{rej.}}(\Gamma_{t-1}, \gamma(t)) > 0$, we have

$$\begin{aligned}
1 - p_{\text{rej.}}(\Gamma_{t-1}, \gamma(t)) = {} & \frac{1}{2d+4} \sum_{\nu\in\{\pm 1,\ldots,\pm d\}} \min\left(1, \frac{\mathrm{e}^{-\beta\sigma|l^{(t-1)}_{\langle x,x+\hat{\nu}\rangle}+3w|}}{\mathrm{e}^{-\beta\sigma|l^{(t-1)}_{\langle x,x+\hat{\nu}\rangle}|}}\right) \\
& + \frac{1}{2d+4} \sum_{\sigma\in\{\downarrow,\uparrow\}} \min\left(1, \frac{\exp\left(-\beta m|n^{(t-1)}_{x,\sigma}+w| + \beta\mu(n^{(t-1)}_{x,\sigma}+w)\right)}{\exp\left(-\beta m|n^{(t-1)}_{x,\sigma}| + \beta\mu n^{(t-1)}_{x,\sigma}\right)}\right) \\
& \qquad \times \delta(0 \leq n_{x,\sigma} + w \leq 3) \\
& + \frac{1}{2d+4} \sum_{\sigma\in\{\downarrow,\uparrow\}} \min\left(1, \frac{\exp\left(-\beta m|\overline{n}^{(t-1)}_{x,\sigma}+w| + \beta\mu(\overline{n}^{(t-1)}_{x,\sigma}+w)\right)}{\exp\left(-\beta m|\overline{n}^{(t-1)}_{x,\sigma}| + \beta\mu\overline{n}^{(t-1)}_{x,\sigma}\right)}\right) \\
& \qquad \times \delta(-3 \leq \overline{n}_{x,\sigma} + w \leq 0)\,.
\end{aligned}$$

$\gamma(t) = (x, n^{+}_{x,\sigma})_w$**:** The acceptance probability is

$$\begin{aligned}
& \varrho(\Gamma_{t-1}, \gamma(t)) = \\
& \frac{1}{2d+4} \min\left(1, \frac{\exp\left(-\beta m|n^{(t-1)}_{x,\sigma}+w| + \beta\mu(n^{(t-1)}_{x,\sigma}+w)\right)}{\exp\left(-\beta m|n^{(t-1)}_{x,\sigma}| + \beta\mu n^{(t-1)}_{x,\sigma}\right)}\right) \\
& \qquad \times \delta(0 \leq n_{x,\sigma} + w \leq 3)
\end{aligned}$$

If $p_{\text{rej.}}(\Gamma_{t-1}, \gamma(t)) > 0$, we have

$$\begin{aligned}
1 - p_{\text{rej.}}(\Gamma_{t-1}, \gamma(t)) = {} & \frac{1}{2d+4} \sum_{\nu\in\{\pm 1,\ldots,\pm d\}} \min\left(1, \frac{\mathrm{e}^{-\beta\sigma|l^{(t-1)}_{\langle x,x+\hat{\nu}\rangle}+3w|}}{\mathrm{e}^{-\beta\sigma|l^{(t-1)}_{\langle x,x+\hat{\nu}\rangle}|}}\right) \\
& + \frac{1}{2d+4} \sum_{\sigma\in\{\downarrow,\uparrow\}} \min\left(1, \frac{\exp\left(-\beta m|n^{(t-1)}_{x,\sigma}+w| + \beta\mu(n^{(t-1)}_{x,\sigma}+w)\right)}{\exp\left(-\beta m|n^{(t-1)}_{x,\sigma}| + \beta\mu n^{(t-1)}_{x,\sigma}\right)}\right) \\
& \qquad \times \delta(0 \leq n_{x,\sigma} + w \leq 3) \\
& + \frac{1}{2d+4} \sum_{\sigma\in\{\downarrow,\uparrow\}} \min\left(1, \frac{\exp\left(-\beta m|\overline{n}^{(t-1)}_{x,\sigma}+w| + \beta\mu(\overline{n}^{(t-1)}_{x,\sigma}+w)\right)}{\exp\left(-\beta m|\overline{n}^{(t-1)}_{x,\sigma}| + \beta\mu\overline{n}^{(t-1)}_{x,\sigma}\right)}\right) \\
& \qquad \times \delta(-3 \leq \overline{n}_{x,\sigma} + w \leq 0)\,.
\end{aligned}$$

The same analysis applies analogously to $\gamma(t) = (x, \overline{n}^{+}_{x,\sigma})_w$.

$\gamma(t) = (x, n^{-}_{x,\sigma})_w$**:** The acceptance probability is

$$\begin{aligned}
&\varrho(\Gamma_{t-1}, \gamma(t)) = \\
&\frac{1}{4N_\mathrm{s}} \min\left(1, \frac{\exp\left(-\beta m|n^{(t-1)}_{x,\sigma} - w| + \beta\mu(n^{(t-1)}_{x,\sigma} - w)\right)}{\exp\left(-\beta m|n^{(t-1)}_{x,\sigma}| + \beta\mu n^{(t-1)}_{x,\sigma}\right)}\right) \\
&\qquad \times \delta(0 \leq n_{x,\sigma} - w \leq 3)
\end{aligned}$$

The rejection probability is

$$\begin{aligned}
&1 - p_{\mathrm{rej.}}(\Gamma_{t-1}, \gamma(t)) = \\
&+ \frac{1}{4N_\mathrm{s}} \sum_i \sum_{\sigma\in\{\uparrow,\downarrow\}} \min\left(1, \frac{\exp\left(-\beta m|n^{(t-1)}_{i,\sigma} - w| + \beta\mu(n^{(t-1)}_{i,\sigma} - w)\right)}{\exp\left(-\beta m|n^{(t-1)}_{i,\sigma}| + \beta\mu n^{(t-1)}_{i,\sigma}\right)}\right) \\
&\qquad \times \delta(0 \leq n_{i,\sigma} - w \leq 3) \\
&+ \frac{1}{4N_\mathrm{s}} \sum_i \sum_{\sigma\in\{\downarrow,\uparrow\}} \min\left(1, \frac{\exp\left(-\beta m|\overline{n}^{(t-1)}_{i,\sigma} - w| + \beta\mu(\overline{n}^{(t-1)}_{i,\sigma} - w)\right)}{\exp\left(-\beta m|\overline{n}^{(t-1)}_{i,\sigma}| + \beta\mu\overline{n}^{(t-1)}_{i,\sigma}\right)}\right) \\
&\qquad \times \delta(-3 \leq \overline{n}_{i,\sigma} - w \leq 0)\,.
\end{aligned}$$

$\gamma(t) = (x, n^{\pm 3}_{x,\sigma})_w$**:** In this case the probability $p_{\mathrm{rej.}}(\Gamma_{t-1}, \gamma(t))$ is always zero. Assume $n_{x,\sigma} + w$ induces a cyclic change $3 \to 0$. The acceptance probability is then

$$\varrho(\Gamma_{t-1}, \gamma(t)) = \frac{1}{4 \cdot N_\mathrm{s}} \min\left(1, \frac{\exp\left(-\beta m|n_{x,\sigma} - 3| + \beta\mu(n_{x,\sigma} - 3)\right)}{\exp\left(-\beta m|n_{x,\sigma}| + \beta\mu n_{x,\sigma}\right)}\right).$$

All other cases of cyclic changes and $\gamma(t) = (x, \overline{n}^{\pm 3}_{x,\sigma})_w$ are analogous.

$\gamma(t) = [x, n^{\pm 3}_{x,\sigma}]$**:** In this case the probability $p_{\mathrm{rej.}}(\Gamma_{t-1}, \gamma(t))$ is always zero. Assume a baryon is removed: $n_{x,\sigma} = 3 \to 0$. The acceptance probability is then

$$\varrho(\Gamma_{t-1}, \gamma(t)) = \frac{1}{2 \cdot 4 \cdot N_\mathrm{s}} \min\left(1, \frac{\exp\left(-\beta m|n_{x,\sigma} - 3| + \beta\mu(n_{x,\sigma} - 3)\right)}{\exp\left(-\beta m|n_{x,\sigma}| + \beta\mu n_{x,\sigma}\right)}\right).$$

The other possible cases are analogous.

As it is illustrated in Figure B.3, the step $\gamma(t)$ acts on the same configuration Γ_{t-1} as $\gamma^{-1}(t_{\max} + p + m - t + 2)$. We use all these properties to finalize the

proof of detailed balance:

$$\begin{aligned}
\frac{P_\gamma(\Gamma \to \Gamma')}{P_{\gamma^{-1}}(\Gamma' \to \Gamma)} &= \prod_{t=1}^{t_{\max}+p+m} \frac{p(\Gamma_{t-1}, \gamma(t))}{p(\Gamma_{t_{\max}+p+m-t+1}, \gamma^{-1}(t))} \\
&= \left(\prod_{t=1}^{p} \frac{p(\Gamma_{t-1}, \gamma_{\mathrm{B}}(t))}{p(\Gamma_{p-t+1}, \gamma_{\mathrm{E}}^{-1}(t + t_{\max} + m))} \right) \\
&\left(\prod_{t=p+1}^{t_{\max}+p} \frac{p(\Gamma_{t-1}, \gamma_w(t))}{p(\Gamma_{t_{\max}+2p+1-t}, \gamma_w^{-1}(t - p + m))} \right) \\
&\left(\prod_{t=t_{\max}+p+1}^{t_{\max}+p+m} \frac{p(\Gamma_{t-1}, \gamma_{\mathrm{E}}(t))}{p(\Gamma_{2(t_{\max}+p)+m-t}, \gamma_{\mathrm{B}}^{-1}(t - (t_{\max} + p)))} \right)
\end{aligned}$$

Let us evaluate each product separately. First consider

$$\prod_{t=1}^{p} \frac{p(\Gamma_{t-1}, \gamma_{\mathrm{B}}(t))}{p(\Gamma_{p-t+1}, \gamma_{\mathrm{E}}^{-1}(t + t_{\max} + m))} .$$

We rearrange the denominator with $t \to p - t + 1$:

$$\begin{aligned}
&\prod_{t=1}^{p} \frac{p(\Gamma_{t-1}, \gamma_{\mathrm{B}}(t))}{p(\Gamma_{p-t+1}, \gamma_{\mathrm{E}}^{-1}(t + t_{\max} + m))} \\
&= \prod_{t=1}^{p} \frac{p(\Gamma_{t-1}, \gamma_{\mathrm{B}}(t))}{p(\Gamma_{p-(p-t+1)+1}, \gamma_{\mathrm{E}}^{-1}((p - t + 1) + t_{\max} + m))} \\
&= \prod_{t=1}^{p} \frac{p(\Gamma_{t-1}, \gamma_{\mathrm{B}}(t))}{p(\Gamma_t, \gamma_{\mathrm{E}}^{-1}(t_{\max} + p + m + 1 - t))}
\end{aligned}$$

In this form, we see that $\gamma_{\mathrm{B}}(t)$ acts on the configuration Γ_{t-1} and $\gamma_{\mathrm{E}}^{-1}(t_{\max} + p + m + 1 - t)$ acts on Γ_t and undoes the changes of $\gamma_{\mathrm{B}}(t)$. This is nothing else than one Metropolis step and its reverse step. We, therefore, have

$$\begin{aligned}
\frac{p(\Gamma_{t-1}, \gamma_{\mathrm{B}}(t))}{p(\Gamma_t, \gamma_{\mathrm{E}}^{-1}(t_{\max} + p + m + 1 - t))} &= \frac{\min\left(1, \frac{\exp(-\beta m|n \pm 3| + \beta\mu(n \pm 3))}{\exp(-\beta m n + \beta\mu n)}\right)}{\min\left(1, \frac{\exp(-\beta m n + \beta\mu n)}{\exp(-\beta m|n \pm 3| + \beta\mu(|n| \pm 3))}\right)} \\
&= \frac{\exp\left(-\beta m|n \pm 3| + \beta\mu(n \pm 3)\right)}{\exp\left(-\beta m|n| + \beta\mu n\right)} = \frac{\mathrm{e}^{-\beta H(\Gamma_t)}}{\mathrm{e}^{-\beta H(\Gamma_{t-1})}}
\end{aligned}$$

Consequently, the first factor is

$$\prod_{t=1}^{p} \frac{p(\Gamma_{t-1}, \gamma_{\mathrm{B}}(t))}{p(\Gamma_{p-t+1}, \gamma_{\mathrm{E}}^{-1}(t + t_{\max} + m))} = \prod_{t=1}^{p} \frac{\mathrm{e}^{-\beta H(\Gamma_t)}}{\mathrm{e}^{-\beta H(\Gamma_{t-1})}} = \frac{\mathrm{e}^{-\beta H(\Gamma_p)}}{\mathrm{e}^{-\beta H(\Gamma_0)}} .$$

The third factor can be treated analogous to the first factor and, therefore, we have

$$\prod_{t=t_{\max}+p+1}^{t_{\max}+p+m} \frac{p(\Gamma_{t-1}, \gamma_{\mathrm{E}}(t))}{p(\Gamma_{2(t_{\max}+p)+m-t}, \gamma_{\mathrm{B}}^{-1}(t - (t_{\max} + p)))} = \frac{\mathrm{e}^{-\beta H(\Gamma_{t_{\max}+p+m})}}{\mathrm{e}^{-\beta H(\Gamma_{t_{\max}+p})}} .$$

The second factor is a little bit more complicated. We first consider the denominator separately:

$$\prod_{t=p+1}^{t_{\max}+p} \frac{p(\Gamma_{t-1}, \gamma_w(t))}{p(\Gamma_{t_{\max}+2p+1-t}, \gamma_w^{-1}(t-p+m))} = \left(\prod_{t=p+1}^{t_{\max}+p} p(\Gamma_{t-1}, \gamma_w(t))\right) \left(\prod_{t=p+1}^{t_{\max}+p} \frac{1}{p(\Gamma_{t_{\max}+2p+1-t}, \gamma_w^{-1}(t-p+m))}\right).$$

We use the substitution $t = t_{\max} + 2p + 2 - t'$ with $t' \in \{p+2, \ldots, t_{\max}+p+1\}$:

$$\begin{aligned}
&\prod_{t=p+1}^{t_{\max}+p} \frac{p(\Gamma_{t-1}, \gamma_w(t))}{p(\Gamma_{t_{\max}+2p+1-t}, \gamma_w^{-1}(t-p+m))} \\
&= \left(\prod_{t=p+1}^{t_{\max}+p} p(\Gamma_{t-1}, \gamma_w(t))\right) \left(\prod_{t'=p+2}^{t_{\max}+p+1} \frac{1}{p(\Gamma_{t'-1}, \gamma_w^{-1}(t_{\max}+p+m+2-t'))}\right) \\
&= \frac{p(\Gamma_p, \gamma_w(p+1))}{p(\Gamma_{t_{\max}+p}, \gamma_w^{-1}(m+1))} \prod_{t=p+2}^{t_{\max}+p} \frac{p(\Gamma_{t-1}, \gamma_w(t))}{p(\Gamma_{t-1}, \gamma_w^{-1}(t_{\max}+p+m+2-t))}.
\end{aligned}$$

The probabilities of the first ratio only contains the first steps of the inner sequences γ and γ^{-1}. Therefore the rejection probability is not part of these ratios. Therefore, we have

$$\begin{aligned}
&\prod_{t=p+1}^{t_{\max}+p} \frac{p(\Gamma_{t-1}, \gamma_w(t))}{p(\Gamma_{t_{\max}+2p+1-t}, \gamma_w^{-1}(t-p+m))} \\
&= \frac{\varrho(\Gamma_p, \gamma_w(p+1))}{\varrho(\Gamma_{t_{\max}+p}, \gamma_w^{-1}(m+1))} \prod_{t=p+2}^{t_{\max}+p} \frac{1-p_{\text{rej.}}(\Gamma_{t-1}, \gamma_w^{-1}(t_{\max}+p+m+2-t))}{1-p_{\text{rej.}}(\Gamma_{t-1}, \gamma_w(t))} \\
&\qquad \frac{\varrho(\Gamma_{t-1}, \gamma_w(t))}{\varrho(\Gamma_{t-1}, \gamma_w^{-1}(t_{\max}+p+m+2-t))}.
\end{aligned}$$

The ratio of rejection probabilities is one because $p_{\text{rej.}}(\Gamma_{t-1}, \gamma_w^{-1}(t_{\max}+p+m+2-t)) = p_{\text{rej.}}(\Gamma_{t-1}, \gamma_w(t))$. To see this, we just have to take a look at Figure B.4. For the update step $\gamma(t+1)$ acting on Γ_t there is a corresponding update step $\gamma^{-1}(t_{\max}+p+m+1-t)$ also acting on Γ_t. From the figure we notice that the possible steps which could have been rejected before Γ_t are the same for $\gamma(t+1)$ and $\gamma^{-1}(t_{\max}+p+m+1-t)$. Therefore, the rejection probabilities are identical. We now have

$$\begin{aligned}
&\prod_{t=p+1}^{t_{\max}+p} \frac{p(\Gamma_{t-1}, \gamma_w(t))}{p(\Gamma_{t_{\max}+2p+1-t}, \gamma_w^{-1}(t-p+m))} \\
&= \frac{\varrho(\Gamma_p, \gamma_w(p+1))}{\varrho(\Gamma_{t_{\max}+p}, \gamma_w^{-1}(m+1))} \prod_{t=p+2}^{t_{\max}+p} \frac{\varrho(\Gamma_{t-1}, \gamma_w(t))}{\varrho(\Gamma_{t-1}, \gamma_w^{-1}(t_{\max}+p+m+2-t))} \\
&= \prod_{t=p+1}^{t_{\max}+p} \frac{\varrho(\Gamma_{t-1}, \gamma_w(t))}{\varrho(\Gamma_t, \gamma_w^{-1}(t_{\max}+p+m+1-t))}.
\end{aligned}$$

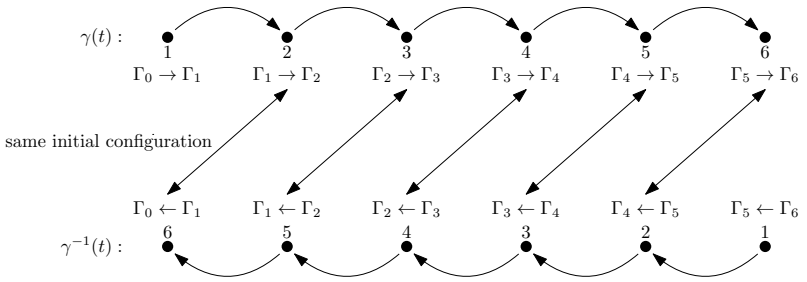

Figure B.3: The configuration Γ_{t-1} is acted upon by $\gamma(t)$ and $\gamma^{-1}(t_{\max}+p+m-t+2)$.

The step $\gamma_w(t_{\max}+p+m+1)$ undoes the step $\gamma_w(t)$ as can be seen from Figure B.4. Consequently, we again have ratios of a Metropolis acceptance probability and the probability of the inverse Metropolis step. This results in

$$\prod_{t=p+1}^{t_{\max}+p} \frac{p(\Gamma_{t-1}, \gamma_w(t))}{p(\Gamma_{t_{\max}+2p+1-t}, \gamma_w^{-1}(t-p+m))} = \frac{\mathrm{e}^{-\beta H(\Gamma_{t_{\max}+p})}}{\mathrm{e}^{-\beta H(\Gamma_p)}}\,.$$

Finally, we put everything together such that

$$\begin{aligned}\frac{P_\gamma(\Gamma \to \Gamma')}{P_{\gamma^{-1}}(\Gamma' \to \Gamma)} &= \prod_{t=1}^{t_{\max}+p+m} \frac{p(\Gamma_{t-1}, \gamma(t))}{p(\Gamma_{t_{\max}+p+m-t+1}, \gamma^{-1}(t))} \\ &= \frac{\mathrm{e}^{-\beta H(\Gamma_p)}}{\mathrm{e}^{-\beta H(\Gamma_0)}} \frac{\mathrm{e}^{-\beta H(\Gamma_{t_{\max}+p})}}{\mathrm{e}^{-\beta H(\Gamma_p)}} \frac{\mathrm{e}^{-\beta H(\Gamma_{t_{\max}+p+m})}}{\mathrm{e}^{-\beta H(\Gamma_{t_{\max}+p})}} \\ &= \frac{\mathrm{e}^{-\beta H(\Gamma_{t_{\max}+p+m})}}{\mathrm{e}^{-\beta H(\Gamma_0)}}\,.\end{aligned}$$

which concludes the proof. For the sake of completeness, a remark is made in the case of the inner sequence only consisting of the step $\gamma_w(p+1) = (x_0, n_0^{\pm 3})_w$. This case is included in the above proof because we then have $t_{\max} = 1$ and

$$\prod_{t=p+1}^{t_{\max}+p} \frac{p(\Gamma_{t-1}, \gamma_w(t))}{p(\Gamma_{t_{\max}+2p+1-t}, \gamma_w^{-1}(t-p+m))} = \frac{\varrho(\Gamma_p, \gamma_w(p+1))}{\varrho(\Gamma_{p+1}, \gamma_w^{-1}(m+1))} = \frac{\mathrm{e}^{-\beta H(\Gamma_{p+1})}}{\mathrm{e}^{-\beta H(\Gamma_p)}}$$

Ergodicity

For the algorithm to be valid, we have to prove ergodicity, i.e. we have to show that a configuration Γ' can be reached from any configuration Γ with a non-vanishing probability in at most M update steps. As described in the previous section, an update step is just a sequence of smaller steps and $P(\Gamma \to \Gamma') > 0 \implies P(\Gamma' \to \Gamma) > 0$. Hence, it is enough to show that we can reach the empty configuration $\{0, 0\}$ from any configuration Γ in at most M steps.

Consider some arbitrary site i with net-quark number q_i. Assume the site is connected with non-zero flux-tube variables to the rest of the lattice. The

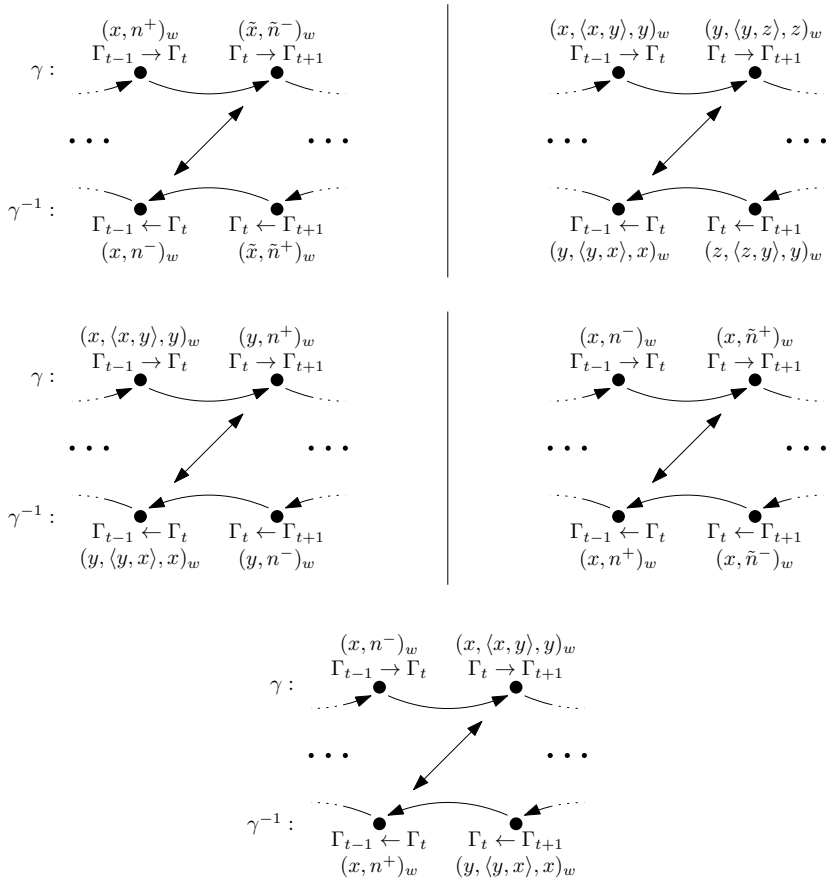

Figure B.4: All possible combinations of consecutive update steps in a sequence γ and its inverse γ^{-1}.

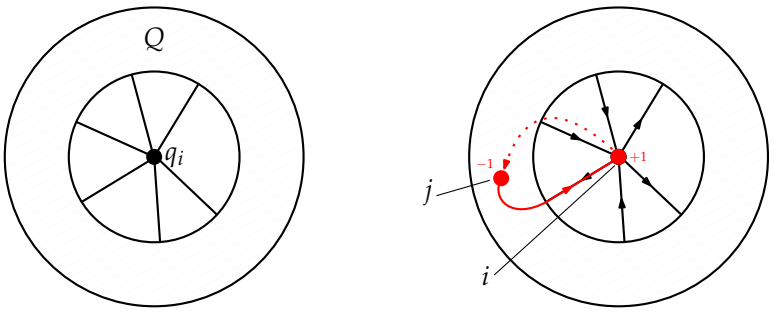

(a) Site i connected to the environment with non-zero flux-tube variables.

(b) Removing some flux tube variable connecting i with its environment.

Figure B.5: Illustration of a site i connected to its environment and the process of removing the connecting flux-tubes by means of the worm algorithm.

situation is illustrated in Figure B.5a. The environment will have the total net-quark number $Q = -q_i \mod 3$ because the total net-quark number must be a multiple of three. We now show that it is possible to remove all flux-tube variables and isolate the site i with a non-vanishing probability. For now we ignore the fact that the occupation numbers of (anti-)quarks are bounded from above and below. In this case, we can easily remove all non-zero flux-tube variables incident with i in at most $2d = 2 \cdot 3 = 6$ update steps. If $l_{\langle i,j \rangle} = w \neq 0$, we can remove the flux-tube variable by adding w to an occupation number at i, jump to another site j, add the value $-w$ to some occupation number at j, update all flux-tube variables with w along a path terminating at i and traversing over $\langle j, i \rangle$. This is demonstrated illustratively in Figure B.5b. Once, we have done this for all remaining non-zero flux-tube variables incident with i, the site i gets isolated. Because there are at most $2d = 6$ links incident with i, we need at most 6 update steps to isolate a site. We repeat the isolation procedure for all remaining sites such that for each site we ignore all sites which already have been isolated. They are not anymore traversed. In total we need at most $6N_\mathrm{s}$ update steps to isolate all sites from each other. The final configuration does not have any flux-tube variables left. All sites are occupied by $q_i = 0 \mod 3$. In practice the occupation number at a site is bounded from below and above. Therefore, we might find ourselves in the situation where we try to add $w \in \{-1, 1\}$ to an occupation number such that we exceed the bounds of the variable. This problem can be circumvented easily. When we insert a meson between i and j, we just prepare both sites with suitable update steps. We choose one occupation number n_i for i and one occupation number n_j for j. We use these variables to add w (at i) or $-w$ (at j). If any of these changes would exceed the corresponding bounds, we just use one update step to induce a cyclic change (e.g. $0 \to 3$) such that the variable is changed to its other bound. Hence, we need at most 3 update steps (preparing i, j and removing the flux-tube variable) to remove a flux-tube variable. We do not need more than $18N_\mathrm{s}$ steps to fully remove all flux-tube variables.

After removing all flux tube variables we are left with a configuration of isolated sites with $q_i = 0 \mod 3$. At a site i, the possible occupation numbers

for quarks and antiquarks are (neglecting the order of spin):

$(\{-3,-3\},\{3,3\})$ $(\{-3,-3\},\{3,0\})$ $(\{-3,-3\},\{2,1\})$
$(\{-3,-3\},\{0,0\})$ $(\{-3,-2\},\{3,2\})$ $(\{-3,-2\},\{2,0\})$
$(\{-3,-2\},\{1,1\})$ $(\{-3,-1\},\{3,1\})$ $(\{-3,-1\},\{2,2\})$
$(\{-3,-1\},\{1,0\})$ $(\{-3,0\},\{3,3\})$ $(\{-3,0\},\{3,0\})$
$(\{-3,0\},\{2,1\})$ $(\{-3,0\},\{0,0\})$ $(\{-2,-2\},\{3,1\})$
$(\{-2,-2\},\{2,2\})$ $(\{-2,-2\},\{1,0\})$ $(\{-2,-1\},\{3,3\})$
$(\{-2,-1\},\{3,0\})$ $(\{-2,-1\},\{2,1\})$ $(\{-2,-1\},\{0,0\})$
$(\{-2,0\},\{3,2\})$ $(\{-2,0\},\{2,0\})$ $(\{-2,0\},\{1,1\})$
$(\{-1,-1\},\{3,2\})$ $(\{-1,-1\},\{2,0\})$ $(\{-1,-1\},\{1,1\})$
$(\{-1,0\},\{3,1\})$ $(\{-1,0\},\{2,2\})$ $(\{-1,0\},\{1,0\})$
$(\{0,0\},\{3,3\})$ $(\{0,0\},\{3,0\})$ $(\{0,0\},\{2,1\})$
$(\{0,0\},\{0,0\})$

For each quark occupation number with $n = 3$ and each antiquark occupation number with $\overline{n} = 3$, we first use one update step with a cyclic change to get $n = 0$ and $\overline{n} = 0$. This will take at most 4 update steps for a site. Afterwards, we are left with the following possible occupation numbers at a site i:

$(\{0,0\},\{0,0\})$ $(\{0,0\},\{2,1\})$ $(\{0,-2\},\{0,2\})$
$(\{0,-2\},\{1,1\})$ $(\{0,-1\},\{0,1\})$ $(\{0,-1\},\{2,2\})$
$(\{-2,-2\},\{2,2\})$ $(\{-2,-2\},\{0,1\})$ $(\{-2,-1\},\{0,0\})$
$(\{-2,-1\},\{2,1\})$ $(\{-1,-1\},\{0,2\})$ $(\{-1,-1\},\{1,1\})$

We can remove all quarks and antiquarks by using insertions of mesons at a site (update with $+w$ and $-w$ at the site) or cyclic changes. The corresponding

updates are given by

$$
\begin{aligned}
&(\{0,0\},\{0,0\}) \\
(\{0,0\},\{2{+}1,1{-}1\}) &\to (\{0,0\},\{3,0\}) \to (\{0,0\},\{0,0\}) \\
(\{0,-2{+}1\},\{0,2{-}1\}) &\to (\{0,-1{+}1\},\{0,1{-}1\}) \to (\{0,0\},\{0,0\}) \\
(\{0,-2{+}1\},\{1{-}1,1\}) &\to (\{0,-1{+}1\},\{0,1{-}1\}) \to (\{0,0\},\{0,0\}) \\
(\{0,-1{+}1\},\{0,1{-}1\}) &\to (\{0,0\},\{0,0\}) \\
(\{0,-1{+}1\},\{2{-}1,2\}) &\to (\{0,0\},\{1{-}1,2{+}1\}) \\
&\to (\{0,0\},\{0,3\}) \to (\{0,0\},\{0,0\}) \\
(\{-2{+}1,-2\},\{2{-}1,2\}) &\to (\{-1{+}1,-2\},\{1{-}1,2\}) \\
&\to (\{0,-2{+}1\},\{0,2{-}1\}) \\
&\to (\{0,-1{+}1\},\{0,1{-}1\}) \to (\{0,0\},\{0,0\}) \\
(\{-2,-2{+}1\},\{0,1{-}1\}) &\to (\{-2{-}1,-1{+}1\},\{0,0\}) \\
&\to (\{-3,0\},\{0,0\}) \to (\{0,0\},\{0,0\}) \\
(\{-2{-}1,-1{+}1\},\{0,0\}) &\to (\{-3,0\},\{0,0\}) \to (\{0,0\},\{0,0\}) \\
(\{-2{-}1,-1{+}1\},\{2,1\}) &\to (\{-3,0\},\{2,1\}) \to (\{0,0\},\{2,1\}) \\
&\to (\{0,0\},\{2{+}1,1{-}1\}) \\
&\to (\{0,0\},\{3,0\}) \to (\{0,0\},\{0,0\}) \\
(\{-1{+}1,-1\},\{0,2{-}1\}) &\to (\{0,-1{+}1\},\{0,1{-}1\}) \to (\{0,0\},\{0,0\}) \\
(\{-1{+}1,-1\},\{1{-}1,1\}) &\to (\{0,-1{+}1\},\{0,1{-}1\}) \to (\{0,0\},\{0,0\})
\end{aligned}
$$

Hence, we need at most $4+5=9$ update steps to remove all quarks and antiquarks from a site i with $q_i = 0 \mod 3$. In total, we need $9N_\mathrm{s}$ update steps to transform a configuration of isolated sites into the empty lattice.

We therefore can reach the empty flux tube configuration $\{0,0\}$ in at most $18N_\mathrm{s} + 9N_\mathrm{s} = 27N_\mathrm{s}$ update steps. This implies we need at most $44N_\mathrm{s}$ update steps to reach a configuration Γ' from any configuration Γ proving ergodicity.

B.7 Fully-dynamic connectivity problem

The FDC-algorithm implements three functions for a graph: Determine whether two vertices i and j are connected by a path of edges, add an edge to the graph and remove an edge from the graph. The main problem is to implement an algorithm which provides these three functions in an efficient way. In our case, the graph is a bond configurations $\{b\}$ of the three dimensional spatial lattice, where the sites are the vertices and the set bonds are the edges. We implement the FDC-algorithm as described in [205] but specifically adapted to bond configurations $\{b\}$.

A bond configuration $\{b\}$ decomposes into clusters of pairwise connected sites i and j and their incident edges. An isolated site is considered to be a cluster of its own. Within a cluster of $\{b\}$, two vertices i and j might be connected by more than one path of edges. In this case, there are edges that we can remove without destroying the connectivity of the cluster. Making

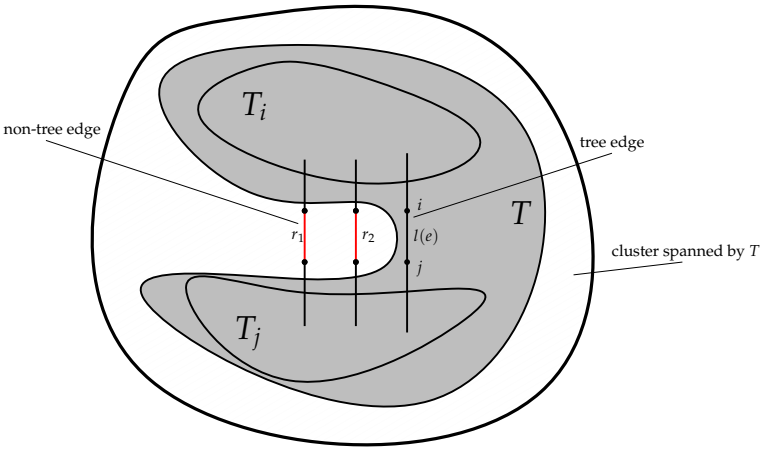

Figure B.6: Illustration of deleting a tree edge of level $l(e)$ where either r_1 or r_2 is promoted to a tree edge restoring the connectivity between the trees T_i and T_j.

all paths between vertices of a cluster unique gives a spanning tree T of the cluster. We use the terminology of [205]. Edges of a spanning tree are called tree edges. All other bonds are denoted non-tree edges. Defining a spanning tree for each cluster of the bond configuration $\{b\}$ gives the spanning forest which contains the full connectivity information. By storing each tree in an efficient way (see further below), we can check the connectivity of two vertices i and j with $\mathcal{O}(\ln N_\mathrm{s})$ operations. We just need to determine the roots of the trees which i and j are part of. If the roots match, both trees are identical and i and j are part of the same cluster.

Every edge e is associated with a level $l(e) \in \{0, 1, \ldots, \lfloor \log_2 N_\mathrm{s} \rfloor\}$. We define the subgraphs F_k of F with $k \in \{0, 1, \ldots, \lfloor \log_2 N_\mathrm{s} \rfloor\}$. A forest F_k includes all tree edges of $F = F_0$ which are of level k at least. The FDC-algorithm starts with a graph containing no edges and maintains the following invariants whenever an edge is removed or inserted:

1. F is a maximal spanning forest: The endpoints i and j of a non-tree edge $e = \{i, j\}$ are not only connected in F but they are also connected in $F_{l(e)}$. In other words, the endpoints of the non-tree edges are connected by a path in F consisting of edges with level $l(e)$ at least.

2. Every tree of a forest F_i contains at most $\lfloor N_\mathrm{s}/2^i \rfloor$ vertices.

Inserting an edge $e = \{i, j\}$ is easy. If the endpoints i and j are already connected, e is inserted, its level is set to zero and it is declared to be a non-tree edge. If the endpoints i and j are not already connected, e is inserted, its level is set to zero, it is declared to be a tree edge and the spanning trees T_i and T_j of the respective clusters C_i and C_j, i and j are part of, are connected in the forest $F = F_0$ at the edge e forming a new cluster spanned by the tree $T \subseteq F$. T is then made of the spanning trees T_i, T_j and the edge e. This process evidently does not change the two invariants.

Deleting an edge $e = \{i, j\}$ is however more involved. For a non-tree edge, we face no difficulties because it can be deleted without changing the invariants or the connectivity of the graph. A tree edge might cause more problems as illustrated in Figure B.6. When a tree edge $e = \{i, j\}$ of a tree T spanning a cluster C is removed, the tree decomposes into two trees T_i and T_j, where T_i contains the endpoint i and T_j contains the endpoint j. The tree T_i (T_j) spans a cluster C_i (C_j) made of all tree edges of T_i (T_j) and all non-tree edges which fully lie in C_i (C_j). There are now two possibilities. Prior to removing the tree edge e, the cluster C was made of C_i and C_j solely connected by the tree edge e, or the cluster C was made of C_i and C_j connected by the tree edge e and non-tree edges between C_i and C_j. The former case just means that we have no loss about the connectivity information by removing the tree edge. The latter case means that the simple removal of e does not give correct spanning trees because C_i and C_j are actually still connected to each other and we have just removed one edge from the otherwise unchanged cluster C. One of the non-tree edges has to be promoted to a tree edge reestablishing a valid spanning tree T of C.

The FDC-algorithm removes a tree edge e with level $k = l(e)$ in the following way. To keep the first invariant, we must search for a replacement edge beginning at level k. As an example, consider Figure B.6. Removing the edge e means that we have to replace it with one of the non-tree edges r_1 or r_2 and insert the replacement at the highest possible level. Assume $l(r_1) < l(r_2)$. Due to the first invariant, we actually must have $l(r_2) \leq k$ because otherwise the endpoints of the non-tree edge r_2 are not connected by a path of tree edges in the forest $F_{l(r_2)}$. From both possible replacement edges r_1 and r_2, the algorithm has to choose r_2, because of its larger level, as the replacement edge and promote it to a tree edge with level $l(r_2)$. Afterwards the newly promoted tree edge is inserted at all levels from 0 to $l(r_2)$ maintaining the definition of F_k. If the algorithm were to choose r_1 as the new replacement edge, the first invariant would become violated because the endpoints of r_2 then are not connected in $F_{l(r_2)}$.

The algorithm starts at the level $l = k$ of the tree edge e. The following steps are conducted:

1. The edge $e = \{i, j\}$ is part of the tree T in F_l. We remove e from T such that T decomposes into the trees T_i and T_j.

2. Without loss of generality, we assume that T_i has less vertices than T_j. Then, T_i does not have more than half the amount of vertices of T. Therefore T_i can be promoted to a tree of the forest F_{l+1} without violating the second invariant. To this end, all tree edges of T_i with level l are increased in their level to $l + 1$ and added to the forest F_{l+1}.

3. The algorithm sweeps over all vertices of T_i until either a non-tree edge r of level l is found which connects T_i and T_j or all non-tree edges of level l have been considered. Every visited non-tree edge of level l which does not connect both trees is promoted to level $l + 1$ because its endpoints lie in T_i. If an edge r has been found, it is a replacement edge and the algorithm jumps to Step 4. Otherwise, if $l > 0$, the algorithm sets

$l \leftarrow l - 1$ and starts at step 1 and repeats the search at the next lower level.

4. The edge e is removed from the remaining levels $0, \ldots l-1$ if $l > 0$.

5. If a replacement edge r has been found, it is promoted to a tree edge of level l and inserted into all forests $F_0, \ldots, F_l$.

The above steps of the algorithm differ slightly to the algorithm's description in [205] which nevertheless should not effect the functionality.

Euler-tour trees

To effectively store a spanning tree such that all basic operations can be done in logarithmic time, we use Euler tours [215]. An Euler tour visits each vertex of the tree T along a specific path over the edges and vertices. The sequence of vertex occurrences is then stored in a balanced tree which is called an ET-tree. The tour visits a vertex v and add it to the end of the sequence, and then enters a subtree of v and traverses all vertices in the subtree before it leaves the subtree to revisit v which means that v is added to the sequence again. Afterwards the next subtree of v is entered till all subtrees of v are visited. If the tour visits a leaf, i.e. a vertex without children, it just adds the leaf to the sequence and goes back to the leaf's parent vertex. The pseudo code of the function `EulerTour(T, r, S)` which generates the Euler tour of a tree `T` with root `r` and initially empty sequence `S` is given by

```
1  void EulerTour(Tree& T, Vertex* currentVertex, Sequence& S){
2
3  addToSequence(S, currentVertex);
4
5  for(int i = 0; i < T.numberOfChildren(currentVertex); i++){
6
7    EulerTour(T, &T.getChild(currentVertex, i), S);
8    addToSequence(S, currentVertex);
9
10 }
11
12 }
```

As an example consider the tree

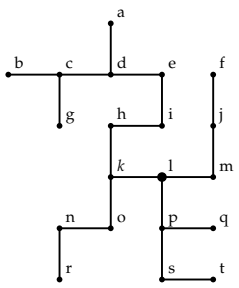

with root l for which

$$\mathrm{l\,m\,j\,f\,j\,m\,l\,p\,s\,t\,s\,p\,q\,p\,l\,k\,o\,n\,r\,n\,o\,k\,h\,i\,e\,d\,c\,g\,c\,b\,c\,d\,a\,d\,e\,i\,h\,k\,l}$$

is a valid Euler tour.

The tree T is never stored in its original form but as an ET-tree. The main advantage of using an Euler tour is that deleting an edge from T, joining T with another tree T' at an edge e or changing the root of T can be done by concatenating, joining, removing subsequences of and inserting vertices into Euler tours which translates to corresponding operations applied to ET-trees [215]. Because the trees are balanced, all these operations can be done in logarithmic time. For the balanced tree structure, we implement AVL-trees [216].

Verification of the implementation

To verify our implementation of the FDC-algorithm, we estimate the universal crossing probabilities $R_1(p_c, N \to \infty)$ in two-dimensional standard bond percolation and compare them to literature values. We consider the case of free (FBC), cylindrical (CBC), where the lattice is connected periodically along the second direction, and periodic (PBC) boundary conditions. The crossing probabilities are determined by computing the values $R_1(p_c, N)$ for various extents N and extrapolating to $N \to \infty$. The results are shown in Figure B.7. Recall that the percolation threshold $p_c = 0.5$ is exactly known for bond percolation [145].

Justified by the data alone, we extrapolate to the limit $N \to \infty$ by fitting the data with the ansatz

$$f(N^{-1}) = f(0) + aN^{-1} + bN^{-1}\,,$$

where we set $b = 0$ for FBC and CBC. We have the following estimates: $f(0) = 0.50001(13)$ for FBC, $f(0) = 0.63679(13)$ for CBC and $f(0) = 0.93486(16)$ for PBC. We compare these estimates to literature. Duality and universality arguments imply $f(0) = 0.5$ in the case of FBC [152, 217]. Our estimate agrees within errors with the analytic result. In the case of PBC, we consider the numerical results $f(0) = 0.93(4)$ of [184] and again notice an agreement with our estimates. For CB, we compare with the estimates $f(0) = 0.63665(80)$ [147], $f(0) = 0.6364(4)$ [218] and $f(0) = 0.6(4)$ [185] and the analytic result $f(0) \approx 0.63645001$ [219]. The estimate based on the FDC-alogrithm agrees within the errors with the numerical results but deviates by roughly 2.61 standard deviations from the analytical result. However, we rule this deviation as insignificant and probably caused by an underestimation of the error and a naive choice of the fit function.

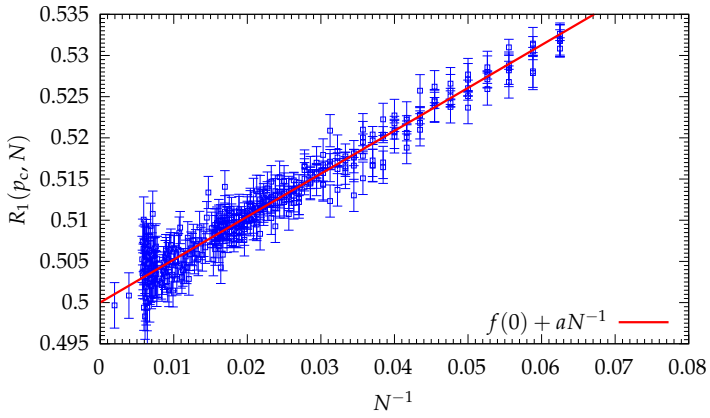

(a) free boundary conditions (FBC)

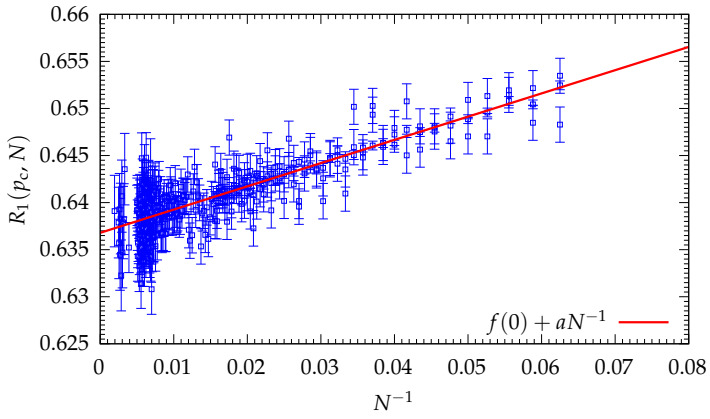

(b) cylindrical boundary conditions (CBC)

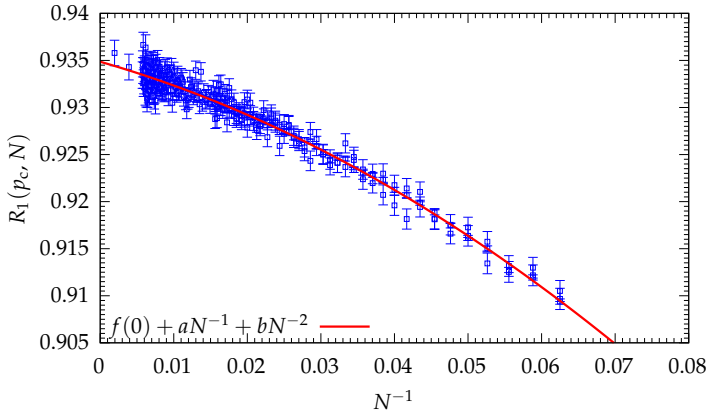

(c) periodic boundary conditions (PBC)

Figure B.7: Two-dimensional spanning probability $R_1(p_c, N)$ evaluated at the critical percolation thresholds p_c for different extents N and boundary conditions. The red curves represent fits of the data. The intersection of a fit function with the vertical axis estimates the extrapolation to $R_1(p_c, N \to \infty)$.

Bibliography

[1] *A schematic model of baryons and mesons*, M. Gell-Mann, 1964, Physics Letters, Vol. 8, No. 3, pp. 214–215, DOI: 10.1016/S0031-9163(64)92001-3

[2] *An SU_3 model for strong interaction symmetry and its breaking*, G. Zweig, 1964, In: DEVELOPMENTS IN THE QUARK THEORY OF HADRONS, Vol. 1, pp. 22–101, DOI: 10.17181/CERN-TH-412

[3] *Very High-Energy Collisions of Hadrons*, R. P. Feynman, 1969, Physical Review Letters, Vol. 23, Issue 24, pp. 1415–1417, DOI: 10.1103/PhysRevLett.23.1415

[4] *Deep inelastic scattering: Experiments on the proton and the observation of scaling*, Henry W. Kendall, 1991, Review of Modern Physics, Vol. 63, Issue 3, pp. 597–614, DOI: 10.1103/RevModPhys.63.597

[5] *Teilchen und Kerne*, 6th edition, B. Povh, K. Rith, C. Scholz, and F. Zetsche, 2004, Springer-Verlag Berlin Heidelberg

[6] *Light cone current algebra*, H. Fritzsch and M. Gell-Mann, 1971, In: International conference on duality and symmetry in hadron physics, Tel Aviv, pp. 317–374

[7] *Current algebra: Quarks and what else?*, H. Fritzsch and M. Gell-Mann, 1972, In: Proceedings, 16th International Conference on High-Energy Physics, Chicago, pp. 135–165

[8] *Advantages of the color octet gluon picture*, H. Fritzsch, M. Gell-Mann, and H. Leutwyler, 1973, Physics Letters B, Vol. 47, No. 4, pp. 365–368, DOI: 10.1016/0370-2693(73)90625-4

[9] *The histroy of QCD*, H. Fritzsch, 2012, CERN Courier, Vol. 52, No. 8, pp. 21–25

[10] *Ultraviolet Behavior of Non-Abelian Gauge Theories*, D. J. Gross and F. Wilczek, 1973, Physical Review Letters, Vol. 30, Issue 26, pp. 1343–1346, DOI: 10.1103/PhysRevLett.30.1343

[11] *Reliable Perturbative Results for Strong Interactions?*, H. D. Politzer, 1973, Physical Review Letters, Vol. 30, Issue 26, pp. 1346–1349, DOI: 10.1103/PhysRevLett.30.1346

[12] *Review of Particle Physics*, S. Navas et al. (Particle Data Group), 2024, Physical Review D, Vol. 110, Issue 3, p. 030001, DOI: 10.1103/PhysRevD.110.030001

[13] *The ALICE experiment: a journey through QCD*, S. Acharya et al. (ALICE Collaboration), 2024, The European Physical Journal C, Vol. 84, No. 8, p. 813, arXiv: 2211.04384, DOI: 10.1140/epjc/s10052-024-12935-y

[14] *The CBM physics book: Compressed baryonic matter in laboratory experiments*, 2011, Lecture Notes in Physics, Vol. 814, DOI: 10.1007/978-3-642-13293-3

[15] *Lattice QCD at High Temperature and Density*, F. Karsch, 2002, Lecture Notes in Physics, Vol. 583, pp. 209–249, DOI: 10.1007/3-540-45792-5_6

[16] *Is there still any T_c mystery in lattice QCD? Results with physical masses in the continuum limit III*, S. Borsanyi, Z. Fodor, C. Hoelbling, S. D. Katz, S. Krieg, C. Ratti, and K. K. Szabo, 2010, Journal of High Energy Physics, Vol. 09, p. 073, arXiv: 1005.3508 (hep-lat), DOI: 10.1007/JHEP09(2010)073

[17] *Chiral and deconfinement aspects of the QCD transition*, A. Bazavov, T. Bhattacharya, M. Cheng, C. DeTar, H.-T. Ding, Steven Gottlieb, R. Gupta, P. Hegde, U. M. Heller, F. Karsch, E. Laermann, L. Levkova, S. Mukherjee, P. Petreczky, C. Schmidt, R. A. Soltz, W. Soeldner, R. Sugar, D. Toussaint, W. Unger, and P. Vranas, 2012, Physical Review D, Vol. 85, Issue 5, p. 054503, DOI: 10.1103/PhysRevD.85.054503

[18] *Towards thermodynamics with $N_f = 2 + 1 + 1$ twisted mass quarks*, F. Burger, G. Hotzel, M. Müller-Preussker, E.-M. Ilgenfritz, and M. P. Lombardo, 2013, Proceedings of Science, Vol. Lattice2013, p. 153, arXiv: 1311.1631 (hep-lat), DOI: 10.22323/1.187.0153

[19] *Equation of state in $(2 + 1)$-flavor QCD*, A. Bazavov, T. Bhattacharya, C. DeTar, H.-T. Ding, S. Gottlieb, R. Gupta, P. Hegde, U. M. Heller, F. Karsch, E. Laermann, L. Levkova, S. Mukherjee, P. Petreczky, C. Schmidt, C. Schroeder, R. A. Soltz, W. Soeldner, R. Sugar, M. Wagner, and P. Vranas, 2014, Physical Review D, Vol. 90, Issue 9, p. 094503, DOI: 10.1103/PhysRevD.90.094503

[20] *Full result for the QCD equation of state with 2+1 flavors*, S. Borsányi, Z. Fodor, C. Hoelbling, S. D. Katz, S. Krieg, and K. K. Szabó, 2014, Physics Letters B, Vol. 730, pp. 99–104, DOI: https://doi.org/10.1016/j.physletb.2014.01.007

[21] *Chiral observables and topology in hot QCD with two families of quarks*, F. Burger, E.-M. Ilgenfritz, M. P. Lombardo, and A. Trunin, 2018, Physical Review D, Vol. 98, No. 9, p. 094501, arXiv: 1805.06001 (hep-lat), DOI: 10.1103/PhysRevD.98.094501

[22] *An Introduction to the Confinement Problem*, J. Greensite, 2011, Lecture Notes in Physics, Vol. 821, DOI: 10.1007/978-3-642-14382-3

[23] *Overview of the QCD phase diagram: Recent progress from the lattice*, J. N. Guenther, 2021, The European Physical Journal A, Vol. 57, No. 4, p. 136, arXiv: 2010.15503 (hep-lat), DOI: 10.1140/epja/s10050-021-00354-6

[24] *QCD at finite temperature and chemical potential from Dyson-Schwinger equations*, C. S. Fischer, 2019, Progress in Particle and Nuclear Physics, Vol. 105, pp. 1–60, DOI: 10.1016/j.ppnp.2019.01.002

[25] *Quantum Field Theory and the Standard Model*, M. D. Schwartz, 2013, Cambridge University Press

[26] *QCD Crossover at Finite Chemical Potential from Lattice Simulations*, S. Borsanyi, Z. Fodor, J. N. Guenther, R. Kara, S. D. Katz, P. Parotto, A. Pasztor, C. Ratti, and K. K. Szabó, 2020, Physical Review Letters, Vol. 125, Issue 5, p. 052001, DOI: 10.1103/PhysRevLett.125.052001

[27] *QCD deconfinement transition line up to $\mu_B = 400$ MeV from finite volume lattice simulations*, S. Borsanyi, Z. Fodor, J. N. Guenther, P. Parotto, A. Pasztor, L. Pirelli, K. K. Szabo, and C. H. Wong, 2024, arXiv: 2410.06216 (hep-lat)

[28] *Deconfinement and percolation*, H. Satz, 1998, Nuclear Physics A, Vol. 642, No. 1, pp. c130–c142, DOI: 10.1016/S0375-9474(98)00508-9

[29] *A flux tube model of the finite temperature deconfining transition in QCD*, A. Patel, 1984, Nuclear Physics B, Vol. 243, No. 3, pp. 411–422, DOI: 10.1016/0550-3213(84)90484-X

[30] *The Quantum Theory of Fields*, S. Weinberg, 1995, Cambridge University Press, DOI: 10.1017/cbo9781139644167

[31] *Local Quantum Physics - Fields, Particles, Algebras*, R. Haag, 1996, Springer-Verlag Berlin Heidelberg

[32] *PCT, Spin and Statistics, and All That*, R. F. Streater and A. S. Wightman, 2000, Princeton University Press, DOI: 10.1515/9781400884230

[33] *An Introduction to Quantum Field Theory*, M. E. Peskin and D. V. Schroeder, 1995, Westview Press

[34] *Gruppentheorie und ihre Anwendung auf die Quantenmechanik der Atomspektren*, E. Wigner, 1931, Vieweg+Teubner Verlag, DOI: 10.1007/978-3-663-02555-9

[35] *Lie Groups, Lie Algebras, and Representations - An Elementary Introduction*, B. C. Hall, 2015, Graduate Texts in Mathematics, Vol. 222, DOI: 10.1007/978-3-319-13467-3

[36] *Feynman diagrams for the Yang-Mills field*, L. D. Faddeev and V. N. Popov, 1967, Physics Letters B, Vol. 25, No. 1, pp. 29–30, DOI: 10.1016/0370-2693(67)90067-6

[37] *Finite-Temperature Field Theory*, J.I. Kapusta and C. Gale, 2006, Cambridge University Press, DOI: 10.1017/cbo9780511535130

[38] *Quantum Chromodynamics on the Lattice*, C. Gattringer and C. B. Lang, 2010, Lecture Notes in Physics, Vol. 788, DOI: 10.1007/978-3-642-01850-3

[39] *Confinement of quarks*, K. G. Wilson, 1974, Physical Review D, Vol. 10, Issue 8, pp. 2445–2459, DOI: 10.1103/PhysRevD.10.2445

[40] *SU(N) gauge theory couplings on asymmetric lattices*, F. Karsch, 1982, Nuclear Physics B, Vol. 205, No. 2, pp. 285–300, DOI: 10.1016/0550-3213(82)90390-X

[41] *Introduction to Quantum Fields on a Lattice*, J. Smit, 2002, Cambridge University Press, DOI: 10.1017/CBO9780511583971

[42] *Chemical potential on the lattice*, P. Hasenfratz and F. Karsch, 1983, Physics Letters B, Vol. 125, No. 4, pp. 308–310, DOI: 10.1016/0370-2693(83)91290-X

[43] *Finite temperature calculations on anisotropic lattices*, I. Bender, T. Hashimoto, F. Karsch, V. Linke, A. Nakamura, M. Schiestl, and I. O. Stamatescu, 1990, Nuclear Physics B - Proceedings Supplements, Vol. 17, pp. 387–390, DOI: 10.1016/0920-5632(90)90279-4

[44] *Lattice fermions: Species doubling, chiral invariance and the triangle anomaly*, L. H. Karsten and J. Smith, 1981, Nuclear Physics B, Vol. 183, No. 1, pp. 103–140, DOI: 10.1016/0550-3213(81)90549-6

[45] *Quarks and Strings on a Lattice*, K. G. Wilson, 1977, In: Zichini, A. (eds) New Phenomena in Subnuclear Physics. The Subnuclear Series, Vol. 13, pp. 69–142, DOI: 10.1007/978-1-4613-4208-3_6

[46] *Hamiltonian formulation of Wilson's lattice gauge theories*, J. Kogut and L. Susskind, 1975, Physical Review D, Vol. 11, No. 2, pp. 395–408, DOI: 10.1103/PhysRevD.11.395

[47] *Absence of neutrinos on a lattice: (I). Proof by homotopy theory*, H. B. Nielsen and M. Ninomiya, 1981, Nuclear Physics B, Vol. 185, No. 1, pp. 20–40, DOI: 10.1016/0550-3213(81)90361-8

[48] *Quantum Fields on a Lattice*, I. Montvay and G. Münster, 1994, Cambridge University Press

[49] *Quarks, Gluons and Lattices*, M. Creutz, 1983, Cambridge University Press, DOI: 10.1017/9781009290395

[50] *Confinement, chiral symmetry, and the lattice*, M. Creutz, 2011, Acta Phys. Slov., Vol. 61, pp. 1–127, arXiv: 1103.3304 (hep-lat), DOI: 10.2478/v10155-011-0001-y

[51] *Gauge Theories as a Problem of Constructive Quantum Field Theory and Statistical Mechanics*, E. Seiler, 1982, Lecture Notes in Physics, Vol. 159, DOI: 10.1007/3-540-11559-5

[52] *The Order of the quantum chromodynamics transition predicted by the standard model of particle physics*, Y. Aoki, G. Endrodi, Z. Fodor, S. D. Katz, and K. K. Szabo, 2006, Nature, Vol. 443, pp. 675–678, arXiv: hep-lat/0611014, DOI: 10.1038/nature05120

[53] *The QCD transition temperature: Results with physical masses in the continuum limit*, Y. Aoki, Z. Fodor, S. D. Katz, and K. K. Szabo, 2006, Physics Letters B, Vol. 643, pp. 46–54, arXiv: hep-lat/0609068, DOI: 10.1016/j.physletb.2006.10.021

[54] *The QCD transition temperature: results with physical masses in the continuum limit II*, Y. Aoki, S. Borsányi, S. Dürr, Z. Fodor, S. D. Katz, S. Krieg, and K. Szabo, 2009, Journal of High Energy Physics, Vol. 2009, No. 06, p. 088, DOI: 10.1088/1126-6708/2009/06/088

[55] *Crystal statistics. 1. A Two-dimensional model with an order disorder transition*, L. Onsager, 1944, Physical Review, Vol. 65, pp. 117–149, DOI: 10.1103/PhysRev.65.117

[56] *Impossibility of Spontaneously Breaking Local Symmetries*, S. Elitzur, 1975, Physical Review D, Vol. 12, pp. 3978–3982, DOI: 10.1103/PhysRevD.12.3978

[57] *Thermal Properties of Gauge Fields and Quark Liberation*, A. M. Polyakov, 1978, Physics Letters B, Vol. 72, pp. 477–480, DOI: 10.1016/0370-2693(78)90737-2

[58] *Critical Behavior at Finite Temperature Confinement Transitions*, B. Svetitsky and L. G. Yaffe, 1982, Nuclear Physics B, Vol. 210, pp. 423–447, DOI: 10.1016/0550-3213(82)90172-9

[59] *Quark Liberation at High Temperature: A Monte Carlo Study of SU(2) Gauge Theory*, L. D. McLerran and B. Svetitsky, 1981, Physical Review D, Vol. 24, p. 450, DOI: 10.1103/PhysRevD.24.450

[60] *The Effective Potential for the Order Parameter of Gauge Theories at Finite Temperature*, N. Weiss, 1981, Physical Review D, Vol. 24, p. 475, DOI: 10.1103/PhysRevD.24.475

[61] *Gauge Fields as Rings of Glue*, A. M. Polyakov, 1979, Nuclear Physics B, Vol. 164, pp. 171–188, DOI: 10.1016/0550-3213(80)90507-6

[62] *Heavy quark anti-quark free energy and the renormalized Polyakov loop*, O. Kaczmarek, F. Karsch, P. Petreczky, and F. Zantow, 2002, Physics Letters B, Vol. 543, pp. 41–47, arXiv: hep-lat/0207002, DOI: 10.1016/S0370-2693(02)02415-2

[63] *Heavy quark free energies and screening in SU(2) gauge theory*, S. Digal, S. Fortunato, and P. Petreczky, 2003, Physical Review D, Vol. 68, p. 034008, arXiv: hep-lat/0304017, DOI: 10.1103/PhysRevD.68.034008

[64] *Deconfining phase transition as a matrix model of renormalized Polyakov loops*, A. Dumitru, Y. Hatta, J. Lenaghan, K. Orginos, and R. D. Pisarski, 2004, Physical Review D, Vol. 70, p. 034511, arXiv: hep-th/0311223, DOI: 10.1103/PhysRevD.70.034511

[65] *Renormalized Polyakov loops in many representations*, S. Gupta, K. Huebner, and O. Kaczmarek, 2008, Physical Review D, Vol. 77, p. 034503, arXiv: 0711.2251 (hep-lat), DOI: 10.1103/PhysRevD.77.034503

[66] *Renormalized Polyakov loops in various representations in finite temperature SU(2) gauge theory*, K. Huebner and C. Pica, 2008, Proceedings of Science, Vol. LATTICE2008, p. 197, arXiv: 0809.3933 (hep-lat), DOI: 10.22323/1.066.0197

[67] *Polyakov loop in 2+1 flavor QCD*, A. Bazavov and P. Petreczky, 2013, Physical Review D, Vol. 87, No. 9, p. 094505, arXiv: 1301.3943 (hep-lat), DOI: 10.1103/PhysRevD.87.094505

[68] *Polyakov loop fluctuations in SU(3) lattice gauge theory and an effective gluon potential*, P. M. Lo, B. Friman, O. Kaczmarek, K. Redlich, and C. Sasaki, 2013, Physical Review D, Vol. 88, p. 074502, arXiv: 1307.5958 (hep-lat), DOI: 10.1103/PhysRevD.88.074502

[69] *Lattice Models of Quark Confinement at High Temperature*, L. Susskind, 1979, Physical Review D, Vol. 20, pp. 2610–2618, DOI: 10.1103/PhysRevD.20.2610

[70] *First Order Phase Transition in the SU(3) Gauge Theory at Finite Temperature*, L. G. Yaffe and B. Svetitsky, 1982, Physical Review D, Vol. 26, p. 963, DOI: 10.1103/PhysRevD.26.963

[71] *A study of the correlation length near a first-order phase transition: The three-dimensional three-state Potts model*, R. V. Gavai, F. Karsch, and B. Petersson, 1989, Nuclear Physics B, Vol. 322, No. 3, pp. 738–758, DOI: 10.1016/0550-3213(89)90235-6

[72] *Thermodynamics of SU(3) lattice gauge theory*, G. Boyd, J. Engels, F. Karsch, E. Laermann, C. Legeland, M. Lütgemeier, and B. Petersson, 1996, Nuclear Physics B, Vol. 469, No. 3, pp. 419–444, DOI: https://doi.org/10.1016/0550-3213(96)00170-8

[73] *Precision study of the continuum SU(3) Yang-Mills theory: How to use parallel tempering to improve on supercritical slowing down for first order phase transitions*, S. Borsanyi, R. Kara, Z. Fodor, D. A. Godzieba, P. Parotto, and D. Sexty, 2022, Physical Review D, Vol. 105, No. 7, p. 074513, arXiv: 2202.05234 (hep-lat), DOI: 10.1103/PhysRevD.105.074513

[74] *Topological features of the deconfinement transition*, S. Borsanyi, Z. Fodor, D. A. Godzieba, R. Kara, P. Parotto, D. Sexty, and R. Vig, 2023, Physical Review D, Vol. 107, No. 5, p. 054514, arXiv: 2212.08684 (hep-lat), DOI: 10.1103/PhysRevD.107.054514

[75] *Equation of state and QCD transition at finite temperature*, A. Bazavov, T. Bhattacharya, M. Cheng, N. H. Christ, C. DeTar, S. Ejiri, Steven Gottlieb, R. Gupta, U. M. Heller, K. Huebner, C. Jung, F. Karsch, E. Laermann, L. Levkova, C. Miao, R. D. Mawhinney, P. Petreczky, C. Schmidt, R. A. Soltz, W. Soeldner, R. Sugar, D. Toussaint, and P. Vranas, 2009, Physical Review D, Vol. 80, Issue 1, p. 014504, DOI: 10.1103/PhysRevD.80.014504

[76] *Properties of the QCD thermal transition with $N_f = 2 + 1$ flavors of Wilson quark*, G. Aarts, C. Allton, J. Glesaaen, S. Hands, B. Jäger, S. Kim, M. P. Lombardo, A. A. Nikolaev, S. M. Ryan, J.-I. Skullerud, and L.-K. Wu, 2022, Physical Review D, Vol. 105, Issue 3, p. 034504, DOI: 10.1103/PhysRevD.105.034504

[77] *Lattice Yang-Mills theory at nonzero temperature and the confinement problem*, C. Borgs and E. Seiler, 1983, Communications in Mathematical Physics, Vol. 91, No. 3, DOI: 10.1007/BF01208780

[78] *Isolating the confining color field in the SU(3) flux tube*, M. Baker, P. Cea, V. Chelnokov, L. Cosmai, F. Cuteri, and A. Papa, 2019, The European Physical Journal C, Vol. 79, No. 6, p. 478, arXiv: 1810.07133 (hep-lat), DOI: 10.1140/epjc/s10052-019-6978-y

[79] *The confining color field in SU(3) gauge theory*, M. Baker, P. Cea, V. Chelnokov, L. Cosmai, F. Cuteri, and A. Papa, 2020, The European Physical Journal C, Vol. 80, No. 6, p. 514, arXiv: 1912.04739 (hep-lat), DOI: 10.1140/epjc/s10052-020-8077-5

[80] *QCD flux tubes across the deconfinement phase transition*, P. Cea, L. Cosmai, F. Cuteri, and A. Papa, 2018, EPJ Web of Conferences, Vol. 175, p. 12006, arXiv: 1710.01963 (hep-lat), DOI: 10.1051/epjconf/201817512006

[81] *Pure gauge QCD flux tubes and their widths at finite temperature*, P. Bicudo, N. Cardoso, and M. Cardoso, 2019, Nuclear Physics B, Vol. 940, pp. 88–112, arXiv: 1702.03454 (hep-lat), DOI: 10.1016/j.nuclphysb.2019.01.012

[82] *Quantum Chromodynamics on a Lattice*, K. G. Wilson, 1977, in: New Developments in Quantum Field Theory and Statistical Mechanics Cargèse 1976, pp. 143–172, DOI: 10.1007/978-1-4615-8918-1_6

[83] *Construction of a selfadjoint, strictly positive transfer matrix for Euclidean lattice gauge theories*, M. Lüscher, 1977, Communications in Mathematical Physics, Vol. 54, No. 3, pp. 283–292, DOI: 10.1007/BF01614090

[84] *The chemical potential in the transfer matrix and in the path integral formulation of QCD on a lattice*, F. Palumbo, 2002, Nuclear Physics B, Vol. 645, No. 1, pp. 309–320, DOI: 10.1016/S0550-3213(02)00827-1

[85] *Transfer matrix and nonperturbative renormalization of fermionic currents in lattice QCD*, V. K. Mitrjushkin, 2002, arXiv: hep-lat/0206024

[86] *Currents, chemical potential and boundary conditions in lattice QCD*, V. K. Mitrjushkin, 2003, Nuclear Physics B - Proceedings Supplements, Vol. 119, pp. 326–328, DOI: 10.1016/S0920-5632(03)01535-4

[87] *On the Gauss law and global charge for quantum chromodynamics*, J. Kijowski and G. Rudolph, 2002, Journal of Mathematical Physics, Vol. 43, No. 4, pp. 1796–1808, DOI: 10.1063/1.1447310

[88] *On the notion of global charge in QCD*, J. Kijowski and G. Rudolph, 2002, Reports on Mathematical Physics, Vol. 49, No. 2, pp. 211–224, DOI: 10.1016/S0034-4877(02)80020-9

[89] *Charge superselection sectors for QCD on the lattice*, J. Kijowski and G. Rudolph, 2005, Journal of Mathematical Physics, Vol. 46, No. 3, p. 032303, DOI: 10.1063/1.1851604

[90] *Quarks and triality in a finite volume*, M. Ghanbarpour and L. von Smekal, 2022, Physical Review D, Vol. 106, Issue 5, p. 054513, DOI: 10.1103/PhysRevD.106.054513

[91] *Entanglement entropy for 2D gauge theories with matters*, S. Aoki, N. Iizuka, K. Tamaoka, and T. Yokoya, 2017, Physical Review D, Vol. 96, Issue 4, p. 045020, DOI: 10.1103/PhysRevD.96.045020

[92] *Gauge fixing, the transfer matrix, and confinement on a lattice*, M. Creutz, 1977, Physical Review D, Vol. 15, No. 4, pp. 1128–1136, DOI: 10.1103/physrevd.15.1128

[93] *The lattice gauge theory approach to quantum chromodynamics*, J. B. Kogut, 1983, Reviews of Modern Physics, Vol. 55, No. 3, pp. 775–836, DOI: 10.1103/revmodphys.55.775

[94] *The connection between the Λ parameters of lattice and continuum QCD*, A. Hasenfratz and P. Hasenfratz, 1980, Physics Letters B, Vol. 93, No. 1, pp. 165–169, DOI: 10.1016/0370-2693(80)90118-5

[95] *One-loop fermion contribution in an asymmetric lattice regularization of SU(N) gauge theories*, R. C. Trinchero, 1983, Nuclear Physics B, Vol. 227, No. 1, pp. 61–74, DOI: 10.1016/0550-3213(83)90143-8

[96] *QCD thermodynamics with light quarks. Quantum corrections to the fermionic anisotropy parameter*, F. Karsch and I. O. Stamatescu, 1989, Physics Letters B, Vol. 227, No. 1, pp. 153–160, DOI: 10.1016/0370-2693(89)91299-9

[97] *Lattice QCD, quark-gluon plasma and heavy-ion collisions*, F. Karsch, 1990, Nuclear Physics B - Proceedings Supplements, Vol. 15, pp. 157–186, DOI: 10.1016/0920-5632(90)90015-M

[98] *Representation Theory of Semisimple Groups*, A. W. Knapp, 1986, Princeton University Press

[99] *Dynamical Symmetry in Particle Physics*, A. Pais, 1966, Reviews of Modern Physics, Vol. 38, No. 2, pp. 215–255, DOI: 10.1103/revmodphys.38.215

[100] *Über die Abgrenzung der Eigenwerte einer Matrix*, S. Geršgorin, 1931, Bulletin de l'Académie des Sciences de l'Union des Républiques Soviétiques Socialistes. VII série. Classe des sciences mathématiques et naturelles, No. 6, pp. 749–754

[101] *Geršgorin and His Circles*, R. S. Varga, 2004, Springer Berlin Heidelberg, DOI: 10.1007/978-3-642-17798-9

[102] *Kernels of trace class operators*, C. Brislawn, 1988, Proceedings of the American Mathematical Society, Vol. 104, No. 4, pp. 1181–1190, DOI: 10.1090/s0002-9939-1988-0929421-x

[103] *YANG-MILLS THEORY AS SCHRODINGER QUANTUM MECHANICS ON THE SPACE OF GAUGE GROUP ORBITS*, K. Gawedzki, 1982, Physical Review D, Vol. 26, pp. 3593–3610, DOI: 10.1103/PhysRevD.26.3593

[104] *Definition and general properties of the transfer matrix in continuum limit improved lattice gauge theories*, M. Lüscher and P. Weisz, 1984, Nuclear Physics B, Vol. 240, No. 3, pp. 349–361, DOI: 10.1016/0550-3213(84)90270-0

[105] *Gauge theories with imaginary chemical potential and the phases of QCD*, A. Roberge and N. Weiss, 1986, Nuclear Physics B, Vol. 275, No. 4, pp. 734–745, DOI: 10.1016/0550-3213(86)90582-1

[106] *Colour screening and quark confinement*, G. Mack, 1978, Physics Letters B, Vol. 78, No. 2, pp. 263–268, DOI: 10.1016/0370-2693(78)90019-9

[107] *Abelian color cycles: A new approach to strong coupling expansion and dual representations for non-abelian lattice gauge theory*, C. Gattringer and C. Marchis, 2017, Nuclear Physics B, Vol. 916, pp. 627–646, DOI: 10.1016/j.nuclphysb.2017.01.025

[108] *Dual representation of lattice QCD with worldlines and worldsheets of Abelian color fluxes*, C. Marchis and C. Gattringer, 2018, Physical Review D, Vol. 97, No. 3, p. 034508, DOI: 10.1103/PhysRevD.97.034508

[109] *A property of electric and magnetic flux in non-Abelian gauge theories*, G. 't Hooft, 1979, Nuclear Physics B, Vol. 153, pp. 141–160, DOI: 10.1016/0550-3213(79)90595-9

[110] *TWISTED BOUNDARY CONDITIONS: A NON-PERTURBATIVE PROBE FOR PURE NON-ABELIAN GAUGE THEORIES*, P. J. van Baal, 1984, PhD thesis, Utrecht University

[111] *Confinement in* SU(N) *lattice gauge theories*, L. G. Yaffe, 1980, Physical Review D, Vol. 21, No. 6, pp. 1574–1590, DOI: 10.1103/PhysRevD.21.1574

[112] *Dual variables for lattice gauge theories and the phase structure of* Z(N) *systems*, A. Ukawa, P. Windey, and A. H. Guth, 1980, Physical Review D, Vol. 21, No. 4, pp. 1013–1036, DOI: 10.1103/PhysRevD.21.1013

[113] *On the phase transition towards permanent quark confinement*, G. 't Hooft, 1978, Nuclear Physics B, Vol. 138, No. 1, pp. 1–25, DOI: 10.1016/0550-3213(78)90153-0

[114] *Comparison of lattice gauge theories with gauge groups Z_2 and SU(2)*, G. Mack and V. B. Petkova, 1979, Annals of Physics, Vol. 123, No. 2, pp. 442–467, DOI: 10.1016/0003-4916(79)90346-4

[115] *Monopole Condensation and the Lattice-Quantum-Chromodynamics Crossover*, R. C. Brower, D. A. Kessler, and H. Levine, 1981, Physical Review Letters, Vol. 47, No. 9, pp. 621–624, DOI: 10.1103/physrevlett.47.621

[116] *Colored monopoles on the lattice*, M. Srednicki and L. Susskind, 1981, Nuclear Physics B, Vol. 179, No. 2, pp. 239–252, DOI: 10.1016/0550-3213(81)90237-6

[117] *Behavior of non-Abelian magnetic fields at high temperature*, T. A. DeGrand and D. Toussaint, 1982, Physical Review D, Vol. 25, No. 2, pp. 526–530, DOI: 10.1103/physrevd.25.526

[118] *Spatial 't Hooft loop, hot QCD and Z_N domain walls*, C. Korthals-Altes, A. Kovner, and M. Stephanov, 1999, Physics Letters B, Vol. 469, No. 1-4, pp. 205–212, DOI: 10.1016/s0370-2693(99)01242-3

[119] *Free energy of an SU(2) monopole-antimonopole pair*, Ch. Hoelbling, C. Rebbi, and V. A. Rubakov, 2001, Physical Review D, Vol. 63, No. 3, DOI: 10.1103/physrevd.63.034506

[120] *Monopoles, vortices and confinement in SU(3) gauge theory*, L. Del Debbio, A. Di Giacomo, and B. Lucini, 2001, Physics Letters B, Vol. 500, No. 3-4, pp. 326–329, DOI: 10.1016/s0370-2693(01)00091-0

[121] *The interaction between center monopoles in SU(2) Yang-Mills*, P. de Forcrand, M. D'Elia, and M. Pepe, 2001, Nuclear Physics B - Proceedings Supplements, Vol. 94, No. 1-3, pp. 494–497, DOI: 10.1016/s0920-5632(01)00890-8

[122] *'t Hooft Loop in SU(2) Yang-Mills Theory*, P. de Forcrand, M. D'Elia, and M. Pepe, 2001, Physical Review Letters, Vol. 86, No. 8, pp. 1438–1441, DOI: 10.1103/PhysRevLett.86.1438

[123] *On 't Hooft's loop operator*, H. Reinhardt, 2003, Physics Letters B, Vol. 557, No. 3-4, pp. 317–323, DOI: 10.1016/s0370-2693(03)00199-0

[124] *Precision lattice calculation of SU(2) 't Hooft loops*, P. de Forcrand and D. Noth, 2005, Physical Review D, Vol. 72, No. 11, DOI: 10.1103/physrevd.72.114501

[125] *The 't Hooft loop in the Hamiltonian approach to Yang-Mills theory in Coulomb gauge*, H. Reinhardt and D. Epple, 2007, Physical Review D, Vol. 76, No. 6, DOI: 10.1103/physrevd.76.065015

[126] *Computation of the Vortex Free Energy in SU(2) Gauge Theory*, T. G. Kovács and E. T. Tomboulis, 2000, Physical Review Letters, Vol. 85, No. 4, pp. 704–707, DOI: 10.1103/physrevlett.85.704

[127] *'t Hooft loops, electric flux sectors, and confinement in SU(2) Yang-Mills theory*, P. de Forcrand and L. von Smekal, 2002, Physical Review D, Vol. 66, No. 1, p. 011504, DOI: 10.1103/PhysRevD.66.011504

[128] *'t Hooft loops and consistent order parameters for confinement*, P. de Forcrand and L. von Smekal, 2002, Nuclear Physics B - Proceedings Supplements, Vol. 106-107, pp. 619–621, DOI: 10.1016/s0920-5632(01)01796-0

[129] *Electric and magnetic fluxes in SU(2) Yang-Mills theory*, L. von Smekal and P. de Forcrand, 2003, Nuclear Physics B - Proceedings Supplements, Vol. 119, pp. 655–657, DOI: 10.1016/s0920-5632(03)01633-5

[130] *SU(2) lattice gauge theory in 2 + 1 dimensions: Critical couplings from twisted boundary conditions and universality*, S. R. Edwards and L. von Smekal, 2009, Physics Letters B, Vol. 681, No. 5, pp. 484–490, DOI: 10.1016/j.physletb.2009.10.063

[131] *SU(3) Deconfinement in (2+1)d from Twisted Boundary Conditions and Self-Duality*, N. Strodthoff, S. R. Edwards, and L. von Smekal, 2010, Proceedings of Science, Vol. LATTICE2010, p. 288, arXiv: 1012.0723 (hep-lat), DOI: 10.22323/1.105.0288

[132] *Universal Aspects of QCD-like Theories*, L. von Smekal, 2012, Nuclear Physics B - Proceedings Supplements, Vol. 228, pp. 179–220, DOI: 10.1016/j.nuclphysbps.2012.06.006

[133] *Algebraic formulation of duality transformations for abelian lattice models*, K. Drühl and H. Wagner, 1982, Annals of Physics, Vol. 141, No. 2, pp. 225–253, DOI: 10.1016/0003-4916(82)90286-x

[134] *Combinatorial Topology*, Vol. 2, P. S. Aleksandrov, 1957, Graylock Press

[135] *Algebra - A Teaching and Source Book*, E. Shult and D. Surowski, 2015, Springer International Publishing Switzerland

[136] *Duality in field theory and statistical systems*, R. Savit, 1980, Reviews of Modern Physics, Vol. 52, No. 2, pp. 453–487, DOI: 10.1103/RevModPhys.52.453

[137] *The Potts model*, F. Y. Wu, 1982, Reviews of Modern Physics, Vol. 54, No. 1, pp. 235–268, DOI: 10.1103/RevModPhys.54.235

[138] *Z(3) interfaces in lattice gauge theory*, S. T. West, 1996, PhD thesis

[139] *High temperature properties of the Z(3) interface in (2+1)-dimensions SU(3) gauge theory*, S. T. West and J. F. Wheater, 1996, Physics Letters B, Vol. 383, pp. 205–211, arXiv: hep-lat/9605040, DOI: 10.1016/0370-2693(96)00731-9

[140] *Tension of the interface between two ordered phases in lattice SU(3) gauge theory*, K. Kajantie, L. Karkkainen, and K. Rummukainen, 1991, Nuclear Physics B, Vol. 357, pp. 693–712, DOI: 10.1016/0550-3213(91)90486-H

[141] *'t Hooft loops and perturbation theory*, P. de Forcrand, B. Lucini, and D. Noth, 2006, Proceedings of Science, Vol. LAT2005, p. 323, arXiv: hep-lat/0510081, DOI: 10.22323/1.020.0323

[142] *CC BY 4.0*, Creative Commons, URL: https://creativecommons.org/licenses/by/4.0/

[143] *Introduction to percolation theory*, D. Stauffer, 1985, Taylor & Francis

[144] *Continuum percolation thresholds in two dimensions*, S. Mertens and C. Moore, 2012, Physical Review E, Vol. 86, Issue 6, p. 061109, DOI: 10.1103/PhysRevE.86.061109

[145] *The critical probability of bond percolation on the square lattice equals 1/2*, H. Kesten, 1980, Communications in Mathematical Physics, Vol. 74, pp. 41–59, DOI: 10.1007/bf01197577

[146] *Renormalization group, scaling and universality in spanning probability for percolation*, J.-P. Hovi and A. Aharony, 1995, Physica A: Statistical Mechanics and its Applications, Vol. 221, No. 1, pp. 68–79, DOI: 10.1016/0378-4371(95)00272-9

[147] *Scaling and universality in the spanning probability for percolation*, J.-P. Hovi and A. Aharony, 1996, Physical Review E, Vol. 53, No. 1, pp. 235–253, DOI: 10.1103/physreve.53.235

[148] *Introduction to the Renormalization Group*, S.-k. Ma, 1973, Reviews of Modern Physics, Vol. 45, No. 4, pp. 589–614, DOI: 10.1103/revmodphys.45.589

[149] *Universal critical amplitudes in finite-size scaling*, V. Privman and M. E. Fisher, 1984, Physical Review B, Vol. 30, No. 1, pp. 322–327, DOI: 10.1103/physrevb.30.322

[150] *Finite Size Scaling and Numerical Simulation of Statistical Systems*, V. Privman, 1990, World Scientific, Singapore

[151] *Bond and site percolation in three dimensions*, J. Wang, Z. Zhou, W. Zhang, T. M. Garoni, and Y. Deng, 2013, Physical Review E, Vol. 87, No. 5, DOI: 10.1103/physreve.87.052107

[152] *Large-cell Monte Carlo renormalization group for percolation*, P. Reynolds, H. Stanley, and W. Klein, 1980, Physical Review B, Vol. 21, No. 3, pp. 1223–1245, DOI: 10.1103/physrevb.21.1223

[153] *Existence of weak singularities when going around the liquid-gas critical point*, J. Kertész, 1989, Physica A: Statistical Mechanics and its Applications, Vol. 161, No. 1, pp. 58–62, DOI: 10.1016/0378-4371(89)90390-7

[154] *Clusters and Ising critical droplets: a renormalisation group approach*, A. Coniglio and W. Klein, 1980, Journal of Physics A: Mathematical and General, Vol. 13, No. 8, pp. 2775–2780, DOI: 10.1088/0305-4470/13/8/025

[155] *Critical droplets and phase transitions in two dimensions*, S. Fortunato, 2003, Physical Review B, Vol. 67, No. 1, p. 014102, DOI: 10.1103/PhysRevB.67.014102

[156] *Cluster percolation and critical behaviour in spin models and SU(N) gauge theories*, S. Fortunato, 2003, Journal of Physics A: Mathematical and General, Vol. 36, No. 15, pp. 4269–4281, DOI: 10.1088/0305-4470/36/15/304

[157] *Cluster percolation and pseudocritical behaviour in spin models*, S. Fortunato and H. Satz, 2001, Physics Letters B, Vol. 509, No. 1, pp. 189–195, DOI: 10.1016/S0370-2693(01)00551-2

[158] *Polyakov loop percolation and deconfinement in SU(2) gauge theory*, S. Fortunato and H. Satz, 2000, Physics Letters B, Vol. 475, No. 3, pp. 311–314, DOI: 10.1016/S0370-2693(00)00091-5

[159] *Percolation and deconfinement in SU(2) gauge theory*, S. Fortunato and H. Satz, 2001, Nuclear Physics A, Vol. 681, No. 1, pp. 466–471, DOI: 10.1016/S0375-9474(00)00554-6

[160] *Percolation and critical behaviour in SU(2) gauge theory*, S. Fortunato, F. Karsch, P. Petreczky, and H. Satz, 2001, Nuclear Physics B - Proceedings Supplements, Vol. 94, No. 1, pp. 398–401, DOI: 10.1016/S0920-5632(01)00984-7

[161] *The structure of projected center vortices in lattice gauge theory*, R. Bertle, M. Faber, J. Greensite, and S. Olejník, 1999, Journal of High Energy Physics, Vol. 1999, No. 03, pp. 019–019, DOI: 10.1088/1126-6708/1999/03/019

[162] *Deconfinement in SU(2) Yang-Mills theory as a center vortex percolation transition*, M. Engelhardt, K. Langfeld, H. Reinhardt, and O. Tennert, 2000, Physical Review D, Vol. 61, No. 5, p. 054504, DOI: 10.1103/PhysRevD.61.054504

[163] *Vortex critical behavior at the deconfinement phase transition*, K. Langfeld, 2003, Physical Review D, Vol. 67, No. 11, DOI: 10.1103/physrevd.67.111501

[164] *Center vortex model for the infrared sector of SU(3) Yang-Mills theory: Confinement and deconfinement*, M. Engelhardt, M. Quandt, and H. Reinhardt, 2004, Nuclear Physics B, Vol. 685, pp. 227–248, arXiv: hep-lat/0311029, DOI: 10.1016/j.nuclphysb.2004.02.036

[165] *Branching of center vortices in SU(3) lattice gauge theory*, F. Spengler, M. Quandt, and H. Reinhardt, 2018, Physical Review D, Vol. 98, Issue 9, p. 094508, DOI: 10.1103/PhysRevD.98.094508

[166] *Impact of Dynamical Fermions on Centre Vortex Structure*, D. Leinweber, J. Biddle, and W. Kamleh, 2021, Proceedings of Science, Vol. LATTICE2021, p. 197, arXiv: 2204.04825 (hep-lat), DOI: 10.22323/1.396.0197

[167] *Centre vortex structure of QCD-vacuum fields and confinement*, D. Leinweber, J. Biddle, and W. Kamleh, 2022, SciPost Physics Proceedings, No. 6, DOI: 10.21468/scipostphysproc.6.004

[168] *Center vortex structure in the presence of dynamical fermions*, J. C. Biddle, W. Kamleh, and D. B. Leinweber, 2023, Physical Review D, Vol. 107, Issue 9, p. 094507, DOI: 10.1103/PhysRevD.107.094507

[169] *Center vortex geometry at finite temperature*, J. A. Mickley, W. Kamleh, and D. B. Leinweber, 2024, Physical Review D, Vol. 110, Issue 3, p. 034516, DOI: 10.1103/PhysRevD.110.034516

[170] *Center vortex evidence for a second finite-temperature QCD transition*, J. A. Mickley, C. Allton, R. Bignell, and D. Leinweber, 2025, Physical Review D, Vol. 111, Issue 3, p. 034508, DOI: 10.1103/PhysRevD.111.034508

[171] *Coherent center domains in SU(3) gluodynamics and their percolation at T_c*, C. Gattringer, 2010, Physics Letters B, Vol. 690, No. 2, pp. 179–182, DOI: 10.1016/j.physletb.2010.05.013

[172] *Center clusters and their percolation properties in lattice QCD*, J. Danzer, C. Gattringer, S. Borsanyi, and Z. Fodor, 2010, Proceedings of Science, Vol. LATTICE2010, p. 176, DOI: 10.22323/1.105.0176

[173] *Coherent center domains from local Polyakov loops*, S. Borsanyi, J. Danzer, Z. Fodor, C. Gattringer, and A. Schmidt, 2011, Journal of Physics: Conference Series, Vol. 312, No. 1, p. 012005, DOI: 10.1088/1742-6596/312/1/012005

[174] *Center clusters in the Yang-Mills vacuum*, C. Gattringer and A. Schmidt, 2011, Journal of High Energy Physics, Vol. 2011, No. 1, p. 51, DOI: 10.1007/JHEP01(2011)051

[175] *Aspects of lattice QCD at finite temperature and density*, J. Danzer, 2011, PhD thesis, Graz U.

[176] *No coincidence of center percolation and deconfinement in SU(4) lattice gauge theory*, M. Dirnberger, C. Gattringer, and A. Maas, 2012, Physics Letters B, Vol. 716, No. 3-5, pp. 465–469, DOI: 10.1016/j.physletb.2012.09.001

[177] *Fractality and other properties of center domains at finite temperature: SU(3) lattice gauge theory*, G. Endrődi, C. Gattringer, and H.-P. Schadler, 2014, Physical Review D, Vol. 89, No. 5, p. 054509, DOI: 10.1103/PhysRevD.89.054509

[178] *Visualizations of coherent center domains in local Polyakov loops*, F. M. Stokes, W. Kamleh, and D. B. Leinweber, 2014, Annals of Physics, Vol. 348, pp. 341–361, DOI: 10.1016/j.aop.2014.05.002

[179] *Center clusters in full QCD at finite temperature and background magnetic field*, G. Endrődi, A. Schäfer, and J. Wellnhofer, 2015, Physical Review D, Vol. 92, No. 1, p. 014509, DOI: 10.1103/PhysRevD.92.014509

[180] *Understanding strongly interacting matter at finite temperature and density from lattice QCD calculations*, H.-P. Schadler, 2015, PhD thesis, Graz U.

[181] *Percolation as a confinement order parameter in $\mathbb{Z}_2$ lattice gauge theories*, S. M. Linsel, A. Bohrdt, L. Homeier, L. Pollet, and F. Grusdt, 2024, Physical Review B, Vol. 110, Issue 24, p. L241101, DOI: 10.1103/PhysRevB.110.L241101

[182] *Percolation renormalization group analysis of confinement in $\mathbb{Z}_2$ lattice gauge theories*, G. Dünnweber, S. M. Linsel, A. Bohrdt, and F. Grusdt, 2025, Physical Review B, Vol. 111, Issue 2, p. 024314, DOI: 10.1103/PhysRevB.111.024314

[183] *Lattice QCD Phase Diagram In and Away from the Strong Coupling Limit*, Ph. de Forcrand, J. Langelage, O. Philipsen, and W. Unger, 2014, Physical Review Letters, Vol. 113, Issue 15, p. 152002, DOI: 10.1103/PhysRevLett.113.152002

[184] *Universal Scaling Functions in Critical Phenomena*, C.-K. Hu, C.-Y. Lin, and J.-A. Chen, 1995, Physical Review Letters, Vol. 75, No. 2, pp. 193–196, DOI: 10.1103/physrevlett.75.193

[185] *Hu Replies:*, C.-K. Hu, 1996, Physical Review Letters, Vol. 76, No. 20, pp. 3875–3875, DOI: 10.1103/physrevlett.76.3875

[186] *Universal finite-size-scaling amplitudes of the Potts model on a torus*, H. Park and M. den Nijs, 1988, Physical Review B, Vol. 38, No. 1, pp. 565–579, DOI: 10.1103/PhysRevB.38.565

[187] *STRONG COUPLING QCD AT FINITE BARYON NUMBER DENSITY*, F. Karsch and K. H. Mütter, 1989, Nuclear Physics B, Vol. 313, pp. 541–559, DOI: 10.1016/0550-3213(89)90396-9

[188] *Baryon bags in strong coupling QCD*, C. Gattringer, 2018, Physical Review D, Vol. 97, Issue 7, p. 074506, DOI: 10.1103/PhysRevD.97.074506

[189] *Bag representation for composite degrees of freedom in lattice gauge theories with fermions*, C. Marchis, C. Gattringer, and O. Orasch, 2018, Proceedings of Science, Vol. LATTICE2018, p. 243, arXiv: 1811.09372 (hep-lat), DOI: 10.22323/1.334.0243

[190] *More on the flux tube model of the deconfining transition*, A. Patel, 1984, Physics Letters B, Vol. 139, No. 5, pp. 394–398, DOI: 10.1016/0370-2693(84)91838-0

[191] *Baryon density correlations in high temperatures hadronic matters*, C. Bernard, T. A. DeGrand, C. DeTar, S. Gottlieb, A. Krasnitz, R. L. Sugar, and D. Toussaint, 1994, Physical Review D, Vol. 49, No. 11, pp. 6051–6062, DOI: 10.1103/PhysRevD.49.6051

[192] *Potts flux tube model at nonzero chemical potential*, J. Condella and C. DeTar, 2000, Physical Review D, Vol. 61, No. 7, p. 074023, DOI: 10.1103/PhysRevD.61.074023

[193] *Centre symmetric 3d effective actions for thermal SU(N) Yang-Mills from strong coupling series*, J. Langelage, S. Lottini, and O. Philipsen, 2011, Journal of High Energy Physics, Vol. 2011, No. 2, p. 57, DOI: 10.1007/JHEP02(2011)057

[194] *The QCD deconfinement transition for heavy quarks and all baryon chemical potentials*, M. Fromm, J. Langelage, S. Lottini, and O. Philipsen, 2012, Journal of High Energy Physics, Vol. 2012, No. 42, DOI: 10.1007/JHEP01(2012)042

[195] *Heavy dense QCD and nuclear matter from an effective lattice theory*, J. Langelage, M. Neuman, and O. Philipsen, 2014, Journal of High Energy Physics, Vol. 2014, No. 9, p. 131, DOI: 10.1007/JHEP09(2014)131

[196] *Ward identities for invariant group integrals*, S. Uhlmann, R. Meinel, and A. Wipf, 2007, Journal of Physics A: Mathematical and Theoretical, Vol. 40, No. 16, pp. 4367–4389, DOI: 10.1088/1751-8113/40/16/008

[197] *Statistical Physics - Statics, Dynamics and Renormalization*, L. P. Kadanoff, 2000, World Scientific

[198] *Statistische Mechanik*, 3rd edition, F. Schwabl, 2010, Springer-Verlag

[199] *Worm Algorithms for Classical Statistical Models*, N. Prokof'ev and B. Svistunov, 2001, Physical Review Letters, Vol. 87, No. 16, p. 160601, DOI: 10.1103/PhysRevLett.87.160601

[200] *Solving the Complex Phase Problem in a QCD Related Model*, Y. Delgado, H. G. Evertz, and C. Gattringer, 2011, Acta Physica Polonica B Proceedings Supplement, Vol. 4, No. 4, p. 703, DOI: 10.5506/APhysPolBSupp.4.703

[201] *QCD Phase Diagram According to the Center Group*, Y. Delgado Mercado, H. G. Evertz, and C. Gattringer, 2011, Physical Review Letters, Vol. 106, No. 22, p. 222001, DOI: 10.1103/PhysRevLett.106.222001

[202] *Worm algorithms for the 3-state Potts model with magnetic field and chemical potential*, Y. Delgado Mercado, H. G. Evertz, and C. Gattringer, 2012, Computer Physics Communications, Vol. 183, No. 9, pp. 1920–1927, DOI: 10.1016/j.cpc.2012.04.014

[203] *Exploring the worldline formulation of the Potts model*, C. Gattringer, D. Göschl, and P. Törek, 2020, Nuclear Physics B, Vol. 956, p. 115008, DOI: 10.1016/j.nuclphysb.2020.115008

[204] *Remarks on the construction of worm algorithms for lattice field theories in worldline representation*, M. Giuliani and C. Gattringer, 2017, arXiv: 1702.04771 (hep-lat)

[205] *Poly-logarithmic deterministic fully-dynamic algorithms for connectivity, minimum spanning tree, 2-edge, and biconnectivity*, J. Holm, K. de Lichtenberg, and M. Thorup, 1998, STOC '98: Proceedings of the Thirtieth Annual ACM Symposium on Theory of Computing, pp. 79–89, DOI: 10.1145/276698.276715

[206] *Solution of the sign problem in the Potts model at fixed fermion number*, A. Alexandru, G. Bergner, D. Schaich, and U. Wenger, 2018, Physical Review D, Vol. 97, No. 11, p. 114503, DOI: 10.1103/physrevd.97.114503

[207] *The three-dimensional, three-state Potts model in an external field*, F. Karsch and S. Stickan, 2000, Physics Letters B, Vol. 488, No. 3-4, pp. 319–325, DOI: 10.1016/s0370-2693(00)00902-3

[208] *First Order Phase Transitions in Renormalization Group Theory*, B. Nienhuis and M. Nauenberg, 1975, Physical Review Letters, Vol. 35, pp. 477–479, DOI: 10.1103/PhysRevLett.35.477

[209] *Finite-size scaling of the three-state Potts model on a simple cubic lattice*, M. Fukugita, H. Mino, M. Okawa, and A. Ukawa, 1990, Journal of Statistical Physics, Vol. 59, No. 5-6, pp. 1397–1429, DOI: 10.1007/bf01334757

[210] *Potts models: Density of states and mass gap from Monte Carlo calculations*, N. A. Alves, B. A. Berg, and R. Villanova, 1991, Physical Review B, Vol. 43, No. 7, pp. 5846–5856, DOI: 10.1103/physrevb.43.5846

[211] *Three-dimensional 3-state Potts model revisited with new techniques*, W. Janke and R. Villanova, 1997, Nuclear Physics B, Vol. 489, No. 3, pp. 679–696, DOI: 10.1016/S0550-3213(96)00710-9

[212] *Flux tube model signals for baryon correlations in heavy ion collisions*, A. Patel, 2012, Physical Review D, Vol. 85, No. 11, DOI: 10.1103/physrevd.85.114019

[213] *Monte-Carlo simulations of a flux tube model*, Z. Burda and P. Sawicki, 1994, Zeitschrift für Physik C Particles and Fields, Vol. 64, No. 2, pp. 291–293, DOI: 10.1007/bf01557400

[214] *ON INVARIANT INTEGRATION OVER SU(N)*, Michael Creutz, 1978, J. Math. Phys., Vol. 19, p. 2043, DOI: 10.1063/1.523581

[215] *Randomized Dynamic Graph Algorithms with Polylogarithmic Time per Operation*, M. R. Henzinger and V. King, 1995, STOC '95 Proceedings of the twenty-seventh annual ACM symposium on Theory of computing, pp. 519–527, DOI: 10.1145/225058.225269

[216] *The Art of Computer Programming - Sorting and Searching*, Vol. 3, second edition, D. E. Knuth, 1998, Addison-Wesley

[217] *On the universality of crossing probabilities in two-dimensional percolation*, R. P. Langlands, C. Pichet, Ph. Pouliot, and Y. Saint-Aubin, 1992, Journal of Statistical Physics, Vol. 67, No. 3-4, pp. 553–574, DOI: 10.1007/bf01049720

[218] *Numerical results for crossing, spanning and wrapping in two-dimensional percolation*, G. Pruessner and N. R. Moloney, 2003, Journal of Physics A: Mathematical and General, Vol. 36, No. 44, pp. 11213–11228, DOI: 10.1088/0305-4470/36/44/003

[219] *Correction-to-scaling exponent for two-dimensional percolation*, R. M. Ziff, 2011, Physical Review E, Vol. 83, No. 2, DOI: 10.1103/physreve.83.020107

Selbstständigkeitserklärung

(gemäß § 17 Absatz 2 der Promotionsordnung der Naturwissenschaftlichen Fachbereiche vom 21.01.2016)

Ich erkläre: Ich habe die vorgelegte Dissertation selbstständig und ohne unerlaubte fremde Hilfe und nur mit den Hilfen angefertigt, die ich in der Dissertation angegeben habe. Alle Textstellen, die wörtlich oder sinngemäß aus veröffentlichten Schriften entnommen sind, und alle Angaben, die auf mündlichen Auskünften beruhen, sind als solche kenntlich gemacht. Ich stimme einer evtl. Überprüfung meiner Dissertation durch eine Antiplagiat-Software zu. Bei den von mir durchgeführten und in der Dissertation erwähnten Untersuchungen habe ich die Grundsätze guter wissenschaftlicher Praxis, wie sie in der „Satzung der Justus-Liebig-Universität Gießen zur Sicherung guter wissenschaftlicher Praxis“ niedergelegt sind, eingehalten.

Ort, Datum	Unterschrift (Milad Ghanbarpour)